

Identification and functional characterisation of oncogenic pathway signatures in malignant Lymphoma

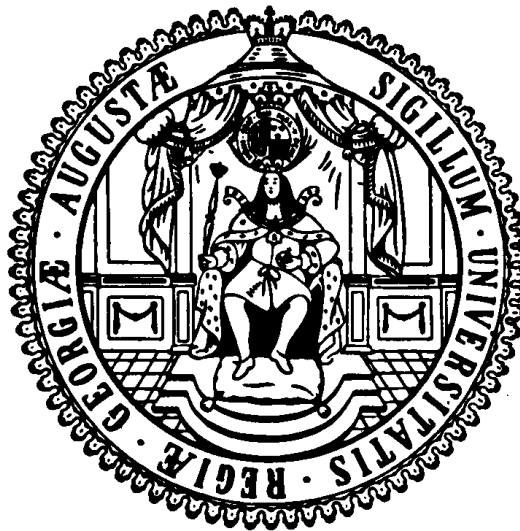
Doctoral Thesis

In partial fulfilment of the requirements for the degree

“Doctor rerum naturalium (Dr. rer. nat.)”

in the Molecular Medicine Study Program

at the Georg-August University Göttingen



Graduate School 1034

submitted by Alexandra Schrader

born in Soest

Göttingen, 2011

Thesis Committee

Prof Dr. Dieter Kube (Supervisor)

E-Mail dkube@med.uni-goettingen.de

Phone 0049-551-391537

Postal Address Universitätsmedizin Göttingen
Zentrum Innere Medizin
Abteilung Hämatologie und Onkologie
Robert-Koch-Straße 40
37075 Göttingen

Prof Dr. Heidi Hahn

E-Mail hhahn@gwdg.de

Phone 0049-551-39-14010

Postal Address Universitätsmedizin Göttingen
Zentrum Hygiene und Humangenetik
Institut für Humangenetik
Heinrich-Düker-Weg 12
37073 Göttingen

Prof Dr. Martin Oppermann

E-Mail mopperm@gwdg.de

Phone 0049-551-395822

Postal Address Universitätsmedizin Göttingen
Zentrum Hygiene und Humangenetik
Abteilung Zelluläre und Molekulare Immunologie
Humboldtallee 34
37073 Göttingen

Date of Disputation: 22.09.2011

Affidavit

By this I declare that I independently authored the presented thesis:

“Identification and functional characterisation of oncogenic pathway signatures in malignant Lymphoma”

and that I did not use other auxiliary means than indicated. Paragraphs that are taken from other publications, by wording or by sense, are marked in every case with a specification of the literary source.

Furthermore I declare that I carried out the scientific experiments following the principles of Good Scientific Practice according to the valid “Richtlinien der Georg-August-Universität Göttingen zur Sicherung guter wissenschaftlicher Praxis”.

Alexandra Schrader

Göttingen, July 2011

Table of Contents

Abstract	I
List of figures	II
List of tables	XII
Abbreviations	XIII
1 Introduction	1
1.1 Burkitt Lymphoma (BL)	2
1.1.1 c-Myc mediates high proliferation of BL cells	3
1.1.2 The c-Myc target gene network affects 15% of all genes	3
1.1.3 Gene expression profiling has enabled the molecular diagnosis of BL ..	4
1.1.4 The microenvironmental factor BAFF might play a role for the survival of BL cells	5
1.1.5 Treatment strategy in BL	5
1.2 Diffuse Large B cell Lymphoma (DLBCL)	6
1.2.1 DLBCL are characterised by a complex karyotype involving the translocation of BCL6	6
1.2.2 DLBCL is characterised by a high aberrant activity of survival signals including NF- κ B	7
1.2.3 Global gene expression profiling identified subgroups of DLBCL	7
1.2.4 Treatment strategy in DLBCL	8
1.3 B cell Development and the Germinal Centre Reaction	9
1.4 B cells are dependent on microenvironmental survival signals	11
1.4.1 Nuclear factor of kappa B light polypeptide gene enhancer in B-cells signalling	12
1.4.2 Mitogen Activated Protein Kinases (MAPKs)	12
1.4.3 BCR activation triggers a variety of signalling pathways including Calcium signalling, NF- κ B, PI3K/AKT and MAPK activation	13
1.4.4 Toll like receptor mediated activation of NF- κ B and MAPK signals	13
1.4.5 CD40 mediates NF- κ B and MAPK signals	14
1.4.6 B cell activating factor of the TNF superfamily (BAFF/ TNFSF13B) can activate distinct TNF receptors that trigger noncanonical NF- κ B and MAPK signalling	15
1.4.7 IL21 signals via IL21R mediated STAT1 and STAT3 activity	16
Aim of the Study	18
2 Materials and Methods	20
2.1 Biological Material	20
2.2 Consumable supplies	21
2.3 Equipment	22
2.4 Chemicals	24
2.5 Chemical Inhibitors	26
2.6 Buffers, Solutions and Media	26
2.7 Plasmids	30

2.8	Recombinant Proteins and Biological Material	30
2.9	Antibodies.....	31
2.10	Oligonucleotides.....	33
2.11	Ready to use Reaction Systems	35
2.12	Cell Biology	36
2.12.1	Cell culture techniques	36
2.12.2	Isolation of Tonsillar Mononuclear Cells from human primary tissue....	36
2.12.3	Enrichment of CD10+ GC B cells	37
2.12.4	Transfection of CD10 ⁺ B cells via non-viral DNA transfer.....	37
2.12.5	Activation of B cells with soluble stimulating factors	38
2.12.6	Inhibitor Treatment	39
2.12.7	Flow cytometry	39
2.12.8	Characterisation of cell populations via flow cytometry	40
2.12.9	Preparative FACS of transfected CD10 ⁺ cells	40
2.12.10	Cell cycle analysis	41
2.12.11	Synchronisation of BL cells using Thymidine treatment	42
2.12.12	Ca ²⁺ Measurement	42
2.13	Protein Biochemistry.....	43
2.13.1	Preparation of cell lysates	43
2.13.2	SDS-PAGE.....	43
2.13.3	Immunoblotting Technique	44
2.14	Molecular Biology	45
2.14.1	Transformation of E.coli.....	45
2.14.2	Isolation of Plasmid DNA.....	45
2.14.3	mRNA Isolation	45
2.14.4	mRNA Amplification.....	46
2.14.5	Reverse Transcription	46
2.14.6	Transcript quantification via qRT-PCR (quantitative Real Time – Polymerase Chain Reaction).....	47
2.14.7	Chromatin Immunoprecipitation.....	48
2.15	Microarray analyses	50
3	Results	54
3.1	High c-Myc activity is an independent negative prognostic factor for diffuse large B cell lymphomas	54
3.1.1	Overexpression of c-Myc in primary human GC B cells	54
3.1.2	Ectopic c-Myc expression triggers a tumour like expression profile in primary GC B cells.....	56
3.1.3	Very high expression of c-Myc target genes is a hallmark of molecular Burkitt lymphomas	59
3.1.4	High expression of c-Myc inducible genes in the group of non-mBL and intermediate lymphomas is associated with shorter overall survival.....	65

3.2	Activation of BL cells with B cell specific microenvironmental factors triggers global changes in gene expression patterns useful to define pathway activity in individual lymphoma	68
3.2.1	anti-IgM, CD40L, IL21, BAFF and LPS stimulation activate an individual, partially overlapping pattern of pathways upon stimulation of Burkitt Lymphoma cells	69
3.2.2	Global changes in gene expression profile through specific in vitro BL cell stimulation.....	72
3.2.3	Distinct stimuli induce the differential expression of overlapping as well as specific target genes	75
3.2.4	Investigation of differential gene expression using qRT-PCR	79
3.2.5	Stimulation mediated gene expression changes in lymphoma precursor cells.....	81
3.2.6	Activated expression of <i>DUSP2</i> , <i>DUSP5</i> , <i>DUSP10</i> and <i>DUSP22</i> through BCR is dominantly mediated by ERK activation in contrast to <i>MYC activation</i> that is dominantly involves PI3K.....	84
3.2.7	rhBAFF stimulation induces differential p38 signals in cell lines of distinct lymphoma entities independent of BAFF receptor expression .	86
3.2.8	Individual aNHL gene expression profiles exhibit a high similarity to the gene expression profiles of <i>in vitro</i> stimulated BL cells, if globally changed genes are considered for this comparison.....	90
3.3	Identification of pathway activities in aNHL using stimulation mediated gene expression changes detected by guided clustering	94
3.3.1	Guided Clustering	95
3.3.2	CD40 and BCR mediated pathway activity is continuously increasing in aggressive NHL samples	96
3.3.3	mBLs are characterised by a missing BCR.1 and a high c-Myc activity	100
3.3.4	The expression of some BCR.1 cluster genes is decreased upon inhibition of c-Myc in BL cell lines.....	101
3.3.5	Changes in BUB1B gene expression in response to BCR crosslink are mediated by altered c-Myc binding to the BUB1B locus.....	103
3.3.6	Prolongation of the G2 phase of the cell cycle in BL cells after BCRx	105
4	Discussion	109
4.1	High c-Myc activity is an independent negative prognostic marker for DLBCL	110
4.2	Identification and characterisation of pathway activities in aNHL	113
5	Conclusion	122
	Bibliography	123
	Appendix	138

Abstract

B cell aggressive non-Hodgkin lymphomas (aNHL) represent a heterogeneous group of lymphatic malignancies comprising Burkitt Lymphoma (BL) and Diffuse Large B cell lymphoma (DLBCL). aNHL have to be treated with high dose chemotherapy regimen. Still 20% of BL and 40% of DLBCL patients do not achieve a complete remission to the so far best treatment. BL cells are characterised by a simple karyotype and an aberrant c-Myc activity that is associated with very high proliferative index of lymphoma cells. DLBCLs are characterised by a complex karyotype and are very heterogeneous in respect to their underlying oncogenic deregulation. Most DLBCL cases harbour a genetic aberration involving *BCL6* as well as constitutive active NF- κ B signalling. So far largely descriptive approaches have been followed to achieve a better understanding of lymphoma biology based on gene expression profiling of aNHL. These include the description of a molecular diagnosis for BL, the mBL signature, as well as the identification of DLBCL subgroups (ABC/GCB). In this study new gene expression patterns holding information about B cell relevant oncogenic pathways were identified. These can be used to infer on the activity of deregulated pathways in malignant lymphoma based on their gene expression profiles. A c-Myc signature was described that comprises genes which are co-regulated with *MYC* in lymphoma precursor cells as well as in aNHL. Using the expression of these genes as a surrogate marker for c-Myc activity (c-Myc index), it was found that high c-Myc activity is an independent negative prognostic factor for DLBCL. To identify functionally important clusters of genes, affected by B cell specific paracrine survival stimuli, the gene expression changes of a BL cell line in response to BCR and CD40 activation as well as Interleukin 21 (IL21), B cell activating factor (BAFF) and Lipopolysaccharide (LPS) stimulation were elucidated. Using the new approach “guided clustering” a gene cluster inhibited upon BCR stimulation (BCR.1) was identified among others. The activity of the BCR.1 gene cluster is negatively correlated with the c-Myc index. The BCR.1 cluster, associated with differences in the expression of cell cycle regulatory factors, provides an explanation for the high chromosomal complexity in a subgroup of DLBCL cases. The gene clusters identified here can help to obtain a better understanding of the biology of so far unclassifiable lymphoma.

List of figures

Figure Page

Figure 1-1 Simplified scheme of the Germinal Centre Reaction. The naïve antigen primed B cell enters secondary lymphatic organs and form a Germinal Centre (GC). GC B cells proliferate in the dark zone. After undergoing somatic hypermutation the cells enter the light zone and affinity maturation of the BCR occurs. Therefore B cells are in close contact with T helper cells and Follicular Dendritic Cells (FDCs), which mediate the needed survival signals via paracrine stimulation of maturing B cells. Subsequent to positive selection and class switch recombination the differentiated B cells leave the GC as memory or plasma cells. Figure taken from (Küppers 2005). 10

Table 2-1 Cell lines.....20

Table 2-2 Consumables21

Table 2-3 Equipment.....22

Table 2-4 Chemicals24

Table 2-5 Chemical Inhibitors.....26

Table 2-7 Vectors30

Table 2-8 Recombinant Proteins30

Table 2-9 Antibodies31

Table 2-10 qRT-PCR Primer33

Table 2-11 Reaction Systems35

Table 2-12 Amount of plasmid DNA used for transfection.....38

Table 2-13 RT Reaction46

Table 2-14 Cycle program RT-PCR47

Table 2-15 Reaction Mix and Cycling Program PCR ChIP.....50

Figure 3-1 Expression of c-Myc in primary human germinal centre B cells. A Flow cytometric analysis of CD10⁺ tonsillar B cells transfected with pcDNA3.1 (upper row) or c-Myc (lower row) together with pMACSΔLNGFR stained with Hoechst Dye to perform live gating. B CD10 and NGFR staining. CD10⁺ and ΔLNGFR⁺, Hoechst negative cells were collected for RNA isolation (see respective gating). C Detection of c-Myc and b-actin in transfected CD10⁺ tonsillar B cells by immunoblot analysis. D Real-time RT-PCR of the relative quantity of c-Myc in c-Myc-expressing and non-expressing GC B cells. All samples were analysed in triplicates and are presented as $2^{-\Delta\Delta CT}$ values compared to vector control. E Multidimensional Scaling (MDS) based on the transcriptional fold-changes of the top 200 c-Myc responsive genes. The plot is a two dimensional visualization (dimension 1 and dimension 2) of the differences between the tonsils with respect to the transcriptional changes induced by c-Myc. F Shown are the transcriptional levels of c-Myc (y-axis) measured by HGU133 Plus 2.0 Affymetrix microarrays in 8 tonsils (x-axis). Each tonsil is represented by a dark green bar and light green bar indicating a pair of transfection experiments (dark green: empty control vector, light green c-Myc expression vector). The scale of the expression data (y-axis) obtained from microarray normalization (variance stabilization) is equivalent to the natural logarithm of the true fold-change: An increase by one unit corresponds to a fold change of e^1 55

Figure 3-2 Gene set enrichment analysis (GSEA) of c-Myc responsive genes. Genes were ranked by their correlation with expression levels of *MYC* in decreasing order from the most positively correlated to most negatively correlated genes. GSEA enrichment scores (y-axis of the top panel) are plotted against the gene list ranked by correlation with *MYC*. A GSEA revealed a strong enrichment of a known c-Myc signature among the genes most correlated with c-Myc in our analysis. This is indicated by the sharp increase in the GSEA enrichment score to the left of the graph and a decrease to the right B In contrast, a known CD40 signature is enriched among the genes negatively correlated with c-Myc. This is indicated by the gradual decrease of the GSEA enrichment score to the left of the graph, and a sharp increase to the right. C GSEA revealed an enrichment of a CANCER NEOPLASTIC META UP gene set which comprises genes that are

upregulated in tumour cells relative to matching normal tissue cells across many tumour entities. For a detailed list of Gene Sets please see Table 3-1.58

Figure 3-3 *FZD7* expression is high in lymphoma precursor cells but reduced in lymphoma cells and negatively correlated to *MYC*-gene expression. *FZD7* and *MYC* gene expression was assessed using qRT-PCR. Ct values were normalized to $\beta 2m$ expression and $\Delta\Delta Ct$ values were calculated compared to respective gene expression in MC116 lymphoma cells. T99, T96, T97, T98, T101 and T102 represent different preparations of tonsillar B cells purified by CD10 MACS. All other analysed samples represent different lymphoma cell lines.64

Figure 3-4 Stratification of NHL patients in mBL and non mBL by expressing c-Myc in GC B cells. Each row in the heatmaps represents a gene and each column represents a microarray sample. The expression levels for each gene were standardized to a mean value of 0 and a standard deviation of 1, and are represented according to a color scale; yellow and blue indicate high and low expression, respectively. A Heatmaps of genes expressed in GC B cells that show a correlation to *MYC* in tonsillar samples and 220 NHL samples (Hummel, Bentink et al. 2006). B Heatmap of gene expression levels of the same genes plotted in (A) this time in 220 NHL samples (Hummel, Bentink et al. 2006) recently classified as mBL, non-mBL or intermediate cases. This classification is colour coded in the top bar (green: mBL, red: non-mBL, grey: intermediate). The patients are arranged according to c-Myc index (increasing from left to right). ...65

Figure 3-5 High expression of c-Myc index genes in the group of non-mBL and intermediate lymphomas is associated with shorter overall survival A Boxplots of the level of the c-Myc index (y-axis) in NHL lymphomas classified as non-mBL, intermediate and mBL (x-axis). B Boxplots of the level of the c-Myc expression index (y-axis) in NHL lymphomas classified as *MYC*-negative, *MYC*-complex and *MYC*-simple (x-axis). Statistical significance of the differences was tested using ANOVA. (C&D) Kaplan Meier plots of the overall survival of non-mBL and intermediate patients stratified by the c-Myc expression index C 88 non-mBL and intermediate patients samples (MMML) were stratified based on the level of their c-Myc expression index into tumours of very low, low, medium and high c-Myc activity. Patients with a tumour of high c-Myc activity have the shortest overall

survival (grey continuous line). D 157 DLBCL patients of the data set published by Dave and colleagues (LLMPP) were grouped as in (C). Patients with high c-Myc index showed shorter overall survival. Statistical significance of the differential survival of these groups was tested using the log rank test..... 67

Figure 3-6 Different pathways activated by IL21, CD40L, anti-IgM (BCRx), BAFF and LPS in human Burkitt Lymphoma cells. BL2 cells were incubated with IL-21 (100ng/ml), CD40L (200ng/ml), anti IgM F(ab)₂ fragments (1.3µg/ml), BAFF (100ng/ml) and LPS (1µg/ml)) for indicated time points. A The activation of calcium signalling was detected using a Ca²⁺ sensitive fluorophor in combination with flowcytometric analyses. BL2 cells were loaded with indo1 and Ca²⁺ influx was measured directly after the stimulation. BCRx (1.3µg/ml) induced an immediate Ca²⁺ accumulation in the cytoplasm as indicated by the increased Indo-1 fluorescence. B BL2 cells stimulated for 30mins as indicated above. The activation of canonical NF-κB signalling was visualized by immunoblot of IκBα. C BL2 cells were stimulated for distinct time points (6hrs for CD40L and LPS, 3hrs for BCRx, 9hrs for BAFF and 2hrs for IL21 stimulation) as described in above. The activation of noncanonical NF-κB signalling was detected monitoring the p52 cleavage product of p100 by immunoblot. D BL2 cells stimulated for 5mins as indicated above. The activation of ERK was shown through immunoblot analyses of phosphorylated ERK1/2. E BL2 cells were stimulated for 30mins as indicated in above. The activation of p38 was detected through detection of phosphorylated p38 via immunoblot. F *In vitro* kinase assay to investigate the activation of JNK in BL2 cells (Kutz, Reisbach et al. 2008). These data were kindly provided by A. Ulrich and A. Kieser. G BL2 cells were stimulated for distinct time points (6hrs for CD40L and LPS, 3hrs for BCR, 9hrs for BAFF and 2hrs for IL21 stimulation) as described in above. The activation of PI3K/AKT signalling was detected using immunoblot detection of phosphorylated AKT1. H&I BL2 cells were stimulated for 30mins as indicated above. The activation of STAT1/STAT3 was detected through the verification of phosphorylated STAT1/STAT3 via immunoblot. 71

Figure 3-7 Identification of anti-IgM (BCRx), CD40L, IL-21, BAFF and LPS regulated genes in BL cells using microarrays. BL2 cell were stimulated as described in Figure 3-6 with A anti IgM F(ab)₂ fragment (3hrs), B CD40L (6hrs), C

IL21 (2hrs), D BAFF (9hrs) and E LPS (6hrs). RNAs from these cells were used to perform whole genome gene expression profiling on Affymetrix HGU-133 plus 2.0 microarray chips. These heatmaps show the TOP 100 most highly changed genes (adj. p-value ≤ 0.05) in response to each stimulus. As distinct microarray chips were used for the microarray analyses of cell perturbation and patient samples (Affymetrix HGU-133A and HGU-133 plus2.0), the list of TOP100 genes had to be adapted to be able to transfer the resulting genes to patient data (see below for additional details). Therefore the lists were shortened since not all probesets were present on both array platforms (BCRx (74 genes), sCD40L (71 genes), rhBAFF (77 genes), rhIL21 (77 genes) and LPS (66 genes)). Each row in the heatmaps represents a gene and each column represents a microarray sample. Yellow and blue indicate high and low expression, respectively.74

Figure 3-8 Overview of high responsive overlapping and stimulus specific genes upregulated in response to BCRx, CD40L, rhBAFF and rhIL21. The lists of genes showing the highest differential expression in response to stimulation (see Appendix table A2, A3, A4, A5) were compared. This comparison was made using VENNY (Oliveros 2007). Genes upregulated in response to BAFF stimulation are represented in the blue ellipsoid (BCR = yellow, CD40L = green, IL21 = red). The overlaps of the gene lists are represented by overlaps of the respective ellipsoids. The number of genes in the respective overlap is indicated.77

Figure 3-9 Overview of high responsive overlapping and stimulus specific genes downregulated in response to BCRx, CD40L, rhBAFF and rhIL21. The lists of genes showing the highest differential expression in response to stimulation (see Appendix table A2, A3, A4, A5) were compared. This comparison was made using VENNY (Oliveros 2007). For a detailed description see Figure 3-8.78

Figure 3-10 qRT-PCR analyses of the expression of a selection of genes after respective stimulation. BL2 cells were stimulated as described in Figure 3-7. One representative experiment out of two is shown. All samples were analysed in triplicates. Results are presented as $2^{-\Delta\Delta CT}$ or ΔCT values, relative to *abl* housekeeper expression and compared to unstimulated control. N.E. = Not Expressed ($\Delta Ct > 10$) A *ID1* B *ICAM1* C *CD58*. D *DUSP2* E *DUSP5* (basal $\Delta Ct >$

10) F *DUSP10* G *DUSP22* H *MYC* I *CXCL10* J *SLAMF7* (basal $\Delta Ct > 10$) K
RGS1 (basal $\Delta Ct > 10$). 80

Figure 3-11 Expression of *ICAM1*, *DUSP2*, *DUSP5*, *DUSP10*, *DUSP22* and *MYC*, *SLAMF7* in CD10⁺ germinal centre B cells in response to sCD40L, BCRx, rhIL21 and rhBAFF stimulation CD10⁺ B cells from distinct tonsillar preparations (T96, T97, T98, T99, T101, T102) were stimulated with 100ng/ml rhIL21, 200ng/ml sCD40L, 1.3 μ g/ml anti IgM/anti IgG F(ab)₂ fragments and rhBAFF for 3hrs. Effects are depicted as $\Delta\Delta Ct$ values normalized to $\beta 2m$ expression and relative to the unstimulated control (NE = not expressed). The statistical significance of the differences in gene expression was calculated for each gene and stimulation separately, using the two paired t-test. A *ICAM1* expression is affected by CD40 ($p=0.0005$) and IL21 ($p=0.0186$). B *DUSP2* expression is affected by BCRx ($p=0.0209$) and IL21 ($p=0.0138$) C *DUSP5* expression is affected by BCRx ($p=0.0378$). D *DUSP10* expression is affected by BCRx ($p<0.0001$). E *DUSP22* expression is highly variable and not affected by any stimulation. F *MYC* expression is affected by BCRx ($p=0.0101$) and CD40 ($p=0.0306$). G *SLAMF7* expression is affected by BCRx ($p=0.0006$)..... 83

Figure 3-12 Pathways involved in the regulation of *DUSP5*, *DUSP2* and *DUSP10* as well as *MYC* in response to BCRx in BL cells. BL2 cells were pre-incubated with specific pathway inhibitors for 3hrs (for detailed information see Methods section chapter 2.12.6). 1.3 μ g/ml anti-IgM F(ab)₂ fragments were added respectively and cells were harvested after additional 3 hrs for qRT-PCR. A-D Expression of *DUSP2*, *DUSP5* and *DUSP10* and *MYC*. Results are presented as $2^{-\Delta\Delta Ct}$ values, relative to *abl* housekeeper expression and compared to unstimulated DMSO control. As *DUSP5* expression (B) is below detectable levels in unstimulated probes, only ΔCt values of stimulated probes relative to DMSO control were compared. One representative experiment out of three biological replicates is shown..... 85

Figure 3-13 rhBAFF stimulation induces differential p38 signals in cell lines of distinct lymphoma entities despite comparable receptor equipment A BL2, Ramos, BL16, SuDHL4 and SuDHL6 cells were stimulated with 100ng/ml rhBAFF for 30 mins. p38 activity was detected using an anti pp38 specific

antibody. B BL2, SuDHL4 and SuDHL6 cells were stimulated as described in A for 9 and 24 h respectively. Activation of the noncanonical NF- κ B pathway was detected using an antibody that detects p100/p52 NFKB2. C&D Surface expression of BAFF-R and TACI was detected on BL2, Ramos, BL16, SuDHL4 and SuDHL6 cells using flow cytometry. D Mean fluorescence intensities of BAFF-R and TACI stained cells are compared. E Expression of BAFF-R, TACI and BCMA mRNA was investigated in BL2, Ramos, SuDHL4 and SuDHL6 cells using qRT-PCR. Δ Ct values were calculated using beta2m expression as housekeeper (NE = not expressed)..... 89

Figure 3-14 Expression of stimulus regulated genes in aNHL. The TOP100 most highly responding genes upon stimulation of BL2 with A rhBAFF, B sCD40L, C anti-IgM F(ab)₂, D rhIL21, fragments, E LPS and (see tables A2-A6 in the appendix) were investigated for their expression in the gene expression profiles of 220 aNHL lymphoma cases (Hummel, Bentink et al. 2006). aNHL cases were ordered from left to right according to the similarity of gene expression to the stimulated status of BL2 cells. The Heatmaps display the expression of target genes (columns) across 220 lymphoma samples (rows). The colour bar above the heatmaps marks mBL in red, non-mBL in green and intermediate lymphoma in yellow. Furthermore the affiliation of samples to ABC/GCB DLBCL subgroups and the presence of an *IG-MYC* translocation is encoded in a bar on top of the map (see legend for colour coding). Relative gene expression is encoded with yellow (high expression) and blue (low expression). 93

Figure 3-15 Comparison of the patient groups that show a gene expression profile of stimulus effected genes most closely to the activated gene expression profile of BL2 cells 55 aNHL samples that show the highest similarity regarding their gene expression profile to the stimulated BL cells in response to CD40L, BCRx, IL21 and BAFF stimulation were compared using Venn Diagrams as described in Figure 3-8..... 93

Figure 3-16 (legend see next page) 99

Figure 3-16 Guided clustering identifies four major clusters of genes regulated by BCR activation and CD40L stimulation. Each row in the heatmaps represents a

gene and each column represents a microarray sample. Yellow and blue indicate high and low expression. left panel: Heatmaps show the gene expression of the respective cluster genes in stimulated BL2 cells compared to control. right panel: Heatmaps show the expression of respective cluster genes in gene expression profiles of tumour samples from 175 intermediate and non-mBL aNHL patients. The patient samples are ordered according to rising BCR.1/CD40.1 index from left to right (symbolized by the red bars). The colour coded bar on top of the heatmaps represents the affiliation of patients to ABC / GCB DLBCL subgroups (orange = ABC tumour sample, blue = GC B tumour sample and grey = unclassifiable sample). A The gene expression of BCR.1 and BCR.2 cluster genes is depicted. B The gene expression of CD40.1 and CD40.2 cluster genes is displayed. 100

Figure 3-17 The BCR.1 index is inversely correlated with the c-Myc index. A&B Correlation coefficients of Pathway Activation Indices in a cohort of 220 aNHL cases. c-Myc index genes, BCR.1, BCR.2, CD40.1 and CD40.2 gene clusters were used to calculate the respective PAIs in gene expression profiles of 220 aNHL diagnosed as mBL (red), non-mBL (green) and intermediate lymphoma (yellow) by Hummel and colleagues (Hummel, Bentink et al. 2006). The parallel activity was estimated plotting the indices against each other and calculating the respective correlation coefficient. A coefficient close to one indicates highly correlated index activities and a high number of lymphoma expressing both gene clusters in an activated state. 102

Figure 3-18 Expression of BCR.1 cluster genes is downregulated by BCR activation and c-Myc inhibition in Burkitt Lymphoma cell lines. A-F BL2 and Ramos cell were pretreated for 3h with 60µM 10058-F4 c-Myc inhibitor or left untreated (DMSO). Cells were stimulated for additional 3h with anti IgM F(ab)2 fragment (1.3µg/ml). qRT-PCR analyses were performed using SYBR green. Foldchanges were calculated using the $\Delta\Delta C_t$ method. One representative experiment of three replicates is shown. 104

Figure 3-19 ChIP of c-Myc reveals a change in c-Myc abundance at the Bub1B promoter upon BCR activation. Chromatin IPs were performed using antibodies directed against IgG as negative control, against c-Myc and against acetylated

histone H3 as positive control (marker for active transcription). To check for c-Myc binding a fragment was amplified that encompasses the previously described E-box in intron 1 of the Bub1B gene (Menssen, Epanchintsev et al. 2007). The lower lane shows a shorter exposure time to infer on differences in acetyl Histone H3 binding..... 105

Figure 3-20 (legend see next page) 108

Figure 3-20 Activation of the BCR leads to a prolonged G2 phase in BL cell lines A & B Asynchronous growing BL2 and Ramos cells were treated with 1.3µg/ml anti IgM F(ab)₂ fragments and 60µM 10058-F4 c-Myc inhibitor for 6h. Cell cycle distribution of cells was measured using Nicoletti buffer and FACS based analyses of the DNA content of the nuclei. C Ramos cells were synchronised in G2 cell cycle phase using 2 rounds of thymidine (2mM) treatment. After removing the Thymidine (0h) the cells started to pass through the cell cycle. Cell cycle distributions were measured over a time course of 0h up to 8h using Nicoletti technique. The 24hrs time point was measured separately. One out of three representative experiments is shown. 109

Table A 1 Gene Set Enrichment Analysis of c-Myc responsive genes. Gene set enrichment analysis (GSEA) of the resulting ranked gene list was performed using the Java implementation of GSEA obtained from <http://www.broadinstitute.org/gsea/>. The ES (Enrichment Score) is given, which is the primary result of the gene set enrichment analysis and reflects the degree to which a gene set is overrepresented in a ranked list of genes. Gene sets are displayed in the order of the NES (Normalized Enrichment Score) which accounts for differences in gene set sizes and correlations between the gene set and the expression dataset. The NOM p-value (Nominal p-value) is a statistical measure for the significance of the enrichment of one single gene set. The FDR q-value (False Discovery Rate) is adjusted for multiple testing. 138

Table A 3 CD40 responsive genes This table shows the effects of sCD40L on the most variable genes. 100 probesets with the highest differential expression were selected from all significantly regulated genes. Probesets that were array specific

and not spotted on the HG U133 plus, which was used for the evaluation of aNHL samples, were discarded and excluded from further analysis..... 141

Table A 4 BCR responsive genes. This table shows the effects of BCRx on the most variable genes. 100 probesets with the highest differential expression were selected from all significantly regulated genes. Probesets that were array specific and not spotted on the HG U133 plus, which was used for the evaluation of aNHL samples, were discarded and excluded from further analysis..... 142

Table A 5 LPS responsive genes This table shows the effects of LPS on the most variable genes. 100 probesets with the highest differential expression were selected from all significantly regulated genes. Probesets that were array specific and not spotted on the HG U133 plus, which was used for the evaluation of aNHL samples, were discarded and excluded from further analysis..... 144

Table A 7 Cluster genes identified by guided clustering 146

List of tables

Table.....	Page
Table 2-1 Cell lines.....	20
Table 2-2 Consumables	21
Table 2-3 Equipment.....	22
Table 2-4 Chemicals	24
Table 2-5 Chemical Inhibitors.....	26
Table 2-6 Buffers, Solutions and Media	26
Table 2-7 Vectors.....	30
Table 2-8 Recombinant Proteins.....	30
Table 2-9 Antibodies	31
Table 2-10 qRT-PCR Primer	33
Table 2-11 Reaction Systems	35
Table 2-12 Amount of plasmid DNA used for transfection.....	38
Table 2-13 RT Reaction	46
Table 2-14 Cycle program RT-PCR	47
Table 2-15 Reaction Mix and Cycling Program PCR ChIP.....	50
Table 3-1 Top 100 genes correlated with <i>MYC</i> in GC B cells and aNHL: The c-Myc index. Genes that are correlated with <i>MYC</i> in primary transfected GC B cells as well as in gene expression profiles of aNHL are listed below. Genes are ordered according to assumed cellular functions and the calculated t-scores. The Pearson Correlation for being expressed in correlation with <i>MYC</i> is also given for each gene.	60

Abbreviations

Abbreviation	Denotation
ABC-like	Activated B cell like
Amp	Ampicilin
aRNA	antisense RNA
BCR	B Cell Receptor
BL	Burkitt Lymphoma
BR	Basic Region
CD	Cluster of Diffrentiation
cDNA	complementary DNA
CIN	Chromosomal Instability
CSR	Class Switch Recombination
CT	Cycle Threshold
CTD	C-Terminal-Domain
ddH ₂ O	Water, double-distilled
DLBCL	Diffuse Large B Cell Lymphoma
DNA	desoxyribonucleic acid
DTT	dithiothreitol
EBV	Epstein Barr Virus
<i>E. coli</i>	<i>Escherichia coli</i>
ECL	enhanced chemiluminescence
EDTA	ethylenediaminetetraacetic acid
et al.	Lat.: et alteri
FACS	Fluorecense Activated Cells Sorting
FBS	Fetal Bovine Serum
FDC	Follicular Dendritic Cell

Abbreviation	Denotation
FITC	Fluoreszeinthiocyanat
FSC	Forward Scatter
GC	Germinal Centre
GCB-like	Germinal Centre B cell like
GFP	Green Fluorescent Protein
HEPES	4-(2-hydroxyethyl)-1-piperazineethanesulfonic acid
HLH	Helix-loop-Helix
HRP	horseradish peroxidase
IG	Immunoglobulin
IVT	<i>In Vitro</i> Transcription
kDa	kilo-Dalton
LB	Luria Bertani
LLMPP	Lymphoma/Leukemia Molecular Profiling Project
LNGFR	Low Affinity Nerve Growth Factor Receptor
LPS	Lipopolysacharide
LZ	Leucine Zipper
MACS™	Magnetic Activated Cell Sorting
MALT	Mucosa Associated Lymphoid Tissue
mBL	Molecular Burkitt Lymphoma
miRNA	micro RNA
mRNA	messenger RNA
MMML	Molecular Mechanisms of Malignant Lymphoma
NF-κB	Nuclear factor of kappa B light polypeptide gene enhancer in B-cells
aNHL	aggressive Non-Hodgkin Lymphoma
PAGE	Polyacrylamide-Gelelectrophoresis
XIV	

Abbreviation	Denotation
PAP	Pathway Activation Pattern
PBS	Phosphate Buffered Saline
PE	Phycoerythrin
PI	Propidium Iodide
PMSF	phenylmethylsulfonylfluoride
qRT-PCR	Quantitative Reverse Transcriptase – Polymerase Chain Reaction
RNA	ribonucleic acid
RNAi	RNA interference
RPM	rounds per minute
RT	roomtemperature
SDS	Sodium-Dodecyl-Sulfate
siRNA	small interfering RNA
SSC	Side Scatter
TAE	Tris-Acetate-EDTA
TBS	Tris Buffered Saline
TEMED	N,N,N',N'-Tetramethylethylenediamin
TMC	Tonsillar Mononuclear Cell
Tris	Tris-hydroxymethyl-aminomethan
Tween	Polyoxyethylensorbitanmonolaurat
VDJ	Variable Diverse Joining
WHO	World Health Organisation
x g	multiple of acceleration of gravity ($g = 9.80665 \text{ m/s}^2$)

1 Introduction

The demographic change approves living circumstances and humans life expectancies. Cancer has become a leading cause of death worldwide. According to the World Health Organization (WHO) cancer accounted for 7.6 million deaths (13% of all) worldwide in 2008 (Ferlay J 2010). It was the biologist Theodor Heinrich Boveri (1862-1915) who first hypothesised that a tumour might arise from one single cell that was not able to separate chromosomes accurately during mitosis (Boveri 1907). Based on his studies with sea urchins he stated: "We may [...] regard it as probable that individual chromosomes have different properties in vertebrates too, and it is this assumption that forms the basis of the tumour hypothesis I have put forward. A malignant tumour cell is [...] a cell with a specific abnormal chromosome constitution." (Boveri 2008). Today it is widely accepted that cancer is a genetic disease and that the deregulation of proto-oncogenes and tumour suppressor genes is the fundamental basis of cellular transformation. The accumulation of multiple independent genetic alterations induce a deregulation of cell signalling pathways crucial for the control of cell growth, cell proliferation, apoptosis, and cell fate. In addition to cell intrinsic genetic aberrations the effects of the tumour environment on the growth of malignant cells has emerged as being particularly important (Hanahan and Weinberg 2011).

The term lymphoma refers to a heterogeneous group of malignancies that originate from B or T lymphocytes. Most of the lymphomas have a B cell origin (95%). B cell lymphoma arise from differentiating B cells during the process of the germinal centre reaction (reviewed in (Küppers 2005). One discriminates two major groups of B cell lymphomas: Hodgkin Lymphoma and Non-Hodgkin Lymphoma (NHL). According to the WHO the Age-World-Standardized incidence rate (ASR (W)) the incidence for NHL was 5.1 new cases per 100 000 persons in 2008. NHL comprises many different types of B cell lymphomas, which can be divided into aggressive (fast-growing) and indolent (slow-growing) types (Jaffe, Harris et al. 1998). B cell aggressive non-Hodgkin lymphomas (aNHL) is a heterogonous group of malignancies that comprises Burkitt's Lymphoma and Diffuse Large B cell lymphoma (DLBCL) (Good and Gascoyne 2008). aNHL have

to be treated with high dose chemotherapy regimens. Despite current treatment advancements still 20% of BL and 40% of DLBCL patients do not achieve a complete response to the so far best treatment regimen. (Yustein and Dang 2007; Friedberg and Fisher 2008; Kahl 2008; Perkins and Friedberg 2008; de Jong and Balague Ponz 2011). A better understanding of aNHL biology and the oncogenic pathway activities that underlie the heterogeneity of aNHL will allow the development of an improved treatment strategy for patients at risk and a better individualized therapy for all patients. Recently major proceedings have been made regarding the characterisation of aNHL based on their tumour gene expression profiles. These transcriptomic gene expression studies allowed the establishment of a molecular diagnosis for BL as well as the discovery of two major subgroups of DLBCL that are indeed different on functional level with respect to their oncogenic dependency (Alizadeh, Eisen et al. 2000; Dave, Fu et al. 2006; Hummel, Bentink et al. 2006). Nevertheless these subgroups still comprise very heterogeneous lymphomas that probably depend on the deregulation of so far uncharacterised pathways.

1.1 Burkitt Lymphoma (BL)

The Burkitt Lymphoma (BL) was first characterised by Denis Burkitt in 1958 as the most prevalent childhood lymphoma mostly localised at the jaw (Burkitt 1958). It is an aggressive form of B cell NHL and accounts for 2% of all lymphoma cases (Küppers 2005). The BL appears in different variants. The endemic form of BL is found in equatorial Africa and is associated with an Epstein-Barr-Virus infection (Rasti, Falk et al. 2005; McNally and Parker 2006). In European areas and in Northern America the sporadic and the immunodeficiency associated forms of BL are predominant (reviewed in (Yustein and Dang 2007). The histology of BL is characterised by monomorphic medium sized B cells that are highly proliferative and silent with respect to NF- κ B and JAK-STAT signals. The tumour has a so called “starry sky” appearance, that is based on the high number of interspersed macrophages in-between the tumour cells (O'Connor, Rappaport et al. 1965).

1.1.1 c-Myc mediates high proliferation of BL cells

BL are characterised by a specific genetic aberration, the translocation of the proto-oncogene *MYC* into one of the immunoglobulin gene loci. BL cells have a simple karyotype with a low number of additional chromosomal aberrations (Hummel, Bentink et al. 2006). The genetic aberration involving *MYC* is regarded as the central event leading to lymphoma genesis of BL (Dalla-Favera, Bregni et al. 1982; Taub, Kirsch et al. 1982). In BL cells the translocated allele of *MYC* is highly expressed whereas the normal allele is usually silent (Eick and Bornkamm 1989).

c-Myc is a Helix-Loop-Helix (HLH) leucine zipper transcription factor which mediates its function only as heterodimer with its HLH partner Max (Adhikary and Eilers 2005). The c-Myc/Max dimer binds specifically to the E-Box sequence in the DNA (consensus “CANNTG”) (Blackwell, Kretzner et al. 1990). High c-Myc activity can factors mediate a high proliferative signal on the one hand and induce apoptosis in the absence of survival on the other hand (Dang, O'Donnell et al. 2006). Thus the extremely high proliferative potential of BL cells can be explained by their aberrant c-Myc activity. One mechanism how high levels of c-Myc can mediate cell cycle progression was explained by the activation of Cyclin D2 (CCND2). Increased presence of CCND2 leads to the sequestration of cyclin dependent kinase (CDK) inhibitor p27 in Cyclin D2–CDK4 complexes. p27 is degraded via the proteasome and release of the Cyclin E - CDK4 complex from p27 leads to promotion of the cell cycle (Pelengaris, Khan et al. 2002). Furthermore, c-Myc target genes that play a role in cell cycle regulation are CDC2 (cdc2 Kinase, also known as cdk1), CCNA2 (Cyclin A2), CCND3 (Cyclin D3) (<http://www.myccancergene.org>), as well as MAD2 and BUB1B (Menssen, Epanchintsev et al. 2007).

1.1.2 The c-Myc target gene network affects 15% of all genes

Among the c-Myc targets, regulators of cell metabolism, cell-cycle control and proliferation are prominent. (Schuhmacher et al., 2001; Cole and Cowling, 2008) c-Myc is proposed to affect a context dependent large network of genes comprising up to 15% of the whole genome (Dang, O'Donnell et al. 2006). Three

major experimental approaches have been used to investigate the actual processes that accompany the deregulated expression of c-Myc: (i) c-Myc overexpression in cell lines or transgenic mice, (ii) respective knockouts or knockdowns of c-Myc or (iii) c-Myc driven chromatin immunoprecipitation in cells with aberrant c-Myc expression in order to identify respective target genes. c-Myc overexpression in mouse B cells can induce the formation of lymphomas (Adams et al., 1985; Kovalchuk et al., 2000; Chesi et al., 2008) While expression in B-cell progenitors or naïve B cells leads to lymphoma cells of the earlier differentiation stage. Ectopic expression during later stages of B-cell development mostly leads to plasmacytoma. (Adams et al., 1985; Kovalchuk et al., 2000; Adams et al., 1983; Chesi et al., 2008). Despite the compelling number of investigations to understand the role of c-Myc in B cell transformation no data available on the potential of c-Myc expression in human lymphoma precursor cells. Recent data demonstrated that c-Myc expression in normal GC B cells is, if at all existing, rather low (Martinez-Valdez et al., 1996; Shaffer et al., 2001; Klein et al., 2003). A first attempt to identify direct c-Myc target genes in primary human GC B cells was not successful, as the effects of c-Myc on the gene expression profiles of B cells were rather low and variable between the distinct biological replicates (M.Sc. Thesis A. Schrader).

1.1.3 Gene expression profiling has enabled the molecular diagnosis of BL

Recently several approaches were utilized to describe and functionally characterise aNHL cases on the basis of gene expression profiles. Hummel and colleagues (Hummel, Bentink et al. 2006) achieved a clear discrimination of BL from other mature aggressive B-cell lymphoma. Using the gene expression profiles of 220 aNHL tumours they developed a molecular classifier for the diagnosis of BL: the mBL signature (58 genes). This gene signature was used to establish a continuous index of 'Burkitt likeness' (I) that enables the classification of aNHL into either molecular Burkitt lymphoma (mBL) ($I > 0.95$), non-mBL ($I < 0.05$) or intermediate lymphomas ($0.95 > I > 0.05$). Most intermediate lymphomas and non-mBL display DLBCL morphology, while mBL includes cases with and without classical BL morphology. Whereas most mBLs harbour a deregulated c-Myc expression as a consequence of an *IG-MYC* translocation, the

majority of non mBLs does not carry *IG-MYC* translocations, but has other genetic abnormalities (reviewed by (Küppers and Dalla-Favera 2001). Although heterogeneous, the intermediate cases are enriched for those with *IG-MYC* or non-*IG-MYC* aberrations on a background of a complex karyotype. The separation of NHL into these different molecular subtypes might be clinically important; cases with the mBL signature and a cytogenetic so called 'MYC-simple' status have a favourable outcome, whereas those with *MYC* breakpoints but lacking a mBL signature have a poor outcome. This study by Hummel and colleagues was published "Back to Back" with a paper from an American consortium (LMPP), which as well established a gene expression signature that discriminates BL from DLBCL (Dave, Fu et al. 2006). Dave and colleagues additionally performed a c-Myc knockdown in a DLBCL cell line with a gene expression close to activated B cells (OCI-Ly10). The combination of c-Myc target genes defined in this vein with large-scale gene expression profiling of lymphoma samples allowed to discriminate to a certain extend between lymphoma subtypes. It is not clear whether these target genes are affected by c-Myc already in lymphoma precursor cells or to which extend the mBL signature itself might be maintained by c-Myc itself.

1.1.4 The microenvironmental factor BAFF might play a role for the survival of BL cells

The role of BAFF for the survival of BL cells was investigated by Ogden and colleagues. They showed *in vitro* that IL10 activated macrophages can rescue BL cells from apoptosis by secreting BAFF (He, Chadburn et al. 2004; Ogden, Pound et al. 2005). Furthermore Saito and colleagues showed that BAFF can inhibit Rituximab as well as BCR triggered apoptosis in a human hairy cell leukemia cell line (Saito, Miyagawa et al. 2008). Nevertheless it still remains elusive whether BL TAMs indeed mediate BAFF signals in the primary tumour and how the BL cells respond in detail to BAFF stimulation.

1.1.5 Treatment strategy in BL

BL is treated with intensive high dose regimens of chemotherapy comparable to the B-ALL scheme. This chemotherapy includes cyclophosphamide, vincristine,

doxorubicin, and high-dose methotrexate (Yustein and Dang 2007; Perkins and Friedberg 2008). Using comparable therapeutic regimens long-term remission can be achieved in approximately 50% of patients. If the disease is not treated it follows a rapid clinical course and can be lethal within several months. Although it is a curable disease, many patients do not achieve complete remission or they relapse.

1.2 Diffuse Large B cell Lymphoma (DLBCL)

DLBCL is the most common lymphoma entity, since it constitutes about 30-40% of all aNHL (Friedberg and Fisher 2008). Diffuse Large B cell lymphoma (DLBCL) is a very heterogeneous disease. In contrast to a relatively high uniformity of BL, DLBCL comprises B cell tumours that morphologically differ and very often are misdiagnosed (Küppers 2005; Friedberg and Fisher 2008). This led to the assumption of the existence of a diversity of oncogenic events underlying these lymphomas. DLBCL tumours are composed of large B cells with a very high percentage of tumour infiltrate. In about 80% of DLBCL cases the tumour cells resemble centroblasts. Apart from this centroblastic type of DLBCL, one differentiates the immunoblastic type of DLBCL (10% of the cases) that shows more than 90% immunoblasts, the T-Cell-Rich/Histiocyte-Rich variant, the anaplastic type and the rare plasmablastic variant.

1.2.1 DLBCL are characterised by a complex karyotype involving the translocation of BCL6

DLBCL tumours present with complex chromosomal aberrations (Dave, Nelson et al. 2002; Iqbal, Gupta et al. 2007). These include in 35% of cases a translocation of the proto-oncogene *BCL6*. Bcl6 is a transcription repressor that is highly expressed during germinal centre reaction and was found to be essential for germinal centre formation (Dent, Shaffer et al. 1997; Fukuda, Yoshida et al. 1997; Ye, Cattoretti et al. 1997). Further genetic aberrations found in DLBCL include for example the translocation of *MYC* to one of the *IGH* or *IGL* gene loci (Weiss, Warnke et al. 1987; Ladanyi, Offit et al. 1991; Baron, Nucifora et al. 1993; Ye, Rao et al. 1993). The high prevalence of chromosomal aberration in DLBCL is

likely a result of an elevated chromosomal instability (CIN). CIN is a frequently observed phenomenon in cancers in general. The aneuploidy resulting from CIN is likely to be induced by a faulty progression of cells through the spindle assembly checkpoint in early M phase (Li, Fang et al. 2009).

1.2.2 DLBCL is characterised by a high aberrant activity of survival signals including NF- κ B

High NF- κ B activity is a hallmark of subsets of DLBCL (Davis, Brown et al. 2001; Feuerhake, Kutok et al. 2005; Lam, Davis et al. 2005; Ngo, Davis et al. 2006). This aberrant activity can be mediated for example by loss of function mutations in I κ B α (Inhibitor of NF- κ B) (Thomas, Wickenhauser et al. 2004) or by mutations in CARD11, necessary for the activation of NF- κ B (Lenz, Davis et al. 2008). Furthermore it has been shown that the aberrant activity of the B cell receptor (BCR) is of high relevance for the acquired survival property of DLBCL cells. Chen and colleagues described a Syk dependent tonic active BCR signalling in DLBCL cell lines and primary tumours. Aiming at therapy of DLBCL with Syk inhibitor, this group showed that cell lines depend on tonic BCR signalling: They undergo apoptosis in response to Syk inhibitor (R406) treatment (Chen, Monti et al. 2008). Furthermore it has been shown *in vitro* that there are subgroups of DLBCL that depend on constitutive active JAK-STAT signalling (Ding, Yu et al. 2008; Lam, Wright et al. 2008). Based on the heterogeneity of DLBCL it is likely that other, so far unidentified pathways are involved in the maintenance of the transformed phenotype of DLBCL.

1.2.3 Global gene expression profiling identified subgroups of DLBCL

Regarding the microarray based investigation of the heterogeneity of DLBCLs four major studies were conducted. Alizadeh and colleagues developed a sub stratification for DLBCL established on their similarity to distinct differentiation stages of normal B cells (ABC = Activated B Cell like and GCB = Germinal Centre B Cell like) (Alizadeh et al. 2000). This study helped to underline the aberrant signalling properties of DLBCL. Based on gene expression profiling it was found that Activated B cell like DLBCL show a high aberrant activity of NF- κ B signalling (Lam, Davis et al. 2005). Monti and colleagues identified three

distinct subtypes of DLBCLs based on their gene expression profiles (Monti, Savage et al. 2005). They described the characteristics of the distinct gene expression profiles as being associated with (i) “oxidative phosphorylation”, (ii) “B cell receptor/proliferation” and (iii) with “host inflammatory response”. These attempts to investigate gene expression profiles of malignant lymphoma have a rather descriptive character. In 2009 Ci and colleagues developed a gene expression profiling based method to infer on Bcl6 activity in primary DLBCL lymphoma (Ci, Polo et al. 2009). Using a Bcl6 driven ChIP-on-Chip assay they defined a group of 1361 target genes in GC B cells and in DLBCL cell lines respectively. They observed that BCL6 target genes are favourably repressed in GCB-type DLBCLs and in the group of BCR type DLBCLs as described by Monti and colleagues (Monti, Savage et al. 2005). In contrast to that Bentink and colleagues used the gene expression data established from ectopic expression of eight oncogenes (including *MYC*, *RAS*, *SRC*, *β -catenin* and *E2F3*) in primary human epithelial cells (Bild, Yao et al. 2006) to model gene modules. These could be used to identify aberrant oncogenic pathway activity in aNHL gene expression profiles (Bentink, Wessendorf et al. 2008). Single gene modules, representing the activity of a defined proto-oncogene, were combined to patterns of oncogene activity called PAPs (Pathway Activation Patterns). BL is characterised by a specific PAP (mBL-PAP). DLBCL can be characterised by four prominent combinations of gene module activities (PAP1-PAP4). One PAP has been defined that comprises aNHLs which cannot be allocated to one of the major PAPs (mindL (molecular individual lymphoma) PAP). The mindL PAP can be used to describe most of the lymphoma which are characterised as “intermediate” by the mBL index. So far the pathway activities are not defined that underline these lymphoma.

1.2.4 Treatment strategy in DLBCL

DLBCL tumours are treated with high dose CHOP therapy. This therapy includes Cyclophosphamid, Hydroxydaunorubicin (Doxorubicin), Vincristin (Oncovin®) and Prednisolon. On top Rituximab, a monoclonal antibody against the B cell specific marker CD20, has further improved the therapy success (R-CHOP) (reviewed in

(Coiffier 2005; Kahl 2008). Nevertheless still 40% of DLBCL patients do not achieve a complete response to this therapy.

1.3 B cell Development and the Germinal Centre Reaction

BL and DLBCL arise from germinal centre B cells (GC B cells) reviewed in (Küppers 2005). B lymphocytes, as part of the adaptive immune response, function as effectors of immune defence. To achieve optimal antigen recognition B cells undergo a strictly regulated maturation process. Maturing B lymphocytes are probably the cells showing the highest dependency on their surrounding microenvironment. The proliferation and survival of activated B cells in secondary lymphatic organs is greatly reliant on paracrine signalling by T cells and follicular dendritic cells. Depending on the antigen affinity of activated B cells, T cells and dendritic cells decide about the fate of the B cell. Positive selection of the right B cell clone promotes proliferation and survival, whereas negative selection leads to the death of the cell (reviewed in (Klein and Dalla-Favera 2008)). Since these signalling pathways are critical for survival and proliferation of B cells it is not surprising that their deregulation can lead to the transformation of B lymphocyte during the GC-reaction.

During early B cell development in the bone marrow the B cell precursor rearranges *IG*-heavy and *IG*-light chain genes. This leads first to the expression of the surrogate B cell receptor and finally to the equipment of the B cell with a functional B cell receptor (BCR). Mature naïve B cells leave the bone marrow and can then be activated by antigen binding to the BCR. Upon BCR activation various signalling pathways are activated including Calcium signalling, PI3K/AKT, NF- κ B and MAPK signals (**described in detail in Chapter 1.4**). Subsequently, activated B cells migrate to secondary lymphatic organs, where they undergo clonal expansion and further differentiation to memory or plasma cells (**Figure 1-1**) (Osmond 1990).

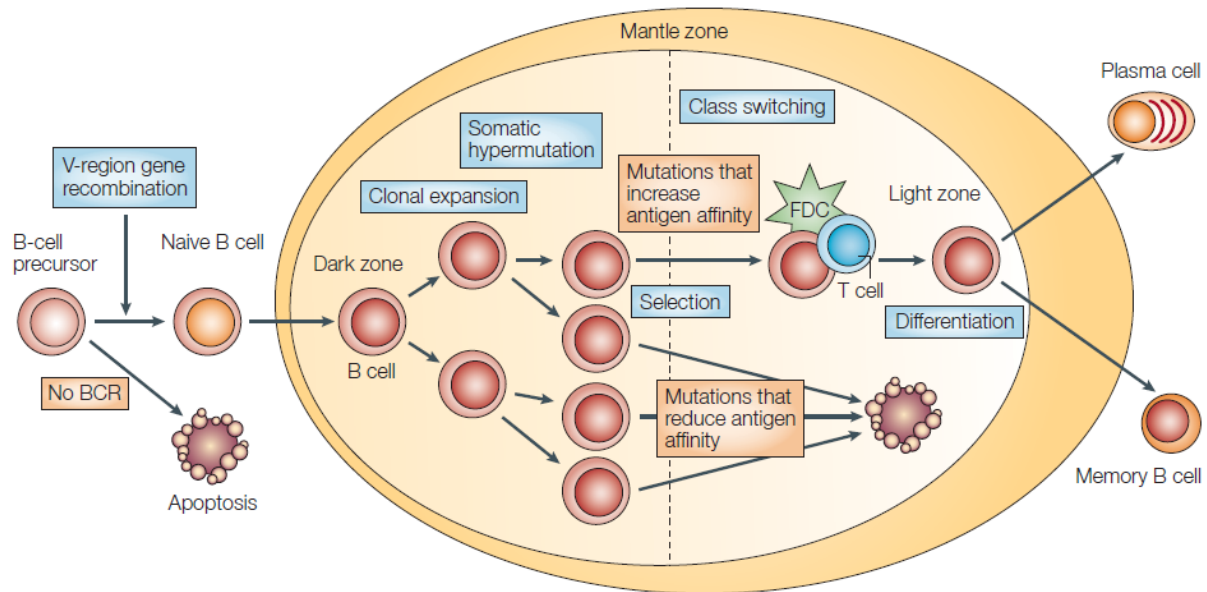


Figure 1-1 Simplified scheme of the Germinal Centre Reaction. The naïve antigen primed B cell enters secondary lymphatic organs and form a Germinal Centre (GC). GC B cells proliferate in the dark zone. After undergoing somatic hypermutation the cells enter the light zone and affinity maturation of the BCR occurs. Therefore B cells are in close contact with T helper cells and Follicular Dendritic Cells (FDCs), which mediate the needed survival signals via paracrine stimulation of maturing B cells. Subsequent to positive selection and class switch recombination the differentiated B cells leave the GC as memory or plasma cells. Figure taken from (Küppers 2005).

During the physiological GC reaction B lymphocytes are selected for an optimal antigen recognition property. First antigen primed B cells enter secondary lymphatic organs and form germinal centres. Germinal centre B cells express the characteristic surface marker CD10 (Klein, Tu et al. 2003). Within the germinal centre distinct regions can be described: a dark zone, a light zone and the surrounding marginal zone. Within the dark zone B cells (centroblasts) proliferate and undergo somatic hypermutation (SHM). SHM is a process leading to mutations in the variable regions of immunoglobulin genes. These modifications are required for the affinity maturation of the BCR. During the process of the GC reaction B cells stay in close contact with T cells and antigen presenting follicular dendritic cells (FDC). These bystander cells supply the maturing B cells with important survival signals including for example CD40L and IL21 expressed by CD4⁺ T cells (see chapter 1.4. for further description). Cells accumulating mutations that increase antigen affinity receive survival signals, provided by T

cells and FDCs (Figure 1-1). If a cell encounters mutations that lead to a lower antigen affinity or defective immunoglobulins it usually undergoes apoptosis. During SHM DNA strand breaks in the immunoglobulin loci are induced. This process involves the AID (activation induced deaminase) (Muramatsu, Kinoshita et al. 2000). SHM induced DNA strand breaks are necessary for genetic changes including deletions or insertions, which display up to 6% of the genetic alterations in SHM. After selection for antigen affinity germinal centre B lymphocytes, then called centrocytes, can switch the class of immunoglobulins they produce. This switch depends on the antigen and respective specific additional signals. During this process of class-switch-recombination (CSR) DNA double strand breaks are employed to achieve a new combination of the variable hypermutated VDJ gene elements with genes encoding for a different heavy chain (Rajewsky 1996). Centrocytes further differentiate to plasma- and memory B cells and leave the germinal centre.

1.4 B cells are dependent on microenvironmental survival signals

One can discriminate B cell intrinsic signalling, that is not dependent on surrounding micro-environmental cells on the one hand and paracrine signalling that is mediated by the microenvironment of the B cell. Central players of intrinsic B cell survival signalling include of course the engagement of the B cell receptor with its specific antigen and furthermore the recognition of non-self molecules by receptors of the innate immune response, the Toll like receptors (TLRs). Important paracrine signals include the T cell mediated co stimulatory activation of CD40. Furthermore IL21 and BAFF function in the sustained survival of activated B cells within the GC (Küppers 2005; D'Orlando, Gri et al. 2007; Khan 2009; Konforte, Simard et al. 2009). In the following paragraphs a brief overview will be given about pathways activated by these factors and the distinct mechanisms employed for the respective pathway activations. As NF- κ B and MAPK signals are central to most of the considered stimuli, they will be explained in more detail.

1.4.1 Nuclear factor of kappa B light polypeptide gene enhancer in B-cells signalling

NF- κ B signalling includes two main processes: canonical and noncanonical pathway (reviewed in (O'Dea and Hoffmann)). Canonical and noncanonical NF- κ B differ in the mode of activation and the utilised NF- κ Bs. The transcription factors of the NF- κ B family include RelA (p65), Rel (c-Rel), and RelB, p50 (the processed form of NFKB1), p50 (the processed active form of p105) or p52 (the processed form of p100). The distinct NF- κ Bs form homo or heterodimers to bind to DNA and act as transcription factors. In the inactive state of the pathway NF- κ Bs are sequestered in the cytoplasm. Upon activation of IKK (I κ B kinase), for example via the CBM complex, I κ B proteins (Inhibitor of NF- κ B) I κ B α , I κ B β and I κ B γ (NEMO) become phosphorylated and are as a consequence proteasomally degraded. This leads to the release of NF- κ B dimers and their translocation into the nucleus (Baldwin 1996; Karin and Ben-Neriah 2000). Noncanonical NF- κ B signalling is activated upon the proteasomal cleavage of the inactive proform of NFKB2, p100, to the active form p52. This cleavage is induced upon phosphorylation of p100 by NIK (NF- κ B inducing kinase).

1.4.2 Mitogen Activated Protein Kinases (MAPKs)

MAPKs comprise ERK/MAPK1, p38 α (MAPK14) and JNK (Jun terminal kinase / MAPK8). In the following paragraph the activation of p38 α (further referred to as p38) will be illustrated as one example for the activation of a MAPK. The primary step in the MAPK cascade is the phosphorylation of MAP3Ks, which can be mediated for example by TNF receptor associated factors like (TRAF2, TRAF3 or TRAF6). Upon activation of MAP3Ks, which include TAK1 or Tpl2, these trigger the phosphorylation and subsequent activation of MAP2Ks. In the case of p38 activation these are MKK4, MKK3 and MKK6. MKK4, MKK3 and MKK6 can be phosphorylated and thereby activate p38. The activation of p38 leads to the phosphorylation and activation of downstream effectors like MAPKKAPK2/5 and subsequently ATFs or CREB, which regulated the transcription of respective target genes. Furthermore, a number of specific serine/threonine phosphatases, tyrosine specific phosphatases and dual specificity phosphatases (DUSPs) have

been identified as negative regulators of the MAPK cascade (Keyse 2000; Saxena and Mustelin 2000; Keyse 2008).

1.4.3 BCR activation triggers a variety of signalling pathways including Calcium signalling, NF- κ B, PI3K/AKT and MAPK activation

Upon antigen recognition BCRs cluster in lipid rafts on the cell surface (Yang and Reth 2010). The BCR itself lacks intracellular signalling domains. Therefore the Igs are linked to CD79A (immunoglobulin-associated alpha) and CD79B (immunoglobulin-associated beta), which mediate the activation of downstream signalling (Reth 1989; Sanchez, Misulovin et al. 1993; Cambier 1995). BCR activation leads to the activation of a variety of signalling pathways including calcium signalling, PI3K/AKT, NF- κ B and MAPK signals reviewed in (Wang and Clark 2003).

BCR activation triggers Src kinases that subsequently lead to the activation of downstream kinases like BTK (Bruton's Tyrosine kinase) and PLC γ 2 (Phospholipase C γ 2). PLC γ 2 activity leads to the hydrolysis of PIP $_2$ (phosphatidyl inositol-4,5-bisphosphate) to IP $_3$ (inositol-1,4,5-trisphosphate) and DAG (diacylglycerol). The rise of intracellular IP $_3$ levels leads to the release of Ca $^{2+}$ from the endoplasmic reticulum and thereby to the activation of Calcineurin and the transcription factor NFAT (nuclear factor of activated T cells). Furthermore PI3K (phosphoinositol 3-kinase) pathway is turned on upon antigen recognition and triggers the phosphorylation and activation of AKT1. Additionally BCR activation triggers MAPK signals (JNK/ERK/p38). These comprise the activation of Ras-Raf-MEK and finally ERK as well as p38 (MAPK14) and JNK. The activation of NF- κ B via BCR is triggered via the formation of the so called CBM (CARMA1-BCL-10-MALT1) complex, which subsequently leads to the activation of NF- κ B (Ruland, Duncan et al. 2001; Wang, You et al. 2002; Egawa, Albrecht et al. 2003; Ruland, Duncan et al. 2003; Bidere, Ngo et al. 2009).

1.4.4 Toll like receptor mediated activation of NF- κ B and MAPK signals

The recognition of bacterial lipopolysaccharides (LPS) via Toll like receptor 4 (TLR-4) is part of the innate immune response (Medzhitov, Preston-Hurlburt et al. 1997; Poltorak, He et al. 1998). TLR-4 belongs to the family of pattern recognition

receptors (PRRs). TLR-4 specifically recognizes Lipopolysaccharide (LPS), which is a component of the cell wall of Gram-negative bacteria (Poltorak, He et al. 1998; Hoshino, Takeuchi et al. 1999). The activation of TLR-4 leads to the recruitment of the adaptor protein MyD88 (Kawai, Adachi et al. 1999). This activation has been shown to trigger the activation of NF- κ B and MAPK signalling (p38 and JNK) via TRAF6 and TAK1 (reviewed in (Palsson-McDermott and O'Neill 2004; Doyle and O'Neill 2006)). It has been shown for some lymphomas that the constant activation of transformed B cells by a persisting microbial antigen is essential for lymphoma growth. This chronic activation can lead for example to the development of MALT lymphomas as a consequence of chronic *Helicobacter pylori* infection (Zucca, Berton et al. 1998; Farinha and Gascoyne 2005).

1.4.5 CD40 mediates NF- κ B and MAPK signals

CD40/TNFRSF5 belongs to the family of TNF receptors. The similarity of the large family of TNF receptors is mainly expressed by their trimetric clustering upon ligand binding (Locksley, Killeen et al. 2001). CD40 is activated via its specific ligand CD40L/CD154 that is expressed either on the surface of or as soluble form by CD4⁺ T helper cells (Armitage, Fanslow et al. 1992; Graf, Korthauer et al. 1992; Hollenbaugh, Grosmaire et al. 1992; Lederman, Yellin et al. 1992). The stimulation of B cells by T helper cells via CD40L is regarded as the “classical” co-stimulatory signal or “help” mediating positive selection of the right B cell clone during immune response (Foy, Shepherd et al. 1993; Van den Eertwegh, Noelle et al. 1993; Foy, Laman et al. 1994). Upon binding of CD40L the receptor trimerizes and a so called “cytokine receptor-assembled signalling complex” (Matsuzawa, Tseng et al. 2008) is formed. It has been proposed that this complex constitutes of TRAF2 (TNF receptor-associated factor 2) and TRAF3 (TNF receptor-associated factor 3), UBE2N (bendless-like ubiquitin conjugating enzyme), c-IAP1 and c-IAP2 (cellular inhibitor of apoptosis proteins 1 and 2), IKK γ (NEMO) and MEKK1 (mitogen-activated protein kinase (MAPK) kinase kinase). MEKK1 is needed for the activation of MAPK signalling via JNK and p38 and IKK activated canonical and noncanonical NF- κ B signalling. In addition to the interaction of TRAF2 and TRAF3 with CD40 (Hu, O'Rourke et al.

1994; Cheng, Cleary et al. 1995; Rothe, Sarma et al. 1995; Sato, Irie et al. 1995), it has also been shown that additional members of the TRAF family bind to the intracellular part of CD40. These include TRAF5 and TRAF6 (Ishida, Mizushima et al. 1996; Ishida, Tojo et al. 1996). TRAF6 leads to the activation of JNK and p38 probably through TAK1 (Matsuzawa, Tseng et al. 2008).

The functionality of CD40 signals for lymphoma cells have extensively been studied *in vitro*. It has been shown by several groups that CD40 activation can have positive effects on cell survival and cell proliferation. This includes for example the rescue of BL and DLBCL cells from apoptosis or BCR induced growth arrest as well as the induction of proliferation of lymphoma cells by CD40 ligation (Santos-Argumedo, Gordon et al. 1994; An and Knox 1996; Wang, Grand et al. 1996; Mackus, Lens et al. 2002; Hristov, Knox et al. 2005; Pham, Tamayo et al. 2005).

1.4.6 B cell activating factor of the TNF superfamily (BAFF/ TNFSF13B) can activate distinct TNF receptors that trigger noncanonical NF- κ B and MAPK signalling

The homeostasis of mature B cells is essentially dependent on B cell Activating Factor of the TNF family (BAFF), also named BLyS/ TALL-1/ TNFSF13B (Moore, Belvedere et al. 1999; Shu, Hu et al. 1999; Schiemann, Gommerman et al. 2001; Mackay, Sierro et al. 2005). An overexpression of BAFF has been shown to induce severe B cell hyperplasia and autoimmune diseases (reviewed in (Mackay, Sierro et al. 2005; Mackay and Leung 2006)). BAFF is expressed by T cells and macrophages either in a membrane bound form or as soluble factor, which is proteolytically cleaved from the cell surface (reviewed in (Bossen and Schneider 2006)). Like other members of the TNF family BAFF occurs as homotrimer. It has been shown that 20 of these trimers can oligomerize to a capsule like structure composed of 60 BAFF proteins (Liu, Hong et al. 2003). BAFF can activate three distinct types of receptors of the TNF receptor superfamily. These include the BAFF-R (BAFF-Receptor/BR3/TNFRSF13C), TACI (transmembrane activator and CAML interactor/TNFRSF13B) and BCMA (B Cell Maturation Antigen/TNFRSF17). Dependent on the quaternary structure of BAFF the ligand shows differing affinities to these receptors (reviewed in (Dillon, Gross et al.

2006)). Trimeric BAFF predominantly binds to and activates BR3. The stimulation of BR3 leads primarily to the activation of the noncanonical NF- κ B pathway via a degradation of TRAF3 by TRAF2, which in turn mediates the accumulation of NIK (MAPK14). NIK induces the activation of NF- κ B2 by phosphorylation induced proteasomal cleavage of p100 to the active form p52 (Claudio, Brown et al. 2002; Bossen and Schneider 2006; Gardam, Sierro et al. 2008; Vallabhapurapu, Matsuzawa et al. 2008). The BAFF 60mer has a higher affinity to TACI and BCMA. The activation of TACI leads to the recruitment of TRAF2 and TRAF6 and the activation of canonical NF- κ B signalling, whereas BCMA activation has been shown to trigger NF- κ B and MAPK signalling (Gross, Johnston et al. 2000; Hatzoglou, Roussel et al. 2000).

Expression of BAFF and BAFF receptors has been detected in lymphoma sections (Rodig, Shahsafaei et al. 2005) and seems to be associated with a bad prognosis for aNHL (DLBCL) patients (Novak, Grote et al. 2004). This is in line with the observation that aNHL patients can show elevated serum levels of BAFF protein (Briones, Timmerman et al. 2002). Autocrine BAFF signalling was shown for CLL, multiple myeloma, DLBCL, MCL and BL cells (He, Chadburn et al. 2004; Novak, Darce et al. 2004; Novak, Grote et al. 2004). Currently an monoclonal antibody directed against human BAFF (belimumab; Lymphostat-B) (Baker, Edwards et al. 2003) is tested in 2nd Phase clinical trials regarding its performance in the therapy of a autoimmune disease (rheumatoid arthritis and SLE) (Ding and Jones 2006). It is discussed that BAFF activity interacts with tonic BCR signalling in a way that the BCR signal leads to the increased expression of NF κ B2/p100 which is needed for BR3 signalling (Stadanlick, Kaileh et al. 2008).

1.4.7 IL21 signals via IL21R mediated STAT1 and STAT3 activity

IL-21 has been identified as potent B cell activator and plasma cell differentiation-inducer (reviewed in (Ettinger, Sims et al. 2005; Davis, Skak et al. 2007; Ettinger, Kuchen et al. 2008). The cytokine IL21 is produced by activated CD4⁺ T cells and NK cells (Parrish-Novak, Dillon et al. 2000; Harada, Magara-Koyanagi et al. 2006; Coquet, Kyparissoudis et al. 2007). IL21 signals through a heterodimeric receptor comprised of the IL-21 receptor (IL-21R) and the common gamma chain of the IL-2 receptor family (Spolski and Leonard 2008). After binding of IL-21 to

the receptor, JAK1 (Janus-activated kinase 1) and JAK3 (Janus-activated kinase 3) are autophosphorylated. As a results from that STAT1 and STAT3 (signal transducer and activator of transcription 1/3) become phosphorylated and thereby activated. This leads to their subsequent translocation to the nucleus and the change of STAT target gene expression (Asao, Okuyama et al. 2001; Zeng, Spolski et al. 2007). In addition to the activation of STATs by IL21R, the receptor can also trigger the activation of MAPK and PI3K/AKT signalling (Zeng, Spolski et al. 2007; Fuqua, Akomeah et al. 2008).

Regarding the effects of IL21 stimulation on BL or DLBCL so far no data exist. It has been shown for follicular lymphoma (FL) that these cells exhibit a high IL-21 receptor expression and that the activation of lymphoma cells via IL21 induces apoptosis (Akamatsu, Yamada et al. 2007).

Aim of the Study

The recent molecular classification of aggressive Non-Hodgkin Lymphoma (NHL) based on global gene expression analyses of individual lymphomas is a major step forward to understand the clinical heterogeneity of aggressive NHL. These transcriptome based analyses aimed to identify oncogenic events in order to describe new biomarkers or elucidate potential targets for individualized therapies of aNHL. An improved understanding of the heterogeneity of pathway deregulation in aggressive NHL is essential to obtain a better prediction of the clinical outcome and treatment responses of aNHL patients.

The heterogeneity of aggressive NHL is fundamentally characterised by differences in proliferative potential and chromosomal complexity of Diffuse Large B Cell Lymphoma and Burkitt Lymphoma (BL). *MYC* is the classical oncogene described for BL. However, it was found that *MYC* is also genetically altered in some non-mBL on a background of additional chromosomal aberrations.

So far the analyses of NHL gene expression profiles contributed to a molecular classification defining two major subgroups: “molecular Burkitt lymphoma (mBL)” and “non-molecular Burkitt lymphoma (non-mBL)”. Apart from candidate gene approach driven investigations the characterisation of primary aggressive NHL using global gene expression analyses is so far largely descriptive. A discrimination of Diffuse Large B C Lymphoma into “Activated B Cell (ABC)-like” and “Germinal Centre B cell (GCB)-like” subtypes was achieved. The so far described molecular classifications differ in the degree of heterogeneity within the defined NHL subgroups. The subgroup of ABC Diffuse Large B Cell Lymphoma for example comprises largely heterogeneous lymphoma cases. Based on *in vitro* experiments it was concluded that ABC lymphoma are mainly characterised by activated NF- κ B and JAK-STAT signals. Regardless these advancements numerous open questions still need to be answered.

- Is there deregulated c-Myc activity in non-mBL lymphoma? Is there any c-Myc activity detectable in non-mBL independent of the genetic *MYC* aberrations? Is this potential c-Myc activity of prognostic relevance for non-mBL patients?

- Is it possible to identify novel pathway activities in malignant lymphoma by transferring gene expression data from *in vitro* perturbations of BL cells to lymphoma gene expression profiles? Can quantitative differences of pathway activities, reflected in gene expression profiles of lymphoma, be detected?
- Which deregulated pathways, apart from NF- κ B and JAK-STAT, underlie the heterogeneity of aggressive NHL? Is it possible to draw conclusions on cell cycle deregulation or chromosomal complexity of aggressive aNHL based on the identified pathway activities.

In order to answer these questions, this study aims to identify and characterise new gene expression patterns that hold information about relevant oncogenic pathway activities. The identification of these patterns was aspired using perturbation experiments in primary lymphoma precursor cells and lymphoma cell lines. In order to improve the knowledge about the deregulated processes in aggressive NHL this study focuses on two distinct approaches: (i) the effect of ectopic expression of the proto-oncogene *MYC* in lymphoma precursor cells and (ii) perturbations of B cell lines by B cell specific paracrine stimuli.

2 Materials and Methods

2.1 Biological Material

Primary material

Primary material of human tonsils from paediatric patients was obtained with informed consent and ethical approval (Ref No.06/Q2702/50) from tonsillectomies performed in the Children's Hospital Birmingham, UK (surgeon: Michael Kuo).

Cell lines

The cell lines that were used in this work are listed in table 2-1.

Table 2-1 Cell lines

Cell line	Source	Distributor	Reference
BL2	B cell, Burkitt Lymphoma (EBV negative)	DSMZ	(Nilsson and Ponten 1975; Kube, Platzer et al. 1995)
BL16	B cell, Burkitt Lymphoma (EBV positive)	Coriell Institute for Medical Research	(Bernheim, Berger et al. 1983)
BL41	B cell, Burkitt Lymphoma (EBV negative)	DSMZ	(Lenoir, Vuillaume et al. 1985)
BL70	B cell, Burkitt Lymphoma (EBV negative)	DSMZ	(Lenoir, Vuillaume et al. 1985)
DG75	B cell, Burkitt Lymphoma (EBV negative)	DSMZ	(Ben-Bassat, Goldblum et al. 1977)
HT	B cell, Diffuse Large B cell lymphoma (GCB)	DSMZ	(Beckwith, Longo et al. 1990)
MC116	B cell, lymphoma undifferentiated	DSMZ	(Magrath, Freeman et al. 1980)
Ramos	B cell, Burkitt Lymphoma	DSMZ	(Klein, Giovanella et al. 1975)
SuDHL4	B cell, Diffuse Large B cell lymphoma (GCB)	DSMZ	(Epstein, Herman et al. 1976)
SuDHL5	B cell, Diffuse Large B cell lymphoma (GCB)	DSMZ	(Epstein, Levy et al. 1978)

SuDHL6	B cell, Diffuse Mixed Small and Large B cell lymphoma (GCB)	DSMZ	(Epstein, Herman et al. 1976)
OCI-Ly1	B cell, Diffuse Large B cell lymphoma (GCB)	University Health Network (Toronto, Canada)	(Epstein, Levy et al. 1978)
OCI-Ly3	B cell, Diffuse Large B cell lymphoma (ABC)	University Health Network (Toronto, Canada)	(Tweeddale, Jamal et al. 1989)
OCI-Ly7	B cell, Diffuse Large B cell lymphoma (GCB)	University Health Network (Toronto, Canada)	(Chang, Blondal et al. 1995)

Bacteria

Escherichia coli (E. coli) TOP10 (Invitrogen, Darmstadt GER) were used for the transformation and amplification of plasmid DNA.

2.2 Consumable supplies

Table 2-2 Consumables

Consumable	Manufacturer
ABI PRISM® 384-Well Clear Optical Reaction Plate	Applied Biosystems, Foster City USA
ABI PRISM® Optical Adhesive Covers	Applied Biosystems, Foster City USA
Cell culture flasks	Sarstedt, Nümbrecht GER
Cryo Box	Nunc, Wiesbaden GER
Cryotubes	Nunc, Wiesbaden GER
Diethylaminoethyl-Cellulose	Whatman®, International Ltd UK
Electroporation Cuvettes	Eurogentec, Cologne GER
FACS tubes	Becton Dickinson Labware, Franklin Lakes, NJ, USA

Materials and Methods

Falcon Tubes 15 ml	Sarstedt, Nümbrecht GER
Falcon Tubes 50 ml	Sarstedt, Nümbrecht GER
Filter Tips, 10 µl, 100 µl, 1000 µl	Starlab, Ahrensburg GER
Micro Touch Examination Gloves	Ansell, München Germany
MACS™ MS columns	Miltenyi-Biotech, Surrey UK
MACS™ pre separation filters	Miltenyi-Biotech, Surrey UK
Nucleofection cuvettes	Amara-biosystems, Cologne GER
Pasteurpipettes	Sarstedt, Nümbrecht GER
Pipette Tips (wo filters)	Sarstedt, Nümbrecht GER
Reactiontubes 1.5ml	Sarstedt, Nümbrecht GER
Reactiontubes 2.0ml	Sarstedt, Nümbrecht GER
Serological pipettes 5 ml	Sarstedt, Nümbrecht GER
Serological pipettes 10 ml	Sarstedt, Nümbrecht GER
Serological pipettes 25 ml	Sarstedt, Nümbrecht GER
Tissue culture dish	Sarstedt, Nümbrecht GER
Tissue culture plates, 6 well	Nunc, Wiesbaden GER
Tissue culture plates, 24 well	Nunc, Wiesbaden GER

2.3 Equipment

Table 2-3 Equipment

Instrument	Manufacturer
3130 Genetic Analyzer	Applied Biosystems, Foster City USA
96-Well Plate Septa	Applied Biosystems, Foster City USA
ABI PRISM 7900HT	Applied Biosystems, Foster City USA
Accu-jet	Brand, Hamburg GER
Amara Nucleofector™ II	Amara-biosystems, Cologne GER

Instrument	Manufacturer
Biofuge Pico	Heraeus Instruments, Hanau GER
Biofuge Primo R	Heraeus Instruments, Hanau GER
Biorupter	Diagnode, Liège, Belgium
Consort E734 Power Supply	Schütt Labortechnik, Göttingen GER
CAT RM 5 horizontal roller	CAT M Zipperer, Staufen GER
Centrifuge 5451D	Eppendorf, Hamburg GER
FACSScan flow cytometer	Becton Dickinson, Heidelberg GER
Hera freeze -80°C freezer	Heraeus Instruments, Hanau GER
IKA KS 260 shaker	IKA, Staufen GER
IKAMAG RCT magnetic stirrer	IKA, Staufen GER
Incubator Galaxy R	RS Biotech, Irvine Scotland, UK
Incubator Cytoperm	Heraeus Instruments, Hanau GER
Incudrive incubator	Schütt Labortechnik, Göttingen GER
LAS-4000 Image Reader	Fujifilm, Düsseldorf GER
Leitz DM IL inverse fluorescence microscope	Leica, Wetzlar GER
MACS™ Separator	Miltenyi-Biotech, Surrey UK
Microflow Laminar Downflow Workstation	Bioquell, England
Microcoolcentrifuge 1-15k	Sigma, Munich GER
Multifuge 3 L-R	Heraeus Instruments, Hanau GER
MoFlow® High-Performance Cell Sorter	Dako, Stockport UK
NanoDrop™	ND-1000 UV/Vis-Spektralphotometer, Wilmington USA
Neubauer Counting Chamber Improved	Lo Labor Optik, Friedrichsdorf GER
Power Pac 300 Power Supply	Bio-Rad, München GER
Reax2 shaker	Heidolph, Schwabach GER
Sunrise™ Microplate Reader	Tecan, Crailsheim GER
Televal 31 inverse light optical microscope	Zeiss, Jena GER

Materials and Methods

Instrument	Manufacturer
Thermocycler Mastercycler	Eppendorf, Hamburg GER
Thermocycler 60	Biomed, Theres GER
Thermocycler T3000	Biometra, Goettingen GER
Thermomixer Compact	Eppendorf, Hambrug GER
Vortex Genie 2	Schütt Labortechnik, Göttingen GER
Vienna Superautomatca	Saeco, Eigeltingen GER
Water bath	Köttermann Labortechnik, Hänigsen GER

2.4 Chemicals

Table 2-4 Chemicals

Chemical	Manufacturer
Agarose	Sigma-Aldrich, Munich GER
Acrylamid/Bisacrylamid 40%	BioRad, Munich GER
Ammonium persulphate	Sigma-Aldrich, Munich GER
Bradford solution	RothiQuant-Roth, Karlsruhe GER
Bromphenol Blue	Sigma-Aldrich, Munich GER
BSA	Serva, Heidelberg GER
DMSO	Sigma-Aldrich, Munich GER
Ethanol (100%)	J.T. Baker, Deventer NL
Ethidiumbromid	Sigma-Aldrich, Munich GER
EDTA	Riedel-de Haën, Seelze GER
FACS Flow	Becton Dickinson, Heidelberg GER
Full Range Rainbow Molecular Weight	GE Healthcare, Munich GER
Formaldehyde	Sigma-Aldrich, Munich GER
Glycerol	Roth, Karlsruhe GER
Glycin	Roth, Karlsruhe GER

Chemical	Manufacturer
HEPES	Sigma-Aldrich, Munich GER
Hydrogen Peroxide	Sigma-Aldrich, Munich GER
Indo-1-AM	Invitrogen/Molecular Probes, Karlsruhe GER
Isopropanol	Sigma-Aldrich, Munich GER
Methanol 100% (p.a.)	J.T. Baker, Deventer NL
Milk powder	Roth, Karlsruhe GER
Nonidet P-40	Sigma-Aldrich, Munich GER
Phosphatase inhibitor Phospho- STOP	Roche, Mannheim GER
Pluronic acid F-127	Sigma-Aldrich, Munich GER
PMSF	Sigma-Aldrich, Munich GER
Protein A Sepharose	GE Healthcare, Munich GER
Propidium iodide	Sigma-Aldrich, Munich GER
Proteaseinhibitor-Mix Complete™	Santa Cruz biotechnology, Heidelberg GER
SDS	Merck, Darmstadt, GER
Sodiumchloride	Merck, Darmstadt, GER
Sodiumdeoxycholat	Merck, Darmstadt, GER
Sodiumvanadat	Sigma-Aldrich, Munich GER
Spectra Multicolor Broad Range	Fermentas, Frankfurt GER
TEMED	Sigma-Aldrich, Munich GER
Trisbase	Sigma-Aldrich, Munich GER
Trypanblue 0.4% in PBS	GIBCO BRL, Life Technologies, Eggenstein GER
Tween-20	Merck, Darmstadt GER
Thymidine (cell culture grade)	Sigma-Aldrich, Munich GER
Water HPLC grade	Merck, Darmstadt GER

2.5 Chemical Inhibitors

The following chemical inhibitors were used for the inhibition of specific pathway components.

Table 2-5 Chemical Inhibitors

Description	Manufacturer	Final concentration
10058F4 (c-Myc)	Sigma-Aldrich, Munich GER	60µM
5Z-7-oxozeaenol (TAK1)	Calbiochem/Merck, Darmstadt, GER	100nM
IKK2 inhibitor VIII	Calbiochem/Merck, Darmstadt, GER	7µM
Ly294002 (PI3K)	Calbiochem/Merck, Darmstadt, GER	10µM
SB203580 (p38/MAPK14)	Sigma-Aldrich, Munich GER	2µM
SP600125 (JNK)	Calbiochem/Merck, Darmstadt, GER	10µM
U0126 (ERK1/2)	Sigma-Aldrich, Munich GER	10µM
VIVIT (NFAT)	Sigma-Aldrich, Munich GER	2.5µM

2.6 Buffers, Solutions and Media

Commonly used buffers solutions and media are summarized below.

Table 2-6 Buffers, Solutions and Media

Liquid	Receipt / Manufacturer
2x SDS loading dye	4% SDS 0.12 M Tris-HCl (pH 6.8) 200mM DTT Pipette Tip of 1% BromphenolBlue
4x loading buffer Roti®-Load	Roth, Karlsruhe GER
AnxV binding buffer	10 mM HEPES/NaOH pH 7.4, 140 mM NaCl, 5 mM CaCl
autoMACS™ buffer	Miltenyi-Biotech, Surrey UK

autoMACS™ buffer plus	autoMACS™ buffer supplemented with: 100 U/ml penicillin + 100 µg/ml streptomycin, Sigma-Aldrich, Dorset UK 10 µg/ml ciprofloxacin, Bayer Cambridge UK 0.25% (v/v) BSA Miltenyi-Biotech, Surrey UK
Cell culture medium I (cell lines - BL)	RPMI-1640 (PAA, Pasching AUS) 10% (v/v) FBS (Sigma-Aldrich, Munich GER) 200U/ml Penicilin + 200µg/ml Streptomycin + 4mM L-Glutamine (Sigma-Aldrich, Munich GER) 50 µM α-Thioglycerol (), 20 nM BCS, 1 mM Sodium pyruvat
Cell culture medium II (cell lines - DLBCL)	RPMI-1640 (PAA, Pasching AUS) 10% (v/v) FBS (Sigma-Aldrich, Munich GER) 200U/ml Penicilin + 200µg/ml Streptomycin + 4mM L-Glutamine (Sigma-Aldrich, Munich GER)
Cell culture medium III	IMDM (PAA) 10% (v/v) FBS (Sigma-Aldrich, Munich GER) 200U/ml Penicilin + 200µg/ml Streptomycin + 4mM L-Glutamine (Sigma-Aldrich, Munich GER) OCI-Ly3 cells were cultivated with 20% FBS
Cell culture medium IV (primary cell isolation)	RPMI 1640 (GIBCO, Paisley UK) 100 U/ml penicillin 100 µg/ml streptomycin (Sigma-Aldrich, Dorset UK) 10 µg/ml ciprofloxacin (Bayer, Newbury UK)
Cell culture medium V (primary cell cultivation)	Cell culture medium IV + 10% (v/v) FBS (Sigma-Aldrich, Dorset UK)
ChIP Puffer	30 ml 5 M NaCl 10 ml 500 mM EDTA (pH 8) 50 ml 1 M Tris (pH 8) 50 ml 10% NP-40 100 ml 10% Triton-X-100 Add 1000ml bidest H ₂ O plus Roche Protease inhibitor cocktail

Materials and Methods

ECL Western Blotting Detection Kit	GE Healthcare, Munich GER
EDTA cell culture grade	0.5 M, Sigma-Aldrich, Munich GER
FACS buffer	1x PBS 0.5% (w/v) BSA
FACS flow	Becton Dickinson (Heidelberg GER)
Freezing medium	90% (v/v) FBS (Biochrom, Berlin GER) 10% (v/v) DMSO (Sigma-Aldrich, Munich GER)
Krebs-Ringer solution (+ Calcium)	10 mM HEPES, pH 7.0, 140 mM NaCl, 4 mM KCl , 1 mM MgCl, 10 mM glucose, 1 mM CaCl ₂
LB-agar	1.5% (w/v) Agar in LB-medium
LB-Medium	0.5% (w/v) Sodium Chloride 0.5% (w/v) Yeast Extract 1% (w/v) Bacto-Trypton
Laemmli buffer (2x)	187.5 mM Tris/HCl pH 6.8 6.0% (w/v) SDS 30.0% (v/v) Glycerin 0.01% (w/v) Bromphenolblue 10% (v/v) β-Mercaptoethanol
Lymphoprep™ ficoll solution	Axis-Shield, Liverpool UK
Nicoletti buffer	0.1% (w/v) Sodium Citrate 0.1% (v/v) TritonX-100 50µg/ml propidium iodide
PCR buffer (10x) for qRT	750 mM Tris-HCl pH 8.8 200 mM Ammonium sulfate (Merck, Darmstadt GER) 0.1% Tween-20 in depc water (DEPC by Roth, Karsruhe GER)
PBS (Phosphate Buffered Saline)	137 mM NaCl 10 mM Phosphate 2.7 mM KCl, pH 7.4.
PBS pH 7.4 (cell culture grade)	Lonza, Verviers BEL

Ponceau-S	5 % (v/v) glacial acetic acid 0.5 % (w/v) Ponceau-S
ReBlot plus mild	Millipore, Schwalbach/Ts. GER
RIPA buffer	1x PBS pH 7.4 1% (v/v) Igepal 0.5% (w/v) Sodium-deoxycholat mg/ml PMSF (solved in isopropanol) 1 mM Sodum-Orthovanadat Complete-Solution (40 µl stocksolutioun for 1 ml RIPA; stocksolution: 1 tablet for 1.5ml H ₂ O, Roche, Grenzach GER)
Running buffer (1x):	25mM Tris-Base 192mM Glycin 34.67 mM SDS
Separation Gel Mix	31.3 % (v/v) Acrylamid/Bis Solution (40 %) 332 mM Tris Base, pH 8,9 3.33 mM EDTA
Stacking Gel Mix	15 % (v/v) Acrylamid/Bis Solution (40 %) 125 mM Tris Base pH 6.8 0.1 % (w/v) SDS 5 mM EDTA
Solution 1 Chemiluminescence Luminol	– 100 mM Tris/HCl pH 8.8 2.5 mM Luminol (Sigma-Aldrich, Munich GER) 4 mM 4-IPBA (Sigma-Aldrich, Munich GER)
Solution 2 Chemiluminescence Peroxide	– 100 mM Tris/HCl pH 8.8 10.6 mM H ₂ O ₂
SybrGreenMix	1x PCR buffer; 3 mM MgCl ₂ (Primetech LTD, Minsk Belarus); 1:80000 SybrGreen (Roche, Grenzach Germany); 0.2 mM dNTP each (Primetech LTD, Minsk Belarus); 20 U/ml taq polymerase (Primetech LTD, Minsk Belarus), 0.25 % TritonX-100 (Roth, Karlsruhe Germany), 0.5 mM trehalose (Roth, Karlsruhe Germany) in depc water
TAE (10x)	400mM Tris 0.01M EDTA (pH 8.3)
TBS (1x)	20mM Tris-Base, 137mM Sodium Chloride (pH 7.6)

Materials and Methods

TBS-T	1x TBS 0.1% (v/v) Tween-20
Transferpuffer (1x):	25mM Tris-Base 192mM Glycin 15% (v/v) MeOH

2.7 Plasmids

Vectors used for the non-viral DNA transfer are summarized in table 2-7 below.

Table 2-7 Vectors

Name	Description	Source
pcDNA3.1	Control vector	Invitrogen, Karlsruhe GER
pcDNA3.1-myc	c-Myc expression vector	kindly provided by Georg Bornkamm (Hörtnagel, Mautner et al. 1995)
pMAX-GFP	GFP control	Amara-biosystems, Cologne GER
pMACS-ΔLNGFR	ΔLNGFR expression vector	Miltenyi-Biotech, Surrey UK

2.8 Recombinant Proteins and Biological Material

The following recombinant proteins were used for the stimulation of BL and DLBCL cell lines as well as primary B cells.

Table 2-8 Recombinant Proteins

Description	Manufacturer
goat anti human IgM F(ab) ² fragment (#109006129)	Jackson ImmunoResearch / Dianova, Hamburg GER
goat anti human IgM / anti IgG F(ab) ² fragment (#109226044)	Jackson ImmunoResearch / Dianova, Hamburg GER
Lipopolysaccharide from <i>E. coli</i> 055:B5 (#62326)	Sigma-Aldrich, Munich GER
rhBAFF (#2149-BF-10)	R&D systems, Wiesbaden-Nordenstadt GER
rhIL21 (#11340213)	ImmunoTools, Friesoythe GER
sCD40L (#ABC159)	AutogenBioclear, Calne, Wiltshire UK

2.9 Antibodies

Antibodies used for immunoblotting, cell sorting and cell characterisation and Chromatin-Immunoprecipitation are summarized below.

Table 2-9 Antibodies

Antibody	Source	Working Dilution
Flow cytometry		
Anti CD3 -PE	BD Biosciences Pharmingen, Oxford UK	1:20 in FACS buffer
Anti CD8 -FITC	BD Biosciences Pharmingen, Oxford UK	1:20 in FACS buffer
Anti CD10 -PE	eBioscience, San Diego USA	1:20 in FACS buffer
Anti CD19 -FITC	Becton Dickinson, Oxford UK	1:20 in FACS buffer
Anti CD20 -FITC	Becton Dickinson, Oxford UK	1:20 in FACS buffer
Anti CD27 -FITC	Becton Dickinson, Oxford UK	1:20 in FACS buffer
Anti CD38 -FITC	Immunotech/BC, Buckinghamshire UK	1:20 in FACS buffer
Anti CD77 -FITC	BD Biosciences Pharmingen, Oxford UK	1:20 in FACS buffer
Anti CD267 -FITC (TACI)	BD Biosciences Pharmingen, Oxford UK	1:20 in FACS buffer
Anti CD268 -PE (BR-3)	BD Biosciences Pharmingen, Oxford UK	1:20 in FACS buffer
Anti IgD -FITC	BD Biosciences Pharmingen, Oxford UK	1:20 in FACS buffer
Anti IgM -FITC	BD Biosciences Pharmingen, Oxford UK	1:20 in FACS buffer
Anti IgG -FITC	BD Biosciences Pharmingen, Oxford UK	1:20 in FACS buffer
Isotype control antibodies, mouse IgG FITC	BD Biosciences Pharmingen, Oxford UK	1:20 in FACS buffer1:20 in FACS buffer
Isotype control antibodies, mouse IgG PE	eBioscience, San Diego USA	1:20 in FACS buffer
Isotype control antibodies, mouse IgG PE	BD Biosciences Pharmingen, Oxford UK	1:20 in FACS buffer

Materials and Methods

ChIP		
anti c-Myc for ChIP (N-262)	Santacruz, Heidelberg GER	2µg/IP
anti acH3 for ChIP (06-599)	Millipore, Schwalbach GER	2µg/IP
anti IgG for ChIP (ab46540)	abcam, Cambridge UK	2µg/IP
Immunoblot		
mouse monoclonal anti α-tubulin (#05-829)	Upstate/Millipore, Schwalbach GER	1:5000 in 3% milkpowder in TBS-T
rabbit anti p-AKT (Ser473) (#9271)	Cell Signalling/ New England Biolabs, Frankfurt am Main GER	1:1000 in 3% BSA in TBS-T
rabbit anti pan AKT (#100-401-401)	Rockland via BioMol, Hamburg GER	1:1000 in 5% BSA in TBS-T
rabbit anti pan AKT (#9272)	Cell Signalling/ New England Biolabs, Frankfurt am Main GER	1:1000 in 3% BSA in TBS-T
rabbit anti p-p38 (#9211)	Cell Signalling/ New England Biolabs, Frankfurt am Main GER	1:1000 in 3% BSA in TBS-T
rabbit anti p38 (#9212)	Cell Signalling/ New England Biolabs, Frankfurt am Main GER	1:1000 in 3% BSA in TBS-T
rabbit anti p-STAT1 (Tyr701) (#9171)	Cell Signalling/ New England Biolabs, Frankfurt am Main GER	1:1000 in 3% BSA in TBS-T
rabbit anti STAT1 (#9172)	Cell Signalling/ New England Biolabs, Frankfurt am Main GER	1:1000 in 3% BSA in TBS-T
rabbit anti p-STAT3 (Ser727) (#9134)	Cell Signalling/ New England Biolabs, Frankfurt am Main GER	1:1000 in 3% BSA in TBS-T
rabbit Anti STAT3 (#9132)	Cell Signalling/ New England Biolabs, Frankfurt am Main GER	1:1000 in 3% BSA in TBS-T
rabbit anti p-STAT5 (#9351)	Cell Signalling/ New England Biolabs, Frankfurt am Main GER	1:1000 in 3% BSA in TBS-T
mouse anti STAT5 (#610191)	BD, Heidelberg GER	1:1000 in 3% BSA in TBS-T
rabbit anti p-STAT6 (Y641) (#9361)	Cell Signalling/ New England Biolabs, Frankfurt am Main GER	1:1000 in 3% BSA in TBS-T
mouse anti STAT6 (S-20) X (#611291)	BD, Heidelberg GER	1:1000 in 3% milkpowder in TBS-T
rabbit anti p100/p52 (#4882)	Cell Signalling/ New England Biolabs, Frankfurt am Main GER	1:1000 in 3% BSA in TBS-T

rabbit anti IkappaB alpha (44D4) (#4812)	Cell Signalling/ New England Biolabs, Frankfurt am Main GER	1:1000 in 3% BSA in TBS-T
Anti mouse HRP polyclonal goat (D1609)	Santa Cruz, Heidelberg GER	1:5000 in 3% milkpowder in TBS-T
Anti rabbit HRP polyclonal goat (E1710)	Santa Cruz, Heidelberg GER	1:1000 in 3% BSA in TBS-T

2.10 Oligonucleotides

The primers used for **SYBR Green qRT-PCR** are listed in table 2-10.

Table 2-10 qRT-PCR Primer

Gene	Oligonucleotide
18 S ribosomal RNA	fwd 5'-AACTTTCGATGGTAGTCGCCG-3' rev 5'-GGATGTGGTAGCCGTTTCTCAG-3'
ABL	fwd 5'-AGCCTGGCCTACAACAAGTTCTC-3' rev 5'-GACATGCCATAGGTAGCAATTTCC-3'
AURKA	fwd 5'-ATCCTGAGGAGGAAGTGGCATC-3' rev 5'-GTCTTCCAAAGCCCACTGCC-3'
beta2 microglobulin (β 2m)	fwd 5'-CTATCCAGCGTACTCCAAAGATTCA-3' rev 5'-TCTCTGCTGGATGACGTGAGTAAA-3'
BAFF	fwd 5'-AAGACCTACGCCATGGGACATC-3' rev 5'-TCTTGGTATTGCAAGTTGGAGTTCA-3'
BAFF-R	fwd 5'-GGAGTTTGGTGTGCTTGCCTT-3' rev 5'-TAGTGCCCCAGCCTTTTGAAG-3'
BCMA	fwd 5'-AATGCGATTCTCTGGACCTGTT-3' rev 5'-CCAGGAGACCTGATCCTGTGTT-3'
BIRC5	fwd 5'-CAAGGACCACCGCATCTCTACA-3' rev 5'-CTCGGCCATCCGCTCC-3'
BUB1B	fwd 5'-CTCAGCATCAAGAAGCTGAGCC-3' rev 5'-GGAGGTGCTTGCAACCGAG-3'

Materials and Methods

CD58	fwd 5' - CTTGAGTCTCTTCCATCTCCCA-3' rev 5' - AAGTCCTCGATGGCTGTTGTAA-3'
CXCL10	fwd 5' - CCATTCTGATTTGCTGCCTTATCT-3' rev 5' -GAGAGAGGTACTCCTTGAATGCCA-3'
MYC (tonsils)	fwd 5' -GCAGAGGAGCAAAAGCTCATT-3' rev 5' -TGATTGCTCAGGACATTTCTGT-3'
MYC var2 (cell lines)	fwd 5' -AAGAGGGTCAAGTTGGACAGTTGC-3' rev 5' -TTTCGGTTGTTGCTGATCTGTCT-3'
DUSP2	fwd 5' -GTACTTCCTGCGAGGAGGCTTC -3' rev 5' -AGGAGCCCTGGAGTCGGAG -3'
DUSP5	fwd 5' - CAGCCACACGGCTGACATTAG-3' rev 5' -GAGATCCCAGCCTCACAGTGG -3'
DUSP10	fwd 5' - CATTGAGGAAGCTCACCAGTGTG-3' rev 5' - CGAGTGTGCTTCATCAAGTAAGCGA-3'
DUSP22	fwd 5' -CCATCAGTATCGGCAGTGGC-3' rev 5' -AGAACTTCAGAATTCCTGGAGCG -3'
FZD7	fwd 5' - GCCACACGAACCAAGAGGAC-3' rev 5' - GGCGCATACATGGAGCATAAG-3'
ICAM1	fwd 5' -TTCACAATGACACTCAGCGGTC -3' rev 5' - AGTGCAAGCTCCCAGTGAAATG-3'
ID1	fwd 5' -CCTCAACGGCGAGATCAGC-3' rev 5' -ATGCGATCGTCCGCAGG -3'
Lef1	fwd 5' - TAATGCACGTGAAGCCTCAGC-3' rev 5' - TTAATGTGAGGTCTTTTTGGCTCC-3'
TACI	fwd 5' -CCATTTGCAACCATCAGAGCC-3' rev 5' -ATGGAGGCACAGCTGATGCAGT-3'

TMEM97	fwd 5'- CTGCTGAAGTGGTATGCTAAGGAGTT-3' rev 5'- TGAGGAAGGCATACGTTGCAA-3'
PBK-TOPK	fwd 5'- GGTGTTATTACTGACAAGGCAGACATATT-3' rev 5'- AATGTGTGGAATCGATAAAGTCATCAT-3'
PARP2	fwd 5'- GGAATCTTGAGCCATGGGCTT-3' rev 5'- GAGCAGCAGTCCTGTATTCTTTAGGC-3'
RGS1	fwd 5'- GAATGGATATGAAAGCATACCTGAGATC-3' rev 5'- CCATTGCATTACTTCAGCAGCA-3'
SlamF7	fwd 5'- GAGCAGCAGTCCTGTATTCTTTAGGC-3' rev 5'- GCTGCTGACCCTGTGAGCTG-3'
ChIP Bub1B	fwd 5'- GACACGGCCTGGTAGGTAAT-3' rev 5'- GCAGCCTTCTTCGCTTTG-3'

2.11 Ready to use Reaction Systems

The following ready to use reaction systems were utilized in this work.

Table 2-11 Reaction Systems

Description	Manufacturer
EndoFree® Plasmid Maxi Kit	Fa. Qiagen, Hilden
ExpressArt® mRNA Amplification Kit	AmpTec, Hamburg GER
PathDetect® in Vivo Signal Transduction Pathway trans-Reporting Systems	Stratagene/Agilent, Waldbronn GER
RNA Isolation Kit	Machery+Nagel, Düren GER
Rneasy® Mini Kit	Qiagen, Hilden GER
SuperscriptII™ RT Kit	Invitrogen, Karlsruhe GER
SignalBoost™ Immunoreaction Enhancer Kit	Calbiochem via Merck, Darmstadt GER

2.12 Cell Biology

2.12.1 Cell culture techniques

Burkitt Lymphoma cell lines were cultivated in cell culture medium I (for details concerning media supplements please refer to table 2.6 Buffers, Solutions and Media) at 37°C, 5% CO₂ and splitted every second day in a ratio depending on observed cell proliferation (cell density: 0.3x10⁵/ml – 1x10⁶/ml). All DLBCL cell lines, apart from OCI-Ly1, OCI-Ly3 and OCI-Ly7, were cultivated in cell culture medium II in a cell density of 5x10⁵/ml – 1x10⁶/ml. OCI cells were cultivated in cell culture medium III supplemented with 10% FBS for OCI-Ly1 and OCI-Ly7 and with 20% FBS for OCI-Ly3 cells. Cells were counted in PBS 0.4% (w/v) Trypanblue using a Neubauer counting chamber. Primary tonsillar mononuclear cells were isolated using cell culture medium IV and cultivated in cell culture medium V in a cell density of 1x10⁶/ml.

To cultivate cells from a frozen aliquot, thawed cells were washed with 10ml of the respective cell culture medium (centrifugation 250xg, 7mins at RT). The cell pellet was resuspended in 5-10ml medium and cells were incubated at 37°C, 5% CO₂. To freeze cells, approximately 1x10⁷ cells were sedimented as described above and resuspended in 500µl freezing medium. Cells were frozen in cryo boxes containing isopropanol to obtain a constant cooling of approximately 1°C/min.

2.12.2 Isolation of Tonsillar Mononuclear Cells from human primary tissue

Primary tonsillar tissue was kept in PBS on ice after tonsillectomy. The tonsillar cells were extracted by mincing the tonsil in cell culture medium IV. The Tonsillar Mononuclear Cells (TMCs) were separated via density gradient centrifugation. Therefore the Lymphoprep™ solution was overlaid with the cell suspension and centrifugation was performed at 400 x g, 30 min at RT without break. The interphase containing the TMCs was collected. TMCs were washed once with cell culture medium IV and a second time with autoMACS™ buffer plus.

2.12.3 Enrichment of CD10⁺ GC B cells

Cell enrichment was performed by an indirect labelling of the GC B cell marker CD10 on the cell surface with an antibody coupled to magnetic beads (MACS™ MicroBeads). The magnetic sorting was performed using MACS™ columns placed in a MACS™ Separator, a strong permanent magnet. Thereby the MACS™ Column provides a magnetic field which retains labelled cells. Elution was achieved by removing the column from the magnet and rinsing the column with buffer.

TMCs were counted and resuspended in autoMACS™ buffer plus (1×10^8 cells/ml). Cells were stained with anti CD10-PE antibody (diluted 1:50) for 15min at 4°C. Cells were washed with autoMACS™ buffer plus (centrifugation 300xg, 10mins, 4°C). Staining with anti-PE microbeads was performed in a dilution of 1:5 in 100µl autoMACS™ buffer plus containing 1×10^7 cells for 15mins at 4°C. Cells were washed with 50x volume of autoMACS™ buffer plus and resuspended in autoMACS™ buffer plus (1×10^8 cells/500µl). CD10⁺ cells were enriched using LS MACS™ separation columns (Miltenyi-Biotec, Surrey UK) topped with pre-separation filters (Miltenyi-Biotec, Surrey UK). After the equilibration of the columns and filters with 500µl autoMACS™ buffer plus in the magnetic field, 1×10^8 cells in 500µl autoMACS™ buffer plus were given onto the column. The columns were washed with 3ml autoMACS™ buffer plus three times. The first washing step was executed through the pre-separation filter. Elution was performed with 5ml autoMACS™ buffer plus. An aliquot of CD10⁺ enriched cells was stored at 4°C for cell characterisation by flow cytometry.

2.12.4 Transfection of CD10⁺ B cells via non-viral DNA transfer

The CD10⁺ cells were transfected by nucleofection using Human B Cell Nucleofector® Kit and the Amaxa Nucleofector® II device. The following vectors were used: pcDNA3.1, pcDNA3.1-myc and pMACS-ΔLNGFR (please refer to table 1-6). pcDNA3.1-myc was used for the transfection of the *MYC*. This construct was kindly provided by Georg Bornkamm (Hörtnagel, Mautner et al. 1995). The ΔLNGFR expression plasmid was cotransfected in all reactions to sort the cells for DNA uptake.

1×10^7 cells in 100 μ l Nucleofection solution B were mixed with specific amounts of plasmid DNA. Cells were transfected in a nucleofection cuvette using the U-15 nucleofection program. For the exact amounts of plasmid DNA please refer to values in table 2-12.

Table 2-12 Amount of plasmid DNA used for transfection

transfection reaction	control	<i>MYC</i>
plasmid	pcDNA3.1	pcDNA3.1-myc
amount	7 μ g	7 μ g
pMACS- Δ LNGFR	3 μ g	3 μ g

Transfected cells were cultivated at 37°C, 5% CO₂ for 12h in a concentration of 0.5×10^7 cells/ml in cell culture medium III and further processed for the preparative FACS. To test protein levels and expression of introduced genetic material 1×10^7 transfected cells were sedimented (10mins, 3000rpm, 4°C) and washed with PBS containing 1mM Sodium orthovanadate. Samples were frozen at -20°C as dry pellets.

2.12.5 Activation of B cells with soluble stimulating factors

Primary B cells - 1×10^6 fresh CD10⁺ B cells were resuspended in cell culture medium V containing 10mM HEPES (1×10^6 cells/ml) and supplemented with sCD40L (200ng/ml), anti human IgM/IgG F(ab)₂ (1.3 μ g/ml), rhIL21 (100ng/ml), rhBAFF (100ng/ml and 200ng/ml) or LPS (1 μ M). Cells were incubated at 37°C, 5% CO₂ for 3hrs for microarray analyses. Cells were harvested (10mins, 300xg, 4°C) and washed with PBS containing 100mM sodium orthovanadate. Samples were frozen at -80°C and RNA was isolated with the RNeasy Kit (Qiagen).

B cell lymphoma cell lines - For the stimulation of lymphoma cell lines, cells were counted and seeded at a concentration of 3×10^5 cells/ml in fresh cell culture medium I 16h prior to the experiment. Next day 1×10^6 cells were resuspended in fresh cell culture medium I containing 10mM HEPES (1×10^6 cells/ml) and supplemented with sCD40L (200ng/ml), anti human IgM F(ab)₂ (1.3 μ g/ml),

rhIL21 (100ng/ml), rhBAFF (100ng/ml and 200ng/ml) or LPS (1µg/ml). Cells were incubated at 37°C, 5% CO₂ for 5 mins, 15mins or 30mins (signalling analyses via WB) or for longer timepoints (sCD40L (6h), anti human IgM/IgG F(ab)₂ (3h), rhIL21 (2h), rhBAFF (9h) or LPS (6h)) for microarray analyses. Cells were harvested (10mins, 300xg, 4°C) and washed with PBS containing 1mM Sodium orthovanadate. Samples for protein analyses were frozen at -20°C as dry pellets and subsequently lysed in supplemented RIPA buffer. Samples for microarray analyses were frozen at -80°C and RNA was isolated with the RNeasy Kit (Qiagen). For the detection of pathway activities in response to stimulation the BL cells were serum starved (16h) prior to stimulation.

2.12.6 Inhibitor Treatment

For cell cycle analyses and analyses of BCR.1 gene expression, BL2 cells were treated with 60µM of the c-Myc inhibitor 10058-F4 in cell culture medium I for 16hrs prior to 3h / 6h / 9h of B cell receptor stimulation (scheme 16h + 3h/6h/9h).

For the gene expression analyses of *MYC* and *DUSPs*, BL2 cells were seeded 16h prior to the experiment in a cell density of 3x10⁵ cells/ml in cell culture medium I containing 0.5%FCS. Next day 1x10⁶ cells/ml in cell culture medium I containing 0.5%FCS were treated with 100nM 5Z-7-oxozeaenol (TAK1 inhibitor), 7µM IKK2 inhibitor, 10µM Ly294002 (PI3K inhibitor), 2µM SB203580 (p38/MAPK14 inhibitor), 10µM SP600125 (JNK inhibitor), 10µM U0126 (ERK1/2 inhibitor) and 2.5µM VIVIT (NFAT inhibitor) for 3h prior to BCR activation. The stimulation was performed for another 3h (scheme 3h + 3h). The cells were harvested at 300xg, 10mins 4°C, washed with PBS containing 1mM sodium orthovanadate and stored at -80°C as dry pellets. To check for pathway activity via WB additional timepoints were harvested (3h + 30min).

2.12.7 Flow cytometry

Flow cytometry is based on the detection of fluorescence which is emitted by a single cell flowing through a liquid stream. A laser beam of a specific wavelength is directed onto the stream of fluid. A number of detectors are aimed at the point where the stream passes through the light beam; one in line with the light beam

(Forward Scatter or FSC) and several vertical to it (Side Scatter (SSC)) and one or more fluorescent detectors. Each cell that passes through the laser beam scatters the light. Fluorescent dyes bound to a cell can be excited and the emitted light can be detected. This combination of scattered and fluorescent light is collected by the distinct detectors. FSC correlates with the cell volume and SSC depends on the inner complexity (granularity) of the cell. Fluorescein (FITC - absorption maximum at 494nm; emission maximum of 521nm) and Phycoerythrin (PE - absorption maximum at 495nm; emission maximum at 575nm) were used as fluorescent dyes coupled to specific antibodies. To adjust the detectors for the “spillover” of one fluorescence signal into the wrong channel, compensation can be performed. FITC, for example, is primarily green but fluorescein also has a significant yellow component to the fluorescence, which appears in the PE channel (Loken, Parks et al. 1977). Compensation can therefore be used to subtract a fraction of the FITC signal from the PE signal (FL1-FL2).

2.12.8 Characterisation of cell populations via flow cytometry

For the characterisation of cell populations approximately 6.5×10^6 cells were used. The CD10⁺ enriched cell population was stained with antibodies against CD27, CD38, CD77, IgM, IgD, IgG and BAFF-R / TACI (see Table 2.9 antibodies). Staining of cells was carried out as follows: 45µl cell suspension was supplemented with 5µl antibody (1:10 in 50µl autoMACS™ buffer plus). The cells were incubated at 4°C for 15mins then washed with 1ml autoMACS buffer plus. Cells were resuspended in 300µl autoMACS™ buffer plus (0.1 µg/ml PI) for the measurement. Data analyses were performed using CellQuest™ (Becton Dickinson, Oxford UK) and FlowJo™ (Treestar, USA) software.

2.12.9 Preparative FACS of transfected CD10⁺ cells

To optimize sensitivity and compensation of the FACS sorter, untransfected TMCs were stained with antibodies labelled with fluorescent dyes that were used for the sorting process (CD10-PE; CD19-FITC). Isotype control IgG monoclonal mouse antibodies coupled to FITC were used to control for the non-specific binding of antibodies directed against cell surface antigens. Cells were cotransfected with a ΔLNGFR expression plasmid that encodes a truncated form

of the membranous Nerve Growth Factor Receptor. The expression of this surface marker only on transfected cells enables to sort for them by a staining with an anti Δ LNGFR-FITC coupled antibody (Kube and Vockerodt 2001). Cells were stained as described above. Antibodies for the controls were used in a dilution of 1:10 in 50 μ l autoMACS™ buffer. The cell suspensions were spiked with propidium iodide (PI 0.1 μ g/ml) or Hoechst Dye (1:100 dilution) (Sanofi Aventis, Frankfurt GER) to ensure selection of viable cells. The cells were stained with a Δ LNGFR-FITC antibody in a dilution of 1:10 in 250 μ l autoMACS™ buffer plus. The transfected cells were sorted for FITC-positivity (Δ LNGFR+), PE-positivity (CD10⁺) and propidium iodide / Hoechst negativity (viability) with the help of MoFlow® High-Performance Cell Sorter (Dako, Stockport UK). Sorted cells were collected into 500 μ l PBS and stored on ice. RNA isolation was performed immediately.

2.12.10 Cell cycle analysis

The cell cycle analysis was performed on the basis of analysing the DNA content in the nuclei of the cells by propidium iodide staining and followed by flow cytometric analyses. Therefore an 200 μ l of the cellsuspension was sedimented (250 x g, 10min, RT) and the pellet was resuspended in 500 μ l hypotonic Nicoletti solution (Nicoletti, Migliorati et al. 1991). This buffer leads to the destruction of the cell membrane due to hypotonic stress, whereas the nucleus stays intact. Propidium iodide respectively DNA content of the nuclei was determined by flow cytometry. Distribution of the cells according to the phase of the cell cycle was performed with the help of FlowJo™ (Treestar, Ashland USA) software according to Dean-Jett-Fox (Fox 1980) and by CellQuest™ (Becton Dickinson, Oxford UK) software. The nuclei of viable cells show three characteristic distributions in the flow cytometric analysis based on their differing DNA content. By this analysis method one can discriminate the cell cycle phases G1, S und G2. Furthermore nuclei from apoptotic cells show an even smaller amount of DNA as cells in the G1 phase and are therefore summarized in the group of SubG1 events.

2.12.11 Synchronisation of BL cells using Thymidine treatment

The treatment of cells with 2mM Thymidine can be used to achieve a cell cycle arrest in S/G2 phase. An overexposure of cells to Thymidine leads to an inhibition of Thymidine kinase which is necessary for DNA synthesis and thereby to an arrest of cells in the S/G2 phase (Stolz, Ertych et al. 2010).

2.12.12 Ca^{2+} Measurement

The calcium signalling response in Burkitt Lymphoma cells was measured using flow cytometry and the Ca^{2+} -sensitive fluorophore Indo-1. Indo-1 (Indo-1-AM) is an uncharged molecule. It can passively diffuse through the plasma membrane. Lipophilic groups are cleaved intracellularly, resulting in a charged molecule which is trapped in the cell due to an altered membrane permeabilization potential. The fluorescence emission maximum of Indo-1 shifts from 475nm (Indo-blue) without Ca^{2+} to 400nm (Indo-violet) after Ca^{2+} binding (excitement at 350nm). Cell loading with the fluorophore is facilitated by the surfactant polyol Pluronic F-127.

To analyse Ca^{2+} signalling 1×10^6 cells were harvested at 300xg, 4°C, 5min. The cells were resuspended in 700µl of cell culture medium I containing 5% FCS. The cells were loaded with Indo-1 for 25min at 30°C. Subsequently, the cell suspension was diluted with 700µl of the corresponding prewarmed medium containing 10% FCS. The cells were incubated for 10min at 37°C and washed twice with Ca^{2+} containing Krebs-Ringer solution. The cells were resuspended in Ca^{2+} -containing Krebs-Ringer solution and kept at 20°C until measurement. The ratio Indo-violet/Indo-blue was measured using LSR II (Becton Dickinson). After 30s, stimulation was performed with 1.3µg/ml anti IgM F(ab')₂ fragment. The Ca^{2+} mobilization profiles were analysed using FlowJo software.

2.13 Protein Biochemistry

2.13.1 Preparation of cell lysates

Cells were sedimented (10mins, 3000rpm, 4°C) and washed with PBS containing 100mM Sodium orthovanadate. Samples were frozen at -20°C as dry pellets until further investigation.

To prepare protein lysates cell pellets were thawed on ice. Cell lysis was carried out by resuspending the cell pellet in RIPA buffer (Table 2.6) and incubating the cell suspensions on ice for 30mins. The cell lysates were centrifuged to sediment the residual cell debris (15mins, 13.000rpm, 4°C). The supernatant was transferred into a new reaction tube. The protein concentrations were examined by Bradford assay (Bradford 1976) with the help of a ready to use Bradford solution and photometric quantification of protein concentrations was performed.

2.13.2 SDS-PAGE

Protein samples in SDS (sodium dodecyl sulphate) containing Laemmli buffer are negatively charged and thus can be separated by size in an electric field using polyacrylamide gelelectrophoresis (PAGE).

Separation of proteins via gel electrophoresis was performed with two different systems. For the investigation of c-Myc expression in transfected GC B cells ready to use gradient gels (Invitrogen, Paisley UK) were utilized in the Xcell Surelock™ chamber (Invitrogen, Paisley UK). The Biorad System (BioRad, München GER) was applied to investigate the activation of signalling pathways. SDS-PAGE gels were used in a concentration of 10% and 12.5% for the separation gel and 5% for the stacking gel.

Immediately after pouring the separation gel, it was covered by 100% isopropanol to obtain a smooth surface of the gel and to protect it from drying out. After polymerization the stacking gel was prepared and poured on top of the separation gel after removing the isopropanol. Differing amounts of protein were used. The exact values are indicated in the depiction of the immunoblot. The protein probe was supplemented with 4x loading buffer Roti®-Load, denaturated

for 5mins at 95°C and loaded on the gel. The gels were run at a current of 20mA for 15mins to ensure proper entering of the probes into the stacking gel. For separation the current was fixed at 40mA in both systems. If the protein concentration was too low to achieve an appropriate amount of protein the whole lysate was loaded onto the gel. For protein size determination the Fullrange rainbow™ marker was used.

2.13.3 Immunoblotting Technique

For further analysis, the proteins separated by SDS-PAGE were transferred onto a nitrocellulose membrane using the western blot technique. The stacking gel was separated from the gel. The nitrocellulose membrane was equilibrated in *aqua dest.* for 1 min. Membrane and the whatman papers were well soaked in transfer buffer prior to arranging them in a pile as follows: Cathode (-); 2 whatman papers; polyacrylamid gel; nitrocellulose membrane; 2 whatman papers; Anode (+). The gel was blotted onto a nitrocellulose membrane (Hybond™-C extra, GE Healthcare, München GER) with the help of the Tank Blot System (BioRad, München, Deutschland) in case of BioRad Gels and with Xcell Surelock™ blotting system (Invitrogen, Paisley UK) in case of invitrogen gradient gels.

The blotting was carried out in transfer buffer at a voltage of 100V, a current of max. 300mA and a power of 300W for 4h. The membrane was washed with TBS-T buffer and blocked with 5% milk powder or 5% BSA in TBS-T for 1h at RT. The staining with primary antibodies was carried out by incubation of the membrane in antibody dilution over night at 4°C. The membrane was washed three times for 10mins with TBS-T and staining with secondary antibodies for 1h at RT was performed. The membrane was washed three times 10mins with TBS-T and the membrane was incubated with ECL-Enhanced Chemiluminescence solution or sel-made ECL (see list of Buffers) for 1min at RT. The detection was performed with the help of Hyperfilm™ ECL (GE Healthcare, München GER) light sensitive films and Hypercasette™ (GE Healthcare, München GER) and with the chemiluminescence camera “LAS-4000 Image Reader” (Fujifilm, Düsseldorf GER). The development of films was performed with Protec Optimax X-Ray Film Processor (Maco, Hamburg GER).

2.14 Molecular Biology

2.14.1 Transformation of E.coli

E.coli bacteria were cultivated in LB medium at 37°C shaking. The bacteria were used for the amplification of plasmid DNA. Therefore the DNA was induced by transformation of the bacteria. Stocks of competent bacteria were stored at -80°C and thawed on ice. 100ng plasmid DNA was mixed with 25µl competent cells. After incubation on ice for 30mins cells underwent a heatshock for 1min at 42°C. The bacteria were again incubated on ice for 10mins immediately after the heatshock. Cells were incubated shaking for 1h in 1ml LB medium without antibiotics. To select positively transformed cells 100µl bacteria suspension was plated on LB agar plates containing 100µg/ml Ampicillin and plates were incubated at 37°C for 16h. To amplify the bacteria a pre culture was inoculated (2ml LB Medium containing antibiotics) and incubated at 37°C for at least 6h. With the help of this pre culture a larger culture was inoculated (150ml LB medium containing antibiotics) and a cryoculture was established (40% (v/v) glycerol-stock) and stored at -80°C.

2.14.2 Isolation of Plasmid DNA

150ml bacterial culture was incubated at 37°C shaking for 16h. Isolation of plasmids was performed with the EndoFree Plasmid Maxi Kit (Qiagen, Hilden). The precipitated DNA was resolved in endotoxin free water and DNA concentrations were measured photometrically.

2.14.3 mRNA Isolation

cell lines - The RNA was isolated with the help of the RNeasy® mini Kit (Qiagen) or the RNA isolation Kit (Machery + Nagel). RNA was eluted with 30µl - 40µl RNase free water. Concentrations were measured by NanoDrop™ measurement.

primary GC B cells - The sorted cells were spun down (10min, 3000rpm, 4°C) and resuspended in 100µl RLT-buffer (RNeasy® microkit) supplemented with 1µl N-carrier solution (ExpressArt®). Lysed cells were stored at -80°C until

further processing. Samples were thawed on ice and isolation of RNA was performed using the RNeasy® microkit, following manufacturer's instructions. The elution was performed twice with 14µl RNase free water (RNeasy® microkit).

2.14.4 mRNA Amplification

To obtain enough RNA of sorted GC B cells the RNA was amplified. RNA was isolated and amplified to be used for microarray analyses and transcript quantification with the help of qRT-PCR. It was described that the amplification process itself does not interfere with the reproducibility of gene regulations estimated by microarray analyses (Puskas, Zvara et al. 2002). Three rounds of amplification of cellular mRNA were performed with the help of ExpressArt® mRNA Amplification Kit from AmpTec according to manufacturer's instructions. The success of the RNA amplification was supervised by analysing the amplification products with the help of agarose gel electrophoresis. The concentrations of antisense aRNAs were determined by NanoDrop™ measurement. Test IVT was performed with the Ambion Mega Script® Kit.

2.14.5 Reverse Transcription

The reverse transcription of RNA from the amplification process was performed with SuperscriptIII™ RT Kit using 500ng aRNA. For the cDNA synthesis from 1µg RNA of cell lines SuperscriptII™ RT Kit was utilized. RT reactions were prepared as follows:

Table 2-13 RT Reaction

Probe reaction Mix	Mastermix
11µl RNA (500ng respectively 1µg)	4µl 5x buffer
1µl random primer (100ng/µl)	1µl DDT (0.1M)
1µl dNTPs (10mM)	1µl RNase out
→ incubation 5mins at 65°C	1µl superscript II / III
→ on ice	
13µl probe reaction Mix + 7µl Mastermix Incubation 50°C 1h 70°C 15mins 4°C	

2.14.6 Transcript quantification via qRT-PCR (quantitative Real Time – Polymerase Chain Reaction)

SYBR® Green is an asymmetrical cyanine dye that binds to double stranded DNA. The resulting DNA-dye-complex absorbs blue light ($\lambda_{\max} = 488 \text{ nm}$) and emits green light ($\lambda_{\max} = 522 \text{ nm}$) (Zipper, Brunner et al. 2004). This attribute can be used for the detection of double stranded PCR products over the time of the PCR reaction. The number of PCR cycles at which a significant exponential increase in fluorescence is detected is directly correlated with the number of copies of DNA template present in the reaction. This value is called the Cycle Threshold (Ct).

Transcript quantification was performed with Fast SYBR® Green (Applied Biosystems, Foster City USA) and a self made SYBR Green Mix (see section Materials). ABI PRISM 7900HT sequence detection system (Applied Biosystems) was used to carry out the PCR reaction and the fluorescence detection. For each real time PCR reaction with the SYBR Green Mix from Applied Biosystems, a 10 μl reaction volume was used with 5 μl Fast SYBR® Green Master Mix (containing all ingredients needed for the PCR) an amount of cDNA that corresponds to 10ng RNA utilized for the cDNA synthesis and 0.3pmol/ μl forward and reverse primer. PCR reactions were performed using a 384well plate sealed with an optical adhesive foil.

Table 2-14 Cycle program RT-PCR

Initial denaturation	95°C 20s	
Deanturation	95°C 1s	
Annealing/Extension	60°C 20s	55 cycles
Dissociation stage	95°C 15s	
	60°C 15s	
	95°C 15s	

The relative expression values for each gene were estimated by normalizing the actual CT values, calculated as means of three independent triplets, to CT values of a housekeeping gene:

$$\Delta\text{CT} = \text{CT}_{\text{gene of interest}} - \text{CT}_{\text{housekeeping gene}}$$

The ΔCT values can then be compared in-between the control and modified samples by calculating $\Delta\Delta CT$:

$$\Delta\Delta CT = \Delta CT_{\text{modified sample}} - \Delta CT_{\text{control}}$$

$\Delta\Delta CT$ is a relative measurement and gives the value for the differences of cycles after the amplicon of the gene of interest can be detected in samples of control transfected cells vs. modified cells. On the basis of $\Delta\Delta CT$ the change of gene expression can be calculated as fold change: fold change = $1 / (2^{\Delta\Delta CT})$

For this study $\beta 2m$ was chosen as a housekeeping gene. The primers for the qRT-PCR reactions were designed on the basis of mRNA sequences published on the NCBI homepage (<http://www.ncbi.nlm.nih.gov/sites/entrez/>) with the help of PrimerExpress™ software (Applied Biosystems, Foster City USA). They were tested for specificity with BLAST (<http://www.ncbi.nlm.nih.gov/blast/Blast.cgi>).

2.14.7 Chromatin Immunoprecipitation

Chromatin-Immunoprecipitation (ChIP) can be used to detect DNA binding of transcription factors to specific sites on the genome. Therefore DNA and bound proteins are crosslinked using formaldehyde. DNA is sheared using ultrasound and the protein DNA complexes are subsequently used for immunoprecipitation of the protein of interest using specific antibodies. In a last step the co-precipitated DNA can be released from the proteins and used for PCR to detect whether specific loci have been co-precipitated. The protocol was performed as follows: 10ml of 1×10^6 BL2 cells/ml were stimulated with 1.3 μ g/ml anti-IgM F(ab)₂ fragments for 3hrs or left untreated as control (stimulations were performed in triplicate). Cells were sedimented and resuspended in 8ml PBS containing 1.42% formaldehyde (in PBS) and incubated for 15min at room temperature. Subsequently the formaldehyde was quenched by adding 1ml 1.25M Glycine (incubation for 5min at room temperature). Cells were washed twice with ice-cold PBS. Cells were resuspended in 1 ml cool IP-buffer +, mixed by pipetting up and down several times, and centrifuged at 12.000g for 1min at 4°C. The supernatant was discarded. The nuclear pellet was washed once with 1 ml IP-buffer + and sedimented (12.000g, 1min., 4°C). The supernatant was discarded and the pellet resuspended in 250 μ l IP-buffer +. Samples were

sonicated using the Biorupter device from Diagenode for 3 x 10 minutes with fresh ice-water (Settings: 10 sec on/off duty time at high power). Protein A Sepharose was blocked by adding 15ml of IP buffer containing 0.5g BSA and 100µl of salmon sperm DNA for 16h at 4°C. The swollen sepharose was washed with IP-buffer (centrifuge 2min at 1000g). 1 volume of IP buffer + was added to the sepharose. For pre-clearing 80 µl blocked sepharose was added to sheared and diluted chromatin and incubated for 1h at 4°C. Sepharose was sedimented at 12.000g, 10min, 4°C and the supernatant was transferred to a new tube. 50µl of each precleared lysate was used for every IP (anti c-Myc, anti acH3, anti IgG control and Input control). 50µl extract was diluted using 450µl IP-buffer. 2µg antibody was added to each sample and incubated at 4°C overnight. In parallel 1µl of GlycoBlue (glycogen) and 100µl 100% ethanol was added to input DNA samples. These were placed at -20 °C overnight. 30µl of protein A - sepharose was added to each sample and probes were incubated at 4°C for 2 hours. In parallel input DNA in EtOH was centrifuged at 4°C, 12.000g for 20min and the DNA pellet was washed once with 500µl 70% EtOH. The pellet was air dried. ChIP immune complexes (sepharose beads) were washed 6 times with 1ml cold IP-buffer. Centrifugation was performed at 2.000g, 4°C, for 2 min. To release DNA from protein immune complexes 100µl 10% (wt/vol) Chelex 100 slurry was added to the washed beads and to the Input DNA pellet. Samples were mixed and heated to 95°C for 10min. After boiling 2µl of 20µg/µl proteinase K was added to the cooled samples. Incubation was performed at 55°C for 30 min on a thermal mixer (shaking at 1000 rpm). Proteinase K was inactivated by incubating samples at 95°C for 10minutes. Samples were centrifuged at 12.000 g for 1min at 4°C and the supernatant (70µl) was transferred to a new tube. Samples were stored at -20°C until PCR reactions were performed. BuB1B PCR was performed using the following cycle protocol:

Table 2-15 Reaction Mix and Cycling Program PCR ChIP

<u>Reaction Mix (25µl):</u>	<u>Cycling Protocol:</u>
1µl DNA	Primary Denaturation: 5 min at 95°C
2.5µl 10x buffer (Primetech, Belarus)	Primary Annealing: 3 min at 60°C
1.5µl 25mM MgCl ₂ (Primetech, Belarus)	Primary Elongation: 3 min at 72 °C
0.1µl Taq (0.5 U) (Primetech, Belarus)	Denaturation: 5 min at 95°C
0.5µl dNTPs (10mM)	Annealing: 3 min at 56°C
18.4µl H ₂ O	Elongation: 3 min at 72 °C
0.5 µl fwd Primer	Final Elongation: 3 min at 72 °C
0.5 µl rev Primer	

2.15 Microarray analyses

cDNA was labelled for microarray hybridization with the help of a labelling IVT reaction. The labelling IVT was performed with the help of Affymetrix GeneChip® IVT Labelling Kit (Affymetrix, High Wycombe UK). Fragmentation and hybridization of labelled aRNA on Human Genome U133A 2.0 Arrays (Affymetrix, High Wycombe UK) was performed by the group around M. Hummel, Charité Berlin, as part of the MMML project. Microarray raw data were sent to Rainer Spang and Katharina Meyer, Insitute of Functional Genomics, University Regensburg for statistical analyses.

Differential gene expression – Data analysis was performed using the statistical computing environment R and the life-science related extension Bioconductor (<http://www.bioconductor.org>). The expression values were background corrected and normalized using the robust multi-array average function from the affy package for c-Myc expression data (Huber, von Heydebreck et al. 2002). Normalized probe intensities were summarized to probeset expression levels using robust additive model as implemented in the RMA approach (Irizarry, Hobbs et al. 2003). For the analyses of stimulation data, the expression values were background corrected and normalized using a variance stabilization method (vsr). Gene expression levels were estimated by fitting an additive model employing a median polish routine. Given the normalized

cell line data from the platform „HG-U133plus2“ and the normalized Patient data from the platform „HG-U133A“ the probe sets from both platforms were intersected. Thus it is possible to change between patient and cell line data without losing genes, previously found on one of the data sets.

Multidimensional Scaling - To explore the coherence of the transcriptional response of the tonsillar B-cells to ectopic c-Myc expression multidimensional scaling was used. Differences in gene-per-gene expression levels between control and c-Myc transfection experiments were computed separately for each tonsil (11 tonsils) by subtracting the expression levels in the control sample from those in the c-Myc transfected sample (log ratio). The top 200 genes showing the highest absolute average log ratios across the tonsils were selected. Euclidean distances between the tonsils based on the log ratios of the top 200 genes were computed and embedded into 2 dimensions for using multidimensional scaling.

c-Myc index - A c-Myc gene signature (c-Myc index) was derived from genes responding to *MYC* expression in both tonsillar B-cells and lymphomas. An integrated gene expression analysis of 220 clinical lymphoma samples and the tonsillar B cell data set was performed. For each gene the Pearson correlation coefficient of its expression across the tonsils compared to that of *MYC* (Affymetrix probeset 202431_s_at) was calculated. The same calculation was performed separately across the lymphomas. Genes were ranked by a weighted average of the correlation coefficients in lymphomas and tonsils with twice as much weight on tonsils. Expression levels of negatively correlated genes were first multiplied by minus one. The expression levels of the top 100 genes was subsequently averaged to a single index. This index is a single number per lymphoma sample reflecting the expression of c-Myc target genes in each sample. Similarly, a truncated c-Myc index was generated that aggregates the expression of all genes in the intersection of the 100 index genes and the genes present on the microarray platform used in the study of Dave and co-workers (Dave, Fu et al. 2006).

Stimulation mediated uniquely regulated genes: To identify genes that are uniquely influenced by only one of the stimuli and not affected by any of the other utilized stimuli, the mean of the control gene expression values was subtracted

from the gene expression values of stimulated samples, resulting in values that solely represent the reaction caused by the stimulation. The gene vectors were correlated to a binary vector. This binary vector includes a “1” only the one stimulation that was investigated to solely regulate genes. The genes were ordered according to the calculated absolute Pearson correlation coefficient. From these two genesets all genes showing a false discovery rate smaller than 0.5 within the genelist calculated by limma were selected. The genes were discretized, in a way that gene values having an FDR smaller than 0.5 within a stimulation were set to one and otherwise to zero.

Pathway Activation Clusters – The identification of pathway activation clusters was performed using a newly developed bioinformatical approach named Guided Clustering (Maneck, Schrader et al. 2011). This algorithm identifies specific groups of genes (clusters) which fulfil 2 criteria at the same time: (i) They are differentially expressed in the guiding dataset (e.g. stimulated vs. unstimulated BL2 cells) and (ii) they show differential expression across distinct lymphoma samples. Thereby one identifies genes which can be used as potential surrogate marker for pathway activity in lymphoma samples. Using the guided clustering approach genes were searched that are differentially expressed among lymphoma samples and as well specifically regulated by one of the utilized stimuli and not affected by the others. Therefore guided clustering was combined with the vector based approach described above.

To infer on gene cluster activity in lymphoma patients, an index value was calculated per gene cluster per lymphoma sample. This index value is calculated by first finding a reference gene that best reflects the set of genes. Then all other genes are turned in the direction of the reference gene. That means if there are genes anti correlated to the reference gene, they are multiplied by minus one. After that, all expression values were averaged using a standard additive model and fitted with a median polish procedure resulting in one value per sample, which includes the overall effect and the sample effect. The index values of genes that were down regulated by a stimulus were multiplied by minus one to enable the interpretation of the indices as absence or presence of stimulation.

GO KEGG and GSEA - Gene set enrichment analysis (GSEA) of ranked gene list was performed using the Java implementation of GSEA obtained from <http://www.broadinstitute.org/gsea/>. GSEA was conducted in the mode for pre-ranked gene lists on the C2 set of curated gene signatures from the Molecular Signature Database (MSigDB). GO and KEGG pathway enrichment analyses were performed using the `gokeggLister` method implemented in the package `compdiagTools`.

Survival Analyses - The prognostic impact of the c-Myc index was evaluated after exclusion of patients with mBL by splitting the remaining lymphomas into groups based on the quartiles of the c-Myc index, i.e. they were split into groups of very low, low, medium, high and very high c-Myc target expression. Survival within the groups was assessed by multivariate Cox regression analysis with patient age (>60 years), Ann Arbor stage, presence of cytogenetically detectable *MYC* aberrations and the presence of an activated B cell (ABC) like lymphoma signature as confounding factors. Cases that could not be assigned an ABC or GCB (germinal centre B cell) label were excluded. In addition, a log-rank test was performed to assess the significance of the survival differences between the groups of lymphomas induced by the c-Myc index. The differences of the c-Myc index in different groups of lymphomas were assessed by ANOVA.

3 Results

3.1 High c-Myc activity is an independent negative prognostic factor for diffuse large B cell lymphomas

Gene expression profiling has recently enabled the reclassification of aggressive Non Hodgkin lymphomas (aNHL) into distinct subgroups. In BL aberrant c-Myc activity results from *IG-MYC* translocations. However, *MYC* aberrations are not limited to BLs and then have a negative prognostic impact. In this study it was investigated to which extend aberrant c-Myc activity plays a functional role in other aNHL and whether it is independent from *MYC* translocations. Based on a combined microarray analysis of human germinal centre (GC) B cells transfected with a c-Myc expression vector and 220 aNHLs cases, a 'c-Myc index' was developed (Schrader, Bentink et al. 2011).

3.1.1 Overexpression of c-Myc in primary human GC B cells

The transcriptional consequences of overexpressing c-Myc in human GC B cells, as the presumed progenitors of BL and DLBCL, were studied first. For this purpose human tonsillar CD10+ B cells were isolated and cotransfected with either a c-Myc expression plasmid or a control plasmid together with a vector encoding the truncated Nerve Growth Factor Receptor (Δ LNGFR) (Figure 3-1 A&B) as previously described (Vockerodt, Morgan et al. 2008; Vrzalikova, Vockerodt et al. 2011). 12 hours after transfection, viable (PI-) cells expressing CD10 and Δ LNGFR were sorted by FACS (Figure 3-1B). This was repeated on 11 separate GC B cell preparations (T15, T16, T17, T21, T28, T29, T51, T55, T56, T57, T58). High c-Myc expression was confirmed in transfected cells. In contrast, control cells showed virtually undetectable levels of endogenous c-Myc. One representative experiment is shown in Figure 3-1 C&D. In a next step microarray analyses were performed using Affymetrix HG U133 plus 2.0 chip.

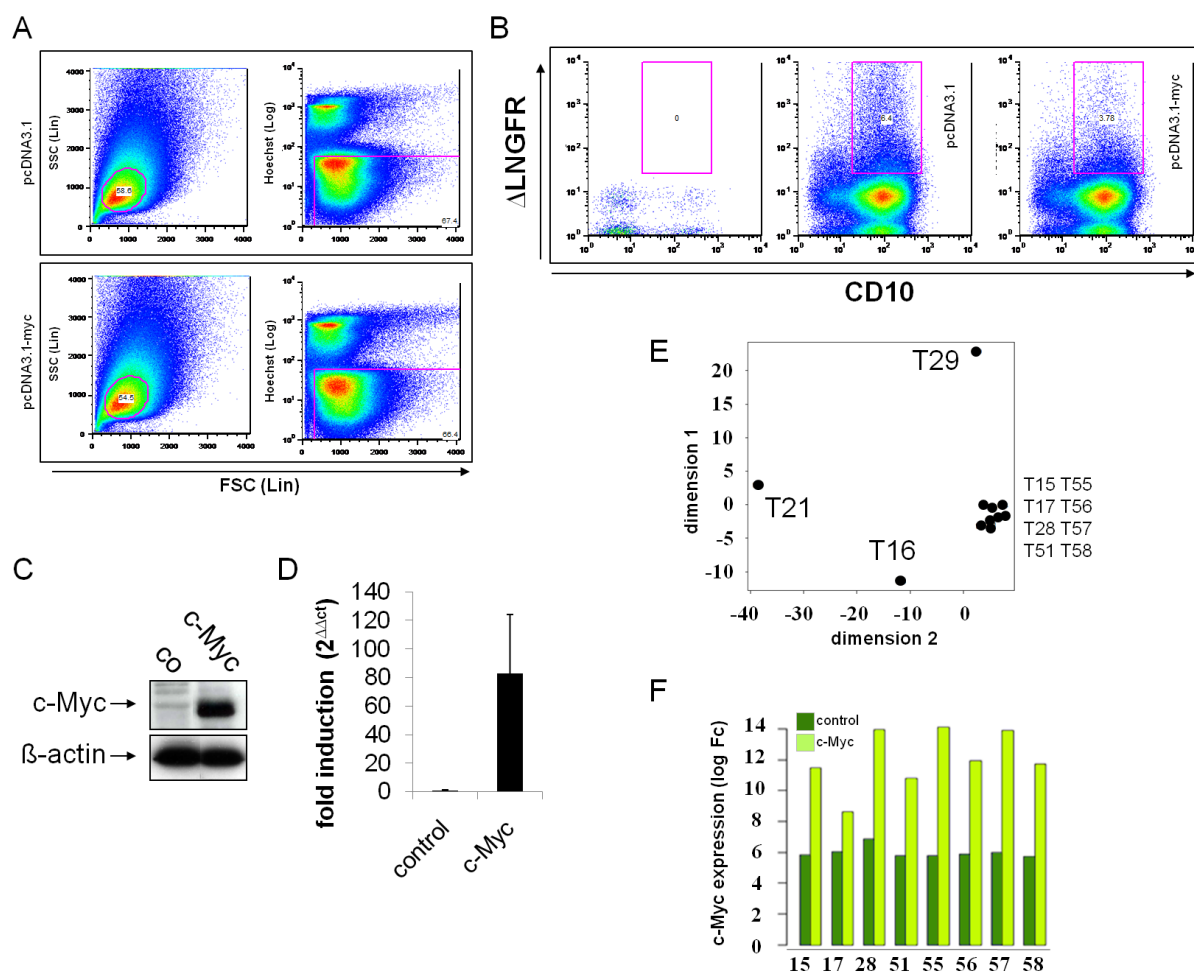


Figure 3-1 Expression of c-Myc in primary human germinal centre B cells. **A** Flow cytometric analysis of CD10⁺ tonsillar B cells transfected with pcDNA3.1 (upper row) or c-Myc (lower row) together with pMACSΔNGFR stained with Hoechst Dye to perform live gating. **B** CD10 and NGFR staining. CD10⁺ and ΔNGFR⁺, Hoechst negative cells were collected for RNA isolation (see respective gating). **C** Detection of c-Myc and β-actin in transfected CD10⁺ tonsillar B cells by immunoblot analysis. **D** Real-time RT-PCR of the relative quantity of c-Myc in c-Myc-expressing and non-expressing GC B cells. All samples were analysed in triplicates and are presented as 2^{-ΔΔCT} values compared to vector control. **E** Multidimensional Scaling (MDS) based on the transcriptional fold-changes of the top 200 c-Myc responsive genes. The plot is a two dimensional visualization (dimension 1 and dimension 2) of the differences between the tonsils with respect to the transcriptional changes induced by c-Myc. **F** Shown are the transcriptional levels of c-Myc (y-axis) measured by HG133 Plus 2.0 Affymetrix microarrays in 8 tonsils (x-axis). Each tonsil is represented by a dark green bar and light green bar indicating a pair of transfection experiments (dark green: empty control vector, light green c-Myc expression vector). The scale of the expression data (y-axis) obtained from microarray normalization (variance stabilization) is equivalent to the natural logarithm of the true fold-change: An increase by one unit corresponds to a fold change of e¹.

To visualize the global response to c-Myc overexpression, the gene expression data was embedded in a two dimensional plane using multiple scaling based on the fold changes of 200 genes with highest average fold-changes between c-Myc overexpressing and control cells across the 11 preparations (Figure 3-1 E). The distances between samples reflect similarity in the response to c-Myc

overexpression rather than any similarity between individual expression profiles. While most tonsils formed a tight cluster indicating a coherent response to c-Myc overexpression, T16, T21 and T29 did not and were removed from further analysis. Consistent with the data shown in Figure 3-1 C&D, the microarray analyses revealed increased c-Myc expression in transfected cells (Figure 3-1 F). However, when compared across all tonsils the average fold changes of the top 200 c-Myc target genes (selected by absolute values of the log fold-change) were small (maximum 4.9 fold). As the effects of c-Myc were rather small, a customized approach was used to extract the information about c-Myc regulated genes from these data.

3.1.2 Ectopic c-Myc expression triggers a tumour like expression profile in primary GC B cells.

To analyse the genes co-regulated with *MYC* an integrated analysis combining two gene expression data sets was performed: CD10⁺ lymphoma precursor cells (data set 1) and 220 aNHL samples (data set 2). This patient cohort of 220 aNHL cases was firstly published by the MMML (Mechanisms of Malignant Lymphoma) consortium (Hummel, Bentink et al. 2006). Within this study a molecular diagnosis of Burkitt Lymphoma, based on the gene expression profiles of these 220 aNHL samples, was developed. According to this so called “index of Burkitt likeness” the patient cohort comprises 45 BL cases, 127 non-mBL cases (of these more than 80% are DLBCL) and 48 unclassifiable so called intermediate cases. All analyses of aNHL microarray samples presented in the following paragraphs were, unless stated otherwise, performed using this study group.

Using this combinatory approach a ranked list of c-Myc-dependent genes was generated. This list comprises genes which are co-regulated with *MYC* in lymphoma precursor cells as well as in the gene expression profiles of malignant lymphoma. Genes were ranked by a weighted average of the correlation coefficients in lymphomas and tonsils with twice as much weight on tonsils. Highly ranked genes thus show a strong response to ectopic c-Myc expression in GC B cells and coherent regulation in lymphomas. It is important to note that these genes show consistent behaviour in both data sets and are not simply differentially expressed between normal and tumour cells (Table 3-1).

Gene set enrichment analysis (GSEA) was used to characterise the ranked list of genes (Subramanian, Tamayo et al. 2005). A significant enrichment of c-Myc target genes previously defined from studies on non lymphoid tissues was found. This is exemplified in Figure 3A by the sharp increase in the GSEA enrichment score to the left of the graph and a decrease to the right. 344 gene sets were found to be significantly (FDR $q < 0.25$) enriched in genes that are positively correlated with *MYC* and 52 gene sets enriched in genes which are negatively correlated with *MYC*. Within the list of 20 gene sets that were most significantly enriched in *MYC* positively correlated genes, 5 were pre-defined c-Myc target gene sets (Figure 3-2 A). This is indicated by the gradual decrease of the GSEA enrichment score to the left of the graph, and a sharp increase to the right. For a detailed list of Gene Sets please see Table A1 in the Appendix. Furthermore, gene sets representing known c-Myc functions like cell cycle regulation or serum response were also enriched in *MYC* positively correlated gene sets. Also in line with previous observations, *MYC* expression was associated with a depletion of gene sets that are described as NF- κ B regulated based on gene expression in CD40 ligand stimulated BL cells (Figure 3-2 B). These results support recent observations of an inverse correlation between *MYC* expression and NF- κ B signalling in lymphomas (Schlee, Holzel et al. 2007; Klapproth, Sander et al. 2009). Most importantly, a significant enrichment of genes from a set called 'CANCER NEOPLASTIC META UP' was observed. This gene set comprises genes that are upregulated in tumour cells relative to matching normal tissue cells across many tumour entities (Figure 3-2 C). This suggests that the c-Myc index includes genes that are reflecting essential transcriptional features of neoplastic transformation.

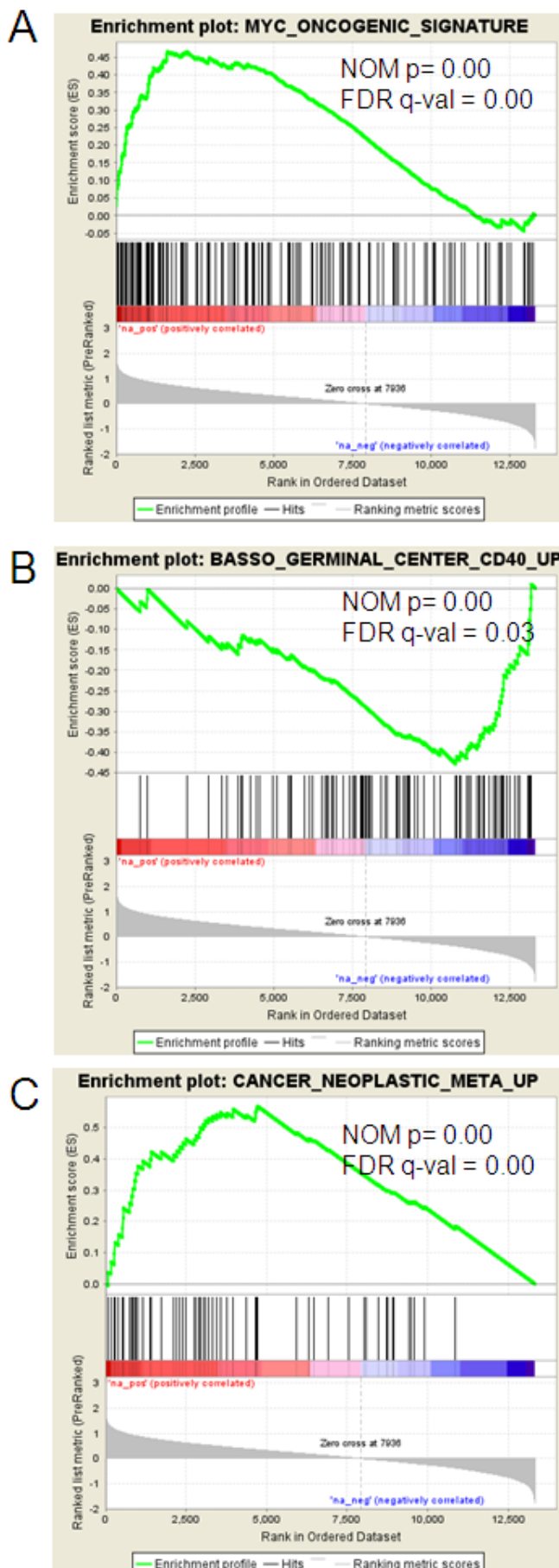


Figure 3-2 Gene set enrichment analysis (GSEA) of c-Myc responsive genes. Genes were ranked by their correlation with expression levels of *MYC* in decreasing order from the most positively correlated to most negatively correlated genes. GSEA enrichment scores (y-axis of the top panel) are plotted against the gene list ranked by correlation with *MYC*. **A** GSEA revealed a strong enrichment of a known c-Myc signature among the genes most correlated with c-Myc in our analysis. This is indicated by the sharp increase in the GSEA enrichment score to the left of the graph and a decrease to the right. **B** In contrast, a known CD40 signature is enriched among the genes negatively correlated with c-Myc. This is indicated by the gradual decrease of the GSEA enrichment score to the left of the graph, and a sharp increase to the right. **C** GSEA revealed an enrichment of a CANCER NEOPLASTIC META UP gene set which comprises genes that are upregulated in tumour cells relative to matching normal tissue cells across many tumour entities. For a detailed list of Gene Sets please see Table 3-1.

Manual inspection of the top 100 MYC correlated genes defining the c-Myc-index, revealed many of them to be involved in functions known to be modulated by c-Myc (Table 3-1 and Table A1 in the Appendix). The observed genes can be grouped to cellular activities as cell cycle regulation and proliferation, transcriptional regulation, chromatin remodelling and DNA-repair, cell metabolism and stress response, regulation of RNA processing and translation as well as cytokines, cell cell communication and intracellular signalling components or drug resistance. Genes involved in cell cell communication show a negative correlation with *MYC*, including the NF- κ B target *ICAM1/CD54* and the 'frizzled' receptor gene family member *FZD7* as part of the Wnt pathway. To test exemplarily for the reverse correlation of *FZD7* and *MYC* expression in lymphoma cell lines as well as in CD10+ germinal center B cells from tonsils qRT-PCR analyses were performed. *MYC* expression was found to be high in BL cell lines DG75, BL2, BL70 and Ramos, but also in cell lines MC116 and OCI-Ly1 and SuDHL4. In these cells *FZD7* expression is detected only at low amounts or is absent (Figure 3-3, page 64). In contrast cell lines OCI-Ly3, HT, OCI-Ly7, SuDHL6 show the opposite pattern. All analysed CD10+ cells from tonsils are clearly characterised by a nearly undetectable *MYC* expression but high for *FZD7*. Thus we conclude that there is an inverse correlation between *MYC* and *FZD7* expression reflecting the described c-Myc index.

3.1.3 Very high expression of c-Myc target genes is a hallmark of molecular Burkitt lymphomas

In a next step the expression of *MYC* co regulated genes was investigated in two independent data sets of aNHL samples. These include the previously mentioned cohort of 220 cases published by Hummel and colleagues and the dataset published by the LLMPP consortium (Dave, Fu et al. 2006). The expression levels of 100 genes in our ranked list were aggregated into a single c-Myc index score for each lymphoma sample (Figure 3-4 A&B page 65, Table A1). The c-Myc index was used as a surrogate marker of c-Myc activity, which is robust to random fluctuations of individual gene expression measures. The c-Myc index measures the extent to which an individual lymphoma expresses genes that are responsive to c-Myc.

Results

Table 3-1 Top 100 genes correlated with MYC in GC B cells and aNHL: The c-Myc index.

Genes that are correlated with *MYC* in primary transfected GC B cells as well as in gene expression profiles of aNHL are listed below. Genes are ordered according to assumed cellular functions and the calculated t-scores. The Pearson Correlation for being expressed in correlation with *MYC* is also given for each gene.

Probeset ID	Cellular activity/gene name	Gene name	MYC correlation	t score
metabolism				
204290_s_at	ALDH6A1	aldehyde dehydrogenase 6 family, member A1	0.52	3.64
209092_s_at	GLOD4	glyoxalase domain containing 4	0.51	2.81
203150_at	RABEPK	Rab9 effector protein with kelch motifs	0.60	2.68
221551_x_at	ST6GALNAC4	ST6 (alpha-N-acetyl-neuraminy-2,3-beta-galactosyl-1,3)-N-acetylgalactosaminide alpha-2,6-sialyltransferase 4	0.53	1.82
201892_s_at	IMPDH2	IMP (inosine monophosphate) dehydrogenase 2	0.54	1.79
210868_s_at	ELOVL6	ELOVL family member 6, elongation of long chain fatty acids (FEN1/Elo2, SUR4/Elo3-like, yeast)	0.49	1.61
208700_s_at	TKT	transketolase	0.53	1.52
211715_s_at	BDH1	3-hydroxybutyrate dehydrogenase, type 1	0.56	1.49
216659_at	LOC1720	dihydrofolate reductase pseudogene	-0.51	-2.47
213572_s_at	SERPINB1	serpin peptidase inhibitor, clade B (ovalbumin), member 1	-0.59	-4.48
208949_s_at	LGALS3	lectin, galactoside-binding, soluble, 3	-0.52	-4.99
Cytokines / cell cell interaction				
209591_s_at	BMP7 (BMP signalling)	bone morphogenetic protein 7	0.56	2.23
209100_at	IFRD2 (Growth factor receptor)	interferon-related developmental regulator 2	0.51	1.94
37408_at	MRC2 (Migration and ECM interaction)	mannose receptor, C type 2	-0.49	-1.76
221378_at	CER1	cerberus 1, cysteine knot superfamily, homolog (Xenopus laevis), BMP antagonist	-0.51	-1.76
211287_x_at	CSF2RA (Growth factor receptor)	colony stimulating factor 2 receptor, alpha, low-affinity (granulocyte-macrophage)	-0.50	-2.09
203175_at	RHOG (G protein coupled Signals)	ras homolog gene family, member G (rho G)	-0.49	-2.50
210904_s_at	IL13RA1 (JAK/STAT signalling)	interleukin 13 receptor, alpha 1	-0.51	-2.85

221958_s_at	GPR177 (G protein coupled Signals)	G protein-coupled receptor 177	-0.54	-3.03
202637_s_at	ICAM1 (cell adhesion and NF-kappaB signalling)	intercellular adhesion molecule 1	-0.51	-3.33
208302_at	HMHB1/HLA-HB1	histocompatibility (minor) HB-1, CTL-response, expressed in EBV-positive B cells	-0.50	-3.50
203706_s_at	FZD7 (Wnt signalling)	frizzled homolog 7 (Drosophila)	-0.49	-4.55
cell cycle / proliferation				
221965_at	MPHOSPH9	M-phase phosphoprotein 9	0.49	2.79
203847_s_at	AKAP8	A kinase (PRKA) anchor protein 8	0.49	2.45
200955_at	IMMT	inner membrane protein, mitochondrial (mitofilin), proliferation induced	0.53	2.14
201970_s_at	NASP	nuclear autoantigenic sperm protein (histone-binding)	0.51	2.09
201856_s_at	ZFR	zinc finger RNA binding protein	0.50	1.62
212899_at	CDC2L6	cell division cycle 2-like 6 (CDK8-like)	-0.59	-4.09
mRNA processing / translation regulation / stability				
200014_s_at	HNRNPC	heterogeneous nuclear ribonucleoprotein C (C1/C2)	0.49	3.79
211787_s_at	EIF4A1	eukaryotic translation initiation factor 4A, isoform 1	0.56	3.03
201530_x_at	(2 probesets)		0.53	2.17
208835_s_at	CROP	cisplatin resistance-associated overexpressed protein / spliceosome	0.54	2.59
217810_x_at	LARS	leucyl-tRNA synthetase	0.53	2.34
208765_s_at	HNRNPR	heterogeneous nuclear ribonucleoprotein R	0.52	2.24
208766_s_at	(2 probesets)		0.55	2.22
211930_at	HNRNPA3	heterogeneous nuclear ribonucleoprotein A3	0.50	2.19
213614_x_at	EEF1A1	eukaryotic translation elongation factor 1 alpha 1	0.51	1.96
215963_x_at	RPL3P7	ribosomal protein L3 pseudogene 7	0.49	1.77
200005_att	EIF3D	eukaryotic translation initiation factor 3, subunit D	0.49	1.20
stress response				
201841_s_at	HSPB1	heat shock 27kDa protein 1	0.49	4.00
215792_s_at	DNAJC11	DnaJ (Hsp40) homolog, subfamily C, member 11	0.63	2.47

Results

211969_at	HSP90AA1	heat shock protein 90kDa alpha (cytosolic), class A member 1	0.55	2.22
Intracellular Signalling				
transcription factors / regulators / scaffolds				
212945_s_at	MGA	MAX gene associated	0.64	5.15
213584_s_at	CREBZF	CREB/ATF bZIP transcription factor	0.56	4.76
209750_at	NR1D2	nuclear receptor subfamily 1, group D, member 2/RORa response associated	0.49	3.30
205446_s_at	ATF2	activating transcription factor 2	0.57	3.22
206912_at	FOXO1	forkhead box E1 (thyroid transcription factor 2)	0.51	2.92
203150_at	RABEPK	Rab9 GTPase effector protein with kelch motifs	0.60	2.68
210543_s_at 208694_at	PRKDC (2 pobesets)	protein kinase, DNA-activated, catalytic polypeptide (DNA repair / gene transcription)	0.59 0.51	1.95 1.62
218406_x_at	NENF	neuron derived neurotrophic factor/activator of Erk/Akt	-0.51	-2.20
203349_s_at	ETV5	ets variant 5	-0.56	-2.26
215228_at	NHLH2	nescient helix loop helix 2/bHLHa34	-0.53	-2.85
35254_at	TRAFD1	TRAF-type zinc finger domain containing 1	-0.49	-3.66
209785_s_at	PLA2G4C	phospholipase A2, group IVC (cytosolic, calcium-independent) produces precursors of signalling molecules	-0.59	-5.78
phosphatases				
216181_at	SYNJ2	synaptojanin 2/inositol-polyphosphate-5- phosphatase	0.55	2.31
219264_s_at	PPP2R3B	protein phosphatase 2 (formerly 2A), regulatory subunit B", beta	0.51	1.73
203030_s_at	PTPRN2	protein tyrosine phosphatase, receptor type, N polypeptide 2	-0.51	-3.34
204015_s_at	DUSP4	dual specificity phosphatase 4	-0.55	-3.53
Chromatin remodelling / DNA-repair				
41386_i_at	JMJD3	jumonji domain containing 3, histone lysine demethylase	0.52	3.93
217815_at	SUPT16H	suppressor of Ty 16 homolog (S. cerevisiae)/FACT complex part	0.53	1.94
200957_s_at	SSRP1/FACT	structure specific recognition protein 1	0.59	1.84
201115_at	POLD2	polymerase (DNA directed), delta 2, regulatory subunit 50kDa	0.58	1.82
201072_s_at	SMARCC1	SWI/SNF related, matrix associated, actin dependent regulator of chromatin, subfamily c, member 1	0.49	1.73

218788_s_at	SMYD3	SET and MYND domain containing 3 histone methyltransferase	0.49	1.45
209731_at	NTHL1	nth endonuclease III-like 1 (E. coli)	0.53	1.15
40446_at	PHF1	PHD finger protein 1/polycomb protein	-0.53	-2.17
211373_s_at	PSEN2	presenilin 2 (Alzheimer disease 4)	-0.55	-3.53
Drug resistance				
212282_at	TMEM97	transmembrane protein 97	0.53	1.97
213485_s_at	ABCC10	ATP-binding cassette, sub-family C (CFTR/MRP), member 10	-0.52	-2.58
Other				
220459_at	MCM3APAS	MCM3AP antisense RNA (non-protein coding)	0.52	3.00
50314_i_at	C20orf27	chromosome 20 open reading frame 27	0.64	2.91
210157_at	C19orf2 (2 probesets)	chromosome 19 open reading frame 2	0.59	2.62
214173_x_at			0.50	1.44
65472_at	C2orf68 2 probesets	chromosome 2 open reading frame 68	0.51	2.54
221878_at			0.51	2.50
218437_s_at	LZTFL1	leucine zipper transcription factor-like 1	0.50	2.20
204559_s_at	LSM7	LSM7 homolog, U6 small nuclear RNA associated (S. cerevisiae)	0.56	1.82
220736_at	SLC19A3	solute carrier family 19, member 3	-0.52	-2.00
220297_at	BTBD7	BTB (POZ) domain containing 7	-0.49	-2.02
206573_at	KCNQ3	potassium voltage-gated channel, KQT-like subfamily, member 3	-0.54	-2.20
220519_s_at	LIM2	lens intrinsic membrane protein 2, 19kDa	-0.49	-2.22
215770_at	LOC100133572	similar to seven transmembrane helix receptor	-0.55	-2.22
217783_s_at	YPEL5	yippee-like 5 (Drosophila)	-0.51	-2.23
206299_at	FAM155B	family with sequence similarity 155, member B	-0.51	-2.32
215754_at	SCARB2/CD36L2	scavenger receptor class B, member 2	-0.50	-2.46
219106_s_at	KBTBD10	kelch repeat and BTB (POZ) domain containing 10	-0.51	-2.47
203242_s_at	PDLIM5	PDZ and LIM domain 5	-0.53	-2.56
220476_s_at	C1orf183	chromosome 1 open reading frame 183	-0.50	-2.59
210135_s_at	SHOX2	short stature homeobox 2	-0.53	-2.87
218765_at	SIDT2	SID1 transmembrane family, member 2	-0.49	-3.00
205138_s_at	UST	uronyl-2-sulfotransferase	-0.50	-3.56

Results

215734_at	C19orf36	chromosome 19 open reading frame 36	-0.55	-3.75
218945_at	C16orf68	chromosome 16 open reading frame 68	-0.50	-4.56
217220_at	NA		-0.60	-4.25
212806_at	NA		-0.52	-3.10
220875_at	NA		-0.51	-2.23
220713_at	NA		0.49	3.64
217166_at	NA		0.52	1.72

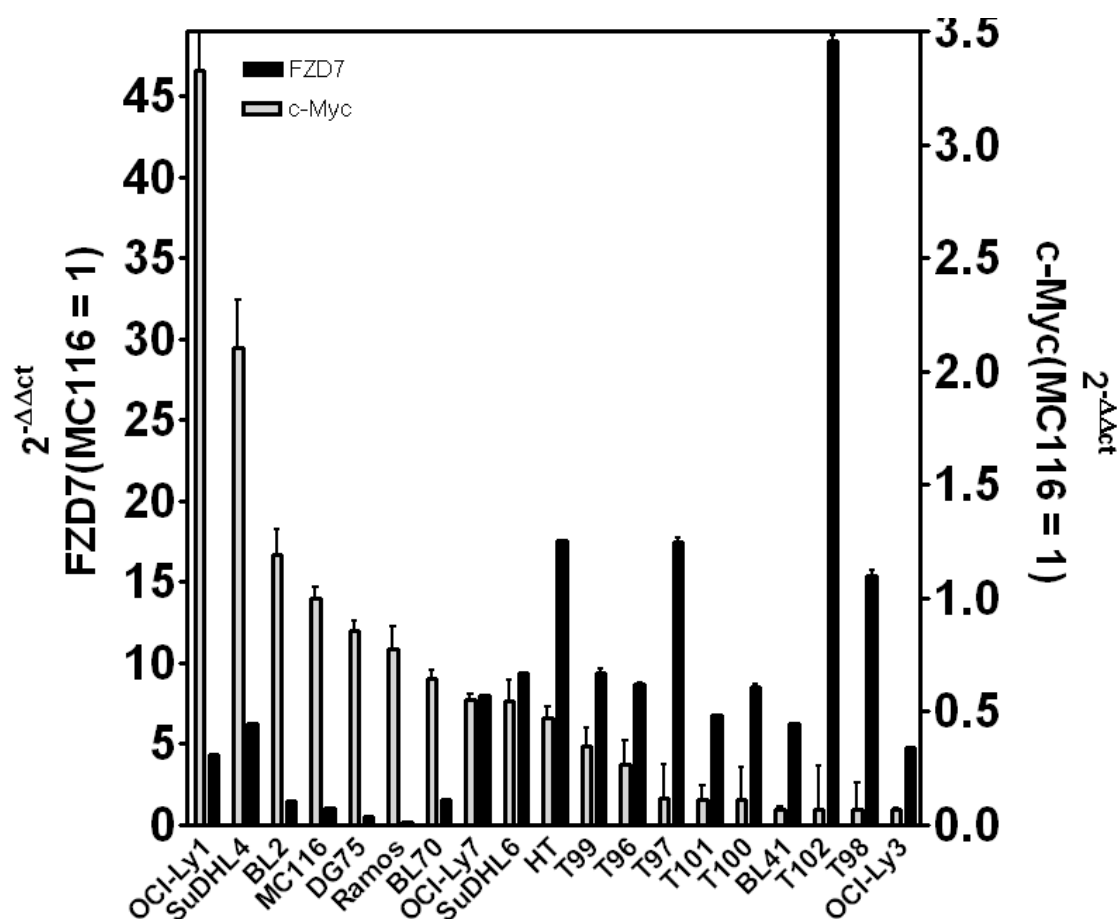


Figure 3-3 *FZD7* expression is high in lymphoma precursor cells but reduced in lymphoma cells and negatively correlated to *MYC*-gene expression. *FZD7* and *MYC* gene expression was assessed using qRT-PCR. Ct values were normalized to $\beta 2m$ expression and $\Delta\Delta Ct$ values were calculated compared to respective gene expression in MC116 lymphoma cells. T99, T96, T97, T98, T101 and T102 represent different preparations of tonsillar B cells purified by CD10 MACS. All other analysed samples represent different lymphoma cell lines.

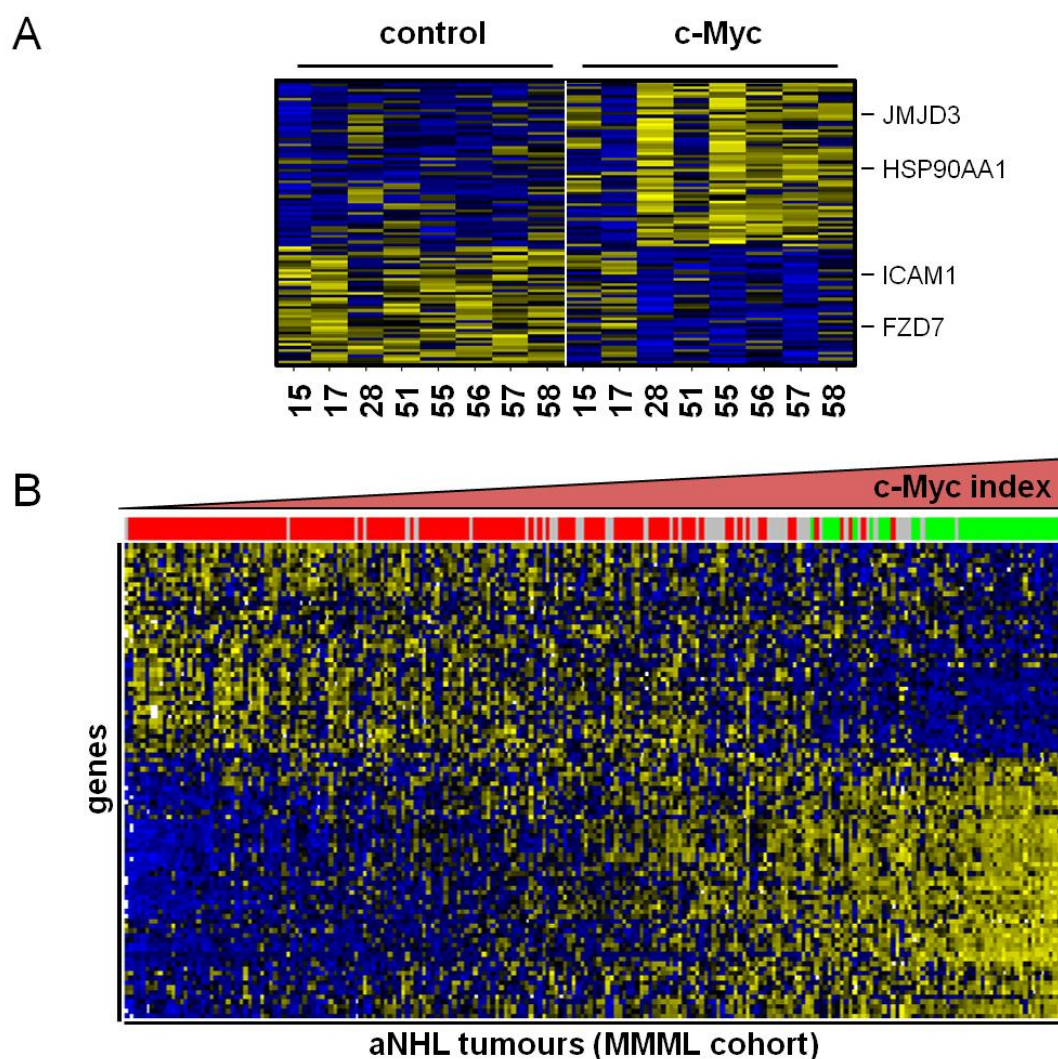


Figure 3-4 Stratification of NHL patients in mBL and non mBL by expressing c-Myc in GC B cells. Each row in the heatmaps represents a gene and each column represents a microarray sample. The expression levels for each gene were standardized to a mean value of 0 and a standard deviation of 1, and are represented according to a color scale; yellow and blue indicate high and low expression, respectively. **A** Heatmaps of genes expressed in GC B cells that show a correlation to *MYC* in tonsillar samples and 220 NHL samples (Hummel, Bentink et al. 2006). **B** Heatmap of gene expression levels of the same genes plotted in (A) this time in 220 NHL samples (Hummel, Bentink et al. 2006) recently classified as mBL, non-mBL or intermediate cases. This classification is colour coded in the top bar (green: mBL, red: non-mBL, grey: intermediate). The patients are arranged according to c-Myc index (increasing from left to right).

3.1.4 High expression of c-Myc inducible genes in the group of non-mBL and intermediate lymphomas is associated with shorter overall survival

Analyses of the c-Myc index across the lymphoma subgroups of 220 aNHL specimens revealed that mBLs consistently showed a higher c-Myc index than

did non-mBLs. This is in line with the assumption that the *IG-MYC* translocation and the resulting aberrant *MYC* expression is the major contributor to the malignant phenotype of BL (Figure 3-5 A&B; see also Figure 3-4 B). Furthermore, other groups of lymphomas defined by their genetic background also show significantly different c-Myc activities. Thus, Figure 3-5 B shows that on average, cases without *MYC* aberrations show the lowest c-Myc index. In contrast, the c-Myc index is higher in cases harbouring *MYC* breakpoints in a background of other complex genetic aberrations and is consistent with a contribution of c-Myc to the pathogenesis of these tumours. The c-Myc induced gene expression pattern is also expressed in lymphoma classified as non-molecular BL.

In the study group of aNHL cases analysed here (MMML cohort) 80% of non-mBL and intermediate cases consisted of DLBCLs. All molecularly defined non-mBL and intermediate lymphomas were ranked according to their c-Myc index and classified into four equally sized groups which were defined as c-Myc very low, low, medium and high. The Kaplan Meier curves in Figure 3-5 C demonstrate a poorer overall survival for patients with non-mBL and intermediate lymphomas that display a high c-Myc index. Significance of the differences between groups was calculated using the log rank test.

Moreover, multivariate Cox regression analysis accounting for the established risk factors of age, Ann Arbor stage, and the ABC/GCB status revealed that the effect of a c-Myc index classified as high on survival was independent of these factors (n=88; hazard ratio for death: 4.2; 95% CI: 1.5-10.1; P=0.0014). To test if the poorer outcome of patients with high c-Myc index tumours can be explained just by the presence of a *MYC* break, which has been shown to be associated with shorter overall survival (Hummel, Bentink et al. 2006), the *MYC* break was included as additional factor in the Cox model. In this model a high c-Myc index is associated with a 3.4 fold increased risk of earlier death, independent of a *MYC* break in these lymphomas (n=86; high c-Myc index: hazard ratio for death: 3.4; 95% CI: 1.4-8.3; P=0.008).

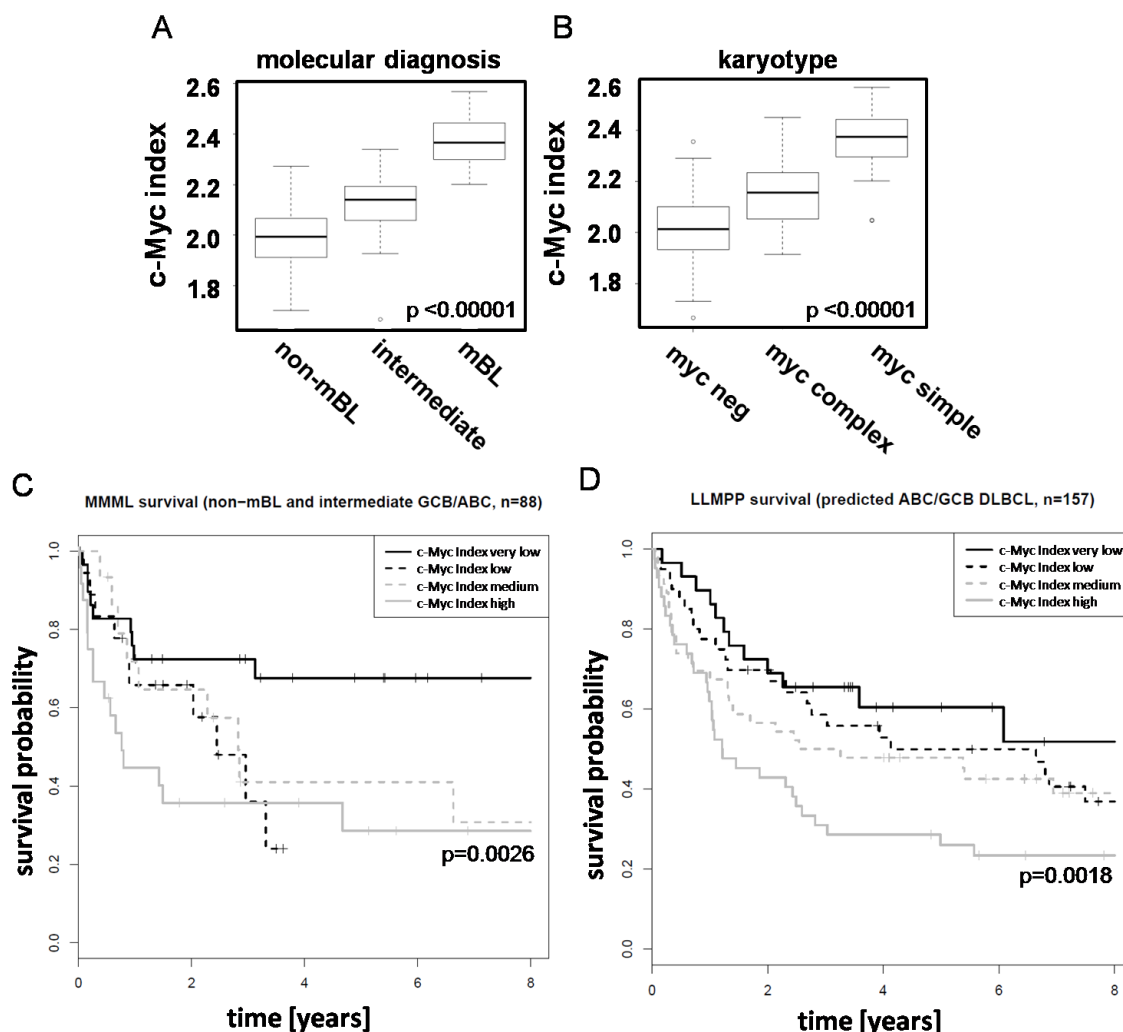


Figure 3-5 High expression of c-Myc index genes in the group of non-mBL and intermediate lymphomas is associated with shorter overall survival **A** Boxplots of the level of the c-Myc index (y-axis) in NHL lymphomas classified as non-mBL, intermediate and mBL (x-axis). **B** Boxplots of the level of the c-Myc expression index (y-axis) in NHL lymphomas classified as *MYC*-negative, *MYC*-complex and *MYC*-simple (x-axis). Statistical significance of the differences was tested using ANOVA. (**C**&**D**) Kaplan Meier plots of the overall survival of non-mBL and intermediate patients stratified by the c-Myc expression index **C** 88 non-mBL and intermediate patients samples (MMML) were stratified based on the level of their c-Myc expression index into tumours of very low, low, medium and high c-Myc activity. Patients with a tumour of high c-Myc activity have the shortest overall survival (grey continuous line). **D** 157 DLBCL patients of the data set published by Dave and colleagues (LLMPP) were grouped as in (**C**). Patients with high c-Myc index showed shorter overall survival. Statistical significance of the differential survival of these groups was tested using the log rank test.

The finding that a high c-Myc index was associated with shorter survival was confirmed in a subgroup of DLBCL patients (n=157) of the dataset published by Dave and colleagues (LLMPP). Since these data were generated on a different array platform, a truncated c-Myc index build from signature genes that are

present on both arrays was used for this analysis. Patients with DLBCL displaying a high c-Myc index were shown to have a significantly shorter overall survival (n=157; hazard ratio for death: 2.0; 95% CI: 1.0-3.8; P=0.045) (Figure 3-5 D).

These results point to an important deregulated function for c-Myc in non-mBL cases, which is not necessarily dependent on the c-Myc translocation, but possibly on other mechanisms that have not been identified so far. The newly described c-Myc index comprises genes that are affected in a variety of tumours compared to normal tissue. This supports the view that aberrant c-Myc expression in GC B cells triggers a tumour like expression pattern. As expected, the c-Myc index is very high in mBL, but more importantly also high within other aNHL. It constitutes a negative prognostic marker independent of established risk factors and of the presence of a *MYC* translocation.

3.2 Activation of BL cells with B cell specific microenvironmental factors triggers global changes in gene expression patterns useful to define pathway activity in individual lymphoma

The microenvironment is a dominant factor for most B cell lymphoma. An improved understanding of signalling modules or their effectors that might play a role in tumour-microenvironment interaction are important to understand elements potentially involved in cell transformation. It is likely that immune response associated signals like B cell receptor activation, innate antigen LPS stimulation or co stimulatory signals mediated via CD40L, B cell activating factor (BAFF) and Interleukin 21 (IL21) are specific mediators in B cell transformation. These stimuli were used to identify modules of genes which can then be utilized to infer on the respective stimulus activity in gene expression profiles of aNHL tumours. In pretests performed in the group of D. Kube it was observed that gene expression changes induced by CD40L in BL cells are probably useful to describe pathway activities in aNHL.

In the present study additional stimuli were utilized that are capable of activating overlapping (e.g. NF- κ B) as well as specific pathways (e.g. JAK-STAT signalling) and thereby mimic oncogenic activities. To infer on the global response of

lymphoma cells the major patterns of gene expression changes in response to the different stimulations were investigated *in vitro* and subsequently used to identify respective patterns in primary lymphoma.

3.2.1 anti-IgM, CD40L, IL21, BAFF and LPS stimulation activate an individual, partially overlapping pattern of pathways upon stimulation of Burkitt Lymphoma cells

The BL cell line BL2 was stimulated in triplicate using anti-IgM antibody to achieve BCR activation (BCRx), recombinant human CD40 ligand (CD40L), recombinant human BAFF (BAFF), recombinant human IL21 (IL21) and LPS to achieve TLR4 activation. To describe the effects of these stimuli on the BL cell line the activation of the following pathways was determined: Ca^{2+} influx, NF- κ B signalling (canonical and noncanonical), MAPK signalling (ERK, p38, JNK), PI3K/AKT signals and JAK/STAT signalling via STAT1 and STAT3. The activation of pathways was monitored using flow cytometry based measurement of Ca^{2+} influx, immunoblots specifically detecting phosphorylation of key pathway components and a kinase assay for the detection of JNK activity. This kinase assay was performed as follows: BL2 cells were transfected with a JNK-HA expression construct. After 24hrs the cells were stimulated with the respective agent for 30mins and subsequently harvested. Cell lysates were incubated with recombinant c-Jun in presence of radioactive phosphor. The induced kinase activity could be verified by detecting phosphorylated c-Jun.

As shown in Figure 3-6 anti IgM treatment of BL cells induces a strong calcium signal. This is expressed by a sharp increase of intracellular Ca^{2+} levels after 5 seconds of anti-IgM stimulation. The Ca^{2+} influx was measured using a specific fluorescent dye that changes the spectrum of emitted light upon binding to Ca^{2+} and flow cytometric analysis of stained cells (Figure 3-6 A). CD40L, BAFF, LPS or IL21 are unable to induce a Ca^{2+} influx. The activation of NF- κ B pathways was detected by monitoring the reduced levels of the NF- κ B inhibitor I κ B α as marker for canonical NF- κ B activity. The cleavage of the p100 (NFKB2) precursor to the p52 form is monitored as marker for noncanonical NF- κ B activity. In contrast to effective induction of Ca^{2+} signals, the activation of the canonical and noncanonical NF- κ B pathway in response to BCRx is only marginal, whereas

CD40L strongly activates noncanonical NF- κ B (Figure 3-6 B & C). The MAPKs p38 (pp38), JNK (p-c-Jun) and ERK (p-ERK) are all activated upon BCR crosslink (Figure 3-6 D-F). Furthermore BCRx leads to the activation of the PI3K/AKT pathways as detected by phosphorylation of AKT upon 30 minutes of anti-IgM stimulation (Figure 3-6 G). The stimulation of BL2 cells with CD40L leads to the activation of canonical and noncanonical NF- κ B pathways (Figure 3-6 B & C). Furthermore an activation of p38 and JNK MAPKs can be detected (Figure 3-6 E&F). In contrast to BCRx an activation of ERK upon CD40L stimulation is not detectable (Figure 3-6 D). BAFF treatment is associated with a low activation of canonical NF- κ B signalling (Figure 3-6 B) and as well a low activation of the noncanonical NF- κ B pathway (Figure 3-6 C). Nevertheless the p38 pathway is induced comparable to BCR crosslink and CD40 activation (Figure 3-6 E). Activation of the PI3K/AKT pathway, as described already for BAFF stimulation (Badr, Borhis et al. 2008), cannot be observed in BL2 cells (Figure 3-6 G). The incubation of BL2 cells with LPS is accompanied with the activation of the canonical NF- κ B pathway but with a delayed kinetic when compared to CD40L (data not shown). An activation of p38 by LPS can only be observed under serum deprivation (Figure 3-6 E). The stimulation of BL2 cells with IL21 is associated with the activation of the STAT1 and STAT3 pathway as shown by the respective phosphorylation of STAT1 and STAT3 (Figure 3-6 H&I). STAT5 and STAT6 were found to be activated to a lesser extend (data not shown). An activation of ERK by IL21, as published by Fuqua and colleagues, cannot be observed in BL2 cells (Figure 3-6 G) (Fuqua, Akomeah et al. 2008).

These results show that the BL cell line BL2 is in general responsive to each of the utilized stimuli and that overlapping as well as specific signalling pathways are activated upon stimulation. Overlapping pathways include for example the activation of p38 by BCRx and CD40L. Furthermore, noncanonical NF- κ B is activated by CD40L and to lesser extent by BAFF. The activation of JNK is limited to CD40L and BCRx. Pathways that are specifically activated by one stimulus include the activation of Ca²⁺, ERK and PI3K by BCRx or the activation of JAK-STAT signalling by IL21. Nevertheless this analysis cannot represent the complete pattern of activated pathways as not all possible time points could be captured for each pathway in response to each stimulus.

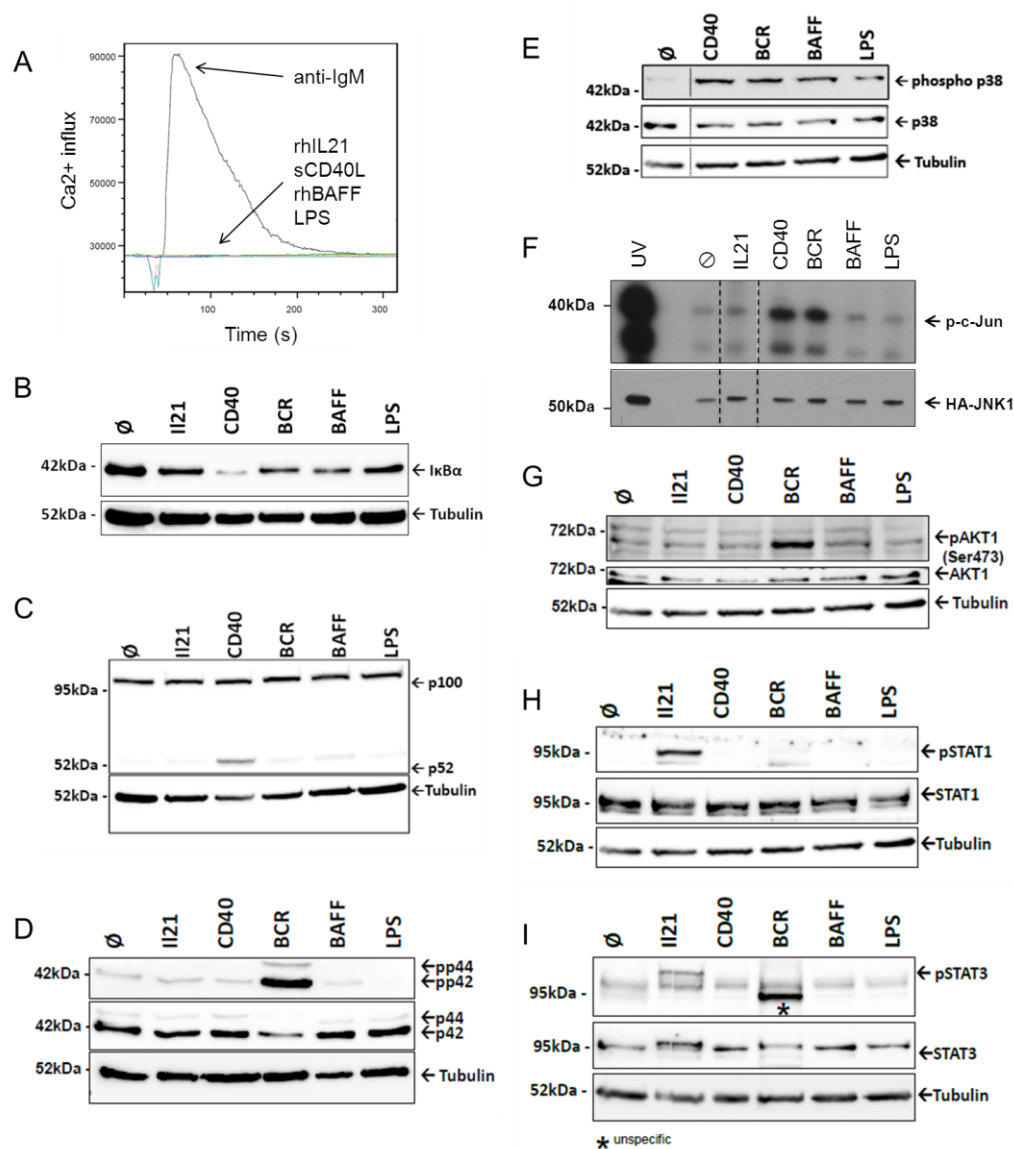


Figure 3-6 Different pathways activated by IL21, CD40L, anti-IgM (BCRx), BAFF and LPS in human Burkitt Lymphoma cells. BL2 cells were incubated with IL-21 (100ng/ml), CD40L (200ng/ml), anti IgM F(ab)₂ fragments (1.3μg/ml), BAFF (100ng/ml) and LPS (1μg/ml) for indicated time points. **A** The activation of calcium signalling was detected using a Ca^{2+} sensitive fluorophor in combination with flowcytometric analyses. BL2 cells were loaded with indo1 and Ca^{2+} influx was measured directly after the stimulation. BCRx (1.3μg/ml) induced an immediate Ca^{2+} accumulation in the cytoplasm as indicated by the increased Indo-1 fluorescence. **B** BL2 cells stimulated for 30mins as indicated above. The activation of canonical NF- κ B signalling was visualized by immunoblot of $\text{I}\kappa\text{B}\alpha$. **C** BL2 cells were stimulated for distinct time points (6hrs for CD40L and LPS, 3hrs for BCRx, 9hrs for BAFF and 2hrs for IL21 stimulation) as described in above. The activation of noncanonical NF- κ B signalling was detected monitoring the p52 cleavage product of p100 by immunoblot. **D** BL2 cells stimulated for 5mins as indicated above. The activation of ERK was shown through immunoblot analyses of phosphorylated ERK1/2. **E** BL2 cells were stimulated for 30mins as indicated in above. The activation of p38 was detected through detection of phosphorylated p38 via immunoblot. **F** *In vitro* kinase assay to investigate the activation of JNK in BL2 cells (Kutz, Reisbach et al. 2008). These data were kindly provided by A. Ulrich and A. Kieser. **G** BL2 cells were stimulated for distinct time points (6hrs for CD40L and LPS, 3hrs for BCR, 9hrs for BAFF and 2hrs for IL21 stimulation) as described in above. The activation of PI3K/AKT signalling was detected using immunoblot detection of phosphorylated AKT1. **H&I** BL2 cells were stimulated for 30mins as indicated above. The activation of

STAT1/STAT3 was detected through the verification of phosphorylated STAT1/STAT3 via immunoblot.

3.2.2 Global changes in gene expression profile through specific in vitro BL cell stimulation

To investigate the gene expression changes that are induced by the distinct stimuli in a global way, gene expression profiling was performed. Therefore for every stimulus the time points were chosen individually. Based on the above described activation of different pathways (3.2.1) and literature based analysis the utilized stimulation periods were defined in the following way: (i) Harvest cells as early as possible to avoid autocrine effects of mediated by the induced expression of cytokines in response to respective stimuli and (ii) Harvest cells as late as possible to get a transcriptional response strong enough to be detected using whole genome microarrays. As CD40L, LPS and BAFF have been described to activate noncanonical NF- κ B, longer time points (6hrs for CD40L and LPS, 9hrs for BAFF) were selected in this case. These were pretested. For BCRx and IL21, which mainly induce short term active signals, shorter time points were chosen (3hrs for BCRx and 2hrs for IL21). Probes were hybridized onto Affymetrix HG U133 plus 2.0 microarrays using three independent biological experiments. Data were analysed with support from K. Meyer/R. Spang from Regensburg. Genes which show a significant (adj. p value ≤ 0.05) change compared to unstimulated cells were considered.

The stimulation of BL2 cells through BCRx lead to the differential expression of 6596 genes. In the following the alterations of gene expressions are given as absolute logarithmic fold changes (logFC). Of these 3039 were upregulated with the highest absolute fold change of 5.5. 3557 genes showed significantly lower expression in response to BCRx with the highest absolute fold change of 2.7. This is the strongest response observed in this study. Activation of CD40 with CD40L alters the expression of 1194 genes (689 upregulated (logFC = 1.8); 496 downregulated (logFC = 2.0)). Stimulation of BL2 cells with IL21 induced the differential expression of 902 genes. Of these 463 genes were upregulated with a maximal absolute fold change of 3.15. 439 genes were found to be significantly downregulated in response to IL21 treatment (logFC = 1.936). BAFF stimulation

significantly affected 129 genes. Of these 89 genes were upregulated with a maximal absolute fold change of 5 ($\log_{2}FC = 0.8$). In response to BAFF the expression of 39 genes is significantly inhibited ($\log_{2}FC = 2.1$). Activation of BL cells with LPS induced the differential expression of 283 genes. Of these 114 genes are upregulated with a $\log_{2}FC$ of 1.1 and 169 show a reduced expression in response to LPS with a $\log_{2}FC$ of 1.9.. The genes differentially expressed with the highest fold changes were summarized in a heatmap (Figure 3-7). This dataset comprises a highly comprehensive amount of data. Therefore only specific differentially expressed genes will be considered for the detailed description in the following paragraph.

The effects of a prolonged CD40L stimulation (24hrs) on Ramos BL cells have been investigated previously by Basso and colleagues. They thereby obtained information suitable to mirror potential CD40 associated processes in the course of the germinal centre reaction (Basso, Klein et al. 2004). The group around Basso used an older version of arrays and thus identified a lower number of differentially expressed genes. Nevertheless they identified comparable global changes in gene expression in response to CD40L stimulation of BL cells. This is for example expressed by the regulation of the same target genes (e.g. *ICAM1*, *CD58*, *DUSP2* and *ID1*). This indicates that some genes are affected at earlier time points but are still detectable at later time points.

Furthermore in the study presented here it was observed that BCRx, CD40L and IL21 stimulation induce the largest changes in global gene expression profiles in BL2 cells. This observation is in line with the study of Zhu and colleagues from 2004 (Zhu, Hart et al. 2004). They investigated the gene expression changes in mouse splenic B cells in response to the stimulation with CD40L, LPS, BCRx, BAFF and 29 additional single ligands. Zhu and colleagues as well identified BCRx as the most potent inducer of gene expression changes. In contrast to the marginal effects of LPS on the global gene expression profile of BL cells, Zhu and colleagues observed a change in gene expression in response to LPS that is comparable to anti-IgM treatment. This could be explained by the distinct cell systems used. Zhu and colleagues used primary mouse B cells whereas the presented study focuses on the effects of the distinct stimuli on lymphoma cells.

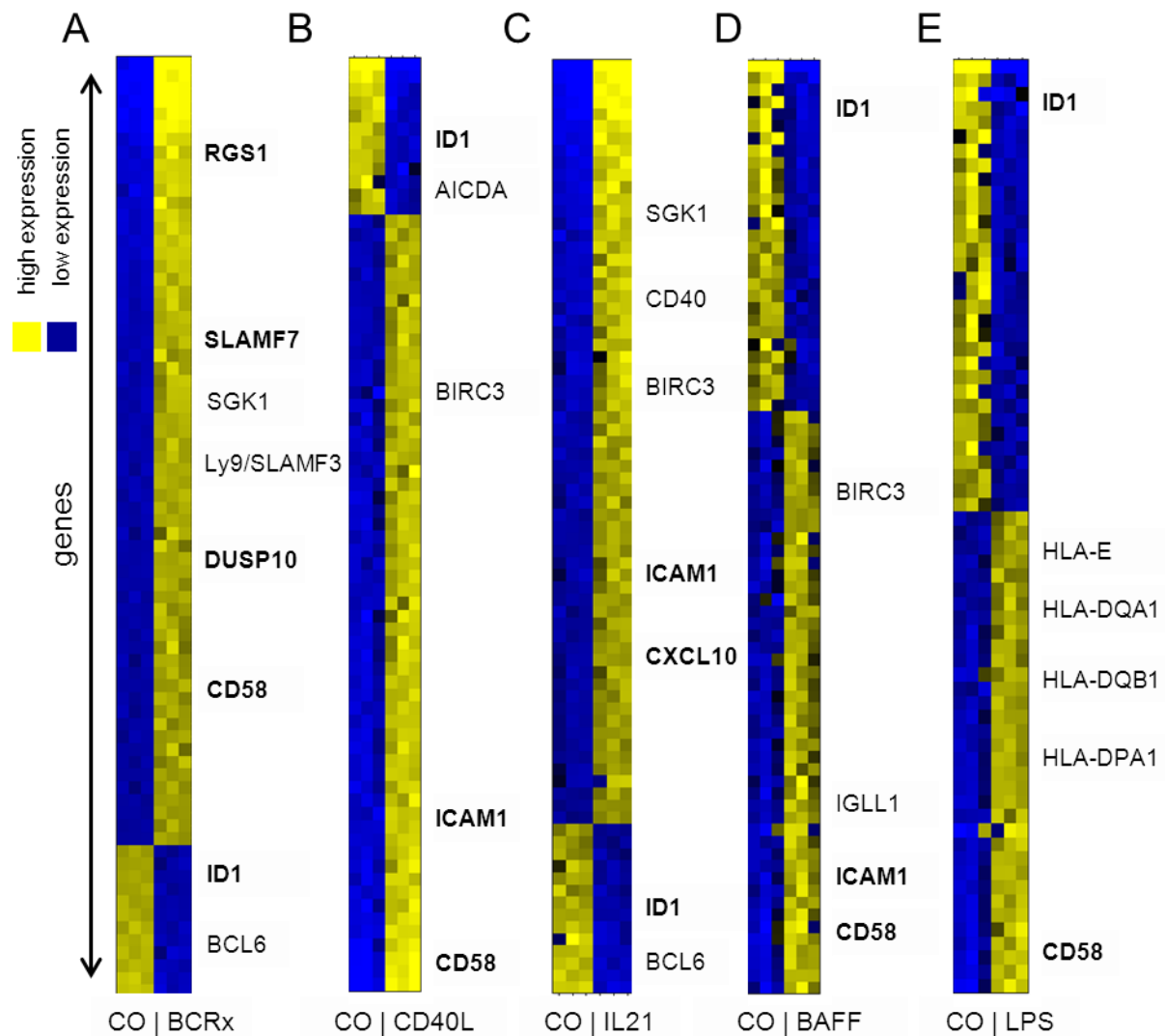


Figure 3-7 Identification of anti-IgM (BCRx), CD40L, IL-21, BAFF and LPS regulated genes in BL cells using microarrays. BL2 cells were stimulated as described in Figure 3-6 with **A** anti IgM F(ab)₂ fragment (3hrs), **B** CD40L (6hrs), **C** IL21 (2hrs), **D** BAFF (9hrs) and **E** LPS (6hrs). RNAs from these cells were used to perform whole genome gene expression profiling on Affymetrix HGU-133 plus 2.0 microarray chips. These heatmaps show the TOP 100 most highly changed genes (adj. p-value ≤ 0.05) in response to each stimulus. As distinct microarray chips were used for the microarray analyses of cell perturbation and patient samples (Affymetrix HGU-133A and HGU-133 plus2.0), the list of TOP100 genes had to be adapted to be able to transfer the resulting genes to patient data (see below for additional details). Therefore the lists were shortened since not all probesets were present on both array platforms (BCRx (74 genes), sCD40L (71 genes), rhBAFF (77 genes), rhIL21 (77 genes) and LPS (66 genes)). Each row in the heatmaps represents a gene and each column represents a microarray sample. Yellow and blue indicate high and low expression, respectively.

3.2.3 Distinct stimuli induce the differential expression of overlapping as well as specific target genes

As shown in chapter 3.2.1 BL2 cells activate overlapping as well as specific signalling pathways upon stimulation. Overlapping pathways include for example the activation of p38 by BCRx and CD40L, the activation of noncanonical NF- κ B by CD40L and to lesser extent by BAFF. Furthermore JNK is commonly activated by CD40L and BCRx. Pathways that are specifically activated by one stimulus include for example the activation of Ca²⁺, ERK and PI3K by BCRx or the activation of JAK-STAT signalling by IL21. Corresponding to this observation in the following paragraph differentially expressed genes which are specifically affected only by one of the stimuli as well as differentially expressed genes which are regulated in response to more than one stimulus will be analysed in more detail. Therefore the lists of genes showing the highest differential expression (see table A2- A6 in the Appendix) in response to BCRx, CD40L, IL21 and BAFF were compared. To allow an overview of genes that are affected on high levels in response to the stimulation the lists of the TOP regulated genes were used for a comparison using Venny (Oliveros 2007) (Figure 3-8 and 3-9). As BCRx, CD40L and IL21 stimulation affect a significantly higher number of genes some of the considered overlapping / specific genes could not be depicted in the utilized Venn Diagrams for all stimuli.

BL2 cells upregulate the expression of *ICAM1* in response to all utilized stimuli (Figure 3-8 and supplementary tables 1-5). *ICAM1* has been described as classical NF- κ B target as well as a STAT1 target gene (Audette, Larouche et al. 2001; Klapproth, Sander et al. 2009). BCRx affected genes furthermore include for example like *CD58*. *CD58* expression is as well upregulated in response to CD40L, BAFF, LPS stimulation, but not affected by IL21 stimulation (Figure 3-8). Genes upregulated by BCR activation as well include several factors involved in negative feedback loops, necessary for shutting down specific pathways. These include *DUSP1*, *DUSP2*, *DUSP5*, *DUSP10*, *DUSP16* and *DUSP22* (Figure 3-8, supplementary table 1), that can dephosphorylate and thereby inhibit MAPKs (Keyse 2008). It can be observed that CD40 and LPS stimulation as well mediate the upregulation of *DUSP22* (supplementary tables 2 & 5). Interestingly a high

overlap can be observed comparing the lists of genes affected by BCRx and IL21 stimulation. IL21 stimulation for example as well induces the upregulation of *DUSP2* expression (Figure 3-8).

Additionally genes have been identified that are upregulated solely by one of the utilized stimuli. BCRx specifically affects genes which are involved in other feedback regulatory mechanisms. One of the strongest upregulated genes in response to BCRx is *RGS1* (Figure 3-8), which encodes a factor that can diminish the signalling activity of G-protein coupled receptors by binding to activated, GTP-bound G-alpha subunits (Blumer 2004). Factors that negatively regulate NF- κ B signalling like TNFAIP3/A20 are as well upregulated in response to BCRx (supplementary table 1). Interestingly IL21 stimulation upregulates the expression of *BCL3* which is a negative modulator of NF- κ B signalling (Figure 3-8) (Zhang, Didonato et al. 1994). Thus IL21 could probably affect NF- κ B signalling mediated by other stimuli.

Remarkably *SLAMF7* is found to be strongly upregulated upon BCR activation. *SLAMF7* is a lymphocyte cell surface signalling molecule which has been shown to be transcriptionally upregulated in response to anti-IgM treatment of Ramos cells and to induce proliferation and autocrine cytokine signalling in human B lymphocytes (Lee, Mathew et al. 2007) (Figure 3-8). The chemokine *CXCL10* is upregulated in response to rhIL21 stimulation (Figure 3-8). *CXCL10* has been implicated in the regulation of the host immune response to the tumour (Wendel, Galani et al. 2008).

Figure 3-8 Overview of high responsive overlapping and stimulus specific genes upregulated in response to BCRx, CD40L, rhBAFF and rhIL21. The lists of genes showing the highest differential expression in response to stimulation (see Appendix table A2, A3, A4, A5) were compared. This comparison was made using VENNY (Oliveros 2007). Genes upregulated in response to BAFF stimulation are represented in the blue ellipsoid (BCR = yellow, CD40L = green, IL21 = red). The overlaps of the gene lists are represented by overlaps of the respective ellipsoids. The number of genes in the respective overlap is indicated.

Results

rhIL21 stimulation (Figure 3-9). Interestingly, the expression of *MYC* was found to be inhibited in response to the activation of the BCR and will be analysed in more detail in the next paragraphs (supplementary table 1).

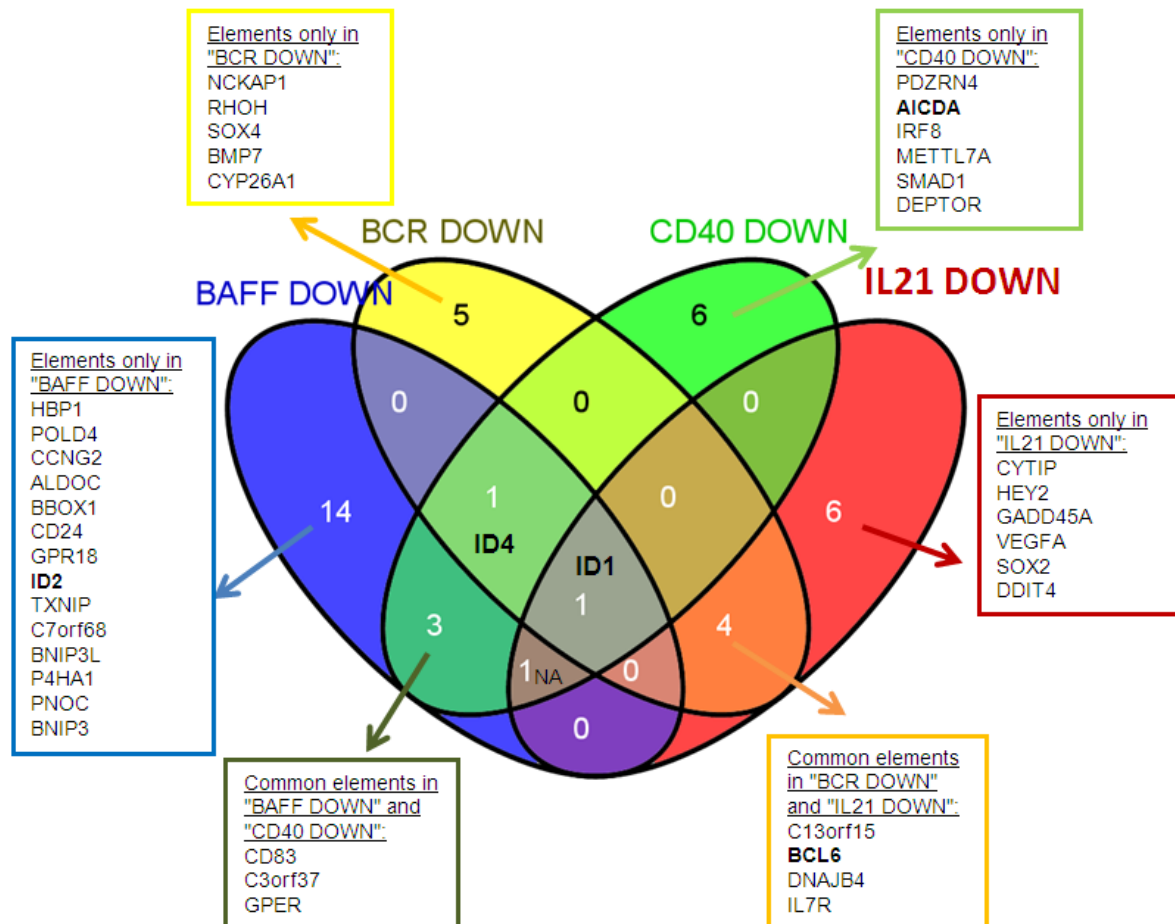


Figure 3-9 Overview of high responsive overlapping and stimulus specific genes downregulated in response to BCRx, CD40L, rhBAFF and rhIL21. The lists of genes showing the highest differential expression in response to stimulation (see Appendix table A2, A3, A4, A5) were compared. This comparison was made using VENNY (Oliveros 2007). For a detailed description see Figure 3-8.

Furthermore it was observed that distinct stimuli change the expression of the same gene in a different way. The expression of *AICDA* for example, is inhibited upon BCRx and CD40L stimulation, but activated upon IL21 stimulation (Figure 3-9 and supplementary tables 1 & 3). Thus it seems to be that the capacity of BL cells to undergo somatic hypermutations can be modulated by paracrine factors.

3.2.4 Investigation of differential gene expression using qRT-PCR

The regulation of a set of genes presented above was investigated using qRT-PCR of two independent stimulations (Figure 3-10 A-K). Stimulation was performed as described for the microarray experiments.

It was observed that *ID1* expression is strongly inhibited in response to all utilized stimuli thus supporting the microarray analyses (Figure 3-10 A). It was found that *ICAM1* expression is activated by all utilized stimuli. The IL21 stimulation has the highest impact on *ICAM1* activation suggesting a dominant function for JAK/STAT signalling for the regulation of this gene (Figure 3-10 B). *CD58* is activated dominantly by CD40L and BCRx treatment and to a lower extent by LPS and BAFF stimulation (Figure 3-10 C). Since various DUSPs have been identified as target genes the expression of *DUSP2*, *DUSP5*, *DUSP10* and *DUSP22* was investigated more detailed. *DUSP2* expression is found to be activated marginally by rhIL21 and strongly by BCRx. This is in line with the obtained array data (Figure 3-10 D). It can be observed that *DUSP5* expression is induced by BCRx (Figure 3-10 E). Comparable to the effects on *DUSP2* expression, *DUSP10* expression is activated in response to BCRx and marginally in response to IL21 stimulation (Figure 3-10 F). For *DUSP22* it can be observed that the activation of CD40 and BCR induces a 2 fold higher expression (Figure 3-10 G), whereas IL21 and LPS stimulation induce only a marginal increase of *DUSP22* mRNA levels. As previously shown the expression of *MYC* is found to be inhibited upon BCRx treatment. This is verified by qRT-PCR demonstrating a up to two fold decreased expression of *MYC* in response to BCR activation (Figure 3-10 H). Furthermore it is confirmed that this inhibition is a BCRx specific effect, which is not mediated by any of the other utilized stimuli. Additionally the expression of *CXCL10* was investigated. *CXCL10* expression is found to be prominently activated by IL21 stimulation, but also affected by sCD40L and LPS stimulation. (Figure 3-10 I). BCRx strongly induces the expression of *SLAMF7* and *RGS1*. This consolidates the studies performed by others (Lee; Jamal) (Figure 3-10 J&K). The results presented here show one representative experiment out of two. As these replicates are highly reproducible and as well comparable to the microarray results only two replicates were performed.

Results

These analyses show that the effects observed on the expression *ID1*, *ICAM1*, *CD58*, *MYC* as well as *SLAMF7* and *RGS1* detected by microarrays analyses can be confirmed in an independent experiment using qRT-PCR analyses. This holds as well true for the observed effects on the expression of the group of DUSPs.

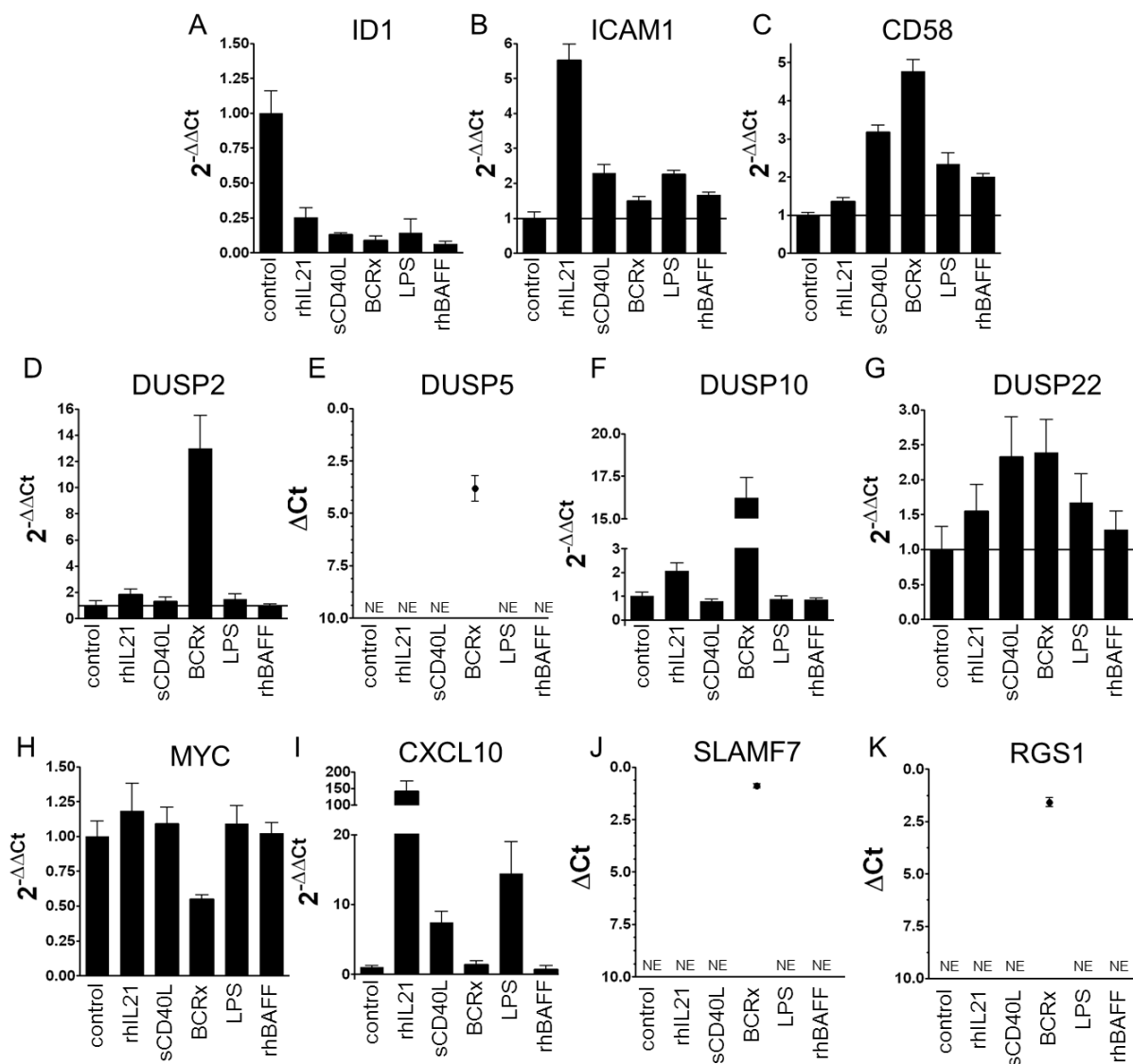


Figure 3-10 qRT-PCR analyses of the expression of a selection of genes after respective stimulation. BL2 cells were stimulated as described in Figure 3-7. One representative experiment out of two is shown. All samples were analysed in triplicates. Results are presented as $2^{-\Delta\Delta Ct}$ or ΔCt values, relative to abl housekeeper expression and compared to unstimulated control. N.E. = Not Expressed ($\Delta Ct > 10$) **A** *ID1* **B** *ICAM1* **C** *CD58*. **D** *DUSP2* **E** *DUSP5* (basal $\Delta Ct > 10$) **F** *DUSP10* **G** *DUSP22* **H** *MYC* **I** *CXCL10* **J** *SLAMF7* (basal $\Delta Ct > 10$) **K** *RGS1* (basal $\Delta Ct > 10$).

3.2.5 Stimulation mediated gene expression changes in lymphoma precursor cells

So far gene expression changes induced by BCRx, CD40L, IL21, BAFF and LPS have been described in BL2 cells. BL cells are used as B cell model in numerous studies as they are very close to GC B cells with respect to their differentiation status (Basso, Klein et al. 2004; Laskov, Berger et al. 2005; Ci, Polo et al. 2009). Nevertheless BL cells are transformed cells that harbour an aberrant c-Myc activity. To test whether BCRx, CD40L, IL21 and BAFF stimulation can mediate the differential expression of selected target genes in a distinct cell system that is close to lymphoma precursor cells, primary human tonsillar CD10⁺ B cells were used for further stimulation experiments. Effects of CD40 and BCR activation as well as IL21 and BAFF stimulation on the expression of a selected set of were investigated. Primary human tonsillar CD10⁺ B cells were isolated according to Vockerodt and colleagues (Vockerodt, Morgan et al. 2008; Vrzalikova, Vockerodt et al. 2011) from 6 distinct tonsillar specimens of paediatric patients (T96, T97, T98, T99, T101, T102). GC B cells were stimulated with 200ng/ml sCD40L, 1.3 µg/ml anti-IgM/anti-IgG F(ab)₂ fragments, 100ng/ml rhIL21 and 100ng/ml rhBAFF for 3hrs.

It was tested for the effects on *ICAM1* as dominantly regulated target gene. As only limited information is available so far regarding the regulation of DUSPs in human B cells, the effects of stimulation on *DUSP2*, *DUSP5*, *DUSP10* and *DUSP22* were investigated. Furthermore in BL2 cells BCRx mediates the differential expression of *MYC* and *SLAMF7*. It was tested whether the observed effects on the expression of these genes were transferable to non-malignant primary B cells (Figure 3-11).

It can be observed that *ICAM1* expression is significantly activated in all investigated biological replicates in response to sCD40L stimulation (Figure 3-11A). It was found that BCRx has a rather inhibitory effect on *ICAM1* expression in 2 of 6 biological replicates. Taking all biological replicates into account, this effect is not significant. The activatory effect of rhIL21 on *ICAM1* expression can be significantly shown in CD10⁺ B cells. rhBAFF treatment has no effect on the expression of *ICAM1*. These results are not directly comparable to the effects

observed in BL cells, where all stimuli lead to an upregulation of *ICAM1* expression. The expression of *DUSP2* is activated in response to CD40 and BCR activation in different biological replicates of stimulated CD10⁺ B cells to varying degrees (Figure 3-11 B). Taking into account the high variability between the biological replicates, only the BCR mediated activation of *DUSP2* expression is statistically significant. The stimulation with rhIL21 has a small inhibitory effect on the expression of *DUSP2*, which is consistent over the distinct replicates. The expression of *DUSP5* is affected on low levels by BCR crosslink (Figure 3-11 C). *DUSP10* expression is reproducibly activated in response to BCRx (Figure 3-11 D). The expression of *DUSP22* is highly variable comparing the distinct tonsillar preparations. Two of the samples show an activation of *DUSP22* expression in response to CD40 activation (Figure 3-11 E). Nevertheless it can only be observed in some of the biological replicates. It can be shown that *MYC* expression is significantly activated in response to CD40 and BCR activation (Figure 3-13 F). This observed upregulation of *MYC* is opposite to the inhibitory effect of BCRx on *MYC* expression in BL cells. *SLAMF7* expression is activated significantly and solely in response to BCRx (Figure 3-13 G).

In summary it was observed that *DUSP10* as well as *SLAMF7* are reproducibly activated in response to BCRx, whereas the activation of *MYC* or *ICAM1* seems to be context depended and therefore different in distinct biological replicates. Overall these results show that some stimulus mediated gene expression changes are indeed transferable to a distinct cell system. These include the regulation of *DUSP2*, *DUSP5*, *DUSP10* and *SLAMF7* in response to BCRx. Nevertheless some effects observed in BL cells in response to stimulation are cell specific. These include for example the inhibition of *MYC* expression in response to BCRx.

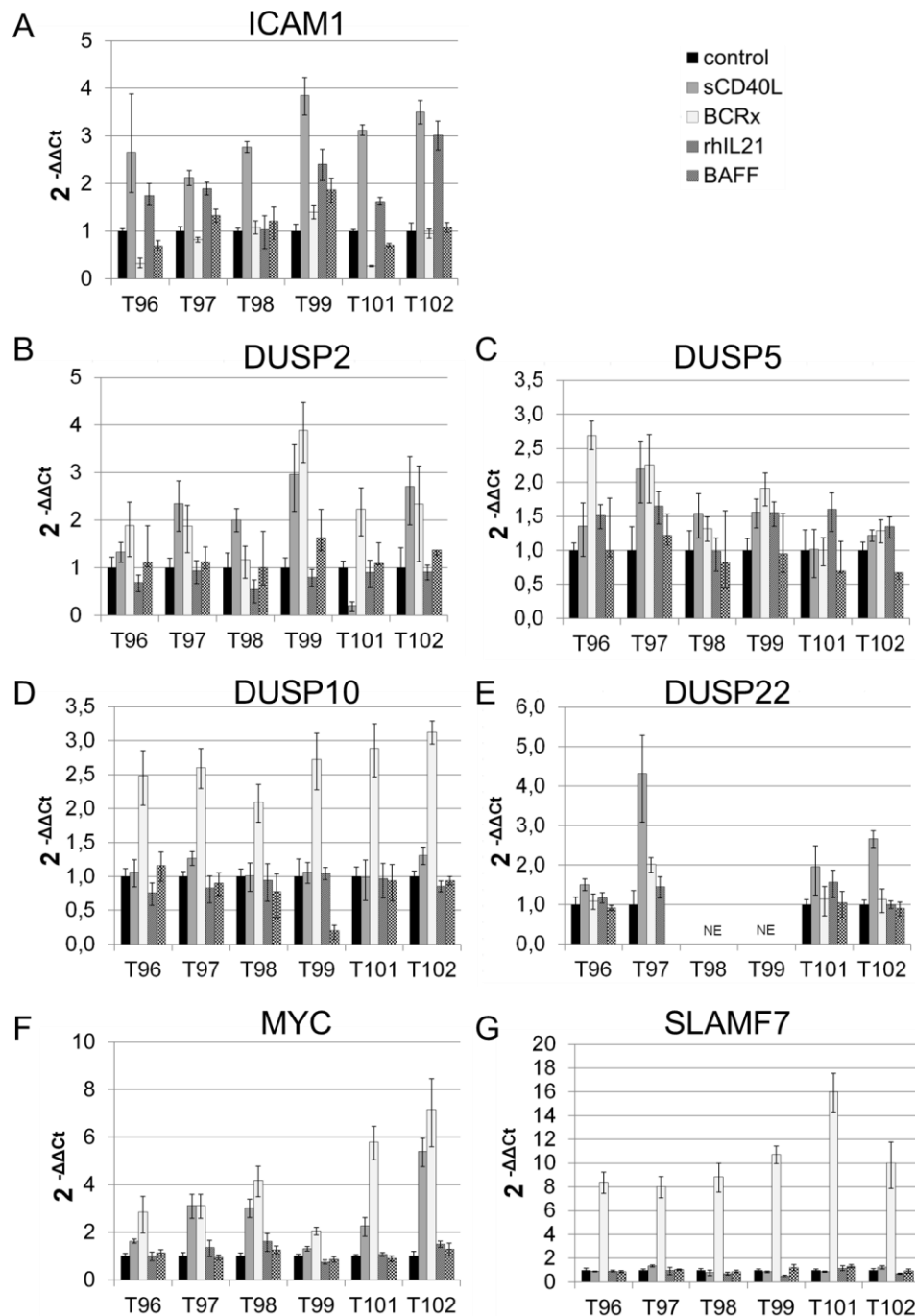


Figure 3-11 Expression of *ICAM1*, *DUSP2*, *DUSP5*, *DUSP10*, *DUSP22* and *MYC*, *SLAMF7* in CD10⁺ germinal centre B cells in response to sCD40L, BCRx, rhIL21 and rhBAFF stimulation CD10⁺ B cells from distinct tonsillar preparations (T96, T97, T98, T99, T101, T102) were stimulated with 100ng/ml rhIL21, 200ng/ml sCD40L, 1.3 μ g/ml anti IgM/anti IgG F(ab)₂ fragments and rhBAFF for 3hrs. Effects are depicted as $\Delta\Delta$ Ct values normalized to β 2m expression and relative to the unstimulated control (NE = not expressed). The statistical significance of the differences in gene expression was calculated for each gene and stimulation separately, using the two paired t-test. **A** *ICAM1* expression is affected by CD40 ($p=0.0005$) and IL21 ($p=0.0186$). **B** *DUSP2* expression is affected by BCRx ($p=0.0209$) and IL21 ($p=0.0138$). **C** *DUSP5* expression is affected by BCRx ($p=0.0378$). **D** *DUSP10* expression is affected by BCRx ($p<0.0001$). **E** *DUSP22* expression is highly variable and not affected by any stimulation. **F** *MYC* expression is affected by BCRx ($p=0.0101$) and CD40 ($p=0.0306$). **G** *SLAMF7* expression is affected by BCRx ($p=0.0006$).

3.2.6 Activated expression of *DUSP2*, *DUSP5*, *DUSP10* and *DUSP22* through BCR is dominantly mediated by ERK activation in contrast to *MYC* activation that is dominantly involves PI3K

The genes encoding for DUSP family members are predominantly affected by an activation of the BCR. These effects are in the main observable in BL cells as well as in primary human GC B cells. To elucidate the pathways involved in the regulation of DUSPs in response to BCRx the expression of *DUSP2*, *DUSP5* and *DUSP10* was investigated in cells pre-treated with inhibitors targeting specific BCRx pathways components. As the inhibition of *MYC* expression in response to BCRx is a BL cell specific phenomenon that cannot be observed in normal B cells (see Figure 3-10 and 3-11) it would be interesting to investigate the pathway that is involved in the regulation of translocated *MYC*.

The pathway components that were considered for the NF- κ B pathway include TAK1, and IKK2. The following specific chemical inhibitors, well known from the literature, were used: 5Z-7-oxozeaenol (TAK1) (Ninomiya-Tsuji, Kajino et al. 2003) and IKK2 inhibitor VIII (IKK2) (Sanda, Iida et al. 2005). To affect MAPK-signalling, SB203580 (p38 MAPK) (Cuenda, Rouse et al. 1995), SP600125 (JNK MAPK) (Bennett, Sasaki et al. 2001) and U0126 (ERK MAPK) (Favata, Horiuchi et al. 1998) were used. It has to be noted that under some conditions TAK1 is also part of MAPK signalling. To inhibit PI3K Ly294002 was used (Vlahos, Matter et al. 1994). To affect Ca^{2+} /NFAT a peptide inhibitor (VIVIT) was utilized (Aramburu, Yaffe et al. 1999).

BL2 cells were preincubated with DMSO, 100nM 5Z-7-oxozeaenol, 7 μ M IKK2 inhibitor VIII, 2 μ M SB203580, 10 μ M SP600125, 10 μ M U0126, 10 μ M Ly294002, or 2.5 μ M VIVIT for 3hrs. Subsequently respective amounts of anti-IgM were added for additional 3 hrs. Cells were harvested and RNA was isolated for qRT-PCR. One representative experiment out of three is shown in Figure 3-12.

Using this approach was shown that the activation of *DUSP2* expression by BCRx is abolished in cells treated with ERK inhibitor U016 indicating the involvement of the Erk-pathway in this process (Figure 3-12 A). The induction of *DUSP5* expression in response to BCRx is diminished in cells treated with TAK1i,

JNKi and completely abolished in cells treated with ERKi (Figure 3-12 B). Thus the ERK-pathway is dominantly involved, whereas JNK and TAK1 are influencing the induction of *DUSP5* only partially. The activation of *DUSP10* is reproducibly diminished in cells treated with PI3Ki and ERKi supporting an involvement of PI3K and ERK signalling in the activation of *DUSP10* expression by BCRx (Figure 3-12 C).

These data show that BCRx mediated induction or activation of *DUSP2*, *DUSP5* or *DUSP10* are predominantly conducted via the activation of ERK. However, to regulate *DUSP5* and *DUSP10* expression through BCR TAK1, JNK or PI3K signalling events have to be taken into account.

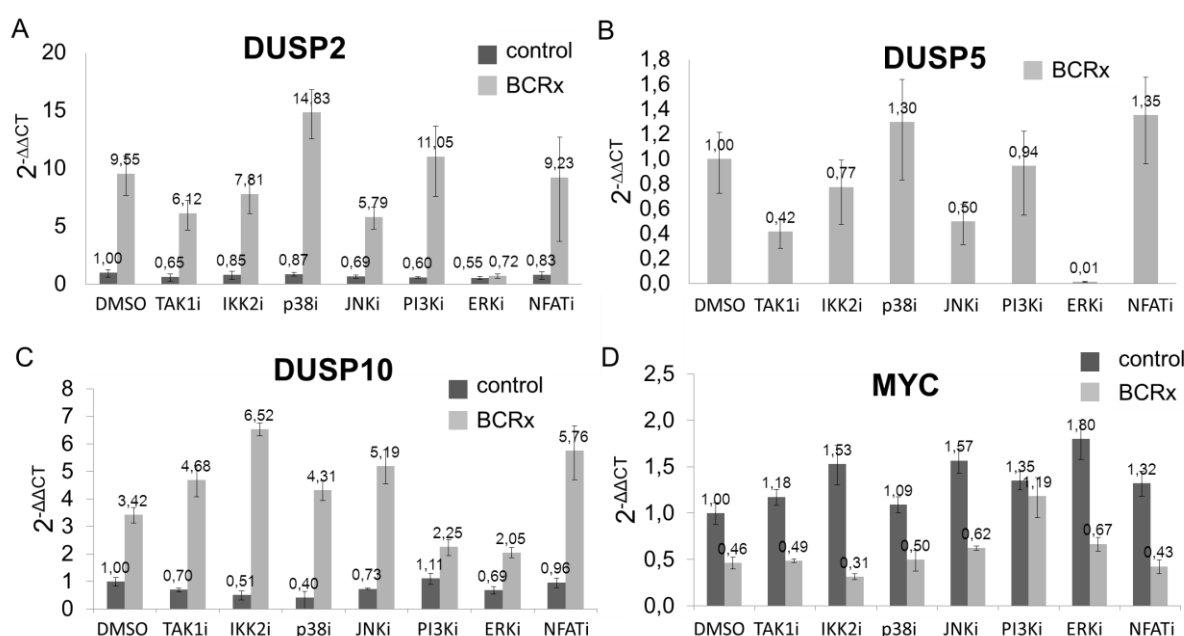


Figure 3-12 Pathways involved in the regulation of *DUSP5*, *DUSP2* and *DUSP10* as well as *MYC* in response to BCRx in BL cells. BL2 cells were pre-incubated with specific pathway inhibitors for 3hrs (for detailed information see Methods section chapter 2.12.6). 1.3 μ M/ml anti-IgM F(ab)₂ fragments were added respectively and cells were harvested after additional 3 hrs for qRT-PCR. **A-D** Expression of *DUSP2*, *DUSP5* and *DUSP10* and *MYC*. Results are presented as $2^{-\Delta\Delta CT}$ values, relative to abl housekeeper expression and compared to unstimulated DMSO control. As *DUSP5* expression (**B**) is below detectable levels in unstimulated probes, only ΔCT values of stimulated probes relative to DMSO control were compared. One representative experiment out of three biological replicates is shown.

The suppression of the aberrant *MYC* gene expression in BL cells in response to BCRx is dependent on PI3K activity as demonstrated by the reversal of the BCRx mediated inhibition by the PI3K inhibitor Ly294002 (Figure 3-12 D). In the future additional and alternative inhibitors have to be used to investigate the observed

involvements of specific kinases for the expression of *DUSPS 2,5,10* and *MYC*. In addition it would be necessary to use RNA-interference to dissect the respective mechanisms in more detail.

From picture 3-12 it becomes obvious that in some cases the inhibitor treatment is associated with an enhanced gene expression after the BCRx. Thus for example the expression of *DUPS2* is enhanced comparing cells treated with anti-IgM antibody and cells treated together with anti-IgM antibody and SB203580 (p38i). A comparable observation is made for *DUSP10*, where the inhibition of IKK2 is associated with a two-fold higher expression after BCRx. Whether the observed effects of TAKi, SB203580, SP600125 or VIVIT are significant remains to be elucidated by additional independent analyses in the future. However, the presented data already suggest the existence of tonic signalling in BL cells suppressing the capacity of the BCR activated pathways to regulate a set of genes as shown here for *DUSPs* and *MYC*. Perceptively such an approach could be used to clarify networks of pathways that interact and depend on each other. This dependency would be reflected in a combined abolishment of gene regulation in cells treated with distinct pathway inhibitors (e.g. TAK1 and p38 as TAK1 is upstream of p38).

3.2.7 rhBAFF stimulation induces differential p38 signals in cell lines of distinct lymphoma entities independent of BAFF receptor expression

As described above it was observed that the stimulation of BL cells with recombinant BAFF induces a predominant activation of p38, rather than a strong activation of the noncanonical NF- κ B signalling as previously described ((He, Chadburn et al. 2004; Mackay, Sierro et al. 2005; Mackay and Leung 2006). Therefore it was tested whether this observed pathway specificity is limited to BL cells or can be observed also in DLBCL cells.

The activation of p38 MAPK signalling was detected using immunoblot analyses to visualize phosphorylation of p38 after short time points of stimulation. It was found that both BL cell lines (Ramos and BL2) respond to BAFF by a respective phosphorylation of p38 (Figure 3-13 A). BL2 and Ramos cells solely differed in the time point of highest p38 phosphorylation (30min vs. 15min respectively). The

activation of p38 by BL16 was utilized as positive control, as it has been shown previously that these cells are capable of activating p38 in response to BAFF stimulation (He, Chadburn et al. 2004). Compared to the observed effect on p38 in BL cells the DLBCL cell lines SuDHL4 and SuDHL6 show very low levels of basal p38 activity and no induction of p38 phosphorylation upon BAFF stimulation (Figure 3-13 A).

As described in chapter 3.2.1, BAFF stimulation induces a rather weak activation of the noncanonical NF- κ B pathway. To investigate the possible differences in the capability of lymphoma cells to activate noncanonical NF- κ B signalling BL and DLBCL cell lines were stimulated with BAFF for 9 and 24h. As marker for NF- κ B activation the cleavage of p100 (inactive precursor of NF κ B2) to p52 was monitored via immunoblot. It can be shown that the DLBCL cell lines SuDHL4 and SuDHL6 show high degradation of p100 to p52 after 9 hrs of stimulation with recombinant human BAFF (Figure 3-13 B). Compared to this effect, BL2 cells show only marginal levels of p52 after 9 hrs and 24 hrs. Ramos cells do not express p100 and therefore cannot activate NF- κ B via this pathway (data not shown).

In a next step it was tested whether a variation in BAFF receptor expression might be the reason for the differences in BAFF response. BAFF-R and TACI expression were investigated via flow cytometry using fluorescently labelled antibodies. Unfortunately BCMA expression could not be investigated due to the lack of the availability of appropriate antibodies. It was observed that BL and DLBCL cell lines are positive for the expression of both receptors (Figure 3-13 C & D). Additionally the mRNA expression of BAFF receptors was investigated using qRT-PCR. Ct values were related to the expression of the housekeeper beta2m. It was observed that the mRNA levels of BAFF-R are highly comparable in BL2, SuDHL4 and SuDHL6 cells (Figure 3-13 E1). Ramos cells showed lower expression of all three BAFF receptor mRNAs. Nevertheless it can be observed that BL2 and SuDHL6 cells show highly comparable levels of the expression of BAFF-R, TACI and BCMA on mRNA level (Figure 3-13 E). These data show, that differences in BAFF receptor equipment are not the basis for distinct responses to BAFF regarding the activation of p38 MAPK.

To get a better insight into the mechanisms leading to these differences additional comprehensive experiments are necessary. However, we decided not to continue this part of the project within the PhD thesis period. However our group started a series of experiments to answer the question whether these differences in BAFF mediated signals are dependent on the different BAFF protein variants. We ask whether the p38 activation specificity of BL cells is still present using native soluble trimetric, 60mer forms or membrane bound BAFF for the stimulation of lymphoma cells. So far a feeder cell line has been developed by K. Moses, that can be used for the stimulation of lymphoma cells with membrane bound and native soluble BAFF. Furthermore, a number of constitutive active BAFF receptor variants for BAFF-receptor (BR3), TACI or BCMA have been cloned. This was realized by a fusion of the signalling domain of BR3, TACI and BCMA to the transmembrane domain of LMP1 following the example of CD40-LMP1 fusions (Hömig-Hölzel, Hojer et al. 2008). This will allow answering the question which receptor might be responsible for the activation of p38 in BL cells or NF- κ B in DLBCL cells or NF- κ B in DLBCL cells. To follow this issue it would be essential to clarify the role of BCMA for the activation of p38 in BL cells (Gross, Johnston et al. 2000; Hatzoglou, Roussel et al. 2000).

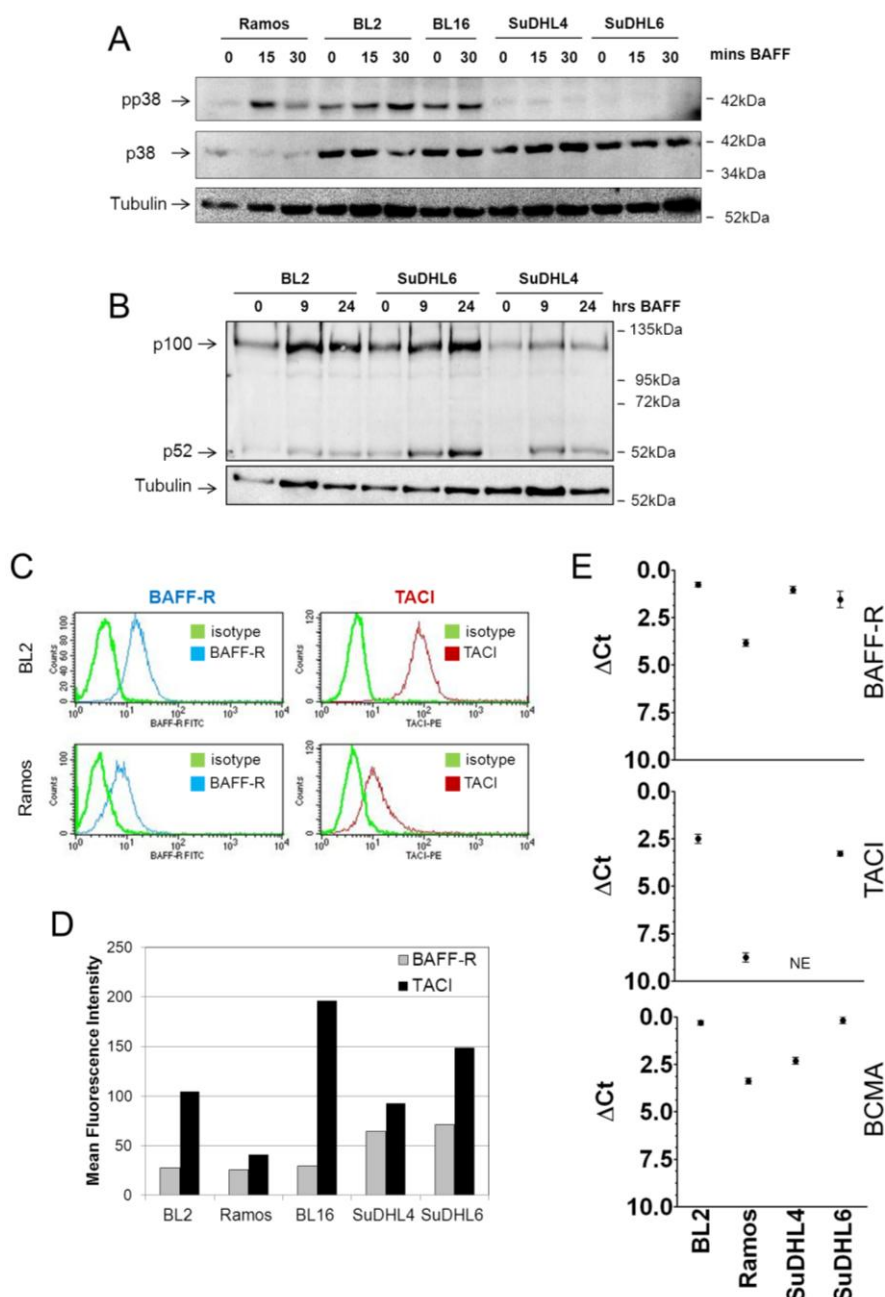


Figure 3-13 rhBAFF stimulation induces differential p38 signals in cell lines of distinct lymphoma entities despite comparable receptor equipment **A** BL2, Ramos, BL16, SuDHL4 and SuDHL6 cells were stimulated with 100ng/ml rhBAFF for 30 mins. p38 activity was detected using an anti pp38 specific antibody. **B** BL2, SuDHL4 and SuDHL6 cells were stimulated as described in A for 9 and 24 h respectively. Activation of the noncanonical NF- κ B pathway was detected using an antibody that detects p100/p52 NFKB2. **C&D** Surface expression of BAFF-R and TACI was detected on BL2, Ramos, BL16, SuDHL4 and SuDHL6 cells using flow cytometry. **D** Mean fluorescence intensities of BAFF-R and TACI stained cells are compared. **E** Expression of BAFF-R, TACI and BCMA mRNA was investigated in BL2, Ramos, SuDHL4 and SuDHL6 cells using qRT-PCR. Δ Ct values were calculated using beta2m expression as housekeeper (NE = not expressed).

3.2.8 Individual aNHL gene expression profiles exhibit a high similarity to the gene expression profiles of *in vitro* stimulated BL cells, if globally changed genes are considered for this comparison

To further proof the functional relevance of BCRx, CD40L, BAFF, IL-21 or LPS target genes identified *in vitro*, it was investigated how the genes, changed with the highest magnitude upon stimulation of BL cells (see tables A2-A6 in the appendix as well as Figures 3-7, 3-8 and 3-9), are expressed in gene expression profiles of 220 aNHL cases. The expression of these genes in gene expression profiles of aNHL cases is summarized in Figure 3-14. It was tested which subgroup of aNHL patients showed an “activated gene expression profile”, meaning an expression of stimulus responsive genes similar to stimulated BL cells. This analysis reveals a relative similarity to the gene expression of stimulated BL cells for each patient sample. Lymphomas showing a high relative similarity of their gene expression to BL cells stimulated with BCRx, CD40L, BAFF, IL-21 or LPS show a higher evidence of respective pathway activity than those with a lower similarity. A high similarity to the respective stimulated gene expression profile will be simplified in the following as “activated pathway activity”.

To analyse the characteristics of aNHL samples in more detail, their affiliation to the mBL/non-mBL and ABC/GCB groups as well as their *MYC* status was plotted in a colour coded bar on top of the respective heatmap. A red bar represents a sample identified as mBL, a yellow bar represents a sample identified as intermediate and a green bar on top of the heatmaps represents a non-mBL sample.

The comparison of gene expression profiles of aNHL cases according to the expression of stimulus responsive genes reveals that mBL cases show a pattern of gene expression that is, as expected, comparable to untreated BL2 (Figure 3-14 A-E). non-mBL cases however show an expression of these stimulus affected genes that is more or less comparable to the treated, activated BL2 cells. Intermediate cases show a transitional expression of stimulated genes. It can be observed that the expression of these genes changes in a continuous way over the aNHL samples. This gradient of pathway activities can be observed among

non-mBL and intermediate lymphoma. This observation is in line with the observed presence of a chromosomal *MYC*-aberration (Figure 3-14 A-E). Lymphomas with a *MYC*-translocation are depleted in all comparisons from those lymphomas characterised by a high pathway activity. Regarding the affiliation of patients to either ABC or GCB DLBCL subgroups no clear picture can be observed. The expression of all stimulus regulated genes is not correlated with an enrichment of either ABC or GCB DLBCL cases.

One could conclude from this observation that the stimulation with BAFF, CD40L, anti-IgM F(ab)₂ fragments, IL21 and LPS shifts the gene expression profile of our BL cell line towards a gene expression detectable in DLBCL cases. To elucidate whether the same cases show an activated gene expression profile disregarding the stimulus used the groups of patients showing an activated gene expression profile (55 cases; right border of the heatmaps) regarding the expression of BCRx, CD40, BAFF and IL21 affected genes were compared (Figure 3-15). Thereby it was observed that 45% of these cases are present in all compared groups. This means disregarding the stimulus used, about 25 lymphoma samples are characterised by a generalized activated gene expression profile. However this does not correspond to the ABC/GCB subgrouping (Figure 3-14). Thus the categorization of aNHL patients according to the expression of these genes is highly insufficient. As one might notice the heatmaps depicted in Figure 3-14 appear rather noisy. This is a result of the high numbers of genes that are regulated in the cell system, but not differentially expressed among the distinct lymphoma cases. Therefore it would be better to focus on genes which are specifically regulated by only one of the stimuli to avoid redundancy of gene activities and to focus on genes which are on the other hand as well differentially expressed among distinct lymphoma samples.

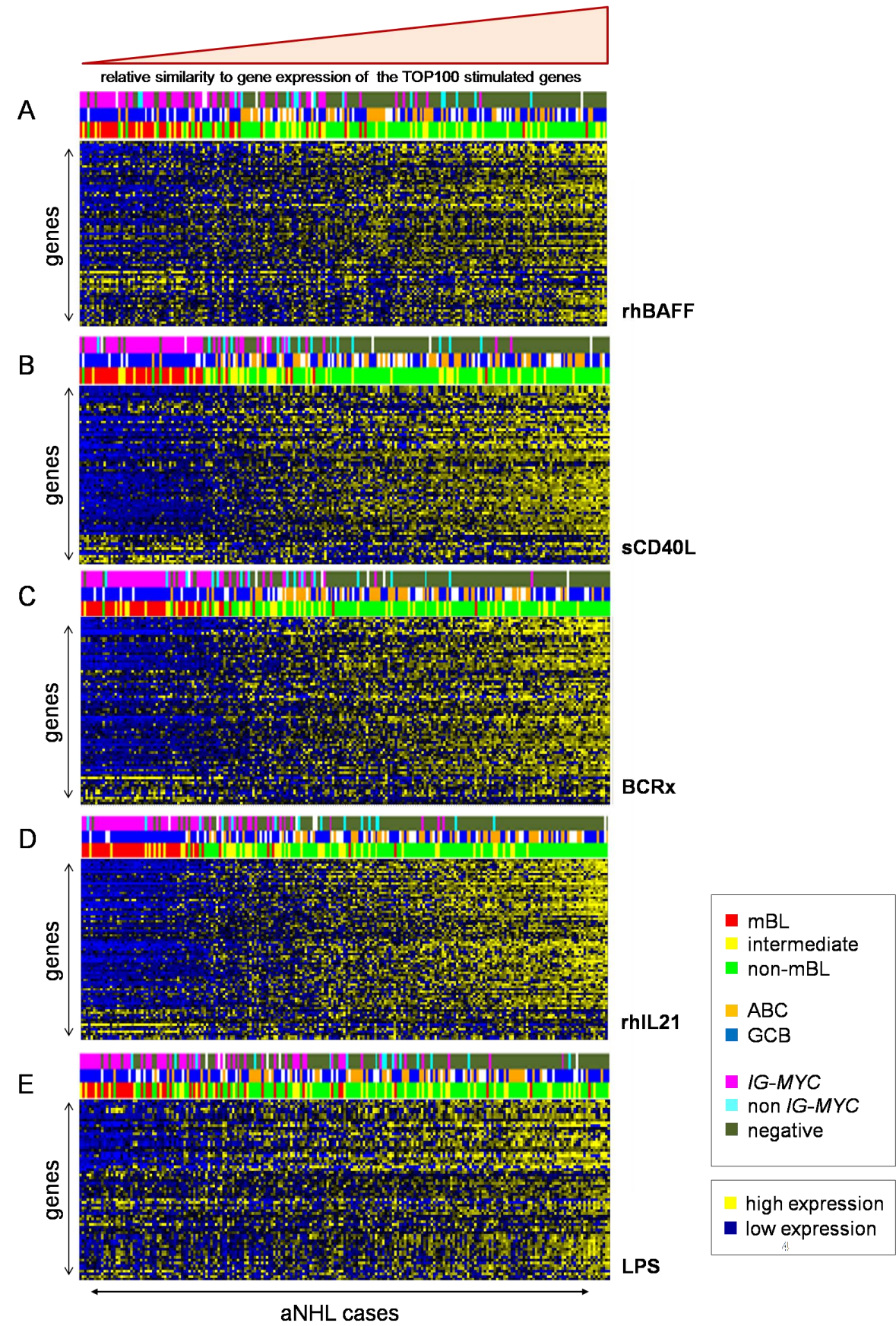


Figure 3-14 (legend see next page)

Figure 3-14 Expression of stimulus regulated genes in aNHL. The TOP100 most highly responding genes upon stimulation of BL2 with **A** rhBAFF, **B** sCD40L, **C** anti-IgM F(ab)₂, **D** rhIL21, fragments, **E** LPS and (see tables A2-A6 in the appendix) were investigated for their expression in the gene expression profiles of 220 aNHL lymphoma cases (Hummel, Bentink et al. 2006). aNHL cases were ordered from left to right according to the similarity of gene expression to the stimulated status of BL2 cells. The Heatmaps display the expression of target genes (columns) across 220 lymphoma samples (rows). The colour bar above the heatmaps marks mBL in red, non-mBL in green and intermediate lymphoma in yellow. Furthermore the affiliation of samples to ABC/GCB DLBCL subgroups and the presence of an *IG-MYC* translocation is encoded in a bar on top of the map (see legend for colour coding). Relative gene expression is encoded with yellow (high expression) and blue (low expression).

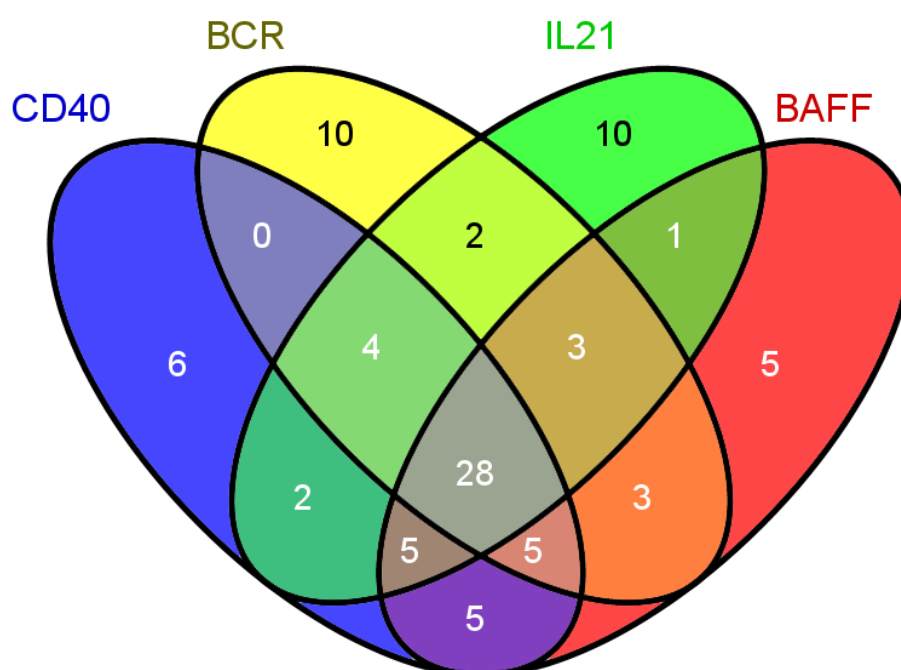


Figure 3-15 Comparison of the patient groups that show a gene expression profile of stimulus effected genes most closely to the activated gene expression profile of BL2 cells 55 aNHL samples that show the highest similarity regarding their gene expression profile to the stimulated BL cells in response to CD40L, BCRx, IL21 and BAFF stimulation were compared using Venn Diagrams as described in Figure 3-8.

It was shown that the activation of BL cells with B cell specific micro-environmental factors triggers different global changes in gene expression patterns to some extent useful in describing pathway activity in individual lymphoma. Thereby a comprehensive repository of gene expression data for CD40L, BCRx, IL21, LPS and BAFF responsive genes in a transformed B cell line is provided. It was observed that anti-IgM treatment has the strongest

capacity to modify gene expression. CD40L and IL21 show intermediate changes, whereas BAFF and LPS affect gene expression at lower levels.

Using qRT-PCR analyses it was verified that a number of genes are regulated by a combination of the used stimuli (e.g. *ICAM1*, *CD58*, *ID1*) or by specifically one of the utilized stimuli (e.g. *MYC*, *SLAMF7*). Furthermore, a selected set of genes involved in the control of negative feedback mechanisms was analysed in more detail (DUSPs). It was observed that the effects of BCRx on DUSPs are in principle transferable to non-malignant B cells and predominantly mediated via ERK.

BL cells are characterised by an *IG-MYC* translocation and thus aberrantly express *MYC*. Interestingly an inhibitory effect of BCRx on *MYC* expression was observed. This seems to be specific for BL cells and is mediated via PI3K. In contrast, in primary human tonsillar CD10+ B cells CD40L and BCR are activating the expression of c-Myc. The findings presented here characterise the BCRx mediated effects as predominantly ERK and PI3K dependent, rather than NF- κ B mediated. This seems to be in contrast to previous studies.

Furthermore, it was shown that upon stimulation highly affected genes are expressed in DLBCL cells with a high relative similarity. The group of lymphomas showing an activated gene expression profile is highly comparable disregarding the stimulus used. However, this generalized activated gene expression profile does not correspond to the ABC categorization and thus needs further investigations.

3.3 Identification of pathway activities in aNHL using stimulation mediated gene expression changes detected by guided clustering

As described above, aNHLs can be distinguished to some extent on molecular level using global gene expression profiling. In the previous paragraphs new insights into potential pathway activities in individual lymphoma have been pointed out. The described c-Myc index was found to be of prognostic significance. The above described relative similarities regarding the global gene expression between *in vitro* perturbed cells and primary lymphoma indicates

the existence of a gradient of pathway activities. However, a real quantification of these activities and the explanation of their functional consequence are still missing.

In order to describe new gene clusters functionally associated to specific paracrine signalling factors, the differentially expressed genes in BL2 cells in response to BAFF, CD40L, IL21 and LPS stimulation as well as BCR activation were used. This data set seems to be well suitable as lymphoma cells activate overlapping but also distinguishing pathways in response to each stimulus. For a better understanding of the functional consequence of aberrant pathway activation in individual lymphomas it was decided to investigate subgroups of gene sets defined as dominantly affected by one of the stimulations described above, and at the same time not affected by any of the other stimuli. We believe that this approach is able to further narrow functional important pathway activities

3.3.1 Guided Clustering

Together with M. Maneck and R. Spang an approach called “guided clustering” was developed (Maneck, Schrader et al.). This methodology enables the identification of specific gene expression modules (clusters) that are affected by the *in vitro* cell line perturbation and as well differentially expressed comparing gene expression profiles of tumour samples. Basically this algorithm identifies genes which fulfil two criteria at the same time: (i) affected by the stimulus and (ii) differently expressed across a set of tumour gene expression profiles. Thereby modules are identified that are functionally associated with the activation by a known stimulus useful to identify pathway activities that are exclusive to a defined lymphoma subgroup. In order to “measure” the activity that is predicted by the expression of these genes in tumour gene expression profiles an index value was used. Therefore, the expression levels of the cluster genes are combined to a single value (index) that quantifies the activity of the identified gene cluster in the tumours (Maneck, Schrader et al.) This value was defined as “Pathway Activation Index”.

To identify genes specifically regulated by one stimulus a vector based bioinformatical approach was embedded into the guided clustering analysis.

Briefly: the mean of the control gene expression values was subtracted from the gene expression values of stimulated samples, resulting in values that solely represent the reaction caused by the stimulation. The gene vectors were correlated to a binary vector. This binary vector includes a “1” only for one stimulation that was investigated to solely regulate genes. The genes were ordered according to the calculated absolute Pearson correlation coefficient.

Using this approach combining stimulus specific gene expression changes of stimulated BL2 cells and gene expression profiles of 220 aggressive NHL a number of specific gene clusters for each stimulus could be described. For each perturbation two pathway indices were identified: an activating and an inhibiting. Among these two clusters changed by LPS stimulation (LPS.1, LPS.2), two clusters regulated upon sCD40L stimulation (CD40.1 and CD40.2), two clusters responding to BAFF (BAFF.1 and BAFF.2), two clusters responding to IL21 stimulation (IL21.1, IL21.2) as well as two clusters changed by BCR activation (BCR.1, BCR.2) were identified (see Appendix table A8).

The data obtained from a single stimulation of BL cells with LPS were used in parallel studies to verify an observation concerning a potential influence of BCL6 on TLR signalling. Therefore an additional LPS driven pathway activation index was identified (LPS.2*) (Maneck, Schrader et al. 2011). It was shown that LPS mediated Toll-like receptor signalling and BCL6 targets are coherently expressed in DLBCL. This supports the hypothesis that BCL6 could potentially modulate Toll-like receptor signalling in DLBCL. For further information please refer to the published manuscript.

In the following paragraphs BCR and CD40 regulated gene clusters will be described in detail.

3.3.2 CD40 and BCR mediated pathway activity is continuously increasing in aggressive NHL samples

As described above, in order to measure gene cluster activity in the gene expression profiles of aNHL samples the expression of the cluster genes was condensed to one single value: the index. This index value was used as a surrogate marker for the activity of a gene cluster in each single patient sample.

Two major gene clusters were identified to be regulated in response to BCRx. One of these gene clusters contains genes which are dominantly inhibited upon BCR activation (BCR.1) whereas the other gene cluster is built up by genes that are specifically activated in response to BCR crosslink (BCR.2) in BL2 cells. (Figure 3-16 A, left panel). The BCR.1 cluster is determined by 288 genes, the BCR.2 cluster encompasses 286 genes. It was striking that within the group of genes summarized as BCR.1 cluster genes involved in DNA-damage response and cell cycle control are highly overrepresented. These include for example *BRCA1*, *AURKA*, *BUB1B*, *CCNA2*, *CCNB1*, *PLK1* and 3, *PBK/TOPK*, *PRC1* and *BIRC5/SURVIVIN*. The BCR.2 cluster comprises 286 genes. These include for example genes encoding for kinases like *SGK1*, *MAPK6* and *MAP2K3* (see Appendix table A8 for detailed information). An expression of these genes according to the stimulated status of the BL cell model will be further referred to as “high index”. Corresponding to that an expression of genes similar to the unstimulated status will be referred to as “low index”. Please note that in the case of the BCR.1 gene cluster a high index corresponds to a low expression of cluster genes.

In order to focus on the heterogeneity of DLBCL the indices based on the expression of BCR.1 and BCR.2 cluster genes were compared in 175 aNHL cases, that have been described as “non-mBL” (127 cases) and “intermediate” (48 cases) with the index of Burkitt-likeness as published by Hummel and colleagues (Hummel, Bentink et al. 2006). These DLBCL gene expression profiles were analysed according to the expression of the respective cluster genes (Figure 3-16 A, right panel). aNHL samples are ordered from left to right according to the BCR.1 index in both heatmaps. BCR.1 and BCR.2 indices show oppositional activities in aNHL gene expression profiles. Lymphoma which exhibit a low expression of BCR.1 cluster genes (index high) show at the same time a low expression of BCR.2 cluster genes (index low). The information derived from these oppositional activities can as well not be used to group ABC and DLBCL patients.

CD40.1 represents a cluster of 288 genes which are activated by CD40 signalling in BL2 cells (Figure 3-16 B left panel). These genes include for example genes

encoding for MHC1 and MHC2 molecules as well as *CD59*, a gene that encodes a cell surface glycoprotein that is involved in lymphocyte signal transduction, *CD160*, encoding a receptor that shows broad specificity for both classical and non-classical MHC class I molecules, as well as *NOTCH2*, which encodes for a cell surface receptor for membrane bound ligand, and may play a role in developmental processes. CD40.2 comprises 71 genes which are mostly inhibited upon CD40 activation. In Figure 3-16 B (right panel) heatmaps of the expression of the CD40 cluster genes in gene expression data of 175 cases (described in A) are depicted. aNHL samples are ordered from left to right according to the CD40.1 index in both heatmaps. Contrary to the oppositional BCR indices, both CD40 indices are basically coherent in DLBCL. A high CD40.1 index (high gene expression of CD40.1 cluster genes) is in most cases accompanied by a high CD40.2 index (low expression of CD40.2 cluster genes). For the affiliation of patients to ABC and GCB DLBCL subgroups (colour coded bar on top of the heatmap) no clear segmentation of patients by one of the CD40 gene cluster activities can be identified. Nevertheless a trend for a higher prevalence of lymphoma samples with the label ABC-like DLBCL can be observed in lymphomas with a high CD40.1 / CD40.2 pathway activation index.

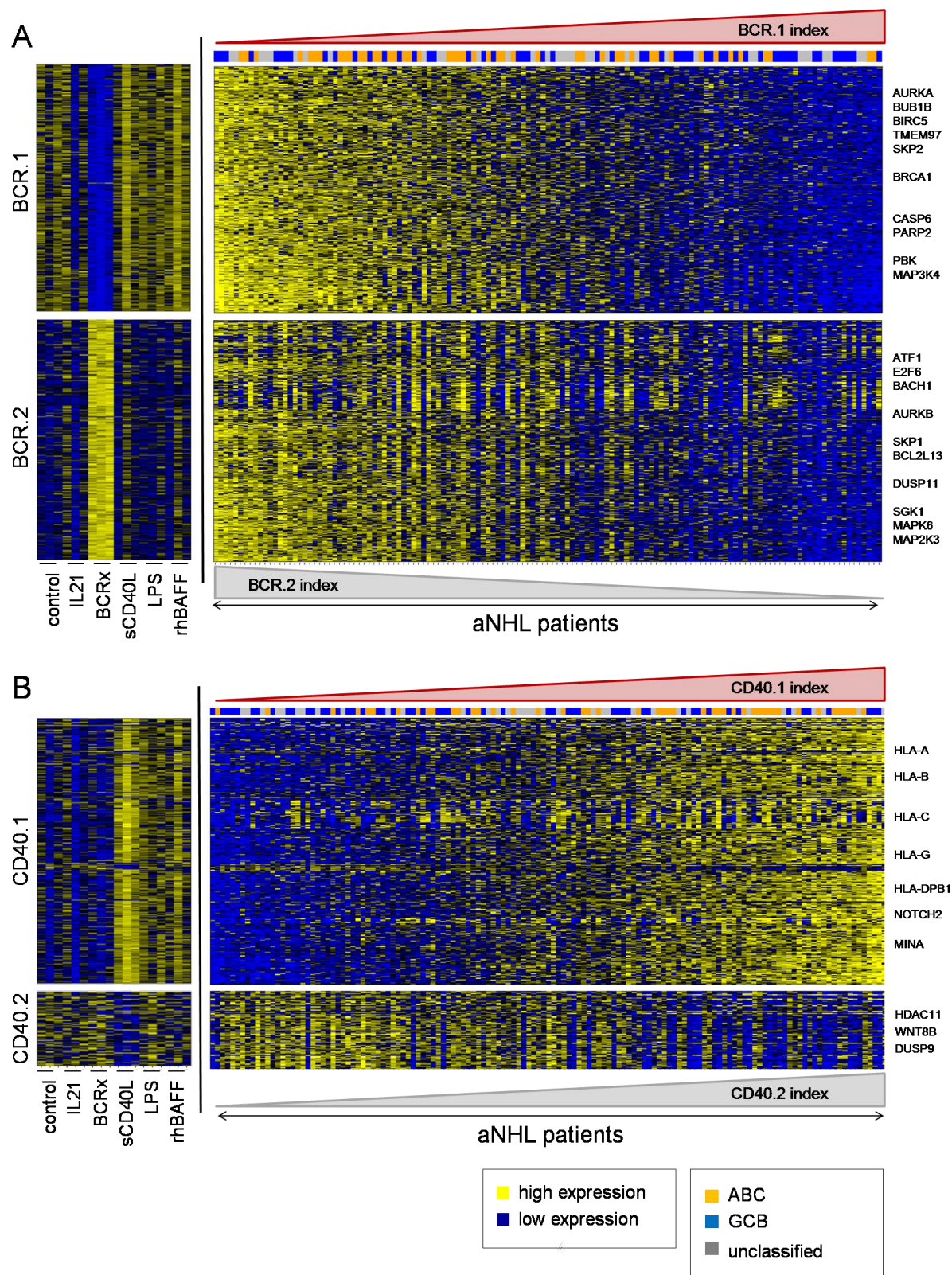


Figure 3-16 (legend see next page)

Figure 3-16 Guided clustering identifies four major clusters of genes regulated by BCR activation and CD40L stimulation. Each row in the heatmaps represents a gene and each column represents a microarray sample. Yellow and blue indicate high and low expression. **left panel:** Heatmaps show the gene expression of the respective cluster genes in stimulated BL2 cells compared to control. **right panel:** Heatmaps show the expression of respective cluster genes in gene expression profiles of tumour samples from 175 intermediate and non-mBL aNHL patients. The patient samples are ordered according to rising BCR.1/CD40.1 index from left to right (symbolized by the red bars). The colour coded bar on top of the heatmaps represents the affiliation of patients to ABC / GCB DLBCL subgroups (orange = ABC tumour sample, blue = GC B tumour sample and grey = unclassifiable sample). **A** The gene expression of BCR.1 and BCR.2 cluster genes is depicted. **B** The gene expression of CD40.1 and CD40.2 cluster genes is displayed.

3.3.3 mBLs are characterised by a missing BCR.1 and a high c-Myc activity

Next, it was investigated whether there are specific interactions of the identified gene clusters which can be better used to identify specific activities of oncogenic gene modules. These modules could then be used to describe new subgroups of DLBCL patients. Furthermore the activities of these gene modules could be used to identify new targets for an improved therapy. This is of particular interest since the identified gene clusters hold functional information about the signalling pathways that underlie the affected genes. As described in Chapter 3.1, a high c-Myc activity was observed in a number of DLBCL cases and found to be an independent risk factor for these DLBCL patients. Therefore it was first asked whether the activity of one of the newly identified gene clusters shows a correlation with high c-Myc activity in DLBCL patients thus implicating a link between c-Myc activity and respective other pathways.

The c-Myc index and the indices representing the expression of CD40 and BCR gene clusters were investigated in gene expression profiles of 220 aNHL cases (Hummel, Bentink et al. 2006). The interactions of the distinct gene cluster activities were investigated by plotting the indices of c-Myc, CD40.1, CD40.2, BCR.1 and BCR.2 against each other (Figure 3-17 A & B, page 102). Thereby the information about the activity of two gene clusters in the gene expression profile of one aNHL sample can be assessed. The most interesting interaction is observed for the BCR.1- and c-Myc-index. In Figure 3-17 B1 it is shown that the BCR.1 index inversely correlates with the c-Myc index. The correlation coefficient is -0.76. That implies that lymphomas which exhibit a high c-Myc activity are characterised by a high expression of BCR.1 genes (low index). mBL cases show

a high c-Myc index but a low BCR.1 index, whereas DLBCL cases show a respectively lower c-Myc index but high BCR.1 index thus reflecting a stronger inhibition of genes defining the BCR.1 index. Intermediate/mindL cases are characterised by an intermediate activity of the c-Myc index and the BCR.1 index. One explanation of this strong inverse correlation could be that BCR.1 genes are regulated directly or indirectly through c-Myc. There might be mechanisms by which a high c-Myc activity accounts for a low BCR.1 activity or vice versa. This indicated a potential direct connection of c-Myc activity with the expression of BCR.1 cluster genes. The other index interactions have to be analysed in more detail in the future.

3.3.4 The expression of some BCR.1 cluster genes is decreased upon inhibition of c-Myc in BL cell lines

As already shown in chapter 3.2 the activation of the BCR is associated with a decreased c-Myc expression. By qRT-PCR it was analysed whether “BCR.1-genes” *BIRC5/SURVIVIN*, *AURKA*, *BUB1B*, *PBK-TOPK* are indeed inhibited by BCRx (validation of microarray data). Furthermore, *TMEM97* as a c-Myc index gene, which is also present within the BCR.1 gene cluster, was analysed. To investigate the possible interaction of c-Myc with BCR.1 cluster genes it was tested whether c-Myc inhibition can reduce the expression of BCR.1 genes. In addition, it was tested whether there is an additive effect of BCRx and c-Myc inhibition on the decreased expression of this selected set of BCR.1 cluster genes. Therefore the mRNA levels of selected cluster genes were assessed in response to BCR activation, c-Myc inhibitor treatment and both (BCRx and c-Myci) using qRT-PCR.

BL2 and Ramos cells were preincubated for 3h with 60µM c-Myc inhibitor 10058-F4 (Berg, Cohen et al. 2002; Yin, Giap et al. 2003) or left untreated (DMSO). DMSO control as well as c-Myci treated cells were stimulated using 1.3µg/ml anti-IgM F(ab)₂ fragments or left unstimulated as control. The inhibition of c-Myc by 10058-F4 can be easily controlled since the 10058-F4 treatment leads to a lower expression of *MYC* itself via a microRNA mediated mechanism (Sampson, Rong et al. 2007). One representative experiment of three replicates is shown in Figure 3-18 (page 104).

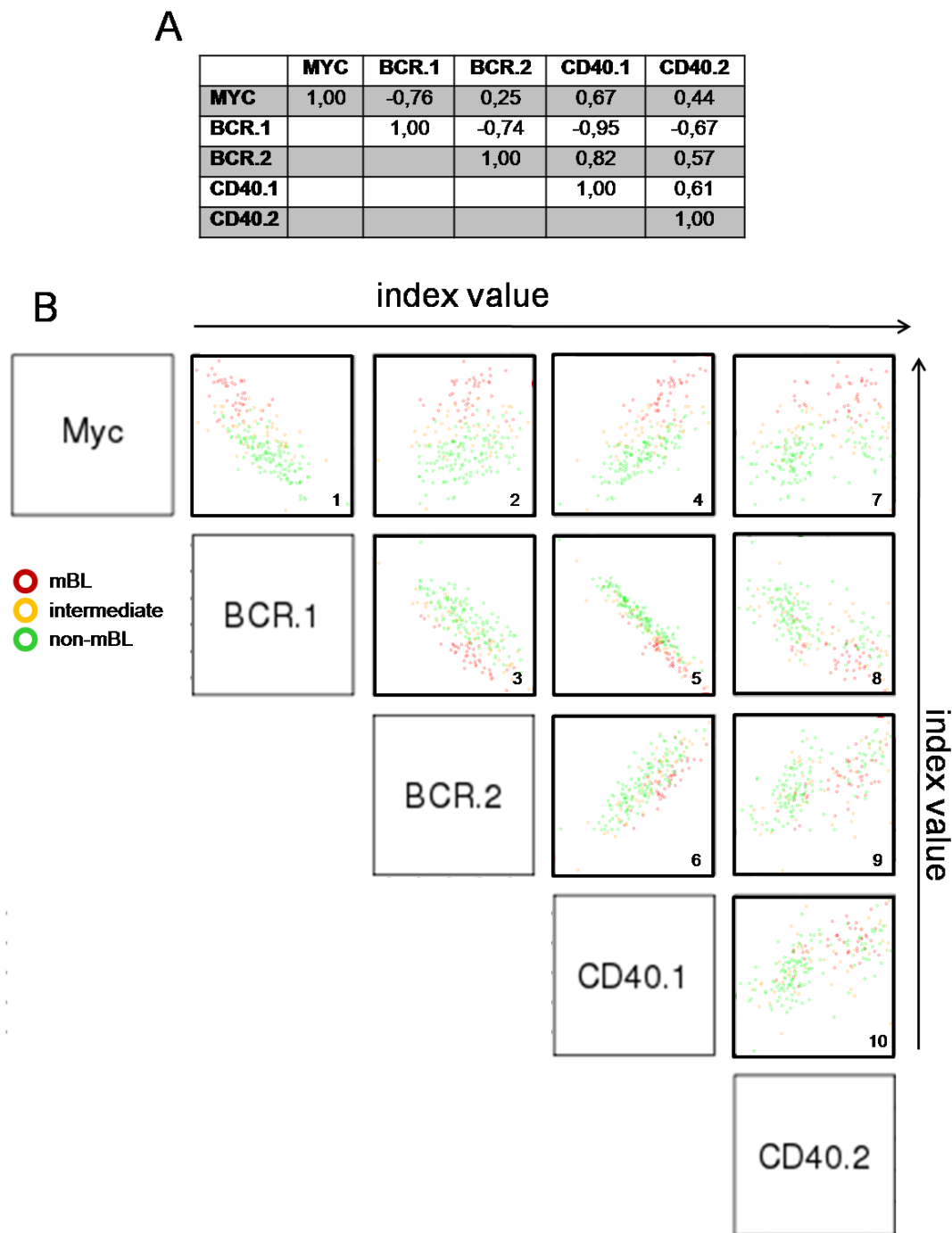


Figure 3-17 The BCR.1 index is inversely correlated with the c-Myc index. A&B Correlation coefficients of Pathway Activation Indices in a cohort of 220 aNHL cases. c-Myc index genes, BCR.1, BCR.2, CD40.1 and CD40.2 gene clusters were used to calculate the respective PAIs in gene expression profiles of 220 aNHL diagnosed as mBL (red), non-mBL (green) and intermediate lymphoma (yellow) by Hummel and colleagues (Hummel, Bentink et al. 2006). The parallel activity was estimated plotting the indices against each other and calculating the respective correlation coefficient. A coefficient close to one indicates highly correlated index activities and a high number of lymphoma expressing both gene clusters in an activated state.

As shown in previous experiments microarray data BCRx is associated with a reduced expression of *MYC* in BL2 and Ramos cells. The same is observed for *BIRC5/SURVIVIN*, *AURKA*, *BUB1B*, *PBK-TOPK* and *TMEM97* expression. Interestingly, the expression of *BIRC5/SURVIVIN*, *AURKA*, *BUB1B*, *PBK-TOPK* and *TMEM97* is also affected by the c-Myc inhibitor 10058-F4. (Figure 3-18 A-F page 104; see also Figure 3-10). *AURKA* and *BUB1B* have been previously described as c-Myc target genes in different cell systems (Menssen, Epanchintsev et al. 2007; den Hollander, Rimpi et al. 2009). Furthermore the BCRx and c-Myc dependent expression of PBK-TOPK is remarkable since it was shown that this kinase could possibly play a role for BL pathogenesis (Simons-Evelyn, Bailey-Dell et al. 2001). This result suggests that the expression of a set of BCR.1 genes is indeed dependent on the aberrant c-Myc activity in BL cells. Combining the inhibition of c-Myc with BCR activation one can observe an additive effect regarding the decreased expression of BCR.1 cluster genes. However, the observed additive effect indicates that there are additional pathways involved by which BCR activation could mediate the inhibition of the investigated BCR.1 cluster genes. One possibility is c-Myc. The second possibility might be mediated by one of the various pathways triggered upon BCR activation but not CD40L, BAFF, IL21 or LPS. Ongoing experiments indicate that ERK and/or PI3K signalling could be involved. However additional experiments are necessary to give a final conclusion on that.

3.3.5 Changes in BUB1B gene expression in response to BCR crosslink are mediated by altered c-Myc binding to the BUB1B locus

To follow the question whether BCR.1 genes might be directly regulated by c-Myc upon BCR activation, the direct promoter binding of c-Myc to one BCR.1 cluster gene, namely *Bub1B*, was investigated. *Bub1B* was selected as example since E-boxes, which serve as direct c-Myc binding sites, have already been published for this gene (Menssen, Epanchintsev et al. 2007). Using ChIP it was tested whether the binding of c-Myc to the E-box containing region in the first intron of the *Bub1B* is altered upon BCR activation. As seen in Figure 3-19 (page 105) the locus of the *Bub1B* gene containing the E-box can be enriched by Immunoprecipitation of c-Myc in unstimulated cells (Figure 3-19 lane 5). Upon

Results

activation of the BCR this enrichment is abolished (Figure 3-19 lane 6). As negative control an IP with an anti IgG antibody was used (Figure 3-19 lane 3&4). As positive control an IP of acetylated histone H3 was used as this is a marker for active description (Figure 3-19 lane 7&8). In a photo with lower exposure time one can observe that acH3 binding to the BUB1B locus is slightly diminished upon BCR crosslink (Figure 3-19 lane 7&8 2). This result points to a direct regulation of the BCR.1 genes by c-Myc.

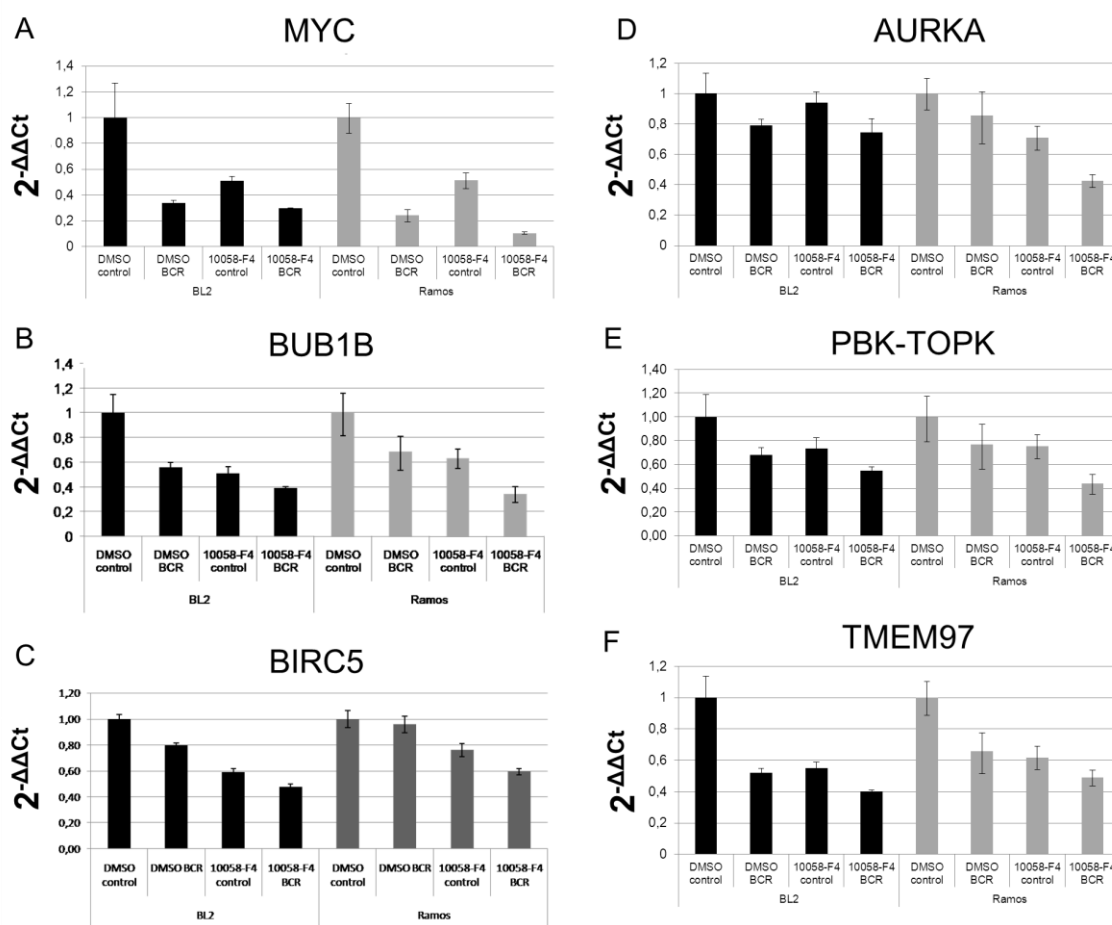


Figure 3-18 Expression of BCR.1 cluster genes is downregulated by BCR activation and c-Myc inhibition in Burkitt Lymphoma cell lines. A-F BL2 and Ramos cell were pretreated for 3h with 60μM 10058-F4 c-Myc inhibitor or left untreated (DMSO). Cells were stimulated for additional 3h with anti IgM F(ab)2 fragment (1.3μg/ml). qRT-PCR analyses were performed using SYBR green. Foldchanges were calculated using the $\Delta\Delta Ct$ method. One representative experiment of three replicates is shown.

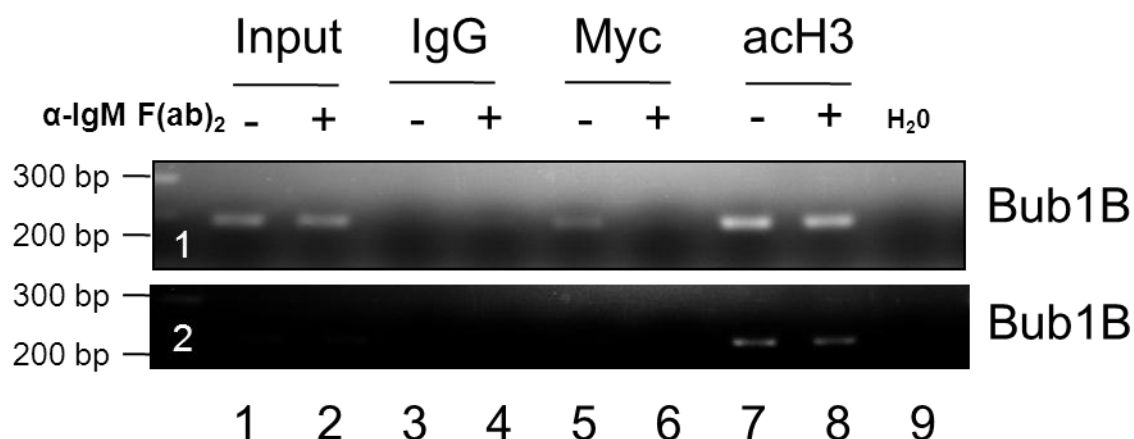


Figure 3-19 ChIP of c-Myc reveals a change in c-Myc abundance at the Bub1B promoter upon BCR activation. Chromatin IPs were performed using antibodies directed against IgG as negative control, against c-Myc and against acetylated histone H3 as positive control (marker for active transcription). To check for c-Myc binding a fragment was amplified that encompasses the previously described E-box in intron 1 of the Bub1B gene (Menssen, Epanchintsev et al. 2007). The lower lane shows a shorter exposure time to infer on differences in acetyl Histone H3 binding.

3.3.6 Prolongation of the G2 phase of the cell cycle in BL cells after BCRx

In parallel to the investigation of a direct c-Myc dependent regulation of BCR.1 gene expression the effect of BCRx on the cell cycle was investigated, as BCR.1 cluster genes are highly enriched in genes associated with G2 cell cycle processes (see table A 9 in the Appendix). Furthermore it was tested whether an inhibition of c-Myc is associated with a comparable effect on the cell cycle as BCR activation. It was hypothesized that c-Myc inhibition could even enhance this biological effect mediated by BCR activation, when both treatments are utilized at the same time.

BL cell lines BL2 and Ramos were incubated with 60 μ M of 10058-F4 c-Myc inhibitor and 1.3 μ g/ml anti IgM F(ab)₂ fragments over a time course of up to 24h. The distribution of cells to distinct cell cycle phases was investigated using Nicoletti buffer followed by FACS analyses of nuclei. One representative experiment of 5 is shown in Figure 3-20 A, page 107 . It could be observed that after 6h of BCR activation the percentage of cells in G2 phase increases from 22% to 29% for Ramos cells and from 20% to 32% for BL2 cells. This effect is even enhanced by the inhibition of c-Myc. Here an increase from 25% to 32% of

Ramos cells and from 32% to 38% of BL2 cells in the G2 phase can be induced by BCR activation. These results are comparable for both BL cell lines. Measurements of the 6h time point are exemplified in figure 3-20 B.

To obtain a more detailed picture of the BCR effects on the passage of BL cell through the cell cycle, Ramos cells were synchronized at the S to G2 phase border using 2 rounds of thymidine treatment (described in Methods Section Chapter 2.12.11 (Stolz, Ertych et al. 2010)). Using this technique it is possible to follow the cells through all cell cycle passages. To relieve the cell cycle block cells were washed three times. At the same time point of the release from cell cycle arrest the cells were stimulated with anti-IgM F(ab)₂ fragments (1.3µg/ml) and treated with 60µM of 10058-F4 c-Myc inhibitor. Thereby one can follow treated compared to control cells over a detailed time course as they re-entry into the cell cycle and pass G2, M, G1 and S phase (Figure 3-20 C). After 8 hours 65% of control cells achieved the passage from G2/M phase to G1. The activation of the BCR decelerates this process. After 8h 48% of BCR activated cells are still within G2/M phase. This effect is enhanced by the inhibition of c-Myc. Of activated Ramos cells with additionally inhibited c-Myc more than 60% of cells were still in G2/M phase after 8h. This observation is in line with the additive negative effect of BCR activation and c-Myc inhibition on the mRNA expression the BCR.1 cluster genes BUB1B, PBK-TOPK, AURKA and BIRC5 (see Figure 3-18).

By investigating direct short term effects on the cell cycle it was found that BCR crosslink leads to a prolonged G2-phase in BL cell lines BL2 and Ramos. It can be shown that the already described G1 arrest is only the final outcome of the influences of BCR signals on the cell cycle that follows the primarily induced prolongation of the G2 phase (Figure 3-20 A, B & C). These results point to the conclusion that the inhibition of G2 phase associated genes represented in the BCR.1 cluster might be indeed the reason for BCR mediated elongation of G2 cell cycle phase. Since the bioinformatic description suggests that DLBCL cases are characterised by a low c-Myc and a high BCR.1 index it could be postulated that the lower expression levels of BCR.1 genes, as observed in a subgroup of DLBCL patients, might be the reason for the differences in growth behaviours of

DLBCL and BL, as it is known that DLBCL tumours show lower growth rates compared to BL. It needs to be investigated on primary lymphoma samples whether there is indeed a longer G2/M-cell cycle transition in DLBCLs compared to BLs.

Using “guided clustering” it was possible to identify new clusters of gene which are affected by paracrine and B cell intrinsic stimuli in the BL cell model. The developed indices are able to quantify pathway activity in individual lymphomas. Most importantly one gene cluster was identified that is inhibited upon BCRx in BL2 cells (BCR.1). BCR.1 activity is inversely correlated with c-Myc activity and separates mBLs from the other analysed aggressive NHLs. The results presented here provide evidence that a lower expression of BCR.1 cluster genes in non-mBLs is probably due to the absence of a strong c-Myc activity or a high activity of paracrine/autocrine signals mimicking BCRx. Furthermore, BCRx leads as short term effect to a prolonged G2 cell cycle phase which could be an explanation for the G1 arrest of the cells observed after longer time points.

Results

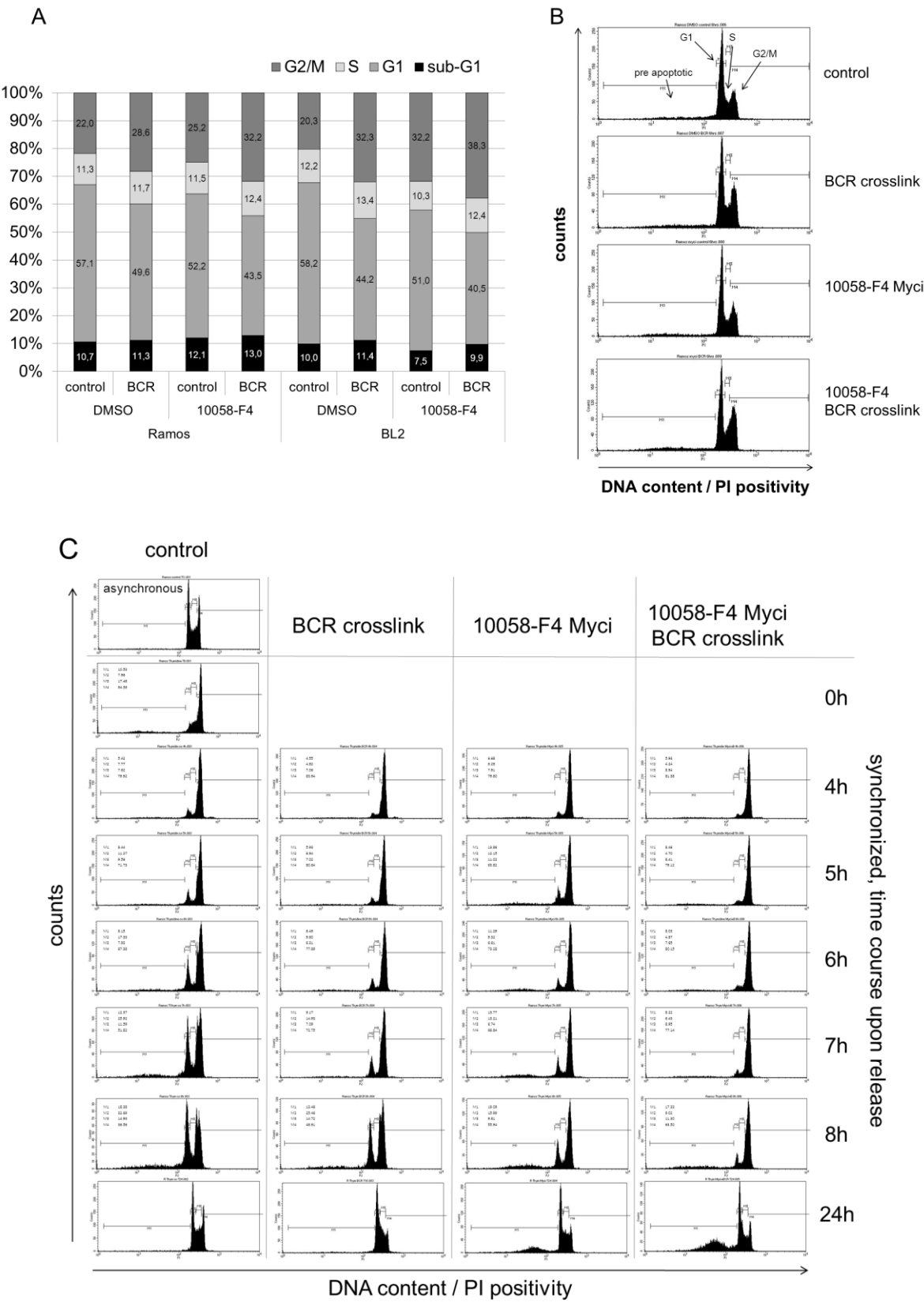


Figure 3-20 (legend see next page)

Figure 3-20 Activation of the BCR leads to a prolonged G2 phase in BL cell lines A & B Asynchronous growing BL2 and Ramos cells were treated with 1.3µg/ml anti IgM F(ab)₂ fragments and 60µM 10058-F4 c-Myc inhibitor for 6h. Cell cycle distribution of cells was measured using Nicoletti buffer and FACS based analyses of the DNA content of the nuclei. **C** Ramos cells were synchronised in G2 cell cycle phase using 2 rounds of thymidine (2mM) treatment. After removing the Thymidine (0h) the cells started to pass through the cell cycle. Cell cycle distributions were measured over a time course of 0h up to 8h using Nicoletti technique. The 24hrs time point was measured separately. One out of three representative experiments is shown.

4 Discussion

Recently the analysis of gene expression profiles of aNHL samples has allowed an advanced understanding of the molecular heterogeneity of these lymphomas (Alizadeh, Eisen et al. 2000; Monti, Savage et al. 2005; Dave, Fu et al. 2006; Hummel, Bentink et al. 2006; Bentink, Wessendorf et al. 2008; Ci, Polo et al. 2009). A molecular definition of BL was described based on different approaches including cell line perturbation experiments. This molecular definition can be used to differentiate molecular BL from DLBCL and other aggressive NHL on the basis of their tumour gene expression profiles (Dave, Fu et al. 2006; Hummel, Bentink et al. 2006). In previous investigations two major DLBCL subgroups were defined comparing at a qualitative level global gene expression of B cells from different differentiation stages with those from primary lymphoma. Thus at the molecular level often a discrimination of the ABC- and GCB-like DLBCLs is performed. The group of ABC DLBCL has been characterised by a worse clinical outcome (Alizadeh, Eisen et al. 2000). However, in a comparable approach a so called OxPhos / BCR-like subgroup was also identified only partially overlapping with ABC- or GCB-like DLBCLs (Monti, Savage et al. 2005). From additional studies on cell lines resembling the ABC- and GCB-like gene expression it is suggested that ABC-like DLBCLs are characterised by highly activated NF-κB and JAK-STAT signals (Feuerhake, Kutok et al. 2005; Lam, Davis et al. 2005; Ngo, Davis et al. 2006; Ding, Yu et al. 2008; Lam, Wright et al. 2008; Hailfinger, Lenz et al. 2009; Davis, Ngo et al. 2010; Ngo, Young et al. 2011). In contrast GCB-like DLBCLs are characterised by deregulated Bcl6 function (Iqbal, Greiner et al. 2007; Choi, Weisenburger et al. 2009; Ci, Polo et al. 2009). Nevertheless, the characterisation of aNHL according to their gene expression profiles is so far

largely descriptive lacking a clear quantitative estimation of pathway activities in individual lymphomas.

In addition, there are a number of open questions, as for example how aberrant c-Myc activity is reflected in non-mBL DLBCL and whether this activity is of functional relevance for these lymphoma. It is not known how the activities of paracrine B cell stimuli contribute to the heterogeneity and the malignant phenotype of DLBCL. It is likely that other oncogenic pathways are involved in the malignancy of DLBCL other than NF- κ B and JAK-STAT signalling. However these so far remain elusive for primary lymphoma. Furthermore it is not understood how the differences in proliferative potential and chromosomal complexity of DLBCL and BL, which highly contribute to the heterogeneity of aNHL, can be explained.

Hence, the aim of this study was to use perturbation experiments in primary lymphoma precursor cells or lymphoma cell lines to identify and characterise new gene expression patterns that hold information about relevant oncogenic pathway activities and their quantitative estimation in individual lymphoma samples. Furthermore, understanding the heterogeneity of pathway deregulation is important for a better understanding of the clinical outcome and prediction of treatment responses not only in lymphoma patients. Thus in this study (i) the effect of ectopic expression of the proto-oncogene *MYC* in lymphoma precursor cells was investigated and (ii) perturbations of B cell lines by B cell specific paracrine stimuli were used to define new groups of genes in order to obtain novel insights into the functional differences underlying the malignant phenotypes of distinct aNHL.

4.1 High c-Myc activity is an independent negative prognostic marker for DLBCL

In this study it was shown that ectopic expression of c-Myc in GC B cells triggers a characteristic expression pattern of c-Myc targets that is also expressed in aNHL. While a very high expression is restricted to Burkitt lymphomas, the expression of c-Myc targets varies on a lower level across non-mBL and

intermediate lymphomas and constitutes a negative prognostic marker in these lymphomas.

The results presented here consolidate the previous conclusions of recent studies with respect to c-Myc activity in aNHL (Dave, Fu et al. 2006; Bentink, Wessendorf et al. 2008). While Dave and coworkers described expression of c-Myc targets as a hallmark of BL, the results presented in this study predict c-Myc activity also for a subset of DLBCL. Like the pattern from Dave et al., the pattern presented here can be found in the expression profiles of Burkitt lymphomas. However, different to their pattern, the c-Myc-index is also displaying a considerable c-Myc activity in DLBCL. Moreover, its expression is prognostic in DLBCL suggesting that c-Myc activity is not limited to BL but exists in some DLBCL and affects their outcome.

Thus, in line with Dave et al., it was demonstrated that sets of c-Myc targets genes can be used to discriminate between BL and DLBCL (Dave, Fu et al. 2006). However oncogenic activity of c-Myc is not restricted to BL but can also be found in other aNHL subtypes. It was observed that within the group of non-mBL and intermediate lymphomas, a high c-Myc index was associated with significantly poorer survival, an effect that was independent of established risk factors and importantly the presence of a detectable *MYC* breakpoint. While recent data suggested genetic aberrations involving *MYC* are associated with a poor prognosis in DLBCL, we demonstrate here that a high c-Myc index is also present in cases without a detectable *MYC* breakpoint (Klapper, Stoecklein et al. 2008; Johnson, Savage et al. 2009; Savage, Johnson et al. 2009) (Barrans, Crouch et al. 2011; Zhang, Chen et al. 2011). Thus, high c-Myc activity is responsible for poor prognosis, irrespective of the nature of the *MYC* abnormality. These abnormalities could include for example copy number variations as recently increased copy numbers of *MYC* have been identified in DLBCL (Stasik, Nitta et al. 2010). Therefore, the assumption, that only those DLBCLs with an *IG-MYC* translocation have a poorer prognosis compared to BL and other types of DLBCL, has to be reconsidered. The c-Myc index gives a more comprehensive risk assessment since it is based on actual c-Myc activity instead of the presence of a *MYC* translocation.

Many of the genes in the c-Myc index have been identified earlier as c-Myc targets in different cellular contexts using different experimental approaches. For example, the GSEA analysis showed a strong enrichment of genes identified by Bild and colleagues, who developed a series of oncogenic signatures based on an analysis of data from c-Myc expression in human primary mammary epithelial cells (Bild, Yao et al. 2006). Also enriched were c-Myc target genes that have been identified in a lymphatic cell line by chromatin immunoprecipitation in combination with human promotor arrays or in inducible c-Myc assays (Schuhmacher, Kohlhuber et al. 2001; Li, Van Calcar et al. 2003). The uniqueness of the c-Myc target list presented here, lies in its focus on genes that are targeted by c-Myc both in GC B cells and in the lymphoma samples. Hence one could conclude that these genes are those most likely to be crucial for the transformation of germinal centre B cells.

It was also observed that CD40 pathway elements are depleted upon c-Myc overexpression. This is mainly reflected by genes that are regulated by NF- κ B and fits with previous observations of others groups (Basso, Klein et al. 2004; Hummel, Bentink et al. 2006; Ding, Yu et al. 2008; Lam, Wright et al. 2008; Compagno, Lim et al. 2009; Fan, Zeller et al. 2010). It is also in line with previously reported *in vitro* studies showing that aberrant c-Myc expression is associated with reduced NF- κ B activity and impaired interferon response (Schlee, Holzel et al. 2007; Klapproth, Sander et al. 2009; Keller, Huber et al. 2010). Furthermore, it also supports the observation that NF- κ B and JAK/STAT regulated genes can distinguish DLBCL from mBL (Ding, Yu et al. 2008; Lam, Wright et al. 2008; Lee, Herrmann et al. 2009).

FZD7 expression was analysed as an example for one of the index genes. The inverse correlation between *MYC* and *FZD7* expression reflects the described c-Myc index. This is of interest as it allows developing new hypotheses regarding the role of Wnt signalling in germinal centre reaction and lymphomagenesis. Linking the two observations that (i) BL cell lines barely respond to stimulation with Wnt3a or Wnt5a (unpublished observation) and (ii) that *MYC* and *FZD7* expression seem to be anti-correlated, it can be suggested that BLs are less responsive towards these stimuli due to a downregulation of FZD receptors for

the Wnt pathways. This is remarkable because the gene encoding the transcription factor Lef-1, as major mediator of β -Catenin signalling, is aberrantly expressed in BLs (Hummel, Bentink et al. 2006). Therefore, a number of new questions arise regarding the role of FZD receptors in the process of mature B cell homeostasis or B cell transformation. It would be interesting to analyse the functional consequences of the observed c-Myc associated reduction of *FZD7* and how this relation might be linked to GC B cell transformation. One hypothesis could be that high c-Myc expression is leading to a disruption of these cell communication pathways and thereby further promote lymphomagenesis. However, this needs more comprehensive experiments in the future.

More recent studies, investigating the time course of c-Myc targets by array based nuclear run-on (ANRO), demonstrated a time-dependent regulation of different pathways by c-Myc (Fan, Zeller et al. 2010). Although the non-viral transient expression assay in primary human GC B cells utilized in the presented study can only picture a small snapshot, this approach demonstrates that c-Myc expression in GC B cells leads to an expression pattern that is still present in fully developed lymphomas. It shall now be extended to study if this gene expression pattern can promote cell survival, reduce spontaneous apoptosis or affect cell proliferation. This observation might open a new discussion about, whether some DLBCL (non-mBL and intermediate lymphomas) have to be treated closer to the scheme used for BL or by modifying the R-CHOP therapy.

4.2 Identification and characterisation of pathway activities in aNHL

Descriptions of global gene expression changes after perturbation of murine splenic B cells or transformed human lymphoma cells are increasingly available (Basso, Klein et al. 2004; Zhu, Hart et al. 2004). However so far these data have not been used to identify and characterise pathway activities in individual lymphomas of B cell origin. Therefore, the global effects of the activation of lymphoma cells by BCR-, CD40-, IL21-, BAFF- or LPS activation /stimulation were analysed. First, it was necessary to identify and describe the major patterns of gene expression changes induced by these stimuli. Secondly these data

repositories were used to identify gene sets allowing to explain differences in cell cycle progression behaviour between BLs and DLBCLs.

It was shown in this study that the BL cell line BL2 is in general responsive to each of the utilized stimuli and that overlapping as well as specific signalling pathways are activated upon stimulation. These include for example the activation of p38 by BCRx and CD40L and the activation of noncanonical NF- κ B in response to CD40L and to lesser extent to BAFF stimulation. Pathways that are activated upon BCR crosslink are predominantly characterised by activation of Ca^{2+} , ERK/MAPK and PI3K/AKT signals. This is in line with observations by others characterising the activated pathways in response to these stimuli in BL cells (An and Knox 1996; Wang, Grand et al. 1996; He, Chadburn et al. 2004; Hristov, Knox et al. 2005; Ogden, Pound et al. 2005). Supporting the presented observation that BCRx predominantly induces ERK MAPK and PI3K/AKT signals it was shown on a selected set of genes (*DUSPs/MYC*) that the effects of BCR activation are dominantly characterised by the activation of ERK MAPK and PI3K/AKT. The activation of NF- κ B by BCRx is rather low but needs to be evaluated in detail in the future (see chapter 3.2.1 and chapter 3.2.6). Such an analysis is in progress and will answer also the question whether the BCR activation reflects indeed an aberrant ERK or PI3K activity and can be used to identify NHLs with high PI3K/ERK-activity. A group of dual specificity phosphatases has been identified as being regulated predominantly by BCRx in BL as well as in GC B cells. This regulation is probably mediated by an ERK dependent mechanism in BL2 cells. So far nothing is known about the regulation of DUSPs in B cells. It has been described by several groups in distinct cell systems that DUSPs can be upregulated in response to external stimuli like for example LPS stimulation of macrophages or the activation of the T cell receptor in developing T cells (Jeffrey, Brummer et al. 2006; Lang, Hammer et al. 2006). Interestingly, a deregulation of DUSPs has been described to be relevant for distinct cancer types (reviewed in Keyse 2008). Based on the findings presented here it would be interesting to investigate the levels of DUSPs expression in B cell lymphoma with potential aberrant MAPK activity resulting from constitutive BCR signalling.

Recently it was shown that ABC-like DLBCL seems to be dependent on a chronic active BCR or related signals as for example TLR mediated processes (Gururajan, Jennings et al. 2006; Ke, Chelvarajan et al. 2009; Davis, Ngo et al. 2010). Until now several studies have linked active BCR signalling in lymphoma solely to an aberrant NF- κ B activity. However there is also evidence that aberrant PI3K signalling could be involved (Uddin, Hussain et al. 2006; Baohua, Xiaoyan et al. 2008). The results presented here point to a coexistence of several pathway activities in aNHL as all analysed stimulations support the view that the relative similarity of gene expression changes are mutual jointly (see chapter 3.2.8). In addition BCR mediated activity of ERK and PI3K seems to be coexisting with NF- κ B activity, as shown by the expression of CD40L stimulated genes. This is consistent with the results obtained recently by Kloo and colleagues. They showed that the activity of the PI3K is essential for some ABC DLBCL cell lines, which have a constitutive BCR signalling mediated by mutations in CD79B (Kloo, Nagel et al. 2011). Kloo and colleagues came to the conclusion, that chronic BCR activity is not only constituted of a constitutive NF- κ B activation but that as well other pathways activated by the BCR have a critical function for the sustained proliferation and survival capacity of malignant aNHLs. However Kloo and colleagues were unable to translate their experimental data on cell lines to individual lymphoma.

The conclusion that the constitutive pathway activities in DLBCL are associated with the aberrant expression of NF- κ B target genes through BCR, TLR or TNF-receptor signalling is based on the cumulative description of mutations in a number of genes involved in parts of the NF- κ B pathways. These are for example genetic alterations in MALT1, MyD88 and CARD11 which have been described for ABC DLBCL (Hailfinger, Lenz et al. 2009; Davis, Ngo et al. 2010). These mutations lead to constitutive activation of NF- κ B signalling and have been identified to be essential for the survival of DLBCL cells (Compagno, Lim et al. 2009; Ngo, Young et al. 2011). The data presented here concerning the comparison of the relative similarity of gene expression changes as described in paragraph 3.2.8 support this view on the presence of a gradient of pathway activities supporting the clinical heterogeneity of aggressive NHLs rather than a sharp discrimination of two or three subgroups.

Using the newly developed bioinformatical method “guided clustering” it was possible to identify new clusters of genes which are affected by paracrine and B cell intrinsic stimuli in the BL cell model, and as well suitable for the stratification of aNHL samples. Thereby the LPS.2* cluster was identified which was shown to be negatively associated with Bcl6 function in the gene expression profiles of aNHL (Maneck, Schrader et al. 2011). This supports the hypothesis that BCL6 could potentially modulate Toll-like receptor signalling in DLBCL, which is in line with the data published by Basso and Dalla-Favera who suggest that Bcl6 could possibly modulate TLR4 signalling (Basso, Saito et al. 2010). This finding is of particular importance as recently oncogenic mutations in MyD88, which is part of the TLR4 signalling pathway, have been identified to be relevant for ABC DLBCL (Ngo, Young et al. 2011). Furthermore the inverse correlation of Bcl6 and TLR4 activity in aNHL represents the main differences in pathway deregulations observed so far between ABC and GCB DLBCL. Our group showed that indeed the Bcl6 activity, detected via the Bcl6 index, is higher in GCB DLBCL than in ABCs. This observation consolidates the findings of Ci and colleagues (Ci, Polo et al. 2009) and further supports the understanding for the oncogenic events underlying the heterogeneity of DLBCL.

A central result presented in this study is the description of one gene cluster that is inhibited upon BCRx in BL2 cells (BCR.1). It was shown that BCR.1 activity is anti correlated with c-Myc activity in aNHL gene expression profiles, most likely as some of the BCR.1 genes are directly regulated by c-Myc. This negative association has not been observed until now. So far c-Myc and BCR signalling have been implied in the genesis of lymphoma as two synergistically acting factors. These observations include for example the critical utilization of c-Myc for BCR triggered B cell proliferation (Murn, Mlinaric-Rascan et al. 2009) as well as a direct interaction of active BCR signalling and *MYC* overexpression for the genesis of B cell lymphoma in a mouse model (Refaeli, Young et al. 2008).

It was shown that the expression of the translocated *MYC* itself is inhibited in response to BCR activation in lymphoma cells harbouring an *IG-MYC* translocation. This is in line with the results published by Kaptein and colleagues (Kaptein, Lin et al. 1996). The study presented here for the first time provides a

hint how this inhibitory effect is mediated, showing that Pi3K activity is needed for this effect. The BCR.1 cluster represents a group of genes which is expressed on lower levels in a subgroup of DLBCLs compared to BLs. The results presented here imply that the low expression of these genes in aNHL is either mediated by a high constitutive BCR signal or by a missing aberrant c-Myc activity. As shown in chapter 3.3.5 and 3.3.6 a group of BCR.1 genes is expressed dependently of high c-Myc function in BL cells and the expression of one of the BCR.1 cluster genes (*BUB1B*) is directly regulated by c-Myc in response to BCR crosslink. The effects observed on the expression of these genes in response to c-Myc inhibition are perfectly in line with previously published findings regarding *AURKA* and *BUB1B*, which have been identified as c-Myc target genes in different cell systems (Menssen, Epanchintsev et al. 2007; den Hollander, Rimpi et al. 2009). The identification of *TMEM97* as being expressed dependently on c-Myc in BL cells in consolidates the c-Myc index described above. *PBK-TOPK* as well as *BIRC5* have so far not been described as target genes of c-Myc.

It was found that BCR activation leads as short term effect to a prolonged G2 cell cycle phase which is accompanied by a downregulated expression of G2 phase associated genes mainly encoding spindle checkpoint factors (BCR.1). Furthermore it could be observed that after 24 h of BCR stimulation BL cells arrest in G1 phase of the cell cycle. So far the effects of BCR activation on cell cycle regulation in lymphoma cells have only been investigated using longer time points of 16-24hrs (Hristov, Knox et al. 2007; Jamal, Ravichandran et al. 2010). These studies found that BCR activation leads to a G1 arrest of BL cells which is consistent with the results presented here. Jamal and colleagues described a complex model of a BCRx induced network involving AKT and ERK, which induces G1 cell cycle arrest in CH1 mouse B cell lymphoma cells. This is in line with the ERK and PI3K dominant effect of BCRx observed in BL2 cells. On top of this, it was shown here that BCR activation leads to a prolonged G2 phase of BL cells cycle in a time frame of 3-9hrs. The findings presented here offer a potential explanation for the G1 cell cycle arrest observed in response to BCR activation. The prolonged G2 phase accompanied by an inhibited expression of spindle checkpoint genes could be a hint for problems of the cell with proper chromosomal segregation during mitosis. Chromosomal miss-segregation in

response to BCR activation could activate a safety mechanism which arrests the cells in G1 phase.

The BCR mediated effect on the G2 phase is enhanced by an additional inhibition of c-Myc. Since several BCR.1 cluster genes e.g. BUB1B and BIRC5 have been identified to be regulated by BCR activation and by c-Myc activity one could conclude that the BCR effect on the cell cycle is, at least in part, mediated by c-Myc. The regulation of the G2 cell cycle phase via BUB1B and MAD2 has already been linked to c-Myc by Menssen and colleagues (Menssen, Epanchintsev et al. 2007). In the study presented by Menssen and colleagues it was shown that the activation of c-Myc leads to a prolonged passage of cells through the G2 phase of the cell cycle. This is contradictory to the findings presented here, where it was shown that highly active c-Myc is needed for a fast progression of BL cells through the G2 cell cycle phase. Menssen and colleagues investigated the effects of c-Myc on the cell cycle in a human colon cancer cell line and a mouse mammary carcinoma cell line both genetically modified to contain a tamoxifen inducible *MYC* allele. Compared to the system presented here, where c-Myc is expressed under the control of an Immunoglobulin enhancer, the cell systems used by Menssen and colleagues are rather inapplicable for the analysis of c-Myc function in lymphoma cells. It has been shown by several groups that the effects of c-Myc are largely context dependent (Dang, O'Donnell et al. 2006). Therefore it is not surprising that the alterations in c-Myc activities have distinct effects in a c-Myc dependent BL cell line compared to a genetically modified colon or mammary carcinoma cell line.

One of the central BCR.1 genes identified here is *BUB1B*. It has been shown that a dysfunction of BUB1B is associated with defects in spindle checkpoint function which lead in consequence to chromosomal instability (CIN) and to the development of tumours due to a tumour suppressor gene loss of heterozygosity (Rao, Yang et al. 2005; Baker, Jin et al. 2009; Li, Fang et al. 2009). It has been shown for CML that the activity of the Bcr-abl tyrosine kinase is associated with an inhibited expression of BRCA1, MAD2, Bub1, Bub3 and BUB1B and thereby induces a weakened spindle checkpoint function accompanied with mitotic slippage upon nocodazole treatment (Wolanin, Magalska et al. 2010). Keeping in

mind that DLBCL lymphoma are characterised by a complex karyotype, one could postulate, that the chronic BCR signal provokes a lower expression of spindle checkpoint regulators like BUB1B in these lymphoma and thereby impairs a proper spindle checkpoint function leading to miss segregation of chromosomes.

Transferred to primary lymphoma one could postulate that the lower expression of the BCR.1 cell cycle genes in the group of DLBCL with high BCR.1 index, could be associated with a longer passage of the lymphoma cells through the G2 phase of the cell cycle. This would be in line with the generally slower growth of DLBCL lymphoma (Ki67 index) compared to BL (Hummel, Bentink et al. 2006) and could serve as explanation for the differences in proliferation rates of BL and DLBCL.

The presented study raises the question how the cell cycle regulation is affected in intermediate lymphoma that have both: active BCR signalling as well as aberrant c-Myc activity. These cases show high BCR.1 index compared to BL, but a lower BCR.1 index compared to DLBCL (lower expression of BCR.1 cluster genes). One could define this group as “Myc high” and “BCR.1 intermediate”. Following the presented model these cells would have a rather high proliferation rate accompanied with a fast passage through the G2 phase and additional impairments regarding the proper progress through G2. This could potentially explain why these lymphomas have been identified as those aNHL cases with a poorer prognosis compared to other DLBCL patients (see Chapter 1). Using treatment strategies that are closer to BL together with targeted therapies against the pathways that inhibit the expression of BCR.1 genes (e.g. the Syk inhibitor proposed by Chen and colleagues (Chen, Monti et al. 2008)) might help to overcome the bad prognosis for these patients.

Another BCR.1 index gene that encodes for a factor involved in spindle checkpoint function is *PLK1* (Polo-Like Kinase 1). In ongoing analyses it is tested whether *PLK1* is as well regulated by c-Myc in response to BCRx. It has been shown that the expression of *PLK1* is associated with a high proliferative index of aNHLs and shortened event free survival (Mito, Kashima et al. 2005; Liu, Zhang et al. 2007). As small molecule inhibitors against PLK1 are already tested in

clinical phase 1 studies (Schoffski 2009), this kinase might be a promising target for individualised therapies for “BCR.1 low” BL and DLBCL cases.

To support the model of BCR induced chromosomal instability, it would be interesting to test whether activated BCR signalling induces chromosomal instability in BL cells harbouring an otherwise simple karyotype. In order to show that the group of “BCR.1 high” lymphoma indeed harbour a longer passage through the G2 phase one strategy could be to stain G2 phase markers, like CyclinB, in histological specimens of DLBCL. Thereby one could be able to check whether the prolonged duration of the G2 phase can be indeed found *in vivo*. As c-Myc is likely not the only factor regulating BCR.1 genes, it would be interesting to investigate which pathways could additionally mediate the inhibition of BCR.1 cluster genes and the BCR mediated cell cycle effect in order to infer on the possibly deregulated pathways in “BCR.1 high” lymphoma. Using a recently published dataset of geneexpression profiles of 900 aNHL cases (Salaverria, Philipp et al. 2011), that includes survival analyses as independent dataset; it would be interesting to investigate the impact of BCR.1 cluster activity on the patient outcome. Identifying the oppositional existence of BCR.1 activity and c-Myc activity reflected in the gene expression profiles of aNHL this study enabled to suggest new models explaining the heterogeneity of aNHL.

As pointed out in paragraph 3.3.2 the newly identified gene clusters representing pathway activities induced by B cell stimuli did not discriminate ABC from GCB DLBCL. These DLBCL subgroups have been identified on the basis of global differences in lymphoma gene expression profiles (Alizadeh, Eisen et al. 2000). Alizadeh and colleagues described that genes which are differentially expressed comparing both DLBCL subgroups are as well differentially expressed comparing normal GC B cells with peripheral blood B lymphocytes activated with a combination of CD40L, anti-IgM and IL-4. Based on the similarity of lymphoma gene expression profiles to these different normal B cell gene expression profiles the subgroups were named ABC like and GCB like DLBCL. This approach is different to the strategy followed in this study. Alizadeh and colleagues did not focus on genes that are activated by specifically one single stimulus but rather considered the global effects of B cell activation. Genes considered for the

discrimination of ABC and GCB lymphoma are expressed in the same way in stimulated peripheral blood cells disregarding the stimulus used and the time point of microarray analysis. Thus this “activated B cell pattern” observed by Alizadeh and colleagues is rather mediated by a combination of distinct activated pathways in the peripheral blood cells as well as in the lymphoma. It has been shown by several studies that the group of ABC DLBCL still comprises heterogeneous lymphomas that depend on distinct oncogenic pathways (Bentink, Wessendorf et al. 2008; Kloos, Nagel et al. 2011). To achieve a discrimination of ABC and GCB using the gene modules presented here, it could therefore be promising to utilize a combination of distinct gene cluster activities. Nevertheless this was not the primary focus of this study.

5 Conclusion

The integration of global gene expression data from *in vitro* perturbation analyses as ectopic expression of c-Myc in GC B cells or stimulation of lymphoma cells provides a robust quantitative measure of oncogenic activity in individual lymphoma. This study offers a comprehensive data repository that enabled the advancement of bioinformatical methods. By providing these gene expression analyses, this study is of high value for lymphoma research in general, as these data open a new scope to signalling events induced by specific B cell stimuli in lymphoma cells. The identification of gene clusters regulated by BCR, CD40, IL21, LPS and BAFF provides new opportunities for the analysis of aberrant signalling in lymphomas.

DLBCLs with high c-Myc activity were identified. It was shown that the c-Myc index is an independent negative prognostic factor for these patients. Furthermore, it was found that the c-Myc index is inversely correlated to a newly identified BCR regulated gene cluster in gene expression profiles of aNHL. This correlation links for the first time active BCR signalling to the growth behaviour differences in aNHL. Furthermore, the results presented in this study propose a new explanation regarding the potential mechanism of the appearance of a higher cytogenetic complexity in DLBCLs: a high BCR signal and low c-Myc activity could be involved in a prolonged G2 phase in some DLBCLs which is followed by defects in spindle checkpoint functions, probably leading to enhanced chromosomal instabilities in these lymphomas. This could have implications for individualized therapies of lymphoma patients regarding the usage of chemotherapeutics targeting G2 phase associated processes.

Integrating the information retrieved from the identified c-Myc index and the BCR.1 cluster it was shown that the effects of a genetic alteration are not per se static, but can be mimicked by external mechanisms as paracrine stimulation of lymphoma cells with micro-environmental factors.

Bibliography

- Adhikary, S. and M. Eilers (2005). "Transcriptional regulation and transformation by Myc proteins." Nat Rev Mol Cell Biol 6(8): 635-645.
- Akamatsu, N., Y. Yamada, et al. (2007). "High IL-21 receptor expression and apoptosis induction by IL-21 in follicular lymphoma." Cancer Lett 256(2): 196-206.
- Alizadeh, A. A., M. B. Eisen, et al. (2000). "Distinct types of diffuse large B-cell lymphoma identified by gene expression profiling." Nature 403(6769): 503-511.
- An, S. and K. A. Knox (1996). "Ligation of CD40 rescues Ramos-Burkitt lymphoma B cells from calcium ionophore- and antigen receptor-triggered apoptosis by inhibiting activation of the cysteine protease CPP32/Yama and cleavage of its substrate PARP." FEBS Lett 386(2-3): 115-122.
- Aramburu, J., M. B. Yaffe, et al. (1999). "Affinity-driven peptide selection of an NFAT inhibitor more selective than cyclosporin A." Science 285(5436): 2129-2133.
- Armitage, R. J., W. C. Fanslow, et al. (1992). "Molecular and biological characterization of a murine ligand for CD40." Nature 357(6373): 80-82.
- Asao, H., C. Okuyama, et al. (2001). "Cutting edge: the common gamma-chain is an indispensable subunit of the IL-21 receptor complex." J Immunol 167(1): 1-5.
- Audette, M., L. Larouche, et al. (2001). "Stimulation of the ICAM-1 gene transcription by the peroxovanadium compound [bpV(Pic)] involves STAT-1 but not NF-kappa B activation in 293 cells." Eur J Biochem 268(6): 1828-1836.
- Badr, G., G. Borhis, et al. (2008). "BAFF enhances chemotaxis of primary human B cells: a particular synergy between BAFF and CXCL13 on memory B cells." Blood 111(5): 2744-2754.
- Baker, D. J., F. Jin, et al. (2009). "Whole chromosome instability caused by Bub1 insufficiency drives tumorigenesis through tumor suppressor gene loss of heterozygosity." Cancer Cell 16(6): 475-486.
- Baker, K. P., B. M. Edwards, et al. (2003). "Generation and characterization of LymphoStat-B, a human monoclonal antibody that antagonizes the bioactivities of B lymphocyte stimulator." Arthritis Rheum 48(11): 3253-3265.
- Baldwin, A. S., Jr. (1996). "The NF-kappa B and I kappa B proteins: new discoveries and insights." Annu Rev Immunol 14: 649-683.
- Baohua, Y., Z. Xiaoyan, et al. (2008). "Mutations of the PIK3CA gene in diffuse large B cell lymphoma." Diagn Mol Pathol 17(3): 159-165.
- Baron, B. W., G. Nucifora, et al. (1993). "Identification of the gene associated with the recurring chromosomal translocations t(3;14)(q27;q32) and t(3;22)(q27;q11) in B-cell lymphomas." Proc Natl Acad Sci U S A 90(11): 5262-5266.
- Barrans, S., S. Crouch, et al. (2011). "Rearrangement of MYC is associated with poor prognosis in patients with diffuse large B-cell lymphoma treated in the era of rituximab." J Clin Oncol 28(20): 3360-3365.
- Basso, K., U. Klein, et al. (2004). "Tracking CD40 signaling during germinal center development." Blood 104(13): 4088-4096.
- Basso, K., M. Saito, et al. (2010). "Integrated biochemical and computational approach identifies BCL6 direct target genes controlling multiple pathways in normal germinal center B cells." Blood 115(5): 975-984.

Bibliography

- Beckwith, M., D. L. Longo, et al. (1990). "Phorbol ester-induced, cell-cycle-specific, growth inhibition of human B-lymphoma cell lines." J Natl Cancer Inst 82(6): 501-509.
- Ben-Bassat, H., N. Goldblum, et al. (1977). "Establishment in continuous culture of a new type of lymphocyte from a "Burkitt like" malignant lymphoma (line D.G.-75)." Int J Cancer 19(1): 27-33.
- Bennett, B. L., D. T. Sasaki, et al. (2001). "SP600125, an anthrapyrazolone inhibitor of Jun N-terminal kinase." Proc Natl Acad Sci U S A 98(24): 13681-13686.
- Bentink, S., S. Wessendorf, et al. (2008). "Pathway activation patterns in diffuse large B-cell lymphomas." Leukemia 22(9): 1746-1754.
- Berg, T., S. B. Cohen, et al. (2002). "Small-molecule antagonists of Myc/Max dimerization inhibit Myc-induced transformation of chicken embryo fibroblasts." Proc Natl Acad Sci U S A 99(6): 3830-3835.
- Bernheim, A., R. Berger, et al. (1983). "Cytogenetic studies on Burkitt's lymphoma cell lines." Cancer Genet Cytogenet 8(3): 223-229.
- Bidere, N., V. N. Ngo, et al. (2009). "Casein kinase 1alpha governs antigen-receptor-induced NF-kappaB activation and human lymphoma cell survival." Nature 458(7234): 92-96.
- Bild, A. H., G. Yao, et al. (2006). "Oncogenic pathway signatures in human cancers as a guide to targeted therapies." Nature 439(7074): 353-357.
- Blackwell, T. K., L. Kretzner, et al. (1990). "Sequence-specific DNA binding by the c-Myc protein." Science 250(4984): 1149-1151.
- Blumer, K. J. (2004). "Vision: the need for speed." Nature 427(6969): 20-21.
- Bossen, C. and P. Schneider (2006). "BAFF, APRIL and their receptors: structure, function and signaling." Semin Immunol 18(5): 263-275.
- Boveri, T. (1907). "Zellenstudien. VI. Eine für die erste Orientierung geeignete Darstellung dieser und anderer Chromosomenprobleme findet sich in meiner Schrift: Ergebnisse über die Konstitution der chromatischen Substanz des Zellkerns." Jena 1904.
- Boveri, T. (2008). "Concerning the origin of malignant tumours by Theodor Boveri. Translated and annotated by Henry Harris." J Cell Sci 121 Suppl 1: 1-84.
- Bradford, M. M. (1976). "A rapid and sensitive method for the quantitation of microgram quantities of protein utilizing the principle of protein-dye binding." Anal Biochem 72: 248-254.
- Briones, J., J. M. Timmerman, et al. (2002). "BLyS and BLyS receptor expression in non-Hodgkin's lymphoma." Exp Hematol 30(2): 135-141.
- Burkitt, D. (1958). "A sarcoma involving the jaws in African children." Br J Surg 46(197): 218-223.
- Cambier, J. C. (1995). "New nomenclature for the Reth motif (or ARH1/TAM/ARAM/YXXL)." Immunol Today 16(2): 110.
- Chang, H., J. A. Blomdal, et al. (1995). "p53 mutations, c-myc and bcl-2 rearrangements in human non-Hodgkin's lymphoma cell lines." Leuk Lymphoma 19(1-2): 165-171.
- Chen, L., S. Monti, et al. (2008). "SYK-dependent tonic B-cell receptor signaling is a rational treatment target in diffuse large B-cell lymphoma." Blood 111(4): 2230-2237.
- Cheng, G., A. M. Cleary, et al. (1995). "Involvement of CRAF1, a relative of TRAF, in CD40 signaling." Science 267(5203): 1494-1498.

- Choi, W. W., D. D. Weisenburger, et al. (2009). "A new immunostain algorithm classifies diffuse large B-cell lymphoma into molecular subtypes with high accuracy." Clin Cancer Res 15(17): 5494-5502.
- Ci, W., J. M. Polo, et al. (2009). "The BCL6 transcriptional program features repression of multiple oncogenes in primary B cells and is deregulated in DLBCL." Blood 113(22): 5536-5548.
- Claudio, E., K. Brown, et al. (2002). "BAFF-induced NEMO-independent processing of NF-kappa B2 in maturing B cells." Nat Immunol 3(10): 958-965.
- Coiffier, B. (2005). "Current strategies for the treatment of diffuse large B cell lymphoma." Curr Opin Hematol 12(4): 259-265.
- Compagno, M., W. K. Lim, et al. (2009). "Mutations of multiple genes cause deregulation of NF-kappaB in diffuse large B-cell lymphoma." Nature 459(7247): 717-721.
- Coquet, J. M., K. Kyriassoudis, et al. (2007). "IL-21 is produced by NKT cells and modulates NKT cell activation and cytokine production." J Immunol 178(5): 2827-2834.
- Cuenda, A., J. Rouse, et al. (1995). "SB 203580 is a specific inhibitor of a MAP kinase homologue which is stimulated by cellular stresses and interleukin-1." FEBS Lett 364(2): 229-233.
- D'Orlando, O., G. Gri, et al. (2007). "Outside inside signalling in CD40-mediated B cell activation." J Biol Regul Homeost Agents 21(3-4): 49-62.
- Dalla-Favera, R., M. Bregni, et al. (1982). "Human c-myc onc gene is located on the region of chromosome 8 that is translocated in Burkitt lymphoma cells." Proc Natl Acad Sci U S A 79(24): 7824-7827.
- Dang, C. V., K. A. O'Donnell, et al. (2006). "The c-Myc target gene network." Semin Cancer Biol 16(4): 253-264.
- Dave, B. J., M. Nelson, et al. (2002). "Cytogenetic characterization of diffuse large cell lymphoma using multi-color fluorescence in situ hybridization." Cancer Genet Cytogenet 132(2): 125-132.
- Dave, S. S., K. Fu, et al. (2006). "Molecular diagnosis of Burkitt's lymphoma." N Engl J Med 354(23): 2431-2442.
- Davis, I. D., K. Skak, et al. (2007). "Interleukin-21 signaling: functions in cancer and autoimmunity." Clin Cancer Res 13(23): 6926-6932.
- Davis, R. E., K. D. Brown, et al. (2001). "Constitutive nuclear factor kappaB activity is required for survival of activated B cell-like diffuse large B cell lymphoma cells." J Exp Med 194(12): 1861-1874.
- Davis, R. E., V. N. Ngo, et al. (2010). "Chronic active B-cell-receptor signalling in diffuse large B-cell lymphoma." Nature 463(7277): 88-92.
- de Jong, D. and O. Balague Ponz (2011). "The molecular background of aggressive B cell lymphomas as a basis for targeted therapy." J Pathol 223(2): 274-282.
- den Hollander, J., S. Rimpì, et al. (2009). "Aurora kinases A and B are up-regulated by Myc and are essential for maintenance of the malignant state." Blood 116(9): 1498-1505.
- Dent, A. L., A. L. Shaffer, et al. (1997). "Control of inflammation, cytokine expression, and germinal center formation by BCL-6." Science 276(5312): 589-592.
- Dillon, S. R., J. A. Gross, et al. (2006). "An APRIL to remember: novel TNF ligands as therapeutic targets." Nat Rev Drug Discov 5(3): 235-246.

Bibliography

- Ding, B. B., J. J. Yu, et al. (2008). "Constitutively activated STAT3 promotes cell proliferation and survival in the activated B-cell subtype of diffuse large B-cell lymphomas." Blood 111(3): 1515-1523.
- Ding, C. and G. Jones (2006). "Belimumab Human Genome Sciences/Cambridge Antibody Technology/GlaxoSmithKline." Curr Opin Investig Drugs 7(5): 464-472.
- Doyle, S. L. and L. A. O'Neill (2006). "Toll-like receptors: from the discovery of NFkappaB to new insights into transcriptional regulations in innate immunity." Biochem Pharmacol 72(9): 1102-1113.
- Egawa, T., B. Albrecht, et al. (2003). "Requirement for CARMA1 in antigen receptor-induced NF-kappa B activation and lymphocyte proliferation." Curr Biol 13(14): 1252-1258.
- Eick, D. and G. W. Bornkamm (1989). "Expression of normal and translocated c-myc alleles in Burkitt's lymphoma cells: evidence for different regulation." EMBO J 8(7): 1965-1972.
- Epstein, A. L., M. M. Herman, et al. (1976). "Biology of the human malignant lymphomas. III. Intracranial heterotransplantation in the nude, athymic mouse." Cancer 37(5): 2158-2176.
- Epstein, A. L., R. Levy, et al. (1978). "Biology of the human malignant lymphomas. IV. Functional characterization of ten diffuse histiocytic lymphoma cell lines." Cancer 42(5): 2379-2391.
- Ettinger, R., S. Kuchen, et al. (2008). "The role of IL-21 in regulating B-cell function in health and disease." Immunol Rev 223: 60-86.
- Ettinger, R., G. P. Sims, et al. (2005). "IL-21 induces differentiation of human naive and memory B cells into antibody-secreting plasma cells." J Immunol 175(12): 7867-7879.
- Fan, J., K. Zeller, et al. (2010). "Time-dependent c-Myc transactomes mapped by Array-based nuclear run-on reveal transcriptional modules in human B cells." PLoS One 5(3): e9691.
- Farinha, P. and R. D. Gascoyne (2005). "Molecular pathogenesis of mucosa-associated lymphoid tissue lymphoma." J Clin Oncol 23(26): 6370-6378.
- Favata, M. F., K. Y. Horiuchi, et al. (1998). "Identification of a novel inhibitor of mitogen-activated protein kinase kinase." J Biol Chem 273(29): 18623-18632.
- Ferlay J, S. H., Bray F, Forman D, Mathers C and Parkin DM. (2010). "GLOBOCAN 2008 v1.2, Cancer Incidence and Mortality Worldwide: IARC CancerBase No. 10 [Internet].", from <http://globocan.iarc.fr>
- Feuerhake, F., J. L. Kutok, et al. (2005). "NFkappaB activity, function, and target-gene signatures in primary mediastinal large B-cell lymphoma and diffuse large B-cell lymphoma subtypes." Blood 106(4): 1392-1399.
- Fox (1980). "A model for the computer analysis of synchronous DNA distributions obtained by flow cytometry." Cytometry 1: 71-77.
- Foy, T. M., J. D. Laman, et al. (1994). "gp39-CD40 interactions are essential for germinal center formation and the development of B cell memory." J Exp Med 180(1): 157-163.
- Foy, T. M., D. M. Shepherd, et al. (1993). "In vivo CD40-gp39 interactions are essential for thymus-dependent humoral immunity. II. Prolonged suppression of the humoral immune response by an antibody to the ligand for CD40, gp39." J Exp Med 178(5): 1567-1575.

- Friedberg, J. W. and R. I. Fisher (2008). "Diffuse large B-cell lymphoma." Hematol Oncol Clin North Am 22(5): 941-952, ix.
- Fukuda, T., T. Yoshida, et al. (1997). "Disruption of the Bcl6 gene results in an impaired germinal center formation." J Exp Med 186(3): 439-448.
- Fuqua, C. F., R. Akomeah, et al. (2008). "Involvement of ERK-1/2 in IL-21-induced cytokine production in leukemia cells and human monocytes." Cytokine 44(1): 101-107.
- Gardam, S., F. Sierro, et al. (2008). "TRAF2 and TRAF3 signal adapters act cooperatively to control the maturation and survival signals delivered to B cells by the BAFF receptor." Immunity 28(3): 391-401.
- Good, D. J. and R. D. Gascoyne (2008). "Classification of non-Hodgkin's lymphoma." Hematol Oncol Clin North Am 22(5): 781-805, vii.
- Graf, D., U. Korthauer, et al. (1992). "Cloning of TRAP, a ligand for CD40 on human T cells." Eur J Immunol 22(12): 3191-3194.
- Gross, J. A., J. Johnston, et al. (2000). "TACI and BCMA are receptors for a TNF homologue implicated in B-cell autoimmune disease." Nature 404(6781): 995-999.
- Gururajan, M., C. D. Jennings, et al. (2006). "Cutting edge: constitutive B cell receptor signaling is critical for basal growth of B lymphoma." J Immunol 176(10): 5715-5719.
- Hailfinger, S., G. Lenz, et al. (2009). "Essential role of MALT1 protease activity in activated B cell-like diffuse large B-cell lymphoma." Proc Natl Acad Sci U S A 106(47): 19946-19951.
- Hanahan, D. and R. A. Weinberg (2011). "Hallmarks of cancer: the next generation." Cell 144(5): 646-674.
- Harada, M., K. Magara-Koyanagi, et al. (2006). "IL-21-induced Bepsilon cell apoptosis mediated by natural killer T cells suppresses IgE responses." J Exp Med 203(13): 2929-2937.
- Hatzoglou, A., J. Roussel, et al. (2000). "TNF receptor family member BCMA (B cell maturation) associates with TNF receptor-associated factor (TRAF) 1, TRAF2, and TRAF3 and activates NF-kappa B, elk-1, c-Jun N-terminal kinase, and p38 mitogen-activated protein kinase." J Immunol 165(3): 1322-1330.
- He, B., A. Chadburn, et al. (2004). "Lymphoma B cells evade apoptosis through the TNF family members BAFF/BLyS and APRIL." J Immunol 172(5): 3268-3279.
- Hollenbaugh, D., L. S. Grosmaire, et al. (1992). "The human T cell antigen gp39, a member of the TNF gene family, is a ligand for the CD40 receptor: expression of a soluble form of gp39 with B cell co-stimulatory activity." EMBO J 11(12): 4313-4321.
- Hömig-Hölzel, C., C. Hojer, et al. (2008). "Constitutive CD40 signaling in B cells selectively activates the noncanonical NF-kappaB pathway and promotes lymphomagenesis." J Exp Med 205(6): 1317-1329.
- Hörtnagel, K., J. Mautner, et al. (1995). "The role of immunoglobulin kappa elements in c-myc activation." Oncogene 10(7): 1393-1401.
- Hoshino, K., O. Takeuchi, et al. (1999). "Cutting edge: Toll-like receptor 4 (TLR4)-deficient mice are hyporesponsive to lipopolysaccharide: evidence for TLR4 as the Lps gene product." J Immunol 162(7): 3749-3752.
- Hristov, K. K., K. A. Knox, et al. (2005). "Regulation of tyrosine phosphorylation during the CD40-mediated rescue of Ramos-BL B cells from BCR-triggered apoptosis." Int J Mol Med 16(5): 937-941.

Bibliography

- Hristov, K. K., K. A. Knox, et al. (2007). "Vanadate-induced inhibition of BCR-triggered apoptosis is coupled with tyrosine phosphorylation and induction of G2M growth arrest in Ramos-BL B cells." Immunol Invest 36(3): 293-306.
- Hu, H. M., K. O'Rourke, et al. (1994). "A novel RING finger protein interacts with the cytoplasmic domain of CD40." J Biol Chem 269(48): 30069-30072.
- Huber, W., A. von Heydebreck, et al. (2002). "Variance stabilization applied to microarray data calibration and to the quantification of differential expression." Bioinformatics 18 Suppl 1: S96-104.
- Hummel, M., S. Bentink, et al. (2006). "A biologic definition of Burkitt's lymphoma from transcriptional and genomic profiling." N Engl J Med 354(23): 2419-2430.
- Iqbal, J., T. C. Greiner, et al. (2007). "Distinctive patterns of BCL6 molecular alterations and their functional consequences in different subgroups of diffuse large B-cell lymphoma." Leukemia 21(11): 2332-2343.
- Iqbal, J., S. Gupta, et al. (2007). "Diffuse large B-cell lymphoma with a novel translocation involving BCL6." Cancer Genet Cytogenet 178(1): 73-76.
- Irizarry, R. A., B. Hobbs, et al. (2003). "Exploration, normalization, and summaries of high density oligonucleotide array probe level data." Biostatistics 4(2): 249-264.
- Ishida, T., S. Mizushima, et al. (1996). "Identification of TRAF6, a novel tumor necrosis factor receptor-associated factor protein that mediates signaling from an amino-terminal domain of the CD40 cytoplasmic region." J Biol Chem 271(46): 28745-28748.
- Ishida, T. K., T. Tojo, et al. (1996). "TRAF5, a novel tumor necrosis factor receptor-associated factor family protein, mediates CD40 signaling." Proc Natl Acad Sci U S A 93(18): 9437-9442.
- Jaffe, E. S., N. L. Harris, et al. (1998). "World Health Organization Classification of lymphomas: a work in progress." Ann Oncol 9 Suppl 5: S25-30.
- Jamal, M. S., S. Ravichandran, et al. (2010). "Defining the antigen receptor-dependent regulatory network that induces arrest of cycling immature B-lymphocytes." BMC Syst Biol 4: 169.
- Jeffrey, K. L., T. Brummer, et al. (2006). "Positive regulation of immune cell function and inflammatory responses by phosphatase PAC-1." Nat Immunol 7(3): 274-283.
- Johnson, N. A., K. J. Savage, et al. (2009). "Lymphomas with concurrent BCL2 and MYC translocations: the critical factors associated with survival." Blood 114(11): 2273-2279.
- Kahl, B. (2008). "Chemotherapy combinations with monoclonal antibodies in non-Hodgkin's lymphoma." Semin Hematol 45(2): 90-94.
- Kaptein, J. S., C. K. Lin, et al. (1996). "Anti-IgM-mediated regulation of c-myc and its possible relationship to apoptosis." J Biol Chem 271(31): 18875-18884.
- Karin, M. and Y. Ben-Neriah (2000). "Phosphorylation meets ubiquitination: the control of NF-[kappa]B activity." Annu Rev Immunol 18: 621-663.
- Kawai, T., O. Adachi, et al. (1999). "Unresponsiveness of MyD88-deficient mice to endotoxin." Immunity 11(1): 115-122.
- Ke, J., R. L. Chelvarajan, et al. (2009). "Anomalous constitutive Src kinase activity promotes B lymphoma survival and growth." Mol Cancer 8: 132.
- Keller, U., J. Huber, et al. (2010). "Myc suppression of Nfkb2 accelerates lymphomagenesis." BMC Cancer 10: 348.

- Keyse, S. M. (2000). "Protein phosphatases and the regulation of mitogen-activated protein kinase signalling." Curr Opin Cell Biol 12(2): 186-192.
- Keyse, S. M. (2008). "Dual-specificity MAP kinase phosphatases (MKPs) and cancer." Cancer Metastasis Rev 27(2): 253-261.
- Khan, W. N. (2009). "B cell receptor and BAFF receptor signaling regulation of B cell homeostasis." J Immunol 183(6): 3561-3567.
- Klapper, W., H. Stoecklein, et al. (2008). "Structural aberrations affecting the MYC locus indicate a poor prognosis independent of clinical risk factors in diffuse large B-cell lymphomas treated within randomized trials of the German High-Grade Non-Hodgkin's Lymphoma Study Group (DSHNHL)." Leukemia 22(12): 2226-2229.
- Klapproth, K., S. Sander, et al. (2009). "The IKK2/NF- κ B pathway suppresses MYC-induced lymphomagenesis." Blood 114(12): 2448-2458.
- Klein, G., B. Giovanella, et al. (1975). "An EBV-genome-negative cell line established from an American Burkitt lymphoma; receptor characteristics. EBV infectibility and permanent conversion into EBV-positive sublines by in vitro infection." Intervirology 5(6): 319-334.
- Klein, U. and R. Dalla-Favera (2008). "Germinal centres: role in B-cell physiology and malignancy." Nat Rev Immunol 8(1): 22-33.
- Klein, U., Y. Tu, et al. (2003). "Transcriptional analysis of the B cell germinal center reaction." Proc Natl Acad Sci U S A 100(5): 2639-2644.
- Kloo, B., D. Nagel, et al. (2011). "Critical role of PI3K signaling for NF-kappaB-dependent survival in a subset of activated B-cell-like diffuse large B-cell lymphoma cells." Proc Natl Acad Sci U S A 108(1): 272-277.
- Konforte, D., N. Simard, et al. (2009). "IL-21: an executor of B cell fate." J Immunol 182(4): 1781-1787.
- Kube, D., C. Platzer, et al. (1995). "Isolation of the human interleukin 10 promoter. Characterization of the promoter activity in Burkitt's lymphoma cell lines." Cytokine 7(1): 1-7.
- Kube, D. and M. Vockerodt (2001). "Transient gene expression and MACS enrichment." Methods Mol Biol 174: 155-164.
- Küppers, R. (2005). "Mechanisms of B-cell lymphoma pathogenesis." Nat Rev Cancer 5(4): 251-262.
- Küppers, R. and R. Dalla-Favera (2001). "Mechanisms of chromosomal translocations in B cell lymphomas." Oncogene 20(40): 5580-5594.
- Kutz, H., G. Reisbach, et al. (2008). "The c-Jun N-terminal kinase pathway is critical for cell transformation by the latent membrane protein 1 of Epstein-Barr virus." Virology 371(2): 246-256.
- Ladanyi, M., K. Offit, et al. (1991). "MYC rearrangement and translocations involving band 8q24 in diffuse large cell lymphomas." Blood 77(5): 1057-1063.
- Lam, L. T., R. E. Davis, et al. (2005). "Small molecule inhibitors of IkappaB kinase are selectively toxic for subgroups of diffuse large B-cell lymphoma defined by gene expression profiling." Clin Cancer Res 11(1): 28-40.
- Lam, L. T., G. Wright, et al. (2008). "Cooperative signaling through the signal transducer and activator of transcription 3 and nuclear factor- κ B pathways in subtypes of diffuse large B-cell lymphoma." Blood 111(7): 3701-3713.

Bibliography

- Lang, R., M. Hammer, et al. (2006). "DUSP meet immunology: dual specificity MAPK phosphatases in control of the inflammatory response." J Immunol 177(11): 7497-7504.
- Laskov, R., N. Berger, et al. (2005). "Differential effects of tumor necrosis factor-alpha and CD40L on NF-kappa B inhibitory proteins I kappa B alpha, beta and epsilon and on the induction of the Jun amino-terminal kinase pathway in Ramos Burkitt lymphoma cells." Eur Cytokine Netw 16(4): 267-276.
- Lederman, S., M. J. Yellin, et al. (1992). "Identification of a novel surface protein on activated CD4+ T cells that induces contact-dependent B cell differentiation (help)." J Exp Med 175(4): 1091-1101.
- Lee, H., A. Herrmann, et al. (2009). "Persistently activated Stat3 maintains constitutive NF-kappaB activity in tumors." Cancer Cell 15(4): 283-293.
- Lee, J. K., S. O. Mathew, et al. (2007). "CS1 (CRACC, CD319) induces proliferation and autocrine cytokine expression on human B lymphocytes." J Immunol 179(7): 4672-4678.
- Lenoir, G. M., M. Vuillaume, et al. (1985). "The use of lymphomatous and lymphoblastoid cell lines in the study of Burkitt's lymphoma." IARC Sci Publ(60): 309-318.
- Lenz, G., R. E. Davis, et al. (2008). "Oncogenic CARD11 mutations in human diffuse large B cell lymphoma." Science 319(5870): 1676-1679.
- Li, M., X. Fang, et al. (2009). "Loss of spindle assembly checkpoint-mediated inhibition of Cdc20 promotes tumorigenesis in mice." J Cell Biol 185(6): 983-994.
- Li, Z., S. Van Calcar, et al. (2003). "A global transcriptional regulatory role for c-Myc in Burkitt's lymphoma cells." Proc Natl Acad Sci U S A 100(14): 8164-8169.
- Liu, L., M. Zhang, et al. (2007). "Expression of PLK1 and survivin in diffuse large B-cell lymphoma." Leuk Lymphoma 48(11): 2179-2183.
- Liu, Y., X. Hong, et al. (2003). "Ligand-receptor binding revealed by the TNF family member TALL-1." Nature 423(6935): 49-56.
- Locksley, R. M., N. Killeen, et al. (2001). "The TNF and TNF receptor superfamilies: integrating mammalian biology." Cell 104(4): 487-501.
- Loken, M. R., D. R. Parks, et al. (1977). "Two-color immunofluorescence using a fluorescence-activated cell sorter." J Histochem Cytochem 25(7): 899-907.
- Mackay, F. and H. Leung (2006). "The role of the BAFF/APRIL system on T cell function." Semin Immunol 18(5): 284-289.
- Mackay, F., F. Sierro, et al. (2005). "The BAFF/APRIL system: an important player in systemic rheumatic diseases." Curr Dir Autoimmun 8: 243-265.
- Mackus, W. J., S. M. Lens, et al. (2002). "Prevention of B cell antigen receptor-induced apoptosis by ligation of CD40 occurs downstream of cell cycle regulation." Int Immunol 14(9): 973-982.
- Magrath, I. T., C. B. Freeman, et al. (1980). "Characterization of lymphoma-derived cell lines: comparison of cell lines positive and negative for Epstein-Barr virus nuclear antigen. II. Surface markers." J Natl Cancer Inst 64(3): 477-483.
- Maneck, M., A. Schrader, et al. (2011). "Genomic data integration using guided clustering." Bioinformatics.
- Matsuzawa, A., P. H. Tseng, et al. (2008). "Essential cytoplasmic translocation of a cytokine receptor-assembled signaling complex." Science 321(5889): 663-668.
- McNally, R. J. and L. Parker (2006). "Environmental factors and childhood acute leukemias and lymphomas." Leuk Lymphoma 47(4): 583-598.

- Medzhitov, R., P. Preston-Hurlburt, et al. (1997). "A human homologue of the Drosophila Toll protein signals activation of adaptive immunity." Nature 388(6640): 394-397.
- Menssen, A., A. Epanchintsev, et al. (2007). "c-MYC delays prometaphase by direct transactivation of MAD2 and BubR1: identification of mechanisms underlying c-MYC-induced DNA damage and chromosomal instability." Cell Cycle 6(3): 339-352.
- Mito, K., K. Kashima, et al. (2005). "Expression of Polo-Like Kinase (PLK1) in non-Hodgkin's lymphomas." Leuk Lymphoma 46(2): 225-231.
- Monti, S., K. J. Savage, et al. (2005). "Molecular profiling of diffuse large B-cell lymphoma identifies robust subtypes including one characterized by host inflammatory response." Blood 105(5): 1851-1861.
- Moore, P. A., O. Belvedere, et al. (1999). "BLyS: member of the tumor necrosis factor family and B lymphocyte stimulator." Science 285(5425): 260-263.
- Muramatsu, M., K. Kinoshita, et al. (2000). "Class switch recombination and hypermutation require activation-induced cytidine deaminase (AID), a potential RNA editing enzyme." Cell 102(5): 553-563.
- Murn, J., I. Mlinaric-Rascan, et al. (2009). "A Myc-regulated transcriptional network controls B-cell fate in response to BCR triggering." BMC Genomics 10: 323.
- Ngo, V. N., R. E. Davis, et al. (2006). "A loss-of-function RNA interference screen for molecular targets in cancer." Nature 441(7089): 106-110.
- Ngo, V. N., R. M. Young, et al. (2011). "Oncogenically active MYD88 mutations in human lymphoma." Nature 470(7332): 115-119.
- Nicoletti, I., G. Migliorati, et al. (1991). "A rapid and simple method for measuring thymocyte apoptosis by propidium iodide staining and flow cytometry." J Immunol Methods 139(2): 271-279.
- Nilsson, K. and J. Ponten (1975). "Classification and biological nature of established human hematopoietic cell lines." Int J Cancer 15(2): 321-341.
- Ninomiya-Tsuji, J., T. Kajino, et al. (2003). "A resorcylic acid lactone, 5Z-7-oxozeaenol, prevents inflammation by inhibiting the catalytic activity of TAK1 MAPK kinase kinase." J Biol Chem 278(20): 18485-18490.
- Novak, A. J., J. R. Darce, et al. (2004). "Expression of BCMA, TACI, and BAFF-R in multiple myeloma: a mechanism for growth and survival." Blood 103(2): 689-694.
- Novak, A. J., D. M. Grote, et al. (2004). "Expression of BLyS and its receptors in B-cell non-Hodgkin lymphoma: correlation with disease activity and patient outcome." Blood 104(8): 2247-2253.
- O'Connor, G. T., H. Rappaport, et al. (1965). "Childhood Lymphoma Resembling "Burkitt Tumor" in the United States." Cancer 18: 411-417.
- O'Dea, E. and A. Hoffmann "The regulatory logic of the NF-kappaB signaling system." Cold Spring Harb Perspect Biol 2(1): a000216.
- Ogden, C. A., J. D. Pound, et al. (2005). "Enhanced apoptotic cell clearance capacity and B cell survival factor production by IL-10-activated macrophages: implications for Burkitt's lymphoma." J Immunol 174(5): 3015-3023.
- Oliveros, J. C. (2007). "VENNY." Retrieved 18/11/2011, 20011, from <http://bioinfogp.cnb.csic.es/tools/venny/index.html>.
- Osmond, D. G. (1990). "B cell development in the bone marrow." Semin Immunol 2(3): 173-180.

Bibliography

- Palsson-McDermott, E. M. and L. A. O'Neill (2004). "Signal transduction by the lipopolysaccharide receptor, Toll-like receptor-4." Immunology 113(2): 153-162.
- Parrish-Novak, J., S. R. Dillon, et al. (2000). "Interleukin 21 and its receptor are involved in NK cell expansion and regulation of lymphocyte function." Nature 408(6808): 57-63.
- Pelengaris, S., M. Khan, et al. (2002). "c-MYC: more than just a matter of life and death." Nat Rev Cancer 2(10): 764-776.
- Perkins, A. S. and J. W. Friedberg (2008). "Burkitt lymphoma in adults." Hematology Am Soc Hematol Educ Program: 341-348.
- Pham, L. V., A. T. Tamayo, et al. (2005). "Constitutive NF-kappaB and NFAT activation in aggressive B-cell lymphomas synergistically activates the CD154 gene and maintains lymphoma cell survival." Blood 106(12): 3940-3947.
- Poltorak, A., X. He, et al. (1998). "Defective LPS signaling in C3H/HeJ and C57BL/10ScCr mice: mutations in Tlr4 gene." Science 282(5396): 2085-2088.
- Puskas, L. G., A. Zvara, et al. (2002). "RNA amplification results in reproducible microarray data with slight ratio bias." Biotechniques 32(6): 1330-1334, 1336, 1338, 1340.
- Rajewsky, K. (1996). "Clonal selection and learning in the antibody system." Nature 381(6585): 751-758.
- Rao, C. V., Y. M. Yang, et al. (2005). "Colonic tumorigenesis in BubR1+/-ApcMin/+ compound mutant mice is linked to premature separation of sister chromatids and enhanced genomic instability." Proc Natl Acad Sci U S A 102(12): 4365-4370.
- Rasti, N., K. I. Falk, et al. (2005). "Circulating epstein-barr virus in children living in malaria-endemic areas." Scand J Immunol 61(5): 461-465.
- Refaeli, Y., R. M. Young, et al. (2008). "The B cell antigen receptor and overexpression of MYC can cooperate in the genesis of B cell lymphomas." PLoS Biol 6(6): e152.
- Reth, M. (1989). "Antigen receptor tail clue." Nature 338(6214): 383-384.
- Rodig, S. J., A. Shahsafaei, et al. (2005). "BAFF-R, the major B cell-activating factor receptor, is expressed on most mature B cells and B-cell lymphoproliferative disorders." Hum Pathol 36(10): 1113-1119.
- Rothe, M., V. Sarma, et al. (1995). "TRAF2-mediated activation of NF-kappa B by TNF receptor 2 and CD40." Science 269(5229): 1424-1427.
- Ruland, J., G. S. Duncan, et al. (2001). "Bcl10 is a positive regulator of antigen receptor-induced activation of NF-kappaB and neural tube closure." Cell 104(1): 33-42.
- Ruland, J., G. S. Duncan, et al. (2003). "Differential requirement for Malt1 in T and B cell antigen receptor signaling." Immunity 19(5): 749-758.
- Saito, Y., Y. Miyagawa, et al. (2008). "B-cell-activating factor inhibits CD20-mediated and B-cell receptor-mediated apoptosis in human B cells." Immunology 125(4): 570-590.
- Salaverria, I., C. Philipp, et al. (2011). "Translocations activating IRF4 identify a subtype of germinal center-derived B-cell lymphoma affecting predominantly children and young adults." Blood 118(1): 139-147.
- Sampson, V. B., N. H. Rong, et al. (2007). "MicroRNA let-7a down-regulates MYC and reverts MYC-induced growth in Burkitt lymphoma cells." Cancer Res 67(20): 9762-9770.
- Sanchez, M., Z. Misulovin, et al. (1993). "Signal transduction by immunoglobulin is mediated through Ig alpha and Ig beta." J Exp Med 178(3): 1049-1055.

- Sanda, T., S. Iida, et al. (2005). "Growth inhibition of multiple myeloma cells by a novel I κ B kinase inhibitor." Clin Cancer Res 11(5): 1974-1982.
- Santos-Argumedo, L., J. Gordon, et al. (1994). "Antibodies to murine CD40 protect normal and malignant B cells from induced growth arrest." Cell Immunol 156(2): 272-285.
- Sato, T., S. Irie, et al. (1995). "A novel member of the TRAF family of putative signal transducing proteins binds to the cytosolic domain of CD40." FEBS Lett 358(2): 113-118.
- Savage, K. J., N. A. Johnson, et al. (2009). "MYC gene rearrangements are associated with a poor prognosis in diffuse large B-cell lymphoma patients treated with R-CHOP chemotherapy." Blood 114(17): 3533-3537.
- Saxena, M. and T. Mustelin (2000). "Extracellular signals and scores of phosphatases: all roads lead to MAP kinase." Semin Immunol 12(4): 387-396.
- Schiemann, B., J. L. Gommerman, et al. (2001). "An essential role for BAFF in the normal development of B cells through a BCMA-independent pathway." Science 293(5537): 2111-2114.
- Schlee, M., M. Holz, et al. (2007). "C-myc activation impairs the NF- κ B and the interferon response: implications for the pathogenesis of Burkitt's lymphoma." Int J Cancer 120(7): 1387-1395.
- Schoffski, P. (2009). "Polo-like kinase (PLK) inhibitors in preclinical and early clinical development in oncology." Oncologist 14(6): 559-570.
- Schrader, A., S. Bentink, et al. (2011). "High myc activity is an independent negative prognostic factor for diffuse large B cell lymphomas." Int J Cancer.
- Schuhmacher, M., F. Kohlhuber, et al. (2001). "The transcriptional program of a human B cell line in response to Myc." Nucleic Acids Res 29(2): 397-406.
- Shu, H. B., W. H. Hu, et al. (1999). "TALL-1 is a novel member of the TNF family that is down-regulated by mitogens." J Leukoc Biol 65(5): 680-683.
- Simons-Evelyn, M., K. Bailey-Dell, et al. (2001). "PBK/TOPK is a novel mitotic kinase which is upregulated in Burkitt's lymphoma and other highly proliferative malignant cells." Blood Cells Mol Dis 27(5): 825-829.
- Spolski, R. and W. J. Leonard (2008). "Interleukin-21: basic biology and implications for cancer and autoimmunity." Annu Rev Immunol 26: 57-79.
- Stadanlick, J. E., M. Kaileh, et al. (2008). "Tonic B cell antigen receptor signals supply an NF- κ B substrate for prosurvival BLyS signaling." Nat Immunol 9(12): 1379-1387.
- Stasik, C. J., H. Nitta, et al. (2010). "Increased MYC gene copy number correlates with increased mRNA levels in diffuse large B-cell lymphoma." Haematologica 95(4): 597-603.
- Stolz, A., N. Ertch, et al. (2010). "The CHK2-BRCA1 tumour suppressor pathway ensures chromosomal stability in human somatic cells." Nat Cell Biol 12(5): 492-499.
- Subramanian, A., P. Tamayo, et al. (2005). "Gene set enrichment analysis: a knowledge-based approach for interpreting genome-wide expression profiles." Proc Natl Acad Sci U S A 102(43): 15545-15550.
- Taub, R., I. Kirsch, et al. (1982). "Translocation of the c-myc gene into the immunoglobulin heavy chain locus in human Burkitt lymphoma and murine plasmacytoma cells." Proc Natl Acad Sci U S A 79(24): 7837-7841.
- Thomas, R. K., C. Wickenhauser, et al. (2004). "Mutational analysis of the I κ B α gene in activated B cell-like diffuse large B-cell lymphoma." Br J Haematol 126(1): 50-54.

Bibliography

- Tweeddale, M., N. Jamal, et al. (1989). "Production of growth factors by malignant lymphoma cell lines." Blood 74(2): 572-578.
- Uddin, S., A. R. Hussain, et al. (2006). "Role of phosphatidylinositol 3'-kinase/AKT pathway in diffuse large B-cell lymphoma survival." Blood 108(13): 4178-4186.
- Vallabhapurapu, S., A. Matsuzawa, et al. (2008). "Nonredundant and complementary functions of TRAF2 and TRAF3 in a ubiquitination cascade that activates NIK-dependent alternative NF-kappaB signaling." Nat Immunol 9(12): 1364-1370.
- Van den Eertwegh, A. J., R. J. Noelle, et al. (1993). "In vivo CD40-gp39 interactions are essential for thymus-dependent humoral immunity. I. In vivo expression of CD40 ligand, cytokines, and antibody production delineates sites of cognate T-B cell interactions." J Exp Med 178(5): 1555-1565.
- Vlahos, C. J., W. F. Matter, et al. (1994). "A specific inhibitor of phosphatidylinositol 3-kinase, 2-(4-morpholinyl)-8-phenyl-4H-1-benzopyran-4-one (LY294002)." J Biol Chem 269(7): 5241-5248.
- Vockerodt, M., S. L. Morgan, et al. (2008). "The Epstein-Barr virus oncoprotein, latent membrane protein-1, reprograms germinal centre B cells towards a Hodgkin's Reed-Sternberg-like phenotype." J Pathol 216(1): 83-92.
- Vrzalikova, K., M. Vockerodt, et al. (2011). "Down-regulation of BLIMP1{alpha} by the EBV oncogene, LMP-1, disrupts the plasma cell differentiation program and prevents viral replication in B cells: implications for the pathogenesis of EBV-associated B-cell lymphomas." Blood 117(22): 5907-5917.
- Wang, D., Y. You, et al. (2002). "A requirement for CARMA1 in TCR-induced NF-kappa B activation." Nat Immunol 3(9): 830-835.
- Wang, H., R. J. Grand, et al. (1996). "Repression of apoptosis in human B-lymphoma cells by CD40-ligand and Bcl-2: relationship to the cell-cycle and role of the retinoblastoma protein." Oncogene 13(2): 373-379.
- Wang, L. D. and M. R. Clark (2003). "B-cell antigen-receptor signalling in lymphocyte development." Immunology 110(4): 411-420.
- Weiss, L. M., R. A. Warnke, et al. (1987). "Molecular analysis of the t(14;18) chromosomal translocation in malignant lymphomas." N Engl J Med 317(19): 1185-1189.
- Wendel, M., I. E. Galani, et al. (2008). "Natural killer cell accumulation in tumors is dependent on IFN-gamma and CXCR3 ligands." Cancer Res 68(20): 8437-8445.
- Wolanin, K., A. Magalska, et al. (2010). "Expression of oncogenic kinase Bcr-Abl impairs mitotic checkpoint and promotes aberrant divisions and resistance to microtubule-targeting agents." Mol Cancer Ther 9(5): 1328-1338.
- Yang, J. and M. Reth (2010). "The dissociation activation model of B cell antigen receptor triggering." FEBS Lett 584(24): 4872-4877.
- Ye, B. H., G. Cattoretti, et al. (1997). "The BCL-6 proto-oncogene controls germinal-centre formation and Th2-type inflammation." Nat Genet 16(2): 161-170.
- Ye, B. H., P. H. Rao, et al. (1993). "Cloning of bcl-6, the locus involved in chromosome translocations affecting band 3q27 in B-cell lymphoma." Cancer Res 53(12): 2732-2735.
- Yin, X., C. Giap, et al. (2003). "Low molecular weight inhibitors of Myc-Max interaction and function." Oncogene 22(40): 6151-6159.
- Yustein, J. T. and C. V. Dang (2007). "Biology and treatment of Burkitt's lymphoma." Curr Opin Hematol 14(4): 375-381.

- Zeng, R., R. Spolski, et al. (2007). "The molecular basis of IL-21-mediated proliferation." Blood 109(10): 4135-4142.
- Zhang, H. W., Z. W. Chen, et al. (2011). "Clinical significance and prognosis of MYC translocation in diffuse large B-cell lymphoma." Hematol Oncol.
- Zhang, Q., J. A. Didonato, et al. (1994). "BCL3 encodes a nuclear protein which can alter the subcellular location of NF-kappa B proteins." Mol Cell Biol 14(6): 3915-3926.
- Zhu, X., R. Hart, et al. (2004). "Analysis of the major patterns of B cell gene expression changes in response to short-term stimulation with 33 single ligands." J Immunol 173(12): 7141-7149.
- Zipper, H., H. Brunner, et al. (2004). "Investigations on DNA intercalation and surface binding by SYBR Green I, its structure determination and methodological implications." Nucleic Acids Res 32(12): e103.
- Zucca, E., F. Bertoni, et al. (1998). "Molecular analysis of the progression from Helicobacter pylori-associated chronic gastritis to mucosa-associated lymphoid-tissue lymphoma of the stomach." N Engl J Med 338(12): 804-810.

Danksagung

Zunächst gilt mein Dank Prof. Dieter Kube, der mich in den letzten drei Jahren kompromisslos unterstützt hat. Sein Engagement und seine Ideen haben diese Arbeit essentiell geprägt. Vielen Dank, dass Du diese Arbeit ermöglicht hast!

Ich möchte mich besonders bei Frederike von Bonin und Neele Walther bedanken. Ihre gute Arbeit und zuverlässige Unterstützung hat entscheidend zur Form dieser Arbeit beigetragen! Dankeschön! Mein ganz besonderer Dank gilt Dr. Martina Vockerodt. Ihre enthusiastische Art und ihre überaus umfassende Betreuung haben mir sehr geholfen. Liebe Martina, die Zusammenarbeit mit dir hat mit immer unglaublich viel Spaß gemacht! ☺ Danke dass Du mir so viel beigebracht hast und danke für den quietschenden LKW in der Zellkultur... Die Zeit in Brum werde ich nie vergessen! At this point I would like to thank Prof. Paul Murray for giving me the possibility to be his guest in his group in Birmingham! Special thanks go to Eszter Nagy, Kate Vrzalikova and all people from the laboratory in Birmingham for their support.

Ich möchte mich ganz herzlich bei Prof. Rainer Spang, Matthias Maneck, Katharina Meyer und der gesamten computational diagnostics group in Regensburg bedanken. Ohne die Kooperation mit Euch und Eure bioinformatische Expertise wäre vieles nicht möglich gewesen. Liebe Katharina, vielen Dank dass Du Dich für unsere Zusammenarbeit so eingesetzt hast und immer ein offenes Ohr für meine nicht enden wollenden Fragen hattest! Außerdem möchte ich mich bei Dr. Stefan Bentink bedanken. Seine Ideen waren essentiell für das Weiterkommen im MYC-Projekt. Lieber Stefan, danke dass Du auch jetzt neben deiner Arbeit so viel investiert hast!

Ich bedanke mich herzlich bei Prof. Michael Hummel und seiner AG, die im Rahmen des MML Verbundes die Hybridisierung der microarrays durchgeführt haben. Außerdem möchte ich mich bei Prof. Georg Bornkamm bedanken, dafür, dass er das *MYC* Expressionsplasmid zur Verfügung gestellt hat. Ein großes Dankeschön geht auch an Prof. Arnd Kieser und seine AG, die uns mit dem JNK-Kinase Assay unterstützt haben. An dieser Stelle möchte ich mich ganz besonders bei Antje Ulrich bedanken, dafür dass sie nach München gefahren ist um den Kinase Assay durchzuführen. ☺

Christina Heemann danke ich speziell für Ihre Hilfe mit den CHIPs. Außerdem möchte ich mich bei Kamila Matulewicz bedanken die mit Ihren Vorarbeiten zu CD40 einen entscheidenden Anstoß zur Weiterentwicklung meines Projekts gegeben hat. Außerdem danke ich Katrin Moses und Katja Hüttner für die gute Zusammenarbeit im

BAFF-Projekt. Ich danke allen meinen Kollegen in der AG Kube für unsere unglaublich tolle Arbeitsatmosphäre und besonders Frederike für jeden Freitags-Witz!

Des Weiteren möchte ich mir bei Prof. Heidi Hahn und Prof. Martin Oppermann bedanken. Ihre Diskussionsbereitschaft und Ihr Interesse in den Thesis Committees haben mich immer wieder auf ein Neues motiviert. Ich danke allen Mitgliedern des GRK1043, insbesonere Prof. Brockmöller und Sven Müller

Ganz besonders möchte ich mich bedanken bei den Mädels aus dem OST-Büro (incl. aller ehemaligen). Bei Euch habe ich gelernt, dass die Wanderung auf dem Grad zum Wahnsinn auch ein lustiger und ausgelassener Tanz sein kann! ☺ Alles wird einfacher wenn man darüber lacht... Insbesondere herzlich danken möchte ich Betty und Julia, die beim Korrekturlesen der Arbeit geholfen haben und Sandra, die immer einen konstruktiven Vorschlag parat hatte!

Für meine Familie und meine Freunde möchte ich an dieser Stelle ein Zitat von Goethe aufgreifen: „Leider lässt sich eine wahrhaftige Dankbarkeit mit Worten nicht ausdrücken.“ (Goethe 1749-1832). Dennoch möchte ich diese Gelegenheit nutzen um einfach mal allen danke zu sagen, die mich bisher, auch im Verlauf der Doktorarbeit, begleitet haben. Ich danke meinen Eltern und meinen Großeltern für Ihre bedingungslose Unterstützung in jeglicher Hinsicht. Frederik danke ich dafür, dass er einfach da ist. Meinen Mädels aus Soest danke ich dafür dass wir es tatsächlich geschafft haben noch immer unser Leben miteinander zu teilen. Gruppe Dino möchte ich danken für eine unvergessliche Studienzeit, insbesondere Julia dafür, dass sie unser zu Hause zu dem gemacht hat was es ist!

This work was supported by the DFG (GRK1034), the German Cancer Aid organisation (MMML), the BMBF (HaematoSys), the “Stiftung der Georg-August-Universität aus Mitteln der Kubeschka/Stricker/Wirth-Stiftung” and the UICC.

Appendix

Chapter 1 The c-Myc index

Table A 1 Gene Set Enrichment Analysis of c-Myc responsive genes. Gene set enrichment analysis (GSEA) of the resulting ranked gene list was performed using the Java implementation of GSEA obtained from <http://www.broadinstitute.org/gsea/>. The ES (Enrichment Score) is given, which is the primary result of the gene set enrichment analysis and reflects the degree to which a gene set is overrepresented in a ranked list of genes. Gene sets are displayed in the order of the NES (Normalized Enrichment Score) which accounts for differences in gene set sizes and correlations between the gene set and the expression dataset. The NOM p-value (Nominal p-value) is a statistical measure for the significance of the enrichment of one single gene set. The FDR q-value (False Discovery Rate) is adjusted for multiple testing.

Gene sets enriched in c-Myc negatively correlated genes					
Name	Size of Geneset	ES	NES	NOM p-val	FDR q-val
WIELAND_HEPATITIS_B_INDUCED	106	-0,44	-2,07	0,000	0,033
BASSO_GERMINAL_CENTER_CD40_UP	97	-0,43	-2,16	0,000	0,026
NO2IL12PATHWAY	15	-0,65	-2,07	0,000	0,043
TAKEDA_NUP8_HOXA9_8D_UP	121	-0,40	-2,06	0,000	0,035
IGF_VS_PDGF_DN	34	-0,52	-2,04	0,004	0,033
P53_BRCA1_UP	28	-0,53	-1,97	0,000	0,058
LINDSTEDT_DEND_8H_VS_48H_UP	64	-0,41	-1,90	0,000	0,086
IFNA_UV-CMV_COMMON_HCMV_6HRS_UP	29	-0,49	-1,90	0,003	0,077
SANA_IFNG_ENDOTHELIAL_UP	60	-0,42	-1,90	0,000	0,071
TNFA_NFKB_DEP_UP	18	-0,57	-1,89	0,000	0,064
VERHAAK_AML_NPM1_MUT_VS_WT_UP	189	-0,34	-1,86	0,000	0,074
STAEGE_EFTS_UP	21	-0,53	-1,86	0,000	0,072
DAC_IFN_BLADDER_UP	16	-0,58	-1,85	0,009	0,067
YANG_OSTECLASTS_SIG	38	-0,46	-1,85	0,000	0,065
TAKEDA_NUP8_HOXA9_3D_UP	150	-0,35	-1,85	0,000	0,063
IFNA_HCMV_6HRS_UP	53	-0,42	-1,84	0,000	0,062
PHOTOSYNTHESIS	20	-0,54	-1,83	0,003	0,062
CMV_HCMV_TIMECOURSE_12HRS_UP	26	-0,50	-1,83	0,006	0,060
HSA04060_CYTOKINE_CYTOKINE_RECEPTOR_INTERACTION	226	-0,32	-1,83	0,000	0,057
TAKEDA_NUP8_HOXA9_16D_UP	135	-0,35	-1,82	0,000	0,058
Gene sets enriched in c-Myc positively correlated genes					
Name	Size of Geneset	ES	NES	NOM p-val	FDR q-val
PENG_GLUTAMINE_DN	248	0,56	2,61	0,000	0,000

BLEO_MOUSE_LYMPH_HIGH_24HRS_DN	34	0,74	2,52	0,000	0,000
MRNA_PROCESSING_REACTOME	102	0,58	2,44	0,000	0,000
MENSSSEN_MYC_UP	31	0,71	2,41	0,000	0,000
MANALO_HYPOXIA_DN	78	0,59	2,40	0,000	0,000
MRNA_PROCESSING	41	0,67	2,38	0,000	0,000
PENG_RAPAMYCIN_DN	188	0,52	2,38	0,000	0,000
PENG_LEUCINE_DN	139	0,54	2,35	0,000	0,000
MYC_TARGETS	39	0,64	2,25	0,000	0,000
CANCER_NEOPLASTIC_META_UP	60	0,57	2,21	0,000	0,000
TRANSLATION_FACTORS	45	0,61	2,20	0,000	0,000
SCHUMACHER_MYC_UP	50	0,59	2,19	0,000	0,002
COLLER_MYC_UP	17	0,75	2,18	0,000	0,003
MTORPATHWAY	23	0,70	2,16	0,000	0,004
BRCA1_OVEREXP_DN	109	0,51	2,16	0,000	0,004
CANTHARIDIN_DN	49	0,58	2,15	0,000	0,004
TARTE_PLASMA_BLASTIC	305	0,45	2,13	0,000	0,006
MYC_ONCOGENIC_SIGNATURE	173	0,47	2,11	0,000	0,006
MRNA_SPLICING	47	0,58	2,09	0,000	0,009
ET743_SARCOMA_DN	246	0,45	2,09	0,000	0,010

Chapter 2 Global gene expression changes

Table A 2 IL21 responsive genes. This table shows the effects of rhIL21 on the most variable genes. 100 probesets with the highest differential expression were selected from all significantly regulated genes. Probesets that were array specific and not spotted on the HG U133 plus, which was used for the evaluation of aNHL samples, were discarded and excluded from further analysis.

	GenSymbols	Probeset-ID	logFC	AveExpr	t	P.Value	adj.P.Val
1	IRF9	203882_at	-3,16	7,46	-39,06	0,00	0,00
2	ICAM1	202638_s_at	-2,92	8,06	-31,38	0,00	0,00
3	SGK1	201739_at	-2,80	9,00	-20,13	0,00	0,00
4	CD83	204440_at	-2,71	10,60	-34,67	0,00	0,00
5	ICAM1	202637_s_at	-2,70	8,39	-28,47	0,00	0,00
6	BATF	205965_at	-2,30	9,42	-34,76	0,00	0,00
7	IFIT1	203153_at	-2,19	6,35	-23,58	0,00	0,00
8	IRF4	204562_at	-2,17	11,00	-24,84	0,00	0,00
9	SLC30A1	212907_at	-1,97	7,68	-13,67	0,00	0,00
10	IRF1	202531_at	-1,97	7,67	-19,28	0,00	0,00
11	BCL2A1	205681_at	-1,94	8,84	-16,07	0,00	0,00
12	IFIT5	203595_s_at	-1,91	6,74	-28,08	0,00	0,00
13	NFKBIE	203927_at	-1,77	8,62	-19,14	0,00	0,00
14	EGR2	205249_at	-1,69	7,44	-15,60	0,00	0,00
15	BIRC3	210538_s_at	-1,66	9,84	-16,54	0,00	0,00
16	STAT1	200887_s_at	-1,66	8,89	-15,00	0,00	0,00
17	ICAM1	215485_s_at	-1,65	7,35	-15,69	0,00	0,00

Appendix

18	MX1	202086_at	-1,64	8,68	-17,78	0,00	0,00
19	TNFAIP3	202644_s_at	-1,64	9,15	-11,68	0,00	0,00
20	CXCL10	204533_at	-1,62	6,58	-25,63	0,00	0,00
21	PTGER4	204897_at	-1,56	9,00	-13,41	0,00	0,00
22	GADD45B	207574_s_at	-1,48	8,85	-10,05	0,00	0,00
23	TNFAIP3	202643_s_at	-1,44	8,43	-10,77	0,00	0,00
24	STAT1	AFFX- HUMISGF3A/ M97935_3_at	-1,44	8,22	-15,70	0,00	0,00
25	RGS16	209324_s_at	-1,44	8,68	-8,34	0,00	0,00
26	NFKBIA	201502_s_at	-1,44	10,84	-10,37	0,00	0,00
27	RGS16	209325_s_at	-1,42	8,68	-10,26	0,00	0,00
28	IRF4	216986_s_at	-1,40	7,81	-17,95	0,00	0,00
29	ZC3H12A	218810_at	-1,38	8,31	-14,00	0,00	0,00
30	GADD45B	209304_x_at	-1,35	8,74	-11,66	0,00	0,00
31	MAP3K8	205027_s_at	-1,33	6,67	-12,96	0,00	0,00
32	IFIT3	204747_at	-1,27	6,84	-13,18	0,00	0,00
33	GADD45B	209305_s_at	-1,27	8,27	-11,49	0,00	0,00
34	USP18	219211_at	-1,23	7,20	-18,06	0,00	0,00
35	IL2RA	206341_at	-1,21	7,03	-14,85	0,00	0,00
36	STAT1	AFFX- HUMISGF3A/ M97935_MB_at	-1,19	7,27	-12,32	0,00	0,00
37	SAMSN1	220330_s_at	-1,18	8,15	-9,38	0,00	0,00
38	BCL3	204908_s_at	-1,16	8,08	-12,80	0,00	0,00
39	IER5	218611_at	-1,16	10,32	-11,09	0,00	0,00
40	CXCR5	206126_at	-1,16	8,08	-17,16	0,00	0,00
41	NUDT4	212183_at	-1,14	8,27	-16,19	0,00	0,00
42	DUSP2	204794_at	-1,13	9,06	-9,07	0,00	0,00
43	MARCKS	201670_s_at	-1,11	8,85	-8,80	0,00	0,00
44	STAT1	209969_s_at	-1,11	7,13	-13,11	0,00	0,00
45	NA	212181_s_at	-1,10	9,81	-18,49	0,00	0,00
46	LRR32	203835_at	-1,10	6,78	-12,56	0,00	0,00
47	JUNB	201473_at	-1,09	8,44	-10,31	0,00	0,00
48	IL2RA	211269_s_at	-1,09	6,92	-14,14	0,00	0,00
49	TAP1	202307_s_at	-1,09	8,34	-17,64	0,00	0,00
50	SNX11	220140_s_at	-1,08	9,08	-13,80	0,00	0,00
51	ZFP36L1	211962_s_at	-1,07	9,16	-7,60	0,00	0,00
52	IER2	202081_at	-1,07	10,04	-13,61	0,00	0,00
53	STAT1	AFFX- HUMISGF3A/ M97935_MA_at	-1,07	7,89	-11,38	0,00	0,00
54	PIM2	204269_at	-1,06	9,28	-14,10	0,00	0,00
55	MCL1	200798_x_at	-1,04	11,19	-11,97	0,00	0,00
56	TLR7	220146_at	-1,04	7,21	-13,25	0,00	0,00
57	MARCKS	201669_s_at	-1,00	10,41	-8,34	0,00	0,00
58	SRSF5	203380_x_at	-1,00	9,98	-9,39	0,00	0,00
59	NA	206302_s_at	-0,98	9,92	-10,54	0,00	0,00
60	ZFP36L1	211965_at	-0,97	7,53	-4,11	0,00	0,02
61	SOCS1	210001_s_at	-0,96	7,38	-13,37	0,00	0,00
62	CD40	215346_at	-0,93	8,82	-16,45	0,00	0,00
63	BCL2L1	215037_s_at	-0,92	7,76	-10,96	0,00	0,00
64	CYTIP	209606_at	0,93	8,04	13,75	0,00	0,00
65	HEY2	219743_at	0,95	7,26	9,33	0,00	0,00
66	GADD45A	203725_at	0,98	8,54	12,98	0,00	0,00
67	VEGFA	210512_s_at	1,12	7,35	9,77	0,00	0,00
68	IL7R	205798_at	1,15	9,65	9,17	0,00	0,00
69	SOX2	213721_at	1,16	7,96	10,16	0,00	0,00
70	DNAJB4	203811_s_at	1,21	8,18	13,88	0,00	0,00
71	C13orf15	218723_s_at	1,24	10,81	10,29	0,00	0,00

72	ID1	208937_s_at	1,49	7,73	14,36	0,00	0,00
73	DDIT4	202887_s_at	1,51	9,39	8,53	0,00	0,00
74	ID3	207826_s_at	1,53	11,03	17,50	0,00	0,00
75	DNAJB4	203810_at	1,59	8,11	17,18	0,00	0,00
76	BCL6	215990_s_at	1,67	8,88	20,75	0,00	0,00
77	BCL6	203140_at	1,90	10,60	20,01	0,00	0,00

Table A 3 CD40 responsive genes This table shows the effects of sCD40L on the most variable genes. 100 probesets with the highest differential expression were selected from all significantly regulated genes. Probesets that were array specific and not spotted on the HG U133 plus, which was used for the evaluation of aNHL samples, were discarded and excluded from further analysis.

	GenSymbols	Probeset-ID	logFC	AveExpr	t	P.Value	adj.P.Val
1	CD58	205173_x_at	-1,62	9,22	-12,40	0,00	0,00
2	CD58	216942_s_at	-1,51	8,52	-11,46	0,00	0,00
3	CD58	211744_s_at	-1,49	8,40	-10,79	0,00	0,00
4	NA	221491_x_at	-1,26	9,31	-12,92	0,00	0,00
5	BTN2A2	205298_s_at	-1,25	7,59	-20,54	0,00	0,00
6	DOCK10	219279_at	-1,20	7,79	-14,55	0,00	0,00
7	HLA-DPA1	213537_at	-1,11	8,83	-8,45	0,00	0,00
8	DENND4A	214787_at	-1,10	8,48	-11,41	0,00	0,00
9	CUX2	213920_at	-1,09	7,81	-12,65	0,00	0,00
10	MAN1A1	208116_s_at	-1,08	8,57	-7,74	0,00	0,00
11	HLA-DQA1	213831_at	-1,07	9,34	-9,35	0,00	0,00
12	CCDC28B	221912_s_at	-1,07	9,28	-16,04	0,00	0,00
13	BATF	205965_at	-1,06	9,42	-16,03	0,00	0,00
14	FNBP1	212288_at	-1,04	9,68	-9,28	0,00	0,00
15	MAN1A1	221760_at	-1,04	10,19	-8,59	0,00	0,00
16	NFKB2	207535_s_at	-1,01	8,23	-11,68	0,00	0,00
17	ICAM1	202638_s_at	-1,01	8,06	-10,81	0,00	0,00
18	HLA-DQA1	203290_at	-1,01	10,45	-12,99	0,00	0,00
19	ICAM1	202637_s_at	-1,00	8,39	-10,51	0,00	0,00
20	HLA-DQB1	212998_x_at	-0,99	10,38	-9,23	0,00	0,00
21	OLFML2A	213075_at	-0,99	8,81	-12,76	0,00	0,00
22	IFIH1	219209_at	-0,99	7,97	-8,76	0,00	0,00
23	HLA-DQB1	209480_at	-0,99	9,25	-7,13	0,00	0,00
24	NA	212671_s_at	-0,98	11,06	-10,00	0,00	0,00
25	HLA-DQB1	209823_x_at	-0,97	8,75	-9,46	0,00	0,00
26	RPS6KA1	203379_at	-0,96	9,11	-8,94	0,00	0,00
27	PLEKHO1	218223_s_at	-0,94	7,90	-13,22	0,00	0,00
28	CTSH	202295_s_at	-0,94	8,65	-12,51	0,00	0,00
29	RUNX3	204198_s_at	-0,93	9,45	-6,30	0,00	0,00
30	BMP2K	59644_at	-0,93	8,17	-8,17	0,00	0,00
31	WNT5A	213425_at	-0,92	7,27	-9,15	0,00	0,00
32	WNT5A	205990_s_at	-0,92	7,76	-13,23	0,00	0,00
33	FNBP1	213940_s_at	-0,91	9,19	-10,06	0,00	0,00
34	ALCAM	201951_at	-0,91	7,59	-10,42	0,00	0,00
35	NFKB2	209636_at	-0,90	7,42	-12,07	0,00	0,00
36	SYNGR2	201079_at	-0,90	9,78	-10,25	0,00	0,00
37	HLA-DQB1	211656_x_at	-0,89	9,69	-9,65	0,00	0,00
38	NA	206302_s_at	-0,89	9,92	-9,54	0,00	0,00
39	HCP5	206082_at	-0,88	7,10	-10,00	0,00	0,00
40	LAT2	221581_s_at	-0,87	8,32	-9,75	0,00	0,00
41	PIK3CD	203879_at	-0,86	9,99	-13,68	0,00	0,00
42	HLA-DQB1	211654_x_at	-0,85	10,22	-10,13	0,00	0,00
43	ANXA7	201366_at	-0,85	9,87	-9,67	0,00	0,00
44	RUNX3	204197_s_at	-0,85	9,10	-11,13	0,00	0,00

Appendix

45	HLA-DQB1	212999_x_at	-0,85	8,04	-6,96	0,00	0,00
46	BIRC3	210538_s_at	-0,85	9,84	-8,42	0,00	0,00
47	HLA-E	200905_x_at	-0,84	9,77	-8,96	0,00	0,00
48	RASSF2	203185_at	-0,84	9,62	-8,32	0,00	0,00
49	ELL2	214446_at	-0,83	7,16	-9,92	0,00	0,00
50	HLA-B	211911_x_at	-0,83	12,27	-13,69	0,00	0,00
51	LOXL2	202998_s_at	-0,83	9,28	-9,55	0,00	0,00
52	NFKBIE	203927_at	-0,83	8,62	-8,97	0,00	0,00
53	BMP2K	219546_at	-0,82	8,19	-7,14	0,00	0,00
54	FDXR	207813_s_at	-0,81	7,77	-13,11	0,00	0,00
55	RFX5	202963_at	-0,81	11,31	-13,10	0,00	0,00
56	HLA-B	208729_x_at	-0,80	12,06	-12,47	0,00	0,00
57	TAP1	202307_s_at	-0,79	8,34	-12,81	0,00	0,00
58	CIITA	205101_at	-0,79	7,26	-6,73	0,00	0,00
59	FAS	215719_x_at	-0,79	6,67	-11,09	0,00	0,00
60	PDZRN4	220595_at	0,81	7,33	12,02	0,00	0,00
61	ID4	209291_at	0,84	8,89	10,82	0,00	0,00
62	GPER	210640_s_at	0,85	7,11	6,27	0,00	0,00
63	AICDA	219841_at	0,86	10,06	10,10	0,00	0,00
64	IRF8	204057_at	0,92	10,84	12,60	0,00	0,00
65	ID3	207826_s_at	0,98	11,03	11,22	0,00	0,00
66	METTL7A	207761_s_at	1,01	9,60	13,40	0,00	0,00
67	CD83	204440_at	1,02	10,60	13,04	0,00	0,00
68	SMAD1	210993_s_at	1,13	9,31	11,49	0,00	0,00
69	DEPTOR	218858_at	1,16	9,52	18,56	0,00	0,00
70	C3orf37	201678_s_at	1,43	9,54	11,46	0,00	0,00
71	ID1	208937_s_at	2,01	7,73	19,30	0,00	0,00

Table A 4 BCR responsive genes. This table shows the effects of BCRx on the most variable genes. 100 probesets with the highest differential expression were selected from all significantly regulated genes. Probesets that were array specific and not spotted on the HG U133 plus, which was used for the evaluation of aNHL samples, were discarded and excluded from further analysis.

	GenSymbols	Probeset-ID	logFC	AveExpr	t	P.Value	adj.P.Val
1	RGS1	216834_at	-5,48	7,65	-19,42	0,00	0,00
2	DUSP5	209457_at	-5,01	7,22	-32,60	0,00	0,00
3	SGK1	201739_at	-4,84	9,00	-34,82	0,00	0,00
4	RGS1	202988_s_at	-4,75	7,11	-24,85	0,00	0,00
5	EGR2	205249_at	-4,52	7,44	-41,72	0,00	0,00
6	BCL2A1	205681_at	-4,30	8,84	-35,53	0,00	0,00
7	CCR7	206337_at	-3,57	8,24	-29,24	0,00	0,00
8	EGR1	201694_s_at	-3,23	7,12	-21,01	0,00	0,00
9	LY9	210370_s_at	-3,19	7,38	-48,30	0,00	0,00
10	LY9	215967_s_at	-3,17	7,68	-50,09	0,00	0,00
11	BHLHE40	201170_s_at	-3,14	7,62	-23,47	0,00	0,00
12	PHLDA1	217996_at	-3,05	6,92	-17,97	0,00	0,00
13	SQSTM1	201471_s_at	-3,04	9,39	-29,95	0,00	0,00
14	DUSP2	204794_at	-3,00	9,06	-24,03	0,00	0,00
15	DDIT3	209383_at	-2,98	7,47	-43,01	0,00	0,00
16	CD83	204440_at	-2,97	10,60	-38,10	0,00	0,00
17	PLEK	203471_s_at	-2,72	9,22	-31,78	0,00	0,00
18	CD1C	205987_at	-2,66	8,15	-23,42	0,00	0,00
19	TNFAIP3	202644_s_at	-2,61	9,15	-18,65	0,00	0,00
20	TNFAIP3	202643_s_at	-2,56	8,43	-19,11	0,00	0,00
21	PLEK	203470_s_at	-2,43	9,27	-33,86	0,00	0,00
22	PHACTR1	213638_at	-2,42	8,74	-23,64	0,00	0,00
23	TRIB3	218145_at	-2,35	9,54	-27,70	0,00	0,00

24	FAM46C	220306_at	-2,34	7,03	-15,34	0,00	0,00
25	ZFP36L1	211962_s_at	-2,33	9,16	-16,52	0,00	0,00
26	RGS16	209325_s_at	-2,32	8,68	-16,80	0,00	0,00
27	TSC22D3	208763_s_at	-2,29	7,68	-25,00	0,00	0,00
28	CD69	209795_at	-2,28	7,15	-18,06	0,00	0,00
29	SLC7A11	217678_at	-2,22	6,89	-35,76	0,00	0,00
30	ARAP2	213618_at	-2,21	7,49	-32,28	0,00	0,00
31	NA	205114_s_at	-2,21	6,61	-21,03	0,00	0,00
32	HLA-DQB1	209480_at	-2,21	9,25	-15,94	0,00	0,00
33	PTGER4	204897_at	-2,20	9,00	-18,91	0,00	0,00
34	FAM102A	212400_at	-2,20	9,06	-23,26	0,00	0,00
35	SLC7A11	209921_at	-2,18	7,13	-30,99	0,00	0,00
36	DUSP10	221563_at	-2,14	7,76	-22,26	0,00	0,00
37	IER2	202081_at	-2,14	10,04	-27,27	0,00	0,00
38	RGS16	209324_s_at	-2,10	8,68	-12,18	0,00	0,00
39	PHLDA1	217997_at	-2,09	6,45	-15,00	0,00	0,00
40	MDFIC	211675_s_at	-2,09	8,34	-31,76	0,00	0,00
41	IL21R	221658_s_at	-2,08	7,91	-28,63	0,00	0,00
42	SLAMF7	219159_s_at	-2,04	6,28	-20,32	0,00	0,00
43	CDKN1A	202284_s_at	-2,03	8,85	-25,53	0,00	0,00
44	UPP1	203234_at	-2,03	7,61	-21,74	0,00	0,00
45	ARL4C	202207_at	-2,03	6,64	-20,93	0,00	0,00
46	JUND	203752_s_at	-2,02	9,35	-14,05	0,00	0,00
47	NAB2	212803_at	-1,98	7,26	-12,70	0,00	0,00
48	KLF6	208961_s_at	-1,97	7,95	-15,99	0,00	0,00
49	NFKBIE	203927_at	-1,96	8,62	-21,23	0,00	0,00
50	RAB8B	219210_s_at	-1,95	7,83	-24,01	0,00	0,00
51	CD58	205173_x_at	-1,95	9,22	-14,90	0,00	0,00
52	NFKB1	209239_at	-1,94	9,97	-20,66	0,00	0,00
53	APOBEC3B	206632_s_at	-1,93	7,66	-15,05	0,00	0,00
54	CTH	217127_at	-1,91	7,99	-30,66	0,00	0,00
55	TNF	207113_s_at	-1,91	6,74	-13,67	0,00	0,00
56	SLC30A1	212907_at	-1,89	7,68	-13,09	0,00	0,00
57	DUSP10	215501_s_at	-1,86	7,34	-30,90	0,00	0,00
58	NA	221491_x_at	-1,86	9,31	-18,99	0,00	0,00
59	TOR3A	218459_at	-1,85	9,65	-25,87	0,00	0,00
60	ARHGAP25	38149_at	-1,85	8,99	-30,42	0,00	0,00
61	DENND4A	214787_at	-1,85	8,48	-19,14	0,00	0,00
62	ARHGAP25	204882_at	-1,85	8,60	-23,06	0,00	0,00
63	NCKAP1	207738_s_at	1,86	9,04	18,13	0,00	0,00
64	C13orf15	218723_s_at	1,95	10,81	16,16	0,00	0,00
65	RHOH	204951_at	2,01	9,74	27,10	0,00	0,00
66	BCL6	203140_at	2,04	10,60	21,41	0,00	0,00
67	ID1	208937_s_at	2,09	7,73	20,12	0,00	0,00
68	DNAJB4	203810_at	2,16	8,11	23,32	0,00	0,00
69	SOX4	201416_at	2,27	9,20	24,61	0,00	0,00
70	SOX4	201417_at	2,34	10,89	33,59	0,00	0,00
71	IL7R	205798_at	2,37	9,65	18,88	0,00	0,00
72	BMP7	209590_at	2,37	9,07	27,89	0,00	0,00
73	ID4	209291_at	2,69	8,89	34,82	0,00	0,00
74	CYP26A1	206424_at	2,75	10,75	24,85	0,00	0,00

Appendix

Table A 5 LPS responsive genes This table shows the effects of LPS on the most variable genes. 100 probesets with the highest differential expression were selected from all significantly regulated genes. Probesets that were array specific and not spotted on the HG U133 plus, which was used for the evaluation of aNHL samples, were discarded and excluded from further analysis.

	GenSymbols	Probeset-ID	logFC	AveExpr	t	P.Value	adj.P.Val
1	NA	221491_x_at	-0,95	9,31	-9,75	0,00	0,00
2	CD58	205173_x_at	-0,83	9,22	-6,39	0,00	0,00
3	HLA-DPA1	213537_at	-0,82	8,83	-6,24	0,00	0,00
4	MAN1A1	221760_at	-0,78	10,19	-6,48	0,00	0,00
5	MAN1A1	208116_s_at	-0,76	8,57	-5,46	0,00	0,00
6	CD58	216942_s_at	-0,76	8,52	-5,77	0,00	0,00
7	CD58	211744_s_at	-0,75	8,40	-5,43	0,00	0,01
8	IKBKE	204549_at	-0,72	8,38	-11,41	0,00	0,00
9	HLA-DQB1	212998_x_at	-0,72	10,38	-6,71	0,00	0,00
10	HLA-DQB1	209480_at	-0,72	9,25	-5,18	0,00	0,01
11	OLFML2A	213075_at	-0,71	8,81	-9,16	0,00	0,00
12	CALR	214315_x_at	-0,70	9,56	-3,99	0,00	0,05
13	BATF	205965_at	-0,70	9,42	-10,61	0,00	0,00
14	HLA-DQB1	212999_x_at	-0,70	8,04	-5,77	0,00	0,00
15	MT1X	204326_x_at	-0,67	7,84	-7,42	0,00	0,00
16	HLA-DQB1	211656_x_at	-0,66	9,69	-7,19	0,00	0,00
17	HLA-DQB1	209823_x_at	-0,65	8,75	-6,27	0,00	0,00
18	ANXA7	201366_at	-0,64	9,87	-7,30	0,00	0,00
19	IKBKE	214398_s_at	-0,64	8,07	-10,88	0,00	0,00
20	HLA-DQB1	211654_x_at	-0,62	10,22	-7,39	0,00	0,00
21	HLA-DQA1	213831_at	-0,62	9,34	-5,43	0,00	0,01
22	FNBP1	212288_at	-0,62	9,68	-5,50	0,00	0,00
23	NA	206302_s_at	-0,60	9,92	-6,49	0,00	0,00
24	NA	212671_s_at	-0,60	11,06	-6,14	0,00	0,00
25	HLA-DQA1	203290_at	-0,59	10,45	-7,61	0,00	0,00
26	IRF4	204562_at	-0,58	11,00	-6,59	0,00	0,00
27	CREBZF	202979_s_at	-0,57	8,23	-4,43	0,00	0,02
28	IGLL1	206660_at	-0,55	9,38	-8,98	0,00	0,00
29	DNAJB1	200664_s_at	-0,54	9,39	-4,63	0,00	0,02
30	IFIT3	204747_at	-0,54	6,84	-5,59	0,00	0,00
31	HLA-E	200905_x_at	-0,54	9,77	-5,72	0,00	0,00
32	PDLIM3	209621_s_at	-0,54	8,96	-7,13	0,00	0,00
33	DNAJB1	200666_s_at	-0,54	10,02	-4,76	0,00	0,01
34	DENND4A	214787_at	-0,54	8,48	-5,54	0,00	0,00
35	NARF	219862_s_at	0,54	9,37	6,32	0,00	0,00
36	SPG11	203513_at	0,54	8,80	7,68	0,00	0,00
37	GPM6A	209469_at	0,55	8,34	4,73	0,00	0,02
38	MYBL1	213906_at	0,56	8,08	5,44	0,00	0,00
39	BNIP3L	221478_at	0,56	9,54	5,51	0,00	0,00
40	STAP1	220059_at	0,56	10,36	7,50	0,00	0,00
41	TRIM22	213293_s_at	0,57	9,60	5,87	0,00	0,00
42	PIK3C2B	204484_at	0,57	8,90	7,36	0,00	0,00
43	GPER	210640_s_at	0,59	7,11	4,33	0,00	0,03
44	KLRC3	207723_s_at	0,59	8,27	7,68	0,00	0,00
45	VEGFA	210512_s_at	0,59	7,35	5,19	0,00	0,01
46	P4HA1	207543_s_at	0,59	9,01	4,38	0,00	0,03
47	SMAD1	210993_s_at	0,59	9,31	6,05	0,00	0,00
48	C7orf68	218507_at	0,60	9,48	4,31	0,00	0,03
49	ID4	209292_at	0,61	7,10	8,77	0,00	0,00
50	TXNIP	201009_s_at	0,62	8,21	4,68	0,00	0,02
51	TXNIP	201008_s_at	0,63	8,13	4,23	0,00	0,03
52	PTPRC	212587_s_at	0,64	9,74	6,77	0,00	0,00
53	PTPRC	207238_s_at	0,67	9,49	8,88	0,00	0,00

54	CCNG2	211559_s_at	0,69	8,54	6,98	0,00	0,00
55	KDM3A	212689_s_at	0,69	8,67	6,16	0,00	0,00
56	CCNG2	202769_at	0,70	9,09	7,25	0,00	0,00
57	CCNG2	202770_s_at	0,72	8,64	7,03	0,00	0,00
58	BNIP3	201848_s_at	0,75	8,40	5,67	0,00	0,00
59	BNIP3	201849_at	0,78	9,75	5,60	0,00	0,00
60	ID4	209291_at	0,78	8,89	10,06	0,00	0,00
61	TXNIP	201010_s_at	0,79	8,40	5,59	0,00	0,00
62	METTL7A	207761_s_at	0,80	9,60	10,66	0,00	0,00
63	ID3	207826_s_at	0,81	11,03	9,25	0,00	0,00
64	DDIT4	202887_s_at	0,83	9,39	4,68	0,00	0,02
65	C3orf37	201678_s_at	0,85	9,54	6,80	0,00	0,00
66	ID1	208937_s_at	1,90	7,73	18,27	0,00	0,00

Table A 6 BAFF responsive genes This table shows the effects of rhBAFF on the most variable genes. 100 probesets with the highest differential expression were selected from all significantly regulated genes. Probesets that were array specific and not spotted on the HG U133 plus, which was used for the evaluation of aNHL samples, were discarded and excluded from further analysis.

	GenSymbols	ID	logFC	AveExpr	t	P.Value	adj.P.Val
1	TCOF1	202384_s_at	-0,74	8,23	-4,42	0,00	0,03
2	HLA-DQA1	203290_at	-0,73	10,45	-9,46	0,00	0,00
3	HLA-DQB1	209823_x_at	-0,73	8,75	-7,06	0,00	0,00
4	HLA-DQB1	212998_x_at	-0,71	10,38	-6,57	0,00	0,00
5	NA	221491_x_at	-0,70	9,31	-7,21	0,00	0,00
6	RUNX3	204198_s_at	-0,70	9,45	-4,74	0,00	0,02
7	EIF5B	214314_s_at	-0,68	7,93	-4,23	0,00	0,04
8	NA	212671_s_at	-0,65	11,06	-6,64	0,00	0,00
9	C1orf63	209006_s_at	-0,65	6,99	-5,29	0,00	0,01
10	EIF5B	201024_x_at	-0,63	10,17	-4,20	0,00	0,04
11	IGLL1	206660_at	-0,61	9,38	-10,13	0,00	0,00
12	HLA-DQB1	211656_x_at	-0,61	9,69	-6,67	0,00	0,00
13	DENND4A	214787_at	-0,60	8,48	-6,20	0,00	0,00
14	LRRFIP1	201862_s_at	-0,59	10,36	-4,08	0,00	0,05
15	OLFML2A	213075_at	-0,59	8,81	-7,54	0,00	0,00
16	SLC23A2	209236_at	-0,59	8,56	-6,87	0,00	0,00
17	RUNX3	204197_s_at	-0,59	9,10	-7,67	0,00	0,00
18	NCOR2	207760_s_at	-0,58	8,95	-4,23	0,00	0,04
19	CD58	205173_x_at	-0,57	9,22	-4,35	0,00	0,03
20	ICAM1	202638_s_at	-0,57	8,06	-6,09	0,00	0,00
21	HLA-DQB1	211654_x_at	-0,56	10,22	-6,59	0,00	0,00
22	DNAJB1	200664_s_at	-0,54	9,39	-4,65	0,00	0,02
23	MAN1A1	221760_at	-0,54	10,19	-4,47	0,00	0,03
24	MT1X	204326_x_at	-0,53	7,84	-5,91	0,00	0,00
25	ICAM1	202637_s_at	-0,53	8,39	-5,61	0,00	0,01
26	PEA15	200787_s_at	-0,53	8,75	-5,10	0,00	0,01
27	HLA-DQA1	213831_at	-0,53	9,34	-4,61	0,00	0,02
28	HSP90B1	200598_s_at	-0,52	10,33	-5,14	0,00	0,01
29	HLA-B	211911_x_at	-0,52	12,27	-8,55	0,00	0,00
30	DNAJB1	200666_s_at	-0,52	10,02	-4,61	0,00	0,02
31	CCDC28B	221912_s_at	-0,51	9,28	-7,72	0,00	0,00
32	LRP8	205282_at	-0,51	7,58	-6,07	0,00	0,00
33	BIRC3	210538_s_at	-0,51	9,84	-5,06	0,00	0,01
34	NFKB2	207535_s_at	-0,50	8,23	-5,79	0,00	0,01
35	HSP90B1	200599_s_at	-0,50	11,68	-5,63	0,00	0,01
36	ILF3	208931_s_at	-0,50	9,33	-4,48	0,00	0,03
37	TOMM40	202264_s_at	-0,50	10,13	-5,13	0,00	0,01
38	CIZ1	213977_s_at	-0,50	8,51	-4,23	0,00	0,04
39	FNBP1	212288_at	-0,49	9,68	-4,41	0,00	0,03

Appendix

40	SRRT	201680_x_at	-0,49	10,85	-8,41	0,00	0,00
41	NAA16	219378_at	-0,49	8,62	-4,78	0,00	0,02
42	PEA15	200788_s_at	-0,49	8,91	-5,23	0,00	0,01
43	HLA-B	208729_x_at	-0,49	12,06	-7,62	0,00	0,00
44	MYBBP1A	219098_at	-0,48	8,89	-4,36	0,00	0,03
45	CSF2RB	205159_at	-0,48	8,77	-5,12	0,00	0,01
46	HSP90B1	216449_x_at	-0,48	9,88	-6,29	0,00	0,00
47	TAF1D	218750_at	-0,48	7,51	-4,29	0,00	0,04
48	KPNB1	208975_s_at	-0,48	10,45	-4,16	0,00	0,04
49	HBP1	209102_s_at	0,48	8,16	5,22	0,00	0,01
50	POLD4	202996_at	0,49	8,28	8,74	0,00	0,00
51	CD83	204440_at	0,51	10,60	6,52	0,00	0,00
52	CCNG2	202770_s_at	0,52	8,64	5,02	0,00	0,01
53	ALDOC	202022_at	0,52	8,26	6,89	0,00	0,00
54	BBOX1	205363_at	0,52	6,82	5,33	0,00	0,01
55	CD24	216379_x_at	0,53	12,11	8,03	0,00	0,00
56	ID4	209293_x_at	0,53	7,79	7,23	0,00	0,00
57	GPR18	210279_at	0,54	9,43	5,98	0,00	0,00
58	C3orf37	201678_s_at	0,56	9,54	4,48	0,00	0,03
59	ID3	207826_s_at	0,56	11,03	6,44	0,00	0,00
60	ID4	209292_at	0,57	7,10	8,21	0,00	0,00
61	CCNG2	202769_at	0,57	9,09	5,95	0,00	0,00
62	CD24	209772_s_at	0,58	10,39	7,39	0,00	0,00
63	ID2	201565_s_at	0,59	10,27	4,98	0,00	0,01
64	TXNIP	201009_s_at	0,62	8,21	4,71	0,00	0,02
65	C7orf68	218507_at	0,63	9,48	4,55	0,00	0,03
66	CCNG2	211559_s_at	0,64	8,54	6,48	0,00	0,00
67	BNIP3L	221479_s_at	0,64	9,06	7,57	0,00	0,00
68	P4HA1	207543_s_at	0,65	9,01	4,83	0,00	0,02
69	PNOC	205901_at	0,67	11,84	10,66	0,00	0,00
70	GPER	210640_s_at	0,68	7,11	5,03	0,00	0,01
71	TXNIP	201008_s_at	0,70	8,13	4,67	0,00	0,02
72	BNIP3	201848_s_at	0,72	8,40	5,47	0,00	0,01
73	BNIP3L	221478_at	0,73	9,54	7,19	0,00	0,00
74	TXNIP	201010_s_at	0,75	8,40	5,31	0,00	0,01
75	BNIP3	201849_at	0,80	9,75	5,75	0,00	0,01
76	ID4	209291_at	0,92	8,89	11,97	0,00	0,00
77	ID1	208937_s_at	2,08	7,73	19,95	0,00	0,00

Chapter 3 Guided Clustering

Table A 7 Cluster genes identified by guided clustering

	IL21.1	IL21.2	CD40.1	CD40.2	BCR.1	BCR.2	LPS.1	LPS.2	BAFF.1	BAFF.2
1	SEC24B	STAT1	SFRS2	PICK1	XPO1	MAPKSP1	LAMA1	GRIN2B	KPNB1	EPHB4
2	RSRC2	IRF1	MRPL46	SOX15	PMS1	ATF1	VNN3	POU2AF1	SLTM	AGRN
3	DYNC1LI1	IFIT3	MUS81	HP	RNASEN	CCDC59	ELAVL3	NRD1	REV1	VGX2
4	USP8	CXCL10	TOE1	TRIM17	LBR	RSL24D1	TSHZ2	FAF1	EIF3A	TBKBP1
5	RABGGTB	APOL6	FARSA	CYP2A13	CETN3	BZW1	MEGF8	TRBV10-2	LSM14A	DNAJC28
6	FAM178A	OASL	EIF4A3	SLC9A3R2	DCK	BNIP2	FOXO4	PDGFB	CKAP5	GPR110
7	NOC3L	IFI44L	MCM3	SDK2	GPN3	ETF1	GRK1	SLC34A1	CENPE	ALDOAP2
8	MTERFD1	IFIT1	NOC3L	APOC4	SLBP	TAF9	ADAMTSL2	NR2E3	ORC6L	SLC18A3
9	ANKRD27	RSAD2	ANKRD27	DCLK2	RHOT1	POMP	TMEM179B	CRTAC1	KIF18B	MLXIPL
10	ZDHHC6	MX1	DNAJA2	CELA2B	CAND1	GNAI3	DOHH	GABRD	ATAD2	DLG4
11	METAP1	IFI44	GPN2	CNPY4	RACGAP1	ARF6	PSD	PDIA2	TOP2A	OSGIN1
12	C2orf49	IFITM1	C16orf80	LTBR4R2	KIF20A	YWHAZ	SNAPC2	ZNF205	ASPM	ENPP3
13	TRA2B	IFITM3	VRK1	GPATCH2	AURKA	GABPB1	NIN	POU4F3	WHSC1	ALPI
14	SFRS1		NDUFV2	KCNQ1	HMMR	CEBPG	FOXO1	ADORA1	SMC2	SOX15
15	KRR1		COX4NB	SULT4A1	NDC80	MAPK6	ZNF646	KCNJ5	MSH2	CADM4
16	RBM25		SHQ1	IGF2AS	CDC20	RBM22	C1orf183	IGF2AS	CACYBP	STBD1
17	NUP50		MCAT	IGFBP5	CENPA	C6orf62	GJA8	ABO	WBP4	SCNN1A
18	ZNHIT6		PRPF4	STMN3	PLK1	ERBB2IP	SIX5	TRGV5	ZC3H13	PFKFB4
19	GNL2		LCMT1	PYY2	NEK2	UBE2B	PTPRS	STMN3	SFRS1	MATN4
20	CCT6A		RFC2	SLC9A3	CCNA2	CSNK1A1	TEX11	PKLR	NASP	PCYT1B

21	POLR3E		RAD51C	ADRA2C	KIF18A	NFE2L2	FOXC2	WFDC8	ACYP1	LRAT
22	RPL23AP7		FEN1	NRXN2	RM1	PLEKH2	SLC2A4	NRXN2	SDCCAG1	OPRD1
23	APIP		TRIP13	AKAP4	PBK	MTMR6	C2orf72	SPTB	LUC7L3	NBR2
24	PSMC6		TRA2B	FAM179B	PRC1	TRIP12	NFKBIL2	OPRL1	KIF20B	NPTXR
25	ZC3H15		SFRS1	PLCH2	BUB1B	TM9SF3	EPO	CEMP1	SUCLA2	KRT16
26	SART3		HNRNPR	ANKRD2	PLK4	DDX5	GPR32	SLC9A3R2	SPAG5	TNXB
27	CHORDC1		PEF1	UCP3	CDCA8	YIPF4	PRDM8	TLX2	MKI67	TUBB4Q
28	C14orf104		C2orf47	ALOX12B	NCAPH	CEP57	PLEKHA4	SYT5	PLK4	SH2D4A
29	WDR3		DLD	HIST1H2AK	TMEM48	MIS12	CYP11B2	NFIX	NCAPH	TGFB2
30	FUBP3		SFRS3	MYCN	OIP5	ZNF330	BARX1	MMP16	PRDX3	WIF1
31	TAF2		DDX19A	SCN2B	CEP55	LARP7	KRT3	SNCA	ADK	MYH15
32	ZMYM4		CIAPIN1	ZNF205	KIF14	NUP88	CEBPE	MAP1LC3C	PAICS	HOXD10
33	ZBTB11		CYC1	EPB41L1	ESPL1	WAPAL	CDKN2B	APCS	EIF2B3	GDF2
34	PRPF38B		PEX14	SLC34A1	POLA2	VPS26A	ZCCHC4	PSPN	NUDC	CCL27
35	BTA1F1		GCDH	NHEJ1	FEN1	UBE2D3	MTHFR		KIN	MAPT
36	TNFAIP8		EXOSC4	HDAC11	BRCA1	RBM15	LRIT1		C12orf48	CRYBB2
37	KIAA0406		PUF60	FKBP6	TUBG1	PITPNB			SSB	TPPP3
38	TM9SF3		REEP4	PCYT1B	MRPL16	TARS			SMC3	FGF20
39	PPWD1		SF4	SNCG	TACC3	MAK16			KIF14	PCDHB17
40	UBXN2B		UBTF	OR3A2	SAC3D1	MTHFD2			POLD1	ADAMTS7
41	LUC7L3		ABCF3	PTCRA	ASPM	SNX5			SCRIB	CABP2
42	GTF2H1		RRP9	ROM1	WDHD1	PDXDC1			REXO4	PRB3
43	PCNP		STX4	NPHS1	BIRC5	DHX15			MSH3	UBTD1
44	ANAPC10		CTCF	SIRT5	CCNB1	DENR			MPHOSPH10	HSPB2
45	RECQL		SMARCAL1	CATSPERB	ASF1B	ZNF410			FASTKD3	PDGFB
46	KLHL2		NOC4L	TCL6	ORC1L	DERL2			ARL6IP4	NR2E3
47	TMM17A		WDR18	HGFAC	KIF2C	HNRNPK			SAFB2	CRTAC1
48	CEP170		PDCD5	CCNJL	CDCA3	C5orf28			CHERP	C14orf115
49	RRS1		MAT2A	HOXC13	FOXM1	DIMT1L			SRRM1	GPR37L1
50	LARP4		AIMP2	ADCY10	RFC3	CDK7			ZNF146	LCN1
51	DNAJB14		MTIF2	ACAP2	ECT2	RAP2C			SUPT16H	NDST1
52	SERBP1		HEATR3	HTR5A	DSCC1	SSFA2			KIAA0406	TRPV6
53	RBM28		DDRKG1	TBL2	C12orf48	JMJD1C			UPF2	HOXA3
54	SSB		THOC1	SLC38A3	WRAP53	EIF1B			LUC7L2	TP53TG5
55	MPHOSPH10		MTHFS	ATP6V1B1	PARP2	ZC3H15			BMS1	TSKS
56	C1orf109		TBL3	PAX3	TRIP13	SAR1A			CHAF1A	KRT19P2
57	NOL7		PPP3CA	RBP3	KIF11	BCAS2			TCOF1	RNLS
58	TCEB1		RPS6KA1	C8orf30A	AASDHPPT	ETFDH			SAFB	XPNPEP3
59	MAGOH		TYMS	PBOV1	FARSA	MMADHC			TOPBP1	DDX25
60	RCHY1		RASSF2	GNG7	CTCF	MRPS30			SSRP1	HSD3B2
61	C9orf82		MRPL12	NPPA	RNASEH2A	MRPL39			SFRS12	ACCN2
62	FBXW2		HSPA14	CLCN7	NEIL3	GMFB			BAZ1A	RGS7
63	ENOPH1		BRMS1	PDGFRA	STIL	TSG101			DAZAP1	TACR2
64	RARS		COPS7B	TASP1	TARDBP	CSNK1D			RPAP3	PSG3
65	TAF1A		PIK3CD	EXOSC1	ARMC1	GDI2			HSPH1	OR7C1
66	VEZF1		ACOX3	WNT8B	MRPL35	LASP1			RSF1	BICC1
67	CEBPZ		IMPDH1	ADORA1	WDR67	CSGALNACT2			TOP1	SYN2
68	AGPAT5		SARS2	DHX29	NUP37	ZBTB1			PPWD1	CAMKV
69	EIF3J		SPIB	TLX2	MRPL12	SLC2A3P1			KTN1	AMBN
70	ZCCHC8		SH3BP5	DUSP9	RAD54L	ZNF217			CENPF	EPB41L1
71	CNIH		DOCK10	KCNJ5	C16orf53	CAPZA1			IARS2	AP3D1
72	UNC50		ARHGAP17		ALG6	HMGCR			BRAP	SPAG9
73	SGMS1		RAB7L1		TROAP	ATP2C1			ACTR6	OR11A1
74	MLX		EIF2B5		CDC7	HSPA5			FABP5	PKLR
75	AHCTF1		MICALL1		RFC4	PPP6C			POLR2F	SHB
76	CEP57		POP4		UNG	TOR1A			ITGB1BP1	ADCY10
77	PIBF1		TTC35		PPAT	JOSD1			GNB1	TGFBRAP1
78	PSMD12		UAP1		FASTKD1	PTBP1			NUP107	TRIM49
79	SDHAF1		ICT1		KIF15	YBX1			TCP1	PCDH1
80	C12orf44		TACO1		ANP32A	EPRS			CCT6A	ATP2B3
81	MFSD1		MRPL34		SRRD	SDCBP			PRPF38B	RAX
82	NPTN		C8orf33		LRRC47	RNF4			CPSF6	CDHR5
83	SOAT1		UCK2		PREB	CAB39			AHSA1	WNT8B
84	SLC35A1		TOMM70A		ZC3H14	YAF2			ERCC3	RHO
85	MT01		AGFG1		TTK	TMEM123			YY1	KRT15
86	GSPT1		LSM12		EFTUD1	TMEM222			CHD8	CACNA1E
87	UTP6		G3BP1		OSBPL11	TFAM			PPIG	LMAN1L
88	ANKRD40		ANXA7		MYCBP	CDK17			DUT	GUCA1B
89	BANP		EXOC1		DYNLL1	USP16			CHORDC1	DNAH9
90	TMEM33		SLC25A46		NIF3L1	GARS			DDX23	NGFR
91	TMED5		TRPM3		MRFAP1L1	CNIH			RUVBL1	GJA3
92	SLC30A5		DDX50		NARG2	RAN			EXO1	MYL10
93	SNW1		EIF4E		SPAST	C11orf57			EIF5B	NR0B1
94	C14orf135		ZC3H14		ZW10	LYRM1			PABPN1	GRAP2
95	POP1		HEATR2		ELF2	SARS			NDUFS8	IFT140
96	ZDHC13		GTF3C2		ADH5	CLIC1			TAF2	LOC645961
97	KIAA1704		TIMM23		ORC4L	MAPRE1			BUB1B	PTPRU

Appendix

98	RSC1A1		POLR3E		ORC2L	SLC25A32			DNM1L	KRT83
99	ATP11B		DHX30		CLINT1	ADIPOR2			FIP1L1	S100A14
100	CUL4A		DPH2		DLAT	E2F6			SMARCA4	NLGN3
101	SUCLA2		WDR1		RIOK2	RAB7A			BPTF	C1orf183
102	DENR		MGAT2		CKAP2	THAP1			NKTR	SOX14
103	TCERG1		ATMIN		NARS2	RNMT			SART3	SLC14A2
104	DNAJA1		UMPS		CEP76	SAT1			MED24	BBOX1
105	SEPHS2		MRPL17		CACYBP	CTMT6			FAM98A	CNTNAP2
106	DNAJC7		ELAC2		TMEM97	WDR26			CCDC99	FBXL12
107	CDC42EP3		ZNF706		POLE2	PYROXD1			MRPS15	NFASC
108	REV1		PRKRA		USP13	PIKFYVE			ANKRD17	PMS2L4
109	TIMM9		CDC5L		RAD1	NIPA2			UBE2K	CCR3
110	XPOT		TUBG1		GCDH	RHOA			CSTF3	TAS2R9
111	HIRA		SAMM50		CPOX	DAZAP2			LSM6	RGS12
112	TXNL1		FBXL15		CLPX	TBC1D15			POLR2E	CPLX2
113	ABHD3		ERCC3		MORC2	C12orf35			EED	C14orf79
114	HSPA8		SAE1		RFC5	WIPF1			MTERFD1	C19orf42
115	C3orf64		CDC25A		RAD51C	C10orf26			TAF5	GRIN2A
116	PNN		UCHL3		RCN2	SKP1			SS18L1	C6orf54
117	CSTF3		ACD		PIGF	KIAA0232			LRDD	UTP14C
118	EXOSC4		PSMB2		ACTR6	CHIC2			NCAPG2	DUSP26
119	NUDC		NAT10		CDC73	ARL8B			SPC25	SLC9A3R2
120	DICER1		C21orf59		MDM1	PPP2R2A			NCOA6	AGER
121	KIAA1012		RNF115		KIAA0528	RNF111			PSPC1	GNG7
122	C11orf58		ELOVL1		PARG	AURKB			LIN37	MUC6
123	KIF23		NECAP2		THAP11	TOP2B			HAUS6	
124	FBXL4		NBN		C12orf52	BC12L13			EXOSC10	
125	HAUS3		GCNT4		PTCD3	ATP6V1E1			IMMT	
126	YEATS2		SEMA3B		CASP6	RAB1A			NAA16	
127	KIAA0753		CLCN1		CTR9	CD164			USP48	
128	HNRNPD		GFM1		MRPL46	PLEKHF2			SPEN	
129	FASTKD3		PNLIP		GPSM2	HECA			PIAS4	
130	ATF2		RCN2		NDUFC1	ITSN2			ABHD3	
131	PUS1		NPAS1		UBE2G1	PPP2R3C			CCDC91	
132	JRK1		DNAJA1		PRPSAP1	RNF11			PSMD1	
133	HSPA4		SF3B2		NCAPD3	ARF4			RECQL4	
134	RPAP3		MRPL39		DPF2	SLC3A2			MTHFD1	
135	TBK1		DDA1		HEATR3	SGPL1			PPP2R5E	
136	EIF4E		WBP11		SHCBP1	MORF4L1			SEC24A	
137	UTP11L		CMAS		C4orf41	PIP4K2A			SAR1B	
138	SUV39H2		CCT6A		SKP2	CHSY1			CEP63	
139	TMEM165		TARDBP		MTX2	FAF2			UCHL5	
140	HNRNPU		IMP3		MUDENG	GOLT1B			RANGAP1	
141	YME1L1		RIOK2		C15orf44	CYP20A1			WDHD1	
142	ETFA		MED22		GINS1	GOT1			DNA2	
143	NUP54		FTSJ3		ZWILCH	ADO			C11orf48	
144	LIN37		ZFR		MRPL18	PSEN1			C10orf2	
145	RIOK2		TFCP2		PEX14	RBMX			PDCD5	
146	QTRTD1		PSME3		TOMM70A	DUSP11			ACOT7	
147	DDX50		MAP2K4		TSN	ATP6V1H			MGM10	
148	NMD3		EFR3A		SFRS4	MAP1LC3B			DDX52	
149			EPS15		HSPH1	IDI1			NCAPD3	
150			TCTN3		FOSL1	NTAN1			LIG1	
151			EIF4ENIF1		KIAA0406	DCTN5			RAD51AP1	
152			ANKRD40		DSN1	CENPN			MRFAP1L1	
153			HPS6		PRPF4B	HNRNPC			TPR	
154			SART3		C13orf34	MARS			PRPF3	
155			ANAPC10		BAG2	YARS			WHSC2	
156			MRS2		ZNHIT3	EDEM1			HAT1	
157			KPNA3		PDHB	DDX18			DNAJC13	
158			APIP		CCDC56	BUD31			ATXN2	
159			BCL10		CUTC	RCHY1			MTDH	
160			CTSH		C14orf104	PRKD3			TCERG1	
161			TBK1		COX11	SWAP70			RAD50	
162			RRP1B		CDK8	LY75			YY1AP1	
163			NUFIP1		C8orf41	CHD1			DLX2	
164			GRPEL1		AURKAIP1	EIF1			DUOX2	
165			CHMP6		IMP3	IMPA1			NDUFS1	
166			YIF1A		MINA	CHMP2B			CEBPZ	
167			NSMCE4A		PUM2	OSBP			NDUFB8	
168			UBE3B		DHX29	RAB5A			EXOSC7	
169			PPCS		COASY	LZTS1			HSPE1	
170			ZBTB11		THAP7	NCRNA00081			C14orf104	
171			NPL		MRPS34	RAB21			ATR	
172			NOTCH2		CCDC51	UGCG			PNN	
173			LAMP2		MRPL17	GABARAPL2			PHIP	
174			RDX		COIL	FBXO28			ZFC3H1	

175		TMEM165	ATMIN	HSD17B12	NUP43
176		PIK3CB	SMARCAL1	YTHDF3	NCOR1
177		HLA-J	COQ9	ECD	TRIM24
178		HLA-F	COBRA1	ABCF1	PSMC6
179		HLA-B	MED20	C15orf24	POLR2B
180		HLA-G	CCDC99	TSPYL1	NCL
181		HLA-C	SIP1	ZEB2	RECQL
182		HCP5	FANCG	CD63	SYNCRIP
183		HLA-A	MCM2	BACH1	MCCC2
184		BTN2A2	CRIP1	PRNP	HSPA4
185		PLEKHO1	GAPVD1	HEXB	PSMD14
186		CSF2RB	CNP	PTTG1IP	C1orf109
187		HLA-DPB1	RAB11A	CEBPB	SLC4A1AP
188		ZNF672	MRPS31	CTSB	MED4
189		RFX5	MRPL34	M6PR	WDR61
190		NUBP1	PHB	LAMP1	AHCTF1
191		TRIP4	POP4	IFI30	MAGOH
192		RAB27A	AGGF1	RIN2	BRD7
193		BID	KIF22	TFEC	NSMCE4A
194		ARIH1	POP7	GPX4	PHF3
195		CD59	DDX23	TLR1	PPP1R12A
196		SLC31A2	ZBED5	TNFRSF14	MAVS
197		FLVCR2	BBS10	GPR137B	ST13
198		CTSC	ZNF638	LY96	SNX1
199		LGALS9	SRBD1	IFNGR1	CBX1
200		RAC2	GTF2E1	SRGN	HNRNPH3
201		HNRNPF	MEN1	CRIM1	RNASEN
202		PSMC6	LSM2	CLEC2B	PRR11
203		SLURP1	SRPK1	CD97	HNRNPD
204		TIMM17A	TTRAP	GPR65	PRPF19
205		MINPP1	ZNF184	CYFIP1	DDX49
206		UBAC1	MICB	IFNGR2	ESPL1
207		C1orf35	TUBD1	ATP6V0E1	EDF1
208		DCC	NFYB	OSTM1	CSF3
209		MTMR4	KIF18B	ACSL1	NIPBL
210		RPS6KB1	PRDM10	WSB2	ASCC3
211		UBE3C	HMGNA4	SGK1	NUP133
212		TMEM70	RAD54B	CSTB	TECR
213		KIAA0947	DTWD1	UPP1	CCNE1
214		LARS2	BRD8	LRP10	KIAA0101
215		C12orf43	TRMT61B	SERINC1	AK2
216		STAM2	RNF34	RAB22A	EXOSC9
217		ISOC1	CDC27	AP2B1	CHCHD3
218		METAP1	EXOC1	C1orf54	RPIA
219		API5	SACM1L	DENND4A	KIAA0562
220		SRPK1	VPS33B	USP12	STK39
221		MFN2	SUCLA2	STK17B	LRRC40
222		SEC23IP	MRS2	GHITM	HNRNPH1
223		CAPRIN1	C6orf211	EIF2S1	C14orf156
224		SEC24B	HMGCB3	TOR1B	PPIH
225		ARFGEF1	GEMIN6	HSPA13	RIOK2
226		CLPX	MRPS16	CD86	RCBTB1
227		UBE2L3	MCM10	FRG1	PRPF4B
228		PDHX	AP1AR	PSMD12	SMS
229		C14orf104	C4orf27	TMEM66	ACIN1
230		BRD7	FASTKD3	ATF4	BRCA1
231		METTL1	CLCN3	POLR2D	EBNA1BP2
232		C9orf114	PRMT5	SHMT2	POLR3K
233		SLC35B1	TDP1	SFPQ	GRPEL1
234		SNX4	LARS2	USP15	CISD1
235		DCTD	BARD1	OSBPL8	SNRNP25
236		PHB	MSH3	LPXN	MELK
237		FAM35A	MPHOSPH6	MAP2K3	TACC3
238		CNPY3	MTIF2	ZHX2	SNRPF
239		ABCB11	ATR	RHOG	PFAS
240		KEAP1	PPP2R5E	CYTSA	USP24
241		DDX42	PSMC6	H3F3B	CMAS
242		CCDC51	ZNF107	PDXK	ROCK1
243		BRIX1	EIF2B4	RAB8B	WDR18
244		RRS1	C9orf40	NFYA	IK
245		WDR3	RTF1	VAMP3	CACNA1S
246		PWP1	MRPL49	AGA	SAP30L
247		MINA	CSE1L	CNIH4	CTNBL1
248		RARS	PLA2G12A	HNMT	DHX30
249		HNRNPA0	ELP4	ARL4C	C14orf166
250		PRLR	UBTF	C3AR1	DHFR
251		HSPA4	GTF3C1	SIRPA	ACD

Appendix

252		SIX3	BCOR	EMP3			GNP3	
253		ADRA1D	C5orf22	MKLN1			PDHB	
254		WDR41	TTC33	ITM2B			PIBF1	
255		ALCAM	PSME4	CCPG1			E4F1	
256		PALB2	PPM1B	CDC42				
257		SYNGR2	PIAS4	KIAA0430				
258		PSMC4	WBP4	TNPO1				
259		RAP2B	ACAP2	TXNDC9				
260		TAF1B	GRSF1	EIF2S2				
261		NUDT21	GADD45GIP1	WARS				
262		YARS2	MSH2	CCL4				
263		DCLRE1B	DTYMK	NINJ1				
264		CINP	FRAT2	LGALS8				
265		IFRD2	STAMBP	RRAGD				
266		SERBP1	C17orf75	ACP5				
267		TTC4	FANCL	C6orf145				
268		C16orf88	SFRS2B	IL32				
269		PSMA7	HMBS	MARCH7				
270		MCCC2	PAAF1	KLF10				
271		TESC	NAA40	SMURF2				
272		LMNB2	NDUFS3	SFT2D2				
273		THAP11	DUT	FAM18B				
274		FNBP1	STRA13	UBL3				
275		EIF4H	HADH	MAFF				
276		CD160	SEPHS1	TMEM30A				
277		TRAPPC3	ABHD10	TMBIM6				
278		FASTKD3	SLC4A1AP	MON1B				
279		CTR9	STRADA	DOCK2				
280		HCK	CBX1	NR3C1				
281		C3orf37	MRPS27	GCH1				
282		PHF16	WRB	SAP30BP				
283		TRIM44	DERA	MATR3				
284		KCNJ1	SAR1B	GCC2				
285		NOL11	MAP3K4	PLXNC1				
286		CPSF4	KIAA1279	HEXA				
287		C7orf23	PPCS					
288		RSRC2	C5orf15					

Table A 8 Gene Set Enrichment Analyses (GO) Gene Set Enrichment for BCR.1 genes was performed using the Geneset annotations implemented in the GO database. The TOP100 most significantly enriched genesets corresponding to biological processes are shown below

Biological Process			
	GO ID	GO Term	downreg. p-value
1	GO:0007017	microtubule-based process	6,00E-16
2	GO:0000278	mitotic cell cycle	7,00E-15
3	GO:0006996	organelle organization	5,00E-14
4	GO:0000226	microtubule cytoskeleton organization	1,00E-13
5	GO:0051301	cell division	2,00E-13
6	GO:0007059	chromosome segregation	3,00E-13
7	GO:0006281	DNA repair	5,00E-12
8	GO:0006974	response to DNA damage stimulus	2,00E-11
9	GO:0007051	spindle organization	4,00E-09
10	GO:0000070	mitotic sister chromatid segregation	8,00E-09
11	GO:0006260	DNA replication	8,00E-09
12	GO:0000819	sister chromatid segregation	1,00E-08
13	GO:0090304	nucleic acid metabolic process	3,00E-08
14	GO:0010564	regulation of cell cycle process	9,00E-08
15	GO:0044260	cellular macromolecule metabolic process	9,00E-08
16	GO:0033554	cellular response to stress	2,00E-07
17	GO:0051276	chromosome organization	2,00E-07
18	GO:0006139	nucleobase, nucleoside, nucleotide and nucleic acid metabolic process	4,00E-07
19	GO:0007098	centrosome cycle	7,00E-07
20	GO:0000075	cell cycle checkpoint	8,00E-07
21	GO:0051640	organelle localization	1,00E-06
22	GO:0040001	establishment of mitotic spindle localization	1,00E-06
23	GO:0051293	establishment of spindle localization	2,00E-06
24	GO:0051653	spindle localization	2,00E-06

25	GO:0051726	regulation of cell cycle	2,00E-06
26	GO:0016043	cellular component organization	3,00E-06
27	GO:0034641	cellular nitrogen compound metabolic process	4,00E-06
28	GO:0006261	DNA-dependent DNA replication	5,00E-06
29	GO:0007052	mitotic spindle organization	9,00E-06
30	GO:0006302	double-strand break repair	1,00E-05
31	GO:0051297	centrosome organization	1,00E-05
32	GO:0000132	establishment of mitotic spindle orientation	1,00E-05
33	GO:0051294	establishment of spindle orientation	1,00E-05
34	GO:0007010	cytoskeleton organization	1,00E-05
35	GO:0009987	cellular process	1,00E-05
36	GO:0006310	DNA recombination	2,00E-05
37	GO:0006807	nitrogen compound metabolic process	2,00E-05
38	GO:0031023	microtubule organizing center organization	2,00E-05
39	GO:0046599	regulation of centriole replication	2,00E-05
40	GO:0050000	chromosome localization	2,00E-05
41	GO:0051303	establishment of chromosome localization	2,00E-05
42	GO:0043170	macromolecule metabolic process	2,00E-05
43	GO:0051656	establishment of organelle localization	3,00E-05
44	GO:0007080	mitotic metaphase plate congression	4,00E-05
45	GO:0051321	meiotic cell cycle	5,00E-05
46	GO:0051983	regulation of chromosome segregation	7,00E-05
47	GO:0007018	microtubule-based movement	7,00E-05
48	GO:0006271	DNA strand elongation involved in DNA replication	1,00E-04
49	GO:0034501	protein localization to kinetochore	1,00E-04
50	GO:0007346	regulation of mitotic cell cycle	1,00E-04
51	GO:0000910	cytokinesis	1,00E-04
52	GO:0051310	metaphase plate congression	1,00E-04
53	GO:0006397	mRNA processing	2,00E-04
54	GO:0007126	meiosis	2,00E-04
55	GO:0051327	M phase of meiotic cell cycle	2,00E-04
56	GO:0044237	cellular metabolic process	3,00E-04
57	GO:0010824	regulation of centrosome duplication	3,00E-04
58	GO:0006270	DNA-dependent DNA replication initiation	3,00E-04
59	GO:0010212	response to ionizing radiation	4,00E-04
60	GO:0051298	centrosome duplication	4,00E-04
61	GO:0033044	regulation of chromosome organization	4,00E-04
62	GO:0032886	regulation of microtubule-based process	5,00E-04
63	GO:0046605	regulation of centrosome cycle	5,00E-04
64	GO:0000236	mitotic prometaphase	6,00E-04
65	GO:0051299	centrosome separation	6,00E-04
66	GO:0006297	nucleotide-excision repair, DNA gap filling	7,00E-04
67	GO:0007062	sister chromatid cohesion	7,00E-04
68	GO:0007099	centriole replication	8,00E-04
69	GO:0022616	DNA strand elongation	8,00E-04
70	GO:0031124	mRNA 3'-end processing	9,00E-04
71	GO:0033043	regulation of organelle organization	1,00E-03
72	GO:0006259	DNA metabolic process	<2e-16
73	GO:0048285	organelle fission	<2e-16
74	GO:0022403	cell cycle phase	<2e-16
75	GO:0000280	nuclear division	<2e-16
76	GO:0007067	mitosis	<2e-16
77	GO:0000087	M phase of mitotic cell cycle	<2e-16
78	GO:0007049	cell cycle	<2e-16
79	GO:0000279	M phase	<2e-16
80	GO:0022402	cell cycle process	<2e-16
81	GO:0007127	meiosis I	0.001
82	GO:0006412	translation	0.001
83	GO:0000724	double-strand break repair via homologous recombination	0.001
84	GO:0000725	recombinational repair	0.001
85	GO:0030010	establishment of cell polarity	0.001
86	GO:0051716	cellular response to stimulus	0.001
87	GO:0007143	female meiosis	0.001
88	GO:0007093	mitotic cell cycle checkpoint	0.001
89	GO:0000375	RNA splicing, via transesterification reactions	0.002
90	GO:0006289	nucleotide-excision repair	0.002
91	GO:0007088	regulation of mitosis	0.002

Appendix

92	GO:0051783	regulation of nuclear division	0.002
93	GO:0070507	regulation of microtubule cytoskeleton organization	0.002
94	GO:0000077	DNA damage checkpoint	0.002
95	GO:0016071	mRNA metabolic process	0.002
96	GO:0045132	meiotic chromosome segregation	0.002
97	GO:0045292	nuclear mRNA cis splicing, via spliceosome	0.002
98	GO:0006396	RNA processing	0.002
99	GO:0034621	cellular macromolecular complex subunit organization	0.003
100	GO:0044238	primary metabolic process	0.003

Curriculum vitae

Personal data

Alexandra Schrader

Born: Soest, Germany

Marital Status: unmarried

Profession since April 2008

Ph.D. student in the Department of Haematology and Oncology, Lymphoma-AG Prof Dr. Dieter Kube (GRK1034 fellowship of the DFG)

Tertiary education

12/2003 – 08/2006 Georg-August-University Goettingen

Studies: Molecular Medicine

Degree: Bachelor of Science

Topic Bachelorthesis: Nucleo-zytoplasmatischer Transport des humanen Transkriptionsfaktors IIA (TFIIA) und der TFIIA-Untereinheiten in höheren Eukaryonten; Department of Molecular Cell Biology, Prof. Dr. Detlef Doenecke

10/2006 – 04/2008 University Medicine Goettingen

Studies: Molecular Medicine

Degree: Master of Science

Topic Masterthesis: Identification of oncogenic pathway signatures in malignant Lymphoma; Department of Haematology and Oncology; PD Dr. Dieter Kube

Language skills

German: native language

English: first language during studies, internet-based TOEFL (Test of English as a Foreign Language)

French: 5 year classes

Extended qualifications

EDV skills in Microsoft Office (Word, Excel, Power Point), Endnote, R

Publications:

High Myc activity is an independent negative prognostic factor for diffuse large B cell lymphomas

A. Schrader, S. Bentink, R. Spang, D. Lenze, M. Hummel, M. Kuo, J.R. Arrand, P.G. Murray, L. Trümper, D. Kube and M. Vockerodt

International Journal of Cancer. 2011 Sep 12. doi: 10.1002/ijc.26423 Epub ahead of print; PMID: 21913186

Genomic data integration using guided clustering

M. Maneck, A. Schrader, D. Kube, R. Spang

Bioinformatics. 2011 Jun 17.; PMID: 21685050

Down-regulation of BLIMP1 α by the EBV oncogene, LMP-1, disrupts the plasma cell differentiation program and prevents viral replication in B cells: implications for the pathogenesis of EBV-associated B-cell lymphomas.

K. Vrzalikova, M. Vockerodt, S. Leonard, A. Bell, W. Wei, A. Schrader, K.L. Wright, D. Kube, M. Rowe, C.B. Woodman, P.G. Murray

Blood. 2011 Jun 2;117(22):5907-17. Epub 2011 Mar 16.; PMID: 21411757

Comparison of major gene expression patterns activated by B cell specific paracrine stimuli

A. Schrader, K. Meyer, N. Walther, M. Vockerodt, E. Hand, A. Ulrich, K. Matulewicz, D. Lenze, M. Hummel, A. Kieser, M. Engelke, M. Kuo, L. Trümper, R. Spang and D. Kube

in preparation

LEF1 is a pro-proliferative factor in Burkitt lymphoma.

A. Ulrich, N. Walther, M. Vockerodt, F. von Bonin, W. Klapper, K. Meyer, A. Schrader, R. Spang, T. Pukrop, P.G. Murray, L. Trümper and D. Kube

in preparation

Congress Participation:

14th STS Meeting 2010 Weimar (Germany)

Poster: "Aberrant expression of the protooncogene c-Myc in normal human germinal centre B cells triggers a tumor like expression pattern that is expressed in Burkitt lymphomas but also some DLBCL"; A. Schrader, S. Bentink, R. Spang, D. Lenze, M. Hummel, M. Kuo, J.R. Arrand, P.G. Murray, L. Trümper, D. Kube and M. Vockerodt

4th Poster Prize

EACR21 Meeting 2010 Oslo (Norway)

Poster: "A c-Myc induced gene expression signature in human germinal center B cells predicts subtypes of aggressive non-Hodgkin Lymphoma."; Schrader A, Bentink S, Spang R, Lenze D, Hummel M, Kuo M, Arrand JR, Murray P, Trümper L, Kube D, Vockerodt

FOR942 Workshop 2009 Göttingen (Germany)

Poster: "Dissecting the molecular events in Burkitt's Lymphoma by expressing Myc in lymphoma precursor cells"; A. Schrader, S. Bentink, R. Spang, D. Lenze, M. Hummel, M. Kuo, J.R. Arrand, P.G. Murray, L. Trümper, D. Kube, M. Vockerodt